REPORT DOCUMENTATION PAGE

Form Approved OMB NO. 0704-0188

1. REPORT DATE (DD-MM-YYYY)	2. REPORT TYPE	3. DATES COVERED (From - To)
30-07-2014	Ph.D. Dissertation	-

4. TITLE AND SUBTITLE
Block Copolymers for Alkaline Fuel Cell Membrane Materials

5a. CONTRACT NUMBER
W911NF-10-1-0520

5b. GRANT NUMBER

5c. PROGRAM ELEMENT NUMBER
611103

6. AUTHORS
Yifan Li

5d. PROJECT NUMBER

5e. TASK NUMBER

5f. WORK UNIT NUMBER

7. PERFORMING ORGANIZATION NAMES AND ADDRESSES
Colorado School of Mines
1500 Illinois St

Golden, CO 80401 -1911

8. PERFORMING ORGANIZATION REPORT NUMBER

9. SPONSORING/MONITORING AGENCY NAME(S) AND ADDRESS (ES)
U.S. Army Research Office
P.O. Box 12211
Research Triangle Park, NC 27709-2211

10. SPONSOR/MONITOR'S ACRONYM(S)
ARO

11. SPONSOR/MONITOR'S REPORT NUMBER(S)
58161-CH-MUR.51

12. DISTRIBUTION AVAILIBILITY STATEMENT
Approved for public release; distribution is unlimited.

13. SUPPLEMENTARY NOTES
The views, opinions and/or findings contained in this report are those of the author(s) and should not contrued as an official Department of the Army position, policy or decision, unless so designated by other documentation.

14. ABSTRACT
Alkaline fuel cells (AFCs) using anion exchange membranes (AEMs) as electrolyte have recently received considerable attention. AFCs offer some advantages over proton exchange membrane fuel cells, including the potential of non-noble metal (e.g. nickel, silver) catalyst on the cathode, which can dramatically lower the fuel cell cost. The main drawback of traditional AFCs is the use of liquid electrolyte (e.g. aqueous potassium hydroxide), which can result in the formation of carbonate precipitates by reaction with carbon dioxide. AEMs with tethered cations can overcome the precipitates formed in traditional AFCs.

15. SUBJECT TERMS
Anion Exchnange Membranes, Block copolymers,

16. SECURITY CLASSIFICATION OF:			17. LIMITATION OF ABSTRACT	15. NUMBER OF PAGES	19a. NAME OF RESPONSIBLE PERSON
a. REPORT	b. ABSTRACT	c. THIS PAGE			Andrew Herring
UU	UU	UU	UU		19b. TELEPHONE NUMBER: 303-384-2082

Report Title

Block Copolymers for Alkaline Fuel Cell Membrane Materials

ABSTRACT

Alkaline fuel cells (AFCs) using anion exchange membranes (AEMs) as electrolyte have recently received considerable attention. AFCs offer some advantages over proton exchange membrane fuel cells, including the potential of non-noble metal (e.g. nickel, silver) catalyst on the cathode, which can dramatically lower the fuel cell cost. The main drawback of traditional AFCs is the use of liquid electrolyte (e.g. aqueous potassium hydroxide), which can result in the formation of carbonate precipitates by reaction with carbon dioxide. AEMs with tethered cations can overcome the precipitates formed in traditional AFCs.

Our current research focuses on developing different polymer systems (blend, block, grafted, and crosslinked polymers) in order to understand alkaline fuel cell membrane in many aspects and design optimized anion exchange membranes with better alkaline stability, mechanical integrity and ionic conductivity. A number of distinct materials have been produced and characterized. A polymer blend system comprised of poly(vinylbenzyl chloride)-b-polystyrene (PVBC-b-PS) diblock copolymer, prepared by nitroxide mediated polymerization (NMP), with poly(2,6-dimethyl-1,4-phenylene oxide) (PPO) or brominated PPO was studied for conversion into a blend membrane for AEM. The formation of a miscible blend matrix improved mechanical properties while maintaining high ionic conductivity through formation of phase separated ionic domains. Using anionic polymerization, a polyethylene based block copolymer was designed where the polyethylene-based block copolymer formed bicontinuous morphological structures to enhance the hydroxide conductivity (up to 94 mS/cm at 80 °C) while excellent mechanical properties (strain up to 205%) of the polyethylene block copolymer membrane was observed. A polymer system was designed and characterized with monomethoxy polyethylene glycol (mPEG) as a hydrophilic polymer grafted through substitution of pendent benzyl chloride groups of a PVBC-b-PS. The incorporation of the hydrophilic polymer allows for an investigation of the effect of hydration on ionic conductivity, resulting in the increase in membrane water affinity, enhancement of conductivity and reduced dependence of conductivity on relative humidity. A study of crosslinking of block copolymers was done wherein the crosslinking occurs in the non-matrix phase in order to maintain mechanical properties. The formation of a cationic crosslinked structure improves the mechanical integrity of the membrane in water while showing little deleterious effect on ionic conductivity and mechanical properties.

BLOCK COPOLYMERS FOR ALKALINE FUEL CELL MEMBRANE MATERIALS

by

Yifan Li

A thesis submitted to the Faculty and the Board of Trustees of the Colorado School of Mines in partial fulfillment of the requirements for the degree of Doctor of Philosophy (Applied Chemistry).

Golden, Colorado

Date _____

Signed: _____

Yifan Li

Signed: _____

Dr. Daniel M. Knauss

Thesis Advisor

Golden, Colorado

Date _____

Signed: _____

Dr. David T. Wu

Professor and Head

Department of Chemistry and Geochemistry

ABSTRACT

Alkaline fuel cells (AFCs) using anion exchange membranes (AEMs) as electrolyte have recently received considerable attention. AFCs offer some advantages over proton exchange membrane fuel cells, including the potential of non-noble metal (e.g. nickel, silver) catalyst on the cathode, which can dramatically lower the fuel cell cost. The main drawback of traditional AFCs is the use of liquid electrolyte (e.g. aqueous potassium hydroxide), which can result in the formation of carbonate precipitates by reaction with carbon dioxide. AEMs with tethered cations can overcome the precipitates formed in traditional AFCs.

Our current research focuses on developing different polymer systems (blend, block, grafted, and crosslinked polymers) in order to understand alkaline fuel cell membrane in many aspects and design optimized anion exchange membranes with better alkaline stability, mechanical integrity and ionic conductivity. A number of distinct materials have been produced and characterized. A polymer blend system comprised of poly(vinylbenzyl chloride)-b-polystyrene (PVBC-b-PS) diblock copolymer, prepared by nitroxide mediated polymerization (NMP), with poly(2,6-dimethyl-1,4-phenylene oxide) (PPO) or brominated PPO was studied for conversion into a blend membrane for AEM. The formation of a miscible blend matrix improved mechanical properties while maintaining high ionic conductivity through formation of phase separated ionic domains. Using anionic polymerization, a polyethylene based block copolymer was designed where the polyethylene-based block copolymer formed bicontinuous morphological structures to enhance the hydroxide conductivity (up to 94 mS/cm at 80 °C) while excellent mechanical properties (strain up to 205%) of the polyethylene block copolymer membrane was observed. A polymer system was designed and characterized with monomethoxy

polyethylene glycol (mPEG) as a hydrophilic polymer grafted through substitution of pendent benzyl chloride groups of a PVBC-b-PS. The incorporation of the hydrophilic polymer allows for an investigation of the effect of hydration on ionic conductivity, resulting in the increase in membrane water affinity, enhancement of conductivity and reduced dependence of conductivity on relative humidity. A study of crosslinking of block copolymers was done wherein the crosslinking occurs in the non-matrix phase in order to maintain mechanical properties. The formation of a cationic crosslinked structure improves the mechanical integrity of the membrane in water while showing little deleterious effect on ionic conductivity and mechanical properties.

TABLE OF CONTENTS

LIST OF FIGURES

LIST OF TABLES

LIST OF SCHEMES

ACKNOWLEDGEMENT

I would like to express my sincere gratitude to my advisor Dr. Daniel Knauss for his invaluable guidance and support during my Ph.D. study and research at Colorado School of Mines. Without all of his inspiration, motivation, patience, and hard work this thesis would not have been possible to complete. I would also like to thank my thesis committee members: Dr. Andrew Herring, Dr. Stephen Boyes, Dr. David Wu, and Dr. John Dorgan for their advice and comments. Special thanks go to Dr. Yuan Yang and Mr. Edward Dempsey for their technical support during the whole of my PhD research. Thanks also go to my group members, especially Dr. Nathaniel Rebeck for his help during my early PhD studies. In addition, thank you to Dr. Fredrick Beyer and Dr. Aaron Jackson at the US Army Research Laboratory for their transmission electron microscopy support.

Thank you to my grandparents, Wenzhao Li and Wenshi Li, who inspired and encouraged me to purse the PhD degree in the United States. I would also express my deep appreciation to my other family members for their tremendous support and understanding. A special thanks to my beloved one – Huiya, for the love, trust, and happiness she provides to me during my most frustrated times.

Finally, I would like to acknowledge the financial support provided by Army Research Office through a Multidisciplinary University Research Initiative (MURI grant # W911NF-10-1-0520). Also, thanks to the teaching assistantship provided by the Department of Chemistry and Geochemistry.

DEDICATION

THIS THESIS IS DEDICATED TO MY BELOVED FAMILY

CHAPTER 1 INTRODUCTION AND BACKGROUND

1.1 Introduction

Over the last few decades, the demand for alternatives to produce clean and efficient energy has dramatically increased. The limited availability of fossil fuels, including coal, oil, and natural gas, provides only a short-term solution for energy. Environmental concerns of reducing greenhouse gas emission and air pollution also motivate the development of renewable energy. On top of this, the incorporation of renewable or non-polluting sources in current energy production becomes unavoidable based on an energy security point of view. Currently, a variety of renewable energy solutions are being developed through using solar, wind, and biofuels to produce clean energies. However, current technologies cannot completely replace fossil fuels and research in all areas of renewable energy is demanded.

Among the various methods to solve energy issues, fuel cells offer a promising solution for application in transportation, stationary power, and portable devices.[1-6] This technology enables the direct conversion of energy from fuels into electrical energy at high efficiency, as fuel cells convert energy electrochemically and are not subject to the limitations of Carnot's cycle. A fuel cell is able to use the fuel from a renewable source (such as hydrogen) to generate zero emissions with only water and heat as byproducts, reducing greenhouse gas emissions and other pollution. Unlike a battery, a fuel cell does not require recharging as long as the fuel is supplied and it provides much longer operating time than batteries because of the higher energy density and lighter weight than an equivalent battery system.

However, high cost, low durability, and other engineering issues are preventing fuel cell from broad application. The electrolyte is one of the main components in a fuel cell. It separates the fuel from the electrodes and selectively transports ions between the electrodes to complete a circuit. A solid-state electrolyte (polymer membrane) is the preferred electrolyte for use in current fuel cells. In order to enhance the performance, extend the lifetime, and lower the cost of fuel cells, a polymer membrane electrolyte has to possess distinct properties. The desired polymer electrolyte needs to be an electron insulator and efficient ionic conductor. The membrane must also possess high chemical, thermal and mechanical stability under the fuel cell operating conditions. Last, but not the least, the ideal polymer membrane material needs to be inexpensive to lower the overall cost of a fuel cell.

Fuel cells can be classified into three types depending on their operation temperatures. One is the high temperature fuel cells, which comprise the solid oxide fuel cell (SOFC) and molten carbonate fuel cells. Phosphoric acid fuel cell (PAFC) is another type of fuel cell that usually operates at intermediate temperature. The other main type is the low temperature fuel cells including proton exchange membrane fuel cell (PEMFC) and alkaline fuel cell (AFC) with operation temperature usually lower than 120 °C.[7, 8] Polymer membrane can be incorporated in the low temperature fuel cells as electrolyte and this review focuses on polymer membrane materials for AFC application.

1.2 Alkaline Fuel Cells

The AFC is the first fuel cell technology to be applied toward practical applications in the 20th century. In the 1950s, NASA began to use AFCs for spacecraft and equipped the Gemini

and Apollo spaceships with this technology.[8] In the AFC, fuel is oxidized on the anode and generates the electrons to flow through the external circuit, whereas electrons reduce the oxygen on the cathode, where hydroxide ions are produced and conduct from cathode to anode (Figure 1.1).

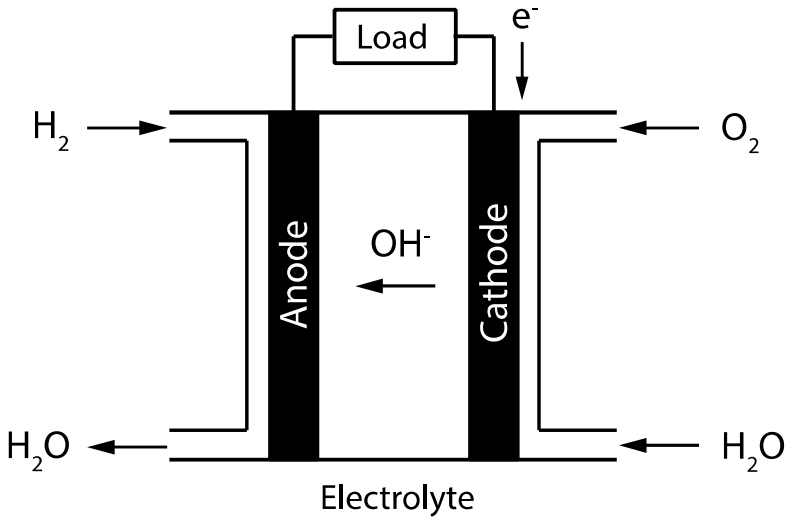

Figure 1.1 Scheme of a hydrogen fueled alkaline fuel cell.

The overall hydrogen fueled AFC reactions are given by:

Anode reaction	$2H_2 + 4OH^- \rightarrow 4H_2O + 4e^-$
Cathode reaction	$O_2 + 2H_2O + 4e^- \rightarrow 4OH^-$
Overall reaction	$2H_2 + O_2 \rightarrow 2H_2O$

AFCs offers many advantages over proton exchange membrane fuel cells (PEMFCs) resulting in the popularity of AFCs in the US space program.[8-11] The primary benefit AFC offered over PEMFC is better electrochemical kinetics on the anode and cathode under the alkaline environment, which results in the ability to use non-precious metal catalyst in this type

of fuel cell to reduce the total costs.[12-15] An AFC usually operates at relatively low temperature (roughly 60 °C),[11] offering a lower possibility of thermal and chemical degradation.

1.2.1 Traditional Alkaline Fuel Cell

Although AFCs offers several benefits, the traditional AFC commonly uses aqueous potassium hydroxide (KOH) as electrolyte,[9, 16] which results in several drawbacks for AFC technology that prohibit extensive application in other than space applications. The main drawback associated with the aqueous KOH electrolyte is the precipitation of potassium carbonate that can form by reaction with carbon dioxide impurities in the fuel and air.[17, 18] The carbon dioxide in the air or fuel reacts with hydroxide to decrease the number of hydroxide ions available for reaction at the anode, thus reducing the fuel cell performance. Furthermore, the formation of a metal carbonate can result in a precipitate that blocks pores in the electrodes, resulting in a further decrease in AFC performance.[8-11]

Another disadvantage of traditional AFC is related to the use of caustic liquid electrolyte. Corrosion management is a problem during the operation because the electrolyte can degrade most materials. Fuel cell materials that come in contact with the electrolyte need to be highly alkaline stable, which also leads to higher cost. The amount of liquid electrolyte also affects the performance, as the electrode can suffer from drying due to the lack of liquid electrolyte, while excess of liquid electrolyte can lead to the flooding of the electrode.

1.2.2 Anion Exchange Membrane Fuel Cell (AEMFC)

Anion exchange membranes have been known for decades in water treatment applications such as electrodialysis,[19-21] but recent research has been directed toward making solid polymer electrolytes for AFCs to overcome the issues in traditional liquid electrolyte AFCs.[8, 11, 22] The anion exchange membrane serves as electrolyte and has less sensitivity to carbon dioxide compared to aqueous KOH due to the absence of free cation in the polymer membrane. As a result, the anion exchange membrane prohibits the carbonate precipitation problem while still maintaining many other advantages of the AFC. Although hydroxide ions are still present in the anion exchange membrane fuel cell (AEMFC), this technology does not have the same corrosion and leakage problems. AEMFCs still has disadvantages compared to PEMFCs. The ion conducted in AEMFC is hydroxide, which is a larger ion than a proton and results in slower ion transport properties from a decreased mobility.[23] Another drawback of AEMFC is its high dependence of ionic conductivity on environmental humidity, which also limits its wide application.[24]

Overall fuel cell performance can be influenced by many factors, and the anion exchange membrane in AEMFCs is one core component. To be effective, the polymer membrane must possess certain desired properties that are directly linked to the fuel cell performance. Foremost, the cationic functional group for hydroxide conduction must be thermally and chemically stable under the AFC operating conditions. It is required that the polymer backbone has adequate mechanical, thermal, and chemical stability to maintain membrane durability under the alkaline conditions. Another important requirement is high ionic conductivity, since the main role of polymer electrolyte is to transport hydroxide from cathode to anode. The ionic conductivity must be high under different temperature and humidity conditions and should not vary. Moreover, the

anion exchange membrane should work as a barrier to prevent electron conduction and fuel crossover in the membrane. Additionally, low cost of the membrane preparation and fabrication is also desired.

A wide range of cationic functional groups and polymer backbones have been studied as anion exchange membranes, and extensive reviews of anion exchange membrane materials are available.[8-11, 22, 25] A few of the important classes of polymer electrolytes studied for use in anion exchange membrane fuel cells (AEMFC) are reviewed here as background information.

1.2.2.1 Polymer Membranes based on Quaternary Ammonium Cation

Functionalization of a polymer backbone with a quaternary ammonium group is the simplest and most widely studied way to introduce a tethered cationic group to form an anion exchange membrane. Among the different types of quaternary ammonium cations, benzyltrimethylammonium [BTMA] is one of the most frequently studied due to the absence of a β-hydrogen in the chemical structure leading to a moderate thermal and chemical stability.[26-29] More prominently, the functionalization of a polymer chain with a [BTMA] cation is relatively straightforward through substitution of a pendent chlorobenzyl group with trimethylamine. The substitution can be done on many different polymers that are functionalized with a chlorobenzyl group, therefore a wide variety of polymer backbones can be studied. Examples of different polymer systems are presented below.

Polystyrene is a readily synthesized material that is considered to be stable in alkaline conditions leading toward its study in alkaline anion exchange membranes. In addition, polystyrene can be incorporated with a variety of functional groups to obtain desired membranes.

The majority of polystyrene based membranes have incorporated quaternary ammonium cation functional groups to conduct hydroxide. Many research groups have taken advantage of this versatile platform to produce various materials for anion exchange membranes.[24, 30-42]

Some early polystyrene based anion exchange membranes were prepared from styrene and divinylbenzene polymer networks. The membrane is obtained by copolymerization of both monomers, followed by chloromethylation and then a trimethylamine quaternization reaction.[30] These membranes exhibited high electrical resistance, however, the brittle nature of polystyrene materials cannot be ignored.

In order to enhance the mechanical properties of styrene-based anion exchange membranes, Zeng, Chen and coworkers prepared an anion exchange membrane based on commercially available polystyrene-poly(ethylene-co-butylene)-polystyrene (SEBS) copolymer.[37, 42] Chloromethylation of the polystyrene block and trimethylamine quaternization were subsequently performed on this polymer (Figure 1.2). Instead of using highly carcinogenic chloromethyl methyl ether, excess formaldehyde and hydrochloric acid gas were used as chloromethylating reagents.[37] The membrane displayed relatively low hydroxide conductivity on the order of 9.37 mS/cm at 80 °C with a low ion exchange capacity (IEC) of 0.3 meq/g and water uptake (12%). Sangeetha and coworkers reported a similar anion exchange membrane modified through a similar synthetic strategy,[38] but after the chloromethylation reaction the polymer was quaternized with triethylamine. The obtained membranes were reported to be flexible, and thermally and mechanically stable. The IECs exhibited a linear relationship with hydroxide conductivity and water uptake. However, the hydroxide conductivity was only 0.69 mS/cm at room temperature for a polymer with an IEC of 0.578 mmol/g.

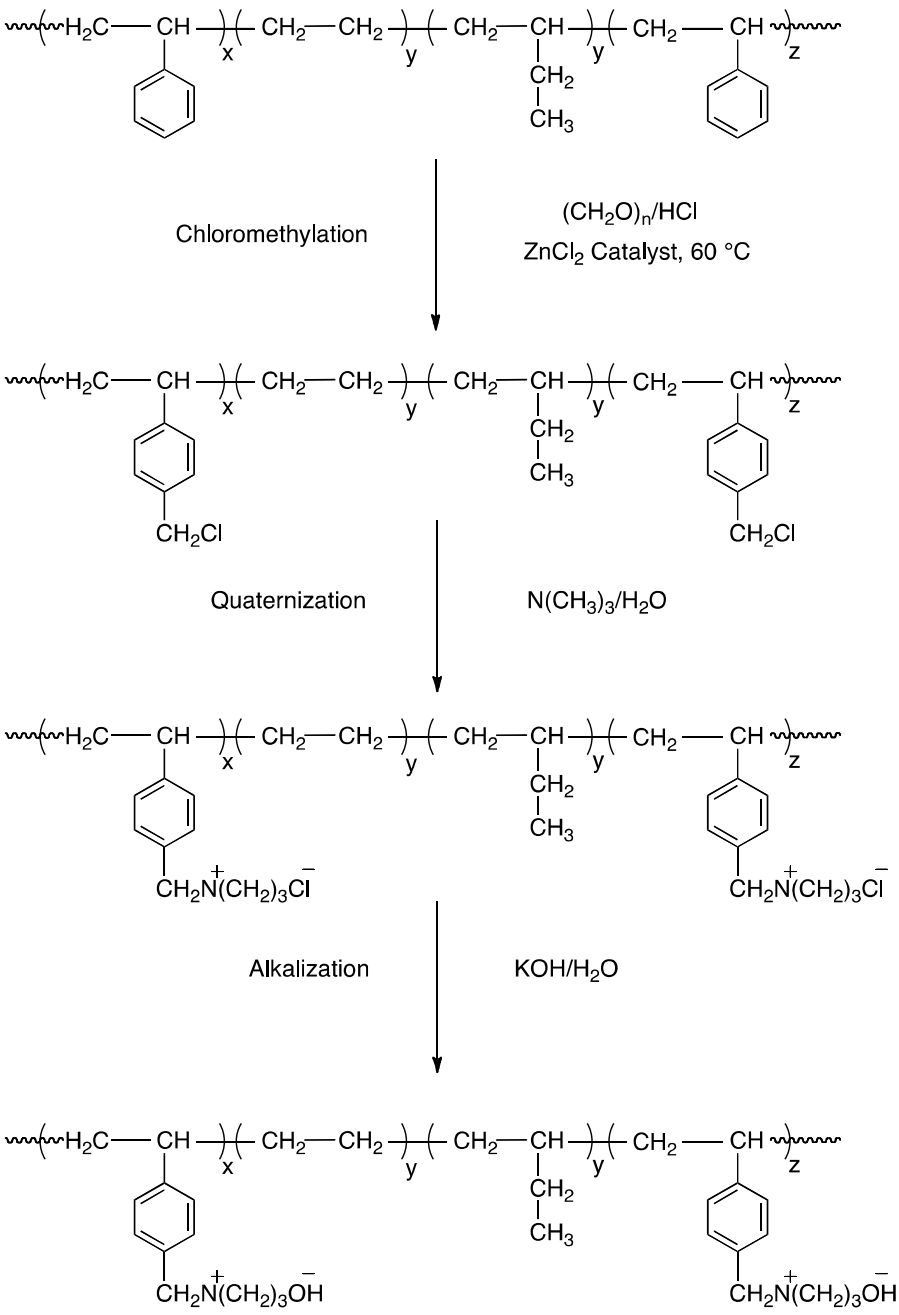

Figure 1.2 Chloromethylation, quaternization, and alkalization reaction of SEBS.

Vinylbenzyl chloride is a styrene derivative monomer containing the benzyl chloride functional group, which can be readily converted to ammonium groups by reaction with tertiary amine reagent without a chloromethylation step. Poly(vinylbenzyl chloride) was radiation grafted into fluorinated or partially fluorinated polymer membranes to prepare an anion exchange

membrane and the properties were extensively studied by researchers at the University of Surrey (Figure 1.3).[24, 31, 32, 34, 35] In their early studies, vinylbenzyl chloride was grafted onto partially fluorinated films of poly(vinylidene fluoride) (PVDF) and fully fluorinated films of poly(tetrafluoroethene-cohexafluoropropylene) (FEP) followed by quaternization and alkalization to prepare anion exchange membrane.[31, 32, 34] Degradation was observed in anion exchange membranes prepared by PVDF, which prohibits this type of membrane for fuel cell application. Nonetheless, FEP film based anion exchange membranes exhibited desired performance in structural stability and hydroxide conductivity of 0.02 S/cm at room temperature. The same graft and functionalization strategy was applied to poly(ethylene-co-tetrafluoroethylene) (ETFE) film leading to a promising hydroxide conductivity of 0.034 S/cm at 50 °C in water.[24, 35] The ETFE based membranes provide higher mechanical properties and lower water uptake than FEP based anion exchange membranes due to a higher crystallinity of ETFE compared to FEP

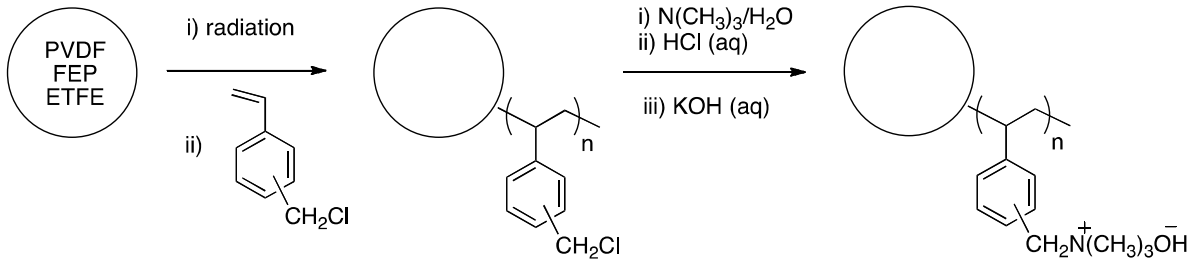

Figure 1.3 The radiation grafting of vinylbenzyl chloride onto PVDF, FEP, AND ETFE polymer films and followed by quaternization and alkalization

Alternative to the grafting modification of commercial copolymer films, vinylbenzyl chloride can be readily incorporated into a polymer backbone to synthesize copolymers with other film forming materials. A polymer membrane was designed based on poly(methyl

methacrylate-co-butyl acrylate-co-vinylbenzyl chloride) (PMBV) random copolymer to study the alkaline fuel cell properties (Figure 1.4).[36] The copolymer was quaternized by trimethylamine in DMF and an anion exchange membrane was prepared from the amphiphilic material. Changing the amount of vinylbenzyl chloride in the copolymer varied the ultimate IEC obtained in the membranes. The methyl methacrylate and butyl acrylate provide the membrane with high mechanical stability and flexibility, although the alkaline stability of the ester groups is expected to be quite low. The increased conductivity is associated with the increase in IEC, however, the quaternized membrane with best hydroxide conductivity (13.5 mS/cm in fully hydrated conditions) shows incredibly high water uptake of 239%.

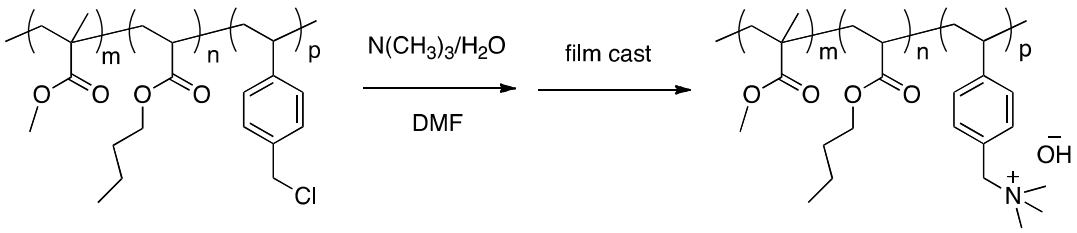

Figure 1.4 Quaternized membrane from poly(methyl methacrylate-co-butyl acrylate-co-vinylbenzyl chloride)

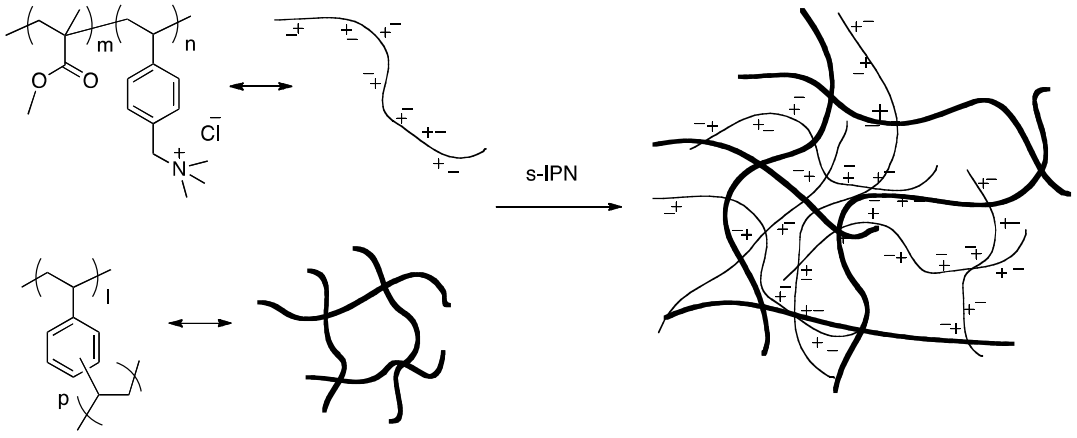

Figure 1.5 Semi-interpenetrated polymer network by crosslinking reaction

Although high water uptake is also associated with high conductivity, the durability of membranes can be dramatically decreased by excessive water uptake and the formation of what approximates a hydrogel. In order to solve this problem, crosslinking steps are commonly involved. It has also been shown that crosslinks in anion exchange membranes can greatly enhance the thermal stability and mechanical durability. Researchers from the same group that produced the PMVB polymers developed a semi-interpenetrated network (s-IPN) based on poly(methyl methacrylate-co-vinylbenzyl chloride) (PMV) random copolymer by polymerization of divinylbenzene in the presence of quaternized PMV solution. The resulting membrane eliminated the butyl acrylate in the copolymer and incorporated crosslinks in the membrane (Figure 1.5).[41] The obtained anion exchange membrane (10 wt% DVB crosslinker of the quaternized PMV membrane) displayed much lower water uptake (63.1%) compared to the non-crosslinked membrane (PMBV based membrane). A durability test under actual fuel cell conditions demonstrated the positive effect on mechanical properties from the formation of crosslinking and removal of butyl acrylate. The conductivity of the crosslinked membrane was determined to be lower than the non-crosslinked version, although still on the order of 10^{-2} S/cm.

Polysulfones are a class of poly(aryl ether) materials that have been widely studied for use in nanofiltration,[43-45] gas separation,[46, 47] and PEMFC.[48, 49] Because of their generally good properties and their ready capability for functionalization to introduce cationic groups, a large number of poly(aryl ether) based anion exchange membranes have been developed for potential application in AEMFCs.[23, 50-58]. The high alkaline stability of polysulfone has been demonstrated by soaking the polymer in 40% NaOH at 70-80 °C for 300 hours, where no degradation was observed.[59] Polysulfones are commonly modified by chloromethylation, followed by quaternization to yield benzyltrimethylammonium groups.

Hibbs and coworkers copolymerized bisphenol with bis(dichlorodiphenyl) sulfone by nucleophilic aromatic substitution polymerization to form a polymer precursor. The obtained polymer was chloromethylated and solvent cast to prepare a membrane. Quaternization with trimethylamine and alkalization were subsequently performed on the membrane to yield an anion exchange membrane in the hydroxide counterion form (Figure 1.6).[23] The chloromethylation reaction took place on the biphenol repeat units and the IEC of the membrane was varied from 0.69 meq/g to 1.89 meq/g depending on the degree of functionalization on the polymer backbone. Increased conductivity was associated with an increase in IEC and in water uptake. The membranes demonstrated hydroxide conductivity up to approximately 35 mS/cm at 30 °C with a water uptake of nearly 100%.

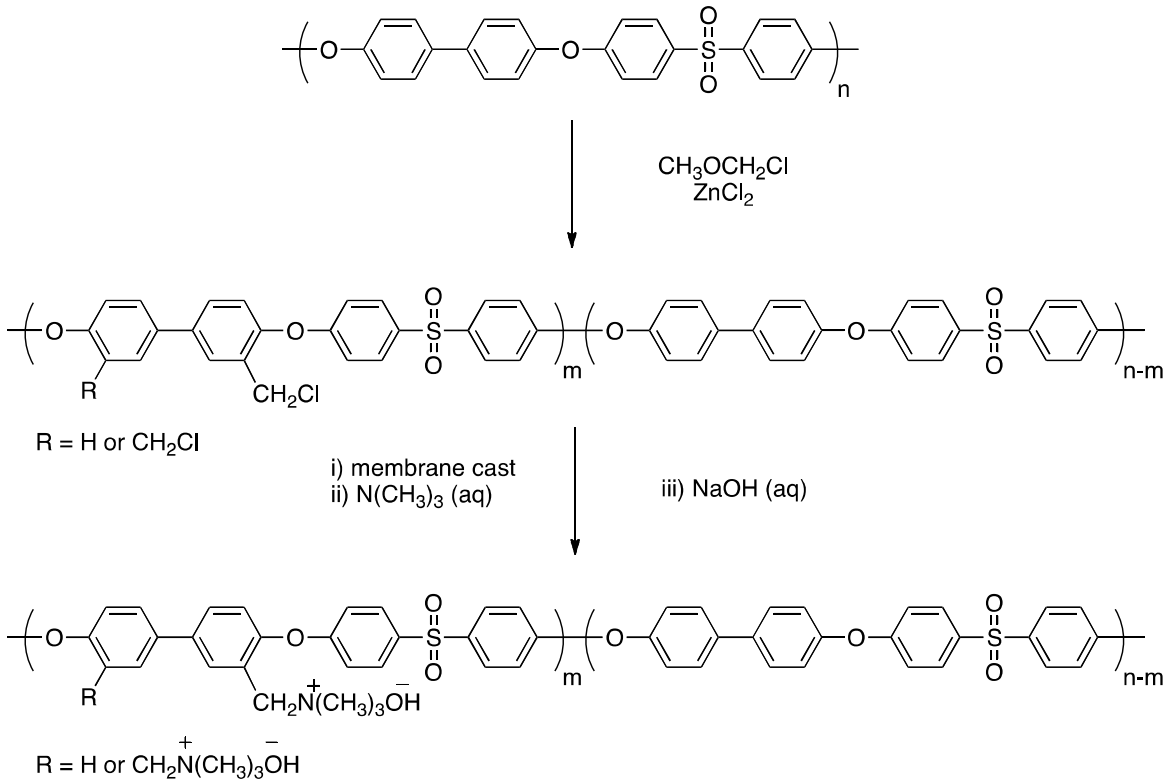

Figure 1.6 Post-modification of polysulfone by chloromethylation, quaternization, and alkalization

Bisphenol A copolymerized polysulfone was also prepared as anion exchange membrane by a similar post-modification method. The chloromethylation reaction was studied to optimize the extent of chloromethyl group functionalization, and it was found that the degree of chloromethylation is a function of temperature and time.[51] Instead of only using trimethylamine as quaternization reagent, other tertiary amines (triethylamine, dimethylethylamine, dimethylisopropylamine, and tetramethylethylenediamine) were also incorporated into the study of the quaternization reaction. The chloromethylated membrane reacting with tetramethylethylenediamine (TMEDA, difunctional crosslinker) and bromoethane produced highest hydroxide conductivity (73 mS/cm at 90 °C) and measured stability in alkaline conditions (Figure 1.7).[51]

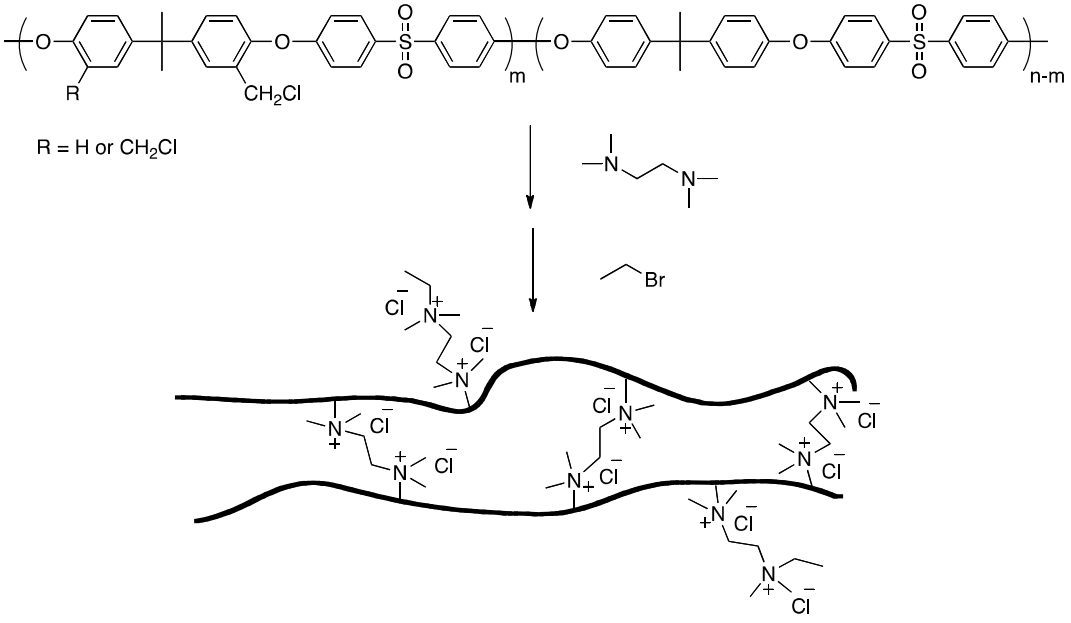

Figure 1.7 TMEDA and bromoethane quaternization of polysulfone

Researchers at Georgia Institute of Technology studied the polysulfone anion exchange membranes based on bisphenol AF (Figure 1.8), which provide fluorenyl functionality in the

polymer backbone to enhance the durability and mechanical stability of fuel cell membrane.[53, 55, 58] In their early study, a high functionality of ammonium cations (as measured by IEC) in their polymer membrane was achieved, which resulted in a high carbonate conductivity of 63 mS/cm at 70 °C.[53] The higher IEC led to an increase in ionic conductivity, however, the high IEC samples also resulted in a high water uptake and low membrane dimensional stability. More recently, researchers from the same group developed a crosslinked polysulfone to overcome the high water uptake issue. An excess of bisphenol AF was designed to ensure phenol end functional groups on polysulfone and an epoxy functional group (tetraphenylol ethane glycidyl ether) was introduced and used to crosslink the polysulfone.[55] The crosslinked structure controlled the water uptake and swelling, and the water uptake decreased from 225% to 50% going from the non-crosslinked membrane to the crosslinked material. However, the hydroxide conductivity of the non-crosslinked membrane was found to be unstable in 1 M hydroxide solution at 50 °C indicating the degradation of quaternary ammonium cation.

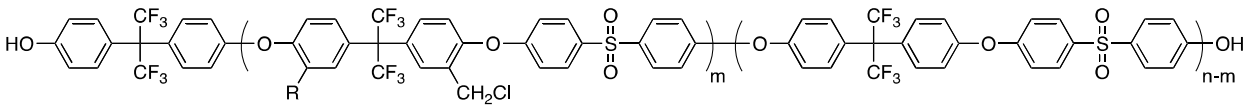

Figure 1.8 Bisphenol AF based polysulfone

As discussed above, the chloromethylation reaction commonly involves with the use of highly carcinogenic chloromethyl methyl ether. Hickner and coworkers developed a less toxic synthetic pathway by incorporating tetramethylbisphenol A as a comonomer in a polysulfone (Figure 1.9).[54] The benzyl methyl groups in the polymer enabled a bromination reaction using N-bromosuccinimide to yield bromomethyl groups on the polysulfone backbone. The

quaternization reaction was performed by both heterogeneous and homogeneous methods. The membrane from heterogeneous amination displayed a higher conductivity than the membrane from the homogeneous method. The membrane in hydroxide form was exposed to air to study the carbon dioxide effect on membrane conductivity. The membranes after 4 days of carbon dioxide exposure reached a similar conductivity to the membrane directly ion exchanged to bicarbonate. A conductivity of 27 mS/cm was obtained for a membrane in bicarbonate form.

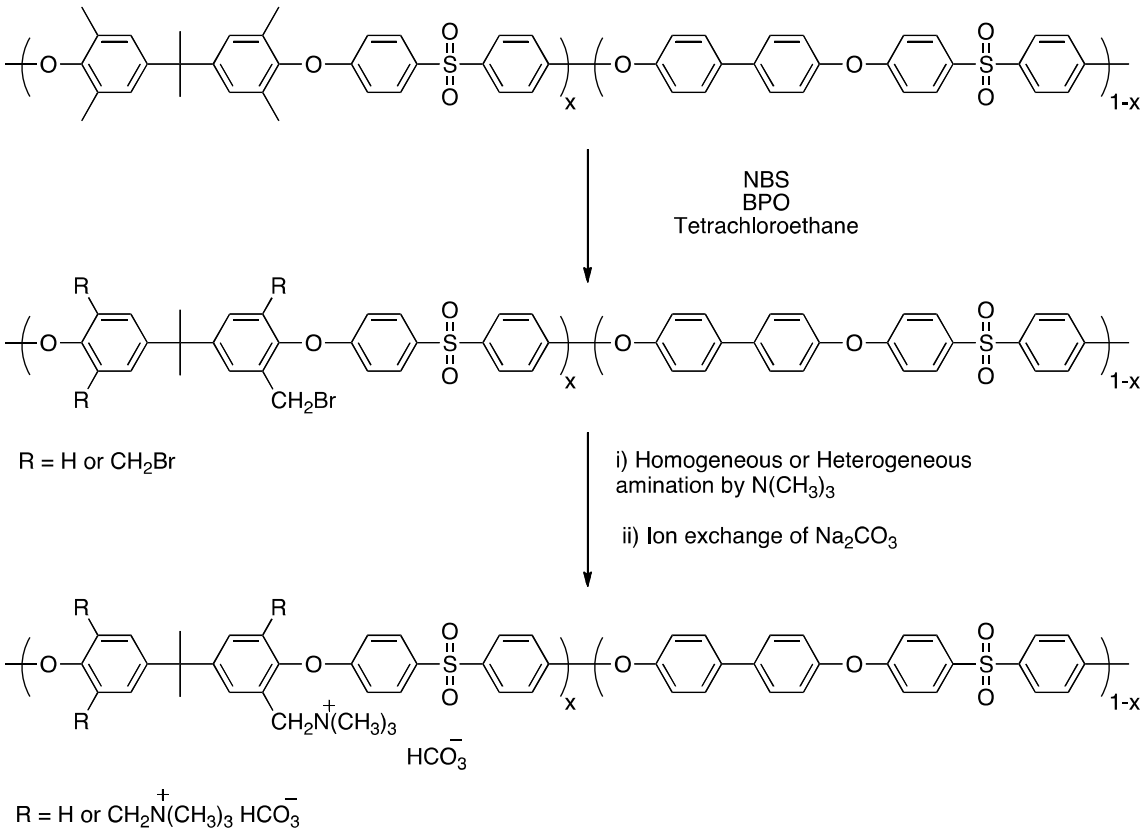

Figure 1.9 Preparation of quaternary ammonium anion exchange membrane based on tetramethylbisphenol A polysulfone

Although the majority of synthetic procedures prepare benzyltrimethylammonium cations through the amination with trimethylamine, alternative methods to functionalize a polysulfone have been examined. Benzylamine functionalized polymers can be synthesized using a

benzyldimethylamine functionalized monomer and then reacted with methyl iodide to form quaternary ammonium cations in the polymer. (Figure 1.10).[52] The functionalized monomer offered control over IEC and cationic group position on the polymer backbone. All membranes showed conductivity on the order of 10^{-2} S/cm at room temperature and the highest hydroxide conductivity reached 80 mS/cm.

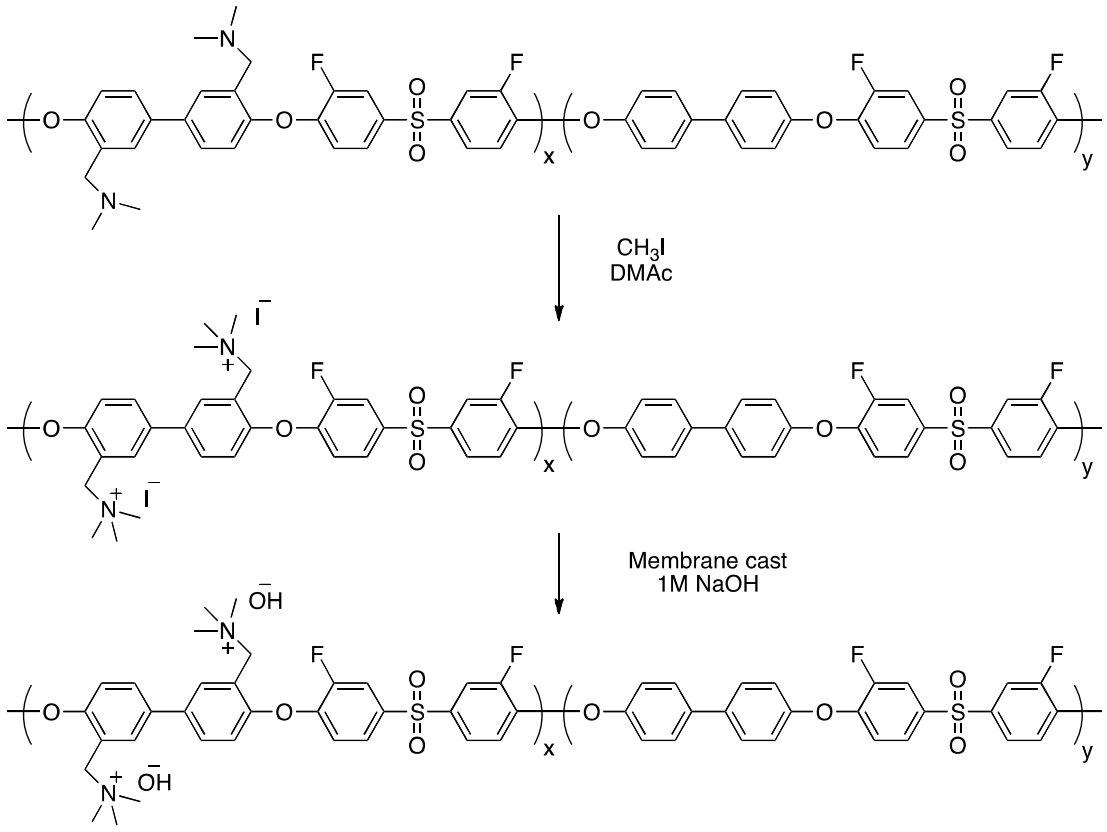

Figure 1.10 Anion exchange membrane by tertiary amine functionalized bisphenol polysulfone

Poly(ether imide)s are another class of polymer backbone that has been used in numerous application areas due to their high thermal, chemical and mechanical stability. The sequence of Chloromethylation and subsequent trimethylamine quaternization has also been used to convert poly(ether imide)s to anion exchange membranes.[60-62] Wang and coworkers developed a

poly(ether imide) based membrane through this process (Figure 1.11) but the hydroxide conductivity was found to be low, ranging from 2.28 to 3.51 mS/cm. Moreover, the poly(ether imide) are potentially susceptible to degradation under alkaline conditions due to possible hydrolysis of the imide group

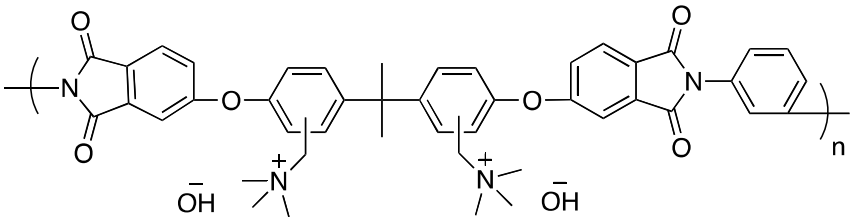

Figure 1.11 Poly(ether imide) for anion exchange membrane[60]

Polyethylene has been studies as membrane material for AEM due to its good chemical and mechanical stability as well as its ease of processing.[63-65] An anion exchange membrane was produced by direct reaction on the polyethylene backbone (Figure 1.12).[66] The sulfonchlorination reaction was performed on a polyethylene film in the presence of sulfur dioxide and chlorine. The diamine reagent was used to substitute the chloride and further quaternized by bromomethane. Although the conductivity of this type of membrane was not reported, the research provided a feasible method for functionalization of polyethylene to produce anion exchange membranes.

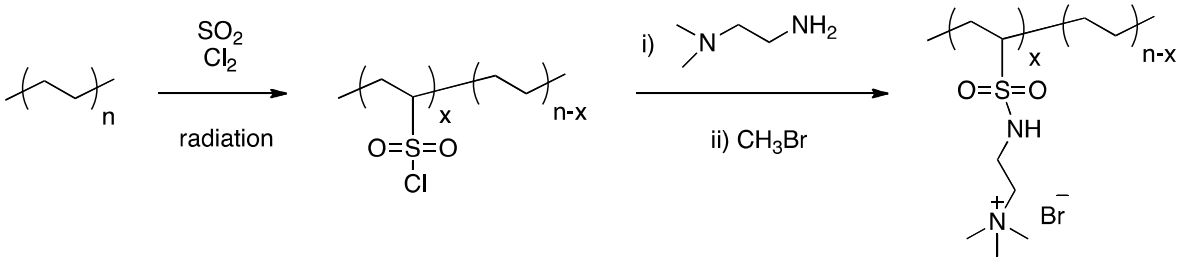

Figure 1.12 Polyethylene derived anion exchange membrane

Coates research group has reported several studies on polyolefin-based membranes, which can be further hydrogenated to form polyethylene based anion exchange membranes.[67-69] Polymer precursors were synthesized by ring opening metathesis polymerization (ROMP) using the Grubbs' second generation catalyst due to the high tolerance of various functional groups. A random copolymer was prepared from non-functionalized cyclooctene and tetraalkylammonium functionalized cyclooctene (Figure 1.13).[68] The IEC varied with the monomer feed ratio in the copolymerization. The unsaturated polymer precursors were hydrogenated by hydrogen gas in the presence of Crabtree's catalyst. The conductivity of hydrogenated membranes reached 65 mS/cm at 50 °C with an IEC of 1.50 mmol/g and water uptake of 132%.

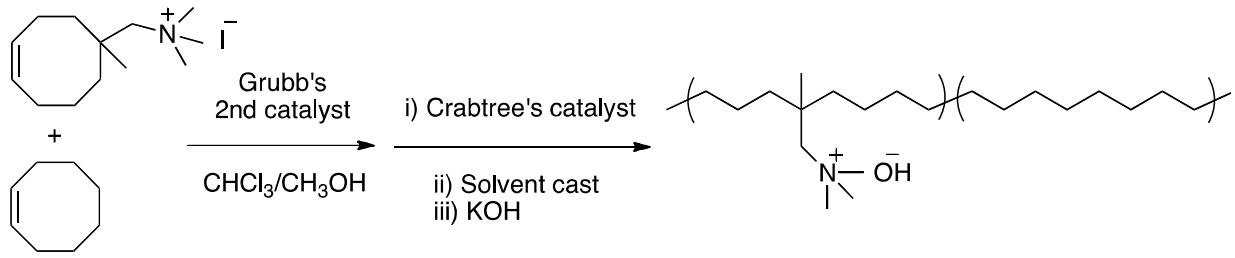

Figure 1.13 Polyethylene based anion exchange membrane

A crosslinked polyethylene based anion exchange membranes were designed with membranes reportedly prepared through the slow evaporation during the polymerization. A tetraalkylammonium-functionalized cross-linkers (two benzyltrimethyl-ammonium groups per monomer) is synthesized to copolymerize with cyclooctene (Figure 1.14).[69] The membranes retained high mechanical properties and conductivities of bromide, chloride, bicarbonate, carbonate, and hydroxide forms were compared and hydroxide exhibited the highest conductivity among all counterions as expected. The crosslinked membrane showed competitive hydroxide

conductivity under hydrated condition, which reached up to 68.7 mS/cm at 20 °C and 111 mS/cm at 50 °C.

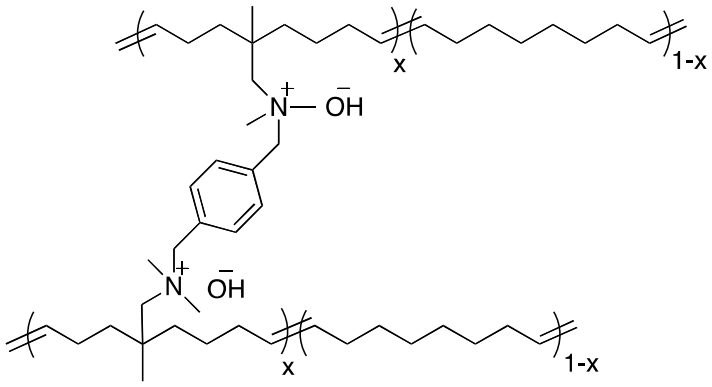

Figure 1.14 Crosslinked anion exchange membrane by functionalized monomer crosslinker

Poly(phenylene oxide) (PPO) is a high performance engineering polymer with high stability. More importantly, the availability of benzyl methyl groups in PPO enable the post functionalization by bromination. PPO based anion exchange membranes have been widely studied by Xu and coworkers.[70-82] The early work on PPO based anion exchange membrane focused on the bromination condition to control the bromine function position.[70] The brominated materials were functionalized to cationic functional groups for different applications. Anion exchange membranes were prepared by blending chloroacetylated PPO (CPPO) with brominated PPO (BrPPO) to form a crosslinked network (Figure 1.15).[76] After functionalization by reaction with trimethylamine, the conductivity showed a proportional relationship with IEC as well as the amount of BrPPO. The water uptake was controlled by the extent of crosslinking reaction between chloroacetyl groups and aromatic ring, and the extent of crosslinking in the membrane was dependent on the amount of CPPO.

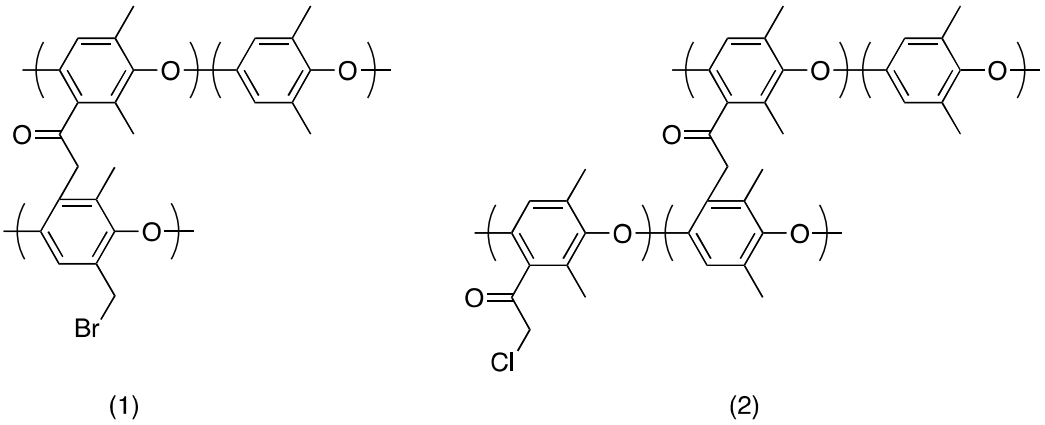

Figure 1.15 Two crosslinking structures in BPPO/CPPO blend membrane

Quaternary ammonium cations other than benzyltrimethylammonium have also been investigated in anion exchange membranes based on PPO. Hickner and coworkers synthesized a series of quaternized PPO containing long alkyl chain quaternary ammonium cations (Figure 1.16).[82] PPO polymer was functionalized through varying degrees of bromination. A series of BPPO polymers were quaternized by N,N-dimethylhexylamine, N,N-dimethyldecylamine, and N,N-dimethyl-hexadecylamine to compare with the BPPO aminated by trimethylamine. The membranes aminated by dimethylhexylamine exhibited the highest conductivity up to 43 mS/cm, which is almost 2 times higher than the membrane with similar IEC in benzyltrimethyl-ammonium cation. Quaternary ammonium cation with long alkyl chains also showed higher alkaline stability than the membranes in benzyltrimethylammonium cation although degradation was reported for all membranes. Quaternized PPOs with multiple alkyl chains displayed significantly lower water uptake due to the increased hydrophobicity resulting from multiple alkyl chains.

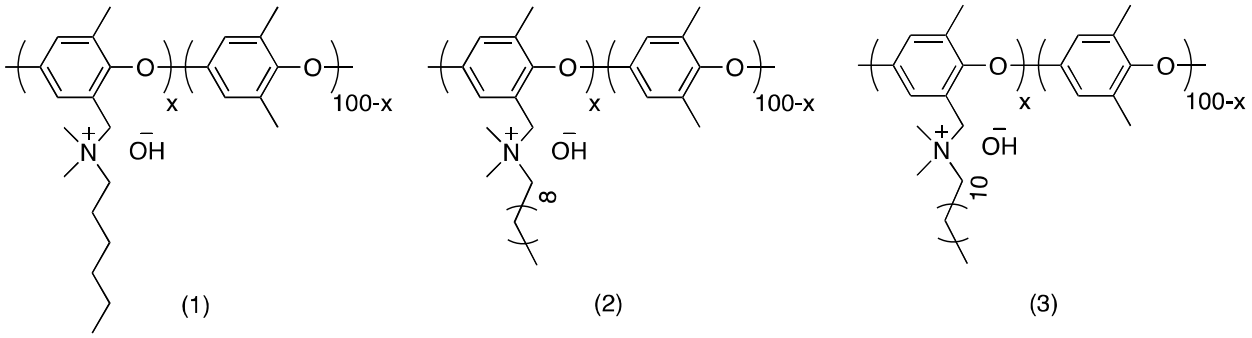

Figure 1.16 Quaternized PPO containing (1) benzyldimethylhexylammonium cation; (2) benzyldimethyldecyl ammonium cation; and (3) benzyldimethylhexadecylammonium cation

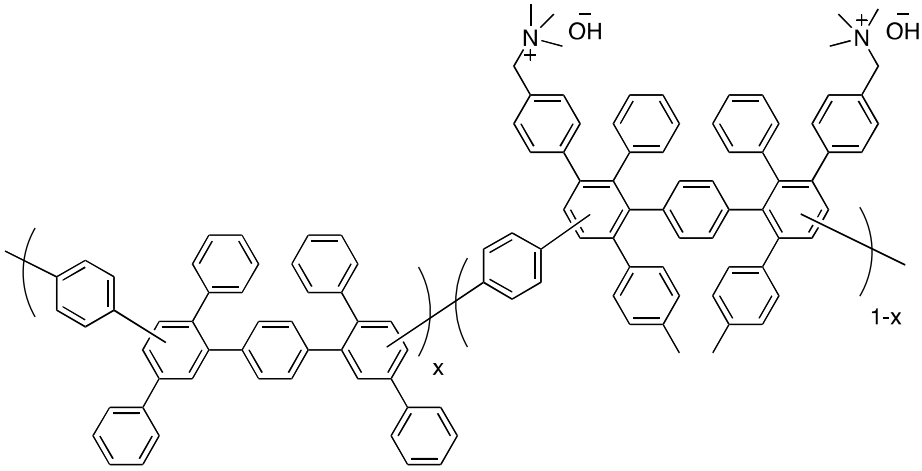

Figure 1.17 Poly(phenylene) based anion exchange membrane

Poly(phenylene) polymer has not been widely studied for anion exchange membrane fuel cell, however, researchers in Sandia National Lab synthesized poly(phenylene) based anion exchange membranes through Diels-Alder reaction (Figure 1.17).[83] Various tetramethyl-poly(phenylene) homopolymers and copolymers were prepared and functionalized to yield a range of IECs. The repeat unit with benzyl methyl groups could undergo bromination by reaction with N-bromosuccinimide initiated by benzoyl peroxide. The resulting bromomethyl groups were subsequently aminated by trimethylamine. The membranes had water uptakes that range

from 23 to 122% with hydroxide conductivity up to 50 mS/cm in water. In addition, the alkaline stability was studied on poly(phenylene) based anion exchange membrane indicating the material is alkaline stable in 4M NaOH at 60 °C.

Anion exchange membranes containing alkyl spacers were also prepared by Friedel–Crafts acylation of 6-bromo-1-hexanoyl chloride on the poly(phenylene) backbone materials (Figure 1.18).[84] The chloride conductivity of membranes with a six-carbon side chain reached 17 mS/cm. The quaternized membrane containing ammonium cations with alkyl side chains was exposed to 4 M KOH at 90 °C for 14 days and no noticeable degradation was observed. The alkaline stability of these membrane displayed improved results compared to the poly(phenylene) membrane tethered by other cations in the same test condition.

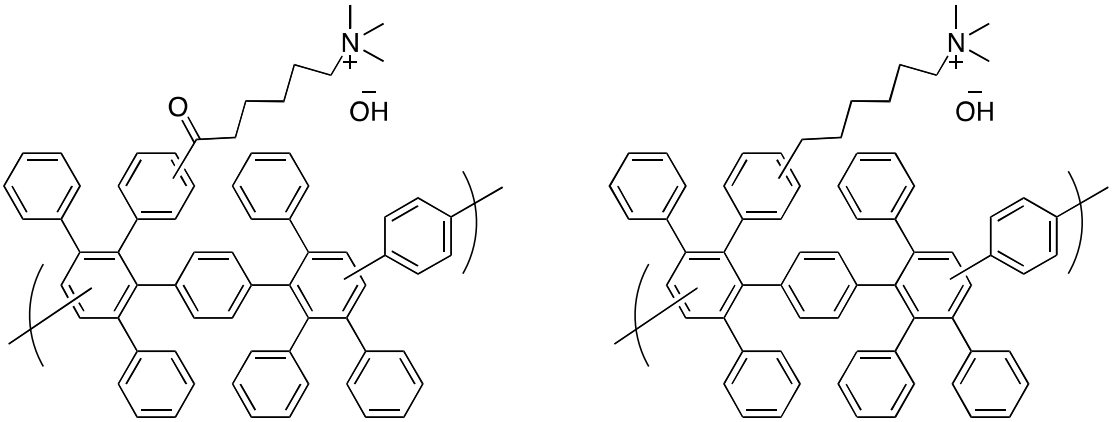

Figure 1.18 Quaternary ammonium cations containing six-carbon side chain

1.2.2.2 Polymer Membranes based on Other Cations

In addition to quaternary ammonium cations, other cations have also been incorporated to produce anion exchange membranes for fuel cells. Quaternary phosphonium cations have demonstrated good ion conduction properties and high stability in alkaline conditions. Yan and

coworkers developed a tris(2,4,6-trimethoxyphenyl) phosphine to tether to a bisphenol A polysulfone,[85, 86] through chloromethylation and chloro substitution with the phosphine. The trimethoxy groups were proposed in this study to increase the stability by reducing the attack by the hydroxide ion. The quaternary phosphonium membrane produced a high ionic conductivity and good fuel cell performance. The conductivity and water uptake were also proportional to IEC in the phosphonium-based membrane. The highest hydroxide conductivity reached 45 mS/cm at 20 °C in water.

The tris(2,4,6-trimethoxyphenyl) phosphine functionalized polysulfone was also reacted with benzyl chloride functional polysulfone to produce self-crosslinking structures at relatively low temperature (Figure 1.19).[87] The crosslinked membrane efficiently reduced the water uptake while mostly retaining hydroxide conductivity of 38 mS/cm under fully hydrated condition at 20 °C.

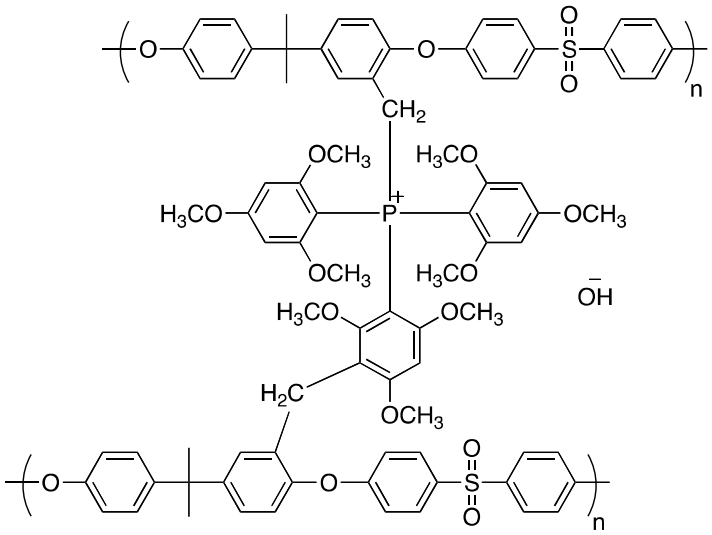

Figure 1.19 Quaternary tris(2,4,6-trimethoxyphenyl) phosphonium cation based anion exchange membrane

Another type of phosphonium cation, tetrakis(dialkylamino)phosphonium cation, was attached to cyclooctene to prepare polyethylene based anion exchange membrane by the Coates research group (Figure 1.20).[88] The alkaline stability of tetrakis(dialkylamino)-phosphonium model compound was evaluated and directly compared with benzyltrimethyl-ammonium cations. The membrane tethered by tetrakis(dialkylamino)phosphonium displayed superior alkaline stability in 15 M KOH at 22 °C and 1 M KOH at 80 °C. Although the cation synthesis required multiple steps, the membrane produced good hydroxide conductivity of 22 mS/cm at 22 °C and high alkaline stability.

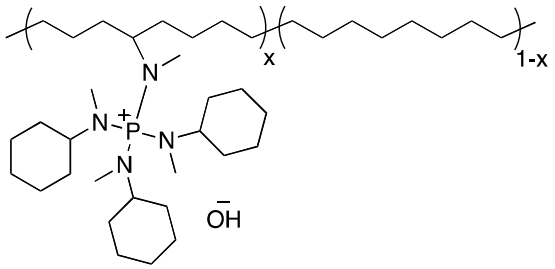

Figure 1.20 Tetrakis(dialkylamino)phosphonium functionalized polyethylene membrane

Guanidinium cation has also been used in anion exchange membrane with speculation that the high basicity can effectively conduct hydroxide ion. Wang and coworkers incorporated guanidinium cation onto biphenol polysulfone backbone and the membranes showed high hydroxide conductivity of 45 mS/cm at 20 °C and 74 mS/cm at 60 °C at an IEC of 1.89 meq/g (Figure 1.21a).[89] More recently, Xu and coworkers incorporated guanidinium cation onto PPO to produce guanidinium PPO (GPPO) membrane in order to study the properties. The GPPO membrane displayed extraordinary hydroxide conductivity of 71 mS/cm at room temperature (Figure 1.21b).[90] The study proposed good chemical stability of the guanidinium cation in hydroxide solution for a short duration (1 M NaOH at 60 °C over 48 hr). Hibbs and coworkers

also studied the alkaline stability of quaternary guanidinium caition tethered on poly(phenylene) (PMGTMPP) membrane. The PMGTMPP membrane exhibited low stability under basic conditions and the ionic conductivity largely decreased after only 24 hours in 4 M KOH at 90 °C.[84]

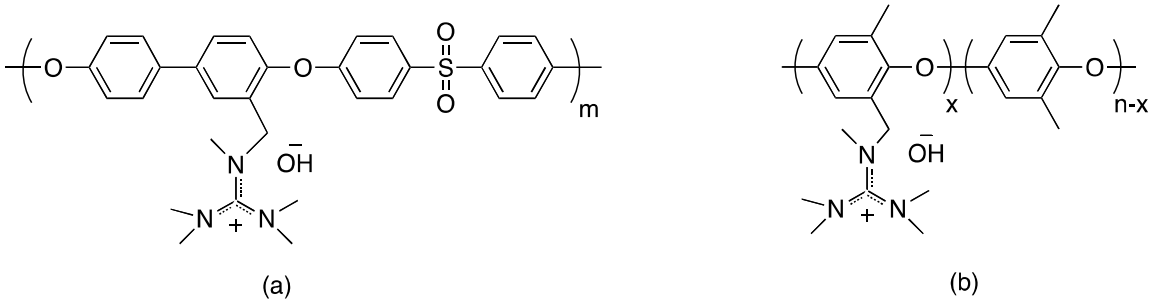

Figure 1.21 Guanidinium functionalized (a) polysulfone and (b) poly(phenylene oxide)

Imidazolium has also been employed in anion exchange membranes as a hydroxide conducting group. Imidazolium can be either prepared in the polymer backbone as poly-benzimidazolium or as pendent cationic group tethered onto the polymer backbone. Poly-benzimidazole was methylated to generate the cation functional polymer and produce anion exchange membrane (Figure 1.22a).[91-93] However, the poor stability of polybenzimidazolium in alkaline condition has impeded application. The similar unstable behavior of imidazolium in alkaline condition was also observed in poly(phenylene) based polymer membrane. The hydroxide conductivity of imidazolium membrane decreased by almost 60% after one day soaking in 4 M KOH solution at 90 °C. In order to increase the alkaline stability of polybenzimidazolium, adjacent bulky groups were designed in polybenzimidazole synthesis (Figure 1.22a). The improved membrane showed hydroxide conductivity of 13.2 mS/cm while

possessing increased alkaline stability, which could correspond to the steric hindrance to hydroxide nucleophilic attack.

Recently, a pendent imidazolium functionalized membrane was prepared based on tetramethylbisphenol A polysulfone block copolymer (Figure 1.22b).[94] The polysulfone polymer was brominated and then functionalized with imidazolium homogeneously. The membrane with an IEC of 1.45 meq/g exhibited high hydroxide conductivity of 100 mS/cm at 80 °C with a reasonable water uptake. The alkaline stability was also investigated with only a slight decrease in hydroxide conductivity observed after immersing in 2 M NaOH solution at 60 °C for 7 days.

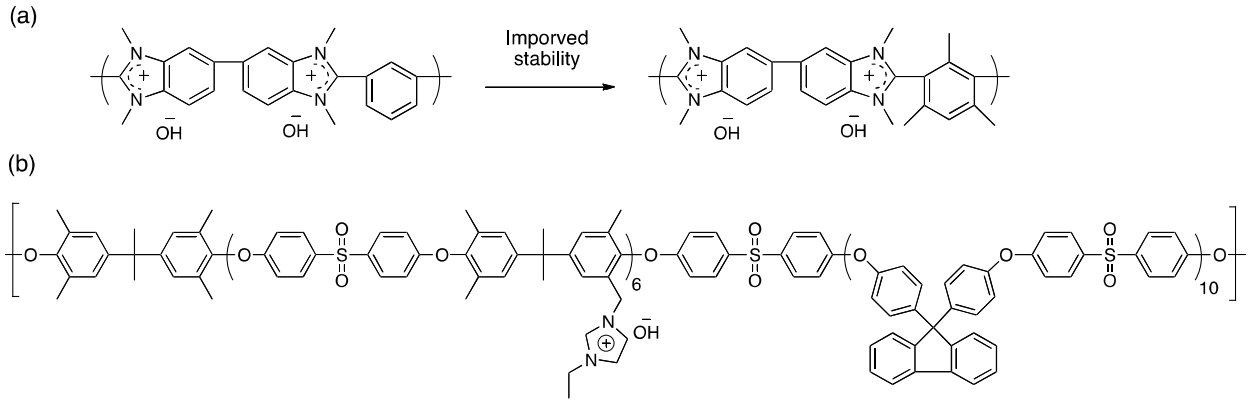

Figure 1.22 Imidazolium functionalized anion exchange membrane

Numerous synthetic strategies have been employed to synthesize cationic functional groups and polymer backbones for potential application as anion exchange membrane fuel cells. While various cationic functional groups and polymer backbones can be selected, enhanced ionic conductivity commonly associates with increased water uptake, correlating to the increase in IEC. However, the high water uptake results in undesirable swelling leading to poor mechanical

integrity of the membrane in water or fuel. Therefore, it is necessary to balance the relationship between membrane ionic conductivity and mechanical performance.

Although benzyltrimethylammonium cation is not the most stable cation for alkaline fuel cell application, the relative ease of synthesis and acceptable ion conducting properties make the benzyltrimethylammonium popular in anion exchange membrane research. Improved cationic functional groups still need to be investigated in order to produce highly conductive materials with improved thermal, and chemical stability through a facile synthetic pathway.

1.3 Phase Separated Materials

Research has demonstrated that the ionic conductivity of polymer electrolyte can be enhanced by the formation of conduction pathways in the membrane through the formation of phase-separated morphology.[25, 95-97] The anion exchange membrane comprises hydrophilic ionic conduction component and a hydrophobic component, where the two parts are not compatible with each other leading to potential phase separated morphology. Additionally, the balance between membrane ionic conductivity and mechanical stability in water is paramount, therefore, the control of phase separation in anion exchange membrane needs to be taken into account to optimize this balance. Most of the reported research on anion exchange membranes deals with random copolymers and the cationic functional groups are randomly distributed through the polymer, which limits microphase separation between hydrophilic and hydrophobic portions. Polymer materials with ordered phase separated morphologies or with the potential for forming ordered phase separation will be presented in the following content.

1.3.1 Perfluorinated Polymer

In the research of Nafion™ as proton exchange membrane, phase separation behavior has been extensively investigated.[95, 96] The hydrophilic side chains constitute the ionic conducting channel while the hydrophobic perfluorinated backbone forms the mechanical component of the membrane material. Although Nafion is a proton exchange membrane material, the material concept provides an example of controlling or manipulating the phase separation in anion exchange membrane to enhance ion exchange membrane properties.

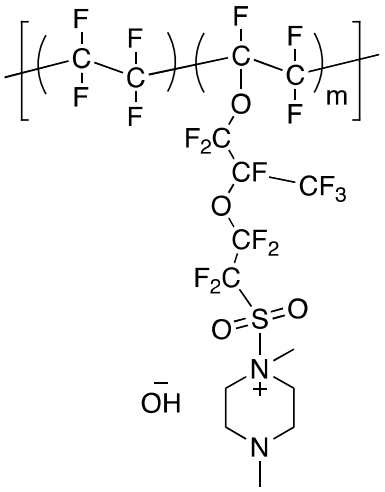

Figure 1.23 Quaternized piperazinium functionalized perfluorinated anion exchange membrane based on Nafion™

Recently, Nafion™ based materials were converted to anion exchange membranes in order to take the advantage of the outstanding membrane performance, and the modified ionomer is expected to provide phase separation behavior.[98-100] A Nafion™ based membrane was functionalized by dimethylpiperazine cations and ion exchanged to hydroxide (Figure 1.23).[100] The cationic modified Nafion™ membranes in both fluoride and hydroxide forms show an ionic peak in small angle x-ray scattering (SAXS), which is attributed to the ordered

phase separation in membrane. However, the Nafion™ modified anion exchange membrane displays lower hydroxide conductivity than chloride, due to the neutralization of hydroxide by carbon dioxide, or more likely the instability of the resulting cation to a nucleophilic hydroxide.

1.3.2 Multi-block Copolymers

Nucleophilic aromatic substitution polymerization has been employed to synthesize multi-block polysulfone copolymers to investigate the membrane properties and their phase separation behavior.[56, 57] A series of mutiblock polymer membranes containing hydrophobic polysulfone block and quaternary ammonium functionalized hydrophilic block were designed by Watanabe and coworkers.[56] In this work, 4,4′-(9-fluorenylidene)diphenol was copolymerized in the polymer for subsequent chloromethylation and the capacity to incorporate a greater number of cationic functional groups. The phase separation between hydrophobic and hydrophilic components was confirmed in the multiblock membrane by scanning transmission electron microscopy (STEM) in Figure 1.24. The ionic conductivity of multiblock membrane outperformed the corresponding random membrane as characterized by electrochemical impedance spectroscopy. The multiblock membranes exhibited hydroxide conductivity up to 144 mS/cm at 80 °C in water.

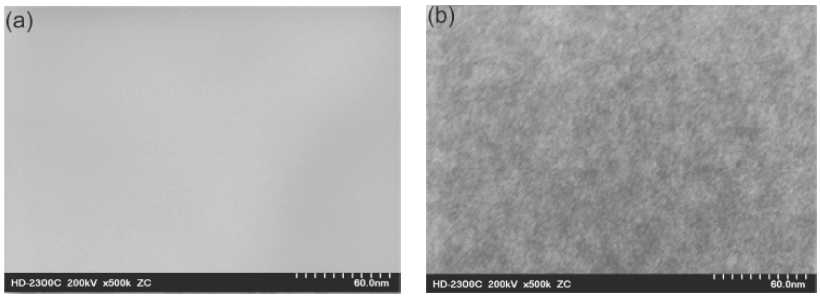

Figure 1.24 STEM images of (a) random copolymer and (b) multiblock copolymer

1.3.3 Block Copolymers

The phase separation behavior of block copolymers with two chemically incompatible blocks has been investigated,[25, 101, 102] and the major morphologies are shown in Figure 1.25.[103] The lamellar (a), gyroidal (b), and cylindrical (c) morphologies arouse the most interests in the anion exchange membrane design due to their continuous structures that can provide continuous ionic conduction pathways. The phase separated block copolymer can lead to a tunable morphology and domain by controlling the relative composition of the two blocks. Controlled block copolymers can be synthesized by a variety of polymerization techniques including living ionic polymerizations and controlled radical polymerizations. As a result, research has been recently directed toward the design of anion exchange membranes with controlled phase separated morphology that could potentially lead to favorable ionic transport and high conductivity.

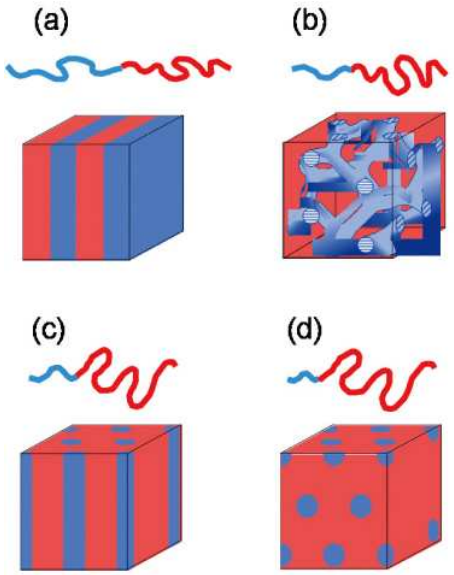

Figure 1.25 Morphology illustration of block copolymer

Controlled phase separation behavior was achieved in anion exchange membranes based on imidazolium functionalized polystyrene-b-polyvinylbenzyl chloride (PS-b-PVBC) synthesized by nitroxide mediated polymerization.[104] Well-defined morphologies of anion exchange membrane were obtained by annealing at high temperature after film formation. Small angel X-ray scattering (SAXS) and transmission electron microscopy confirmed the formation of hexagonal cylinder and cylinder + lamella coexisting morphologies in membranes prepared by solvent casting and melt casting (Figure 1.26). The conductivity comparison was performed between cylindrical sample, lamellar sample, and the corresponding homopolymer (polyvinylbenzylhexyl-imidazolium bis(trifluoromethane-sulfonyl)imide) samples. The conductivity of membranes with lamellar morphology displayed approximately 10-fold higher values than a cylindrical sample and 5 times lower than corresponding homopolymer.

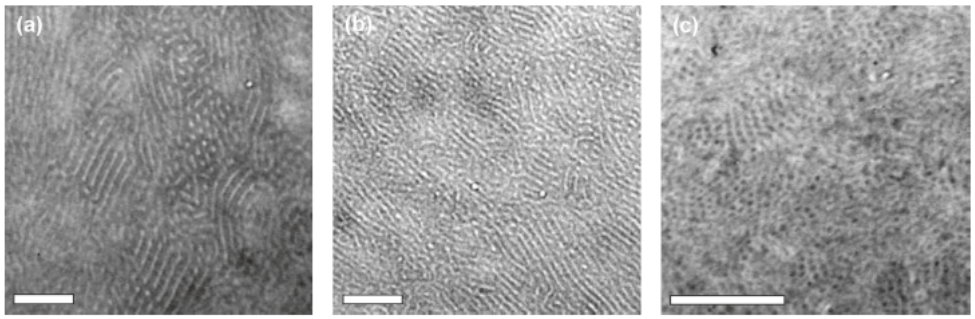

Figure 1.26 TEM images of (a) cylinders + lamellae phase coexistence by solvent casting; (b) cylinders + lamellae phase coexistence by melt casting; and (c) hexagonally packed cylindrical phase by melt casting

A similar polymer system, polystyrene-b-poly(vinylbenzyltrimethylammonium hydroxide) (PS-b-P[VBTMA][OH]) block copolymers, was prepared by atom transfer radical polymerization (ATRP) using benzyltrimethylammonium functionalized monomer in the Coughlin research group.[105] The controlled phase separation was also observed in this set of

polymers, and the spherical, cylindrical, and lamellar morphologies were confirmed by SAXS in Figure 1.27. The conductivity of materials showed strong dependence on IEC, temperature and relative humidity, similar to the dependence observed in random copolymer based anion exchange membranes.

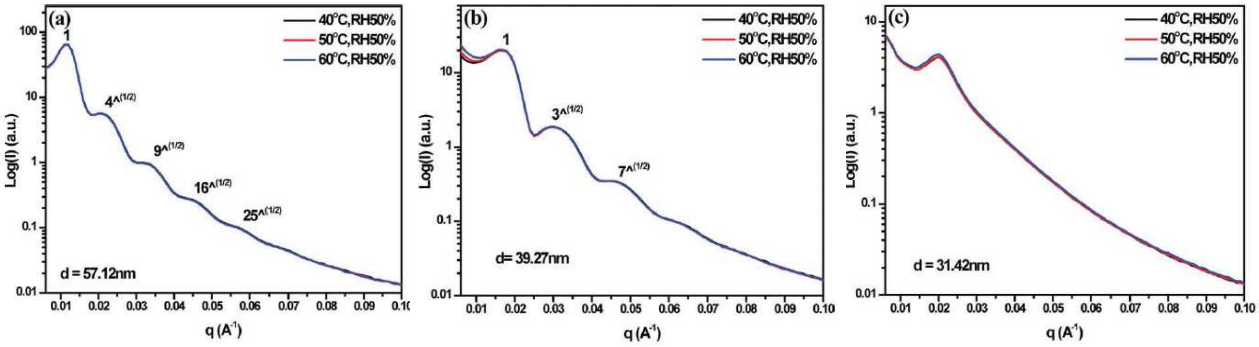

Figure 1.27 SAXS profiles of PS-b-P[VBTMA][OH] block copolymers

The Winey and Elabd research groups investigated the effect of block copolymer and its corresponding random copolymer on ion conducting properties. Block copolymer consisting of methyl methacrylate as membrane formation block and 1-(2-methacryloyloxy)ethyl-3-butylimidazolium hydroxide as ion conduction block were synthesized (Figure 1.28).[106] The block copolymer precursor was synthesized by reversible addition-fragmentation chain transfer (RAFT) polymerization using imidazolium functionalized monomer.[107] Although the ester groups in the polymer could potentially degrade under alkaline conditions, this study investigated the membrane properties between block copolymer and random copolymer with the same IEC. The block copolymer displayed ordered morphology while random copolymers were featureless in the SAXS profile indicating no ordered phase separation. The volume fraction of ionic block was tuned by varying the humidity, which leads to changes in morphology. The hydroxide conductivity (25 mS/cm at 80 °C and 90% humidity) of block copolymer exhibited

one order of magnitude higher value than the random copolymer with the same IEC, which further implies the importance of controlled phase separation on membrane ion transport property.

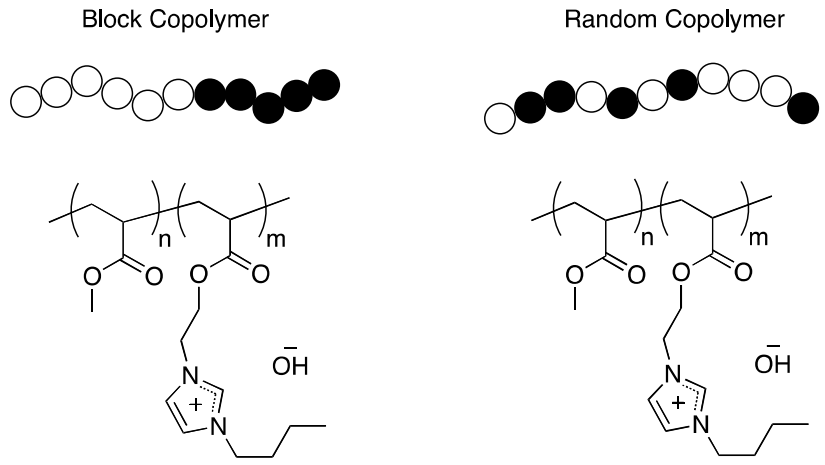

Figure 1.28 Imidazolium functionalized block copolymer and random copolymer

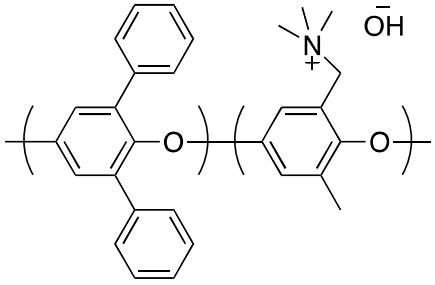

Figure 1.29 Quaternary ammonium functionalized PPO

Another interesting block copolymer was synthesized based on PPO copolymers. 2,6-dimethylphenol and 2,6-diphenylphenol monomers were polymerized to form PPO random and block copolymer (Figure 1.29).[108] The block copolymers were functionalized by bromination and followed by trimethylamine quaternization. Benzyl methyl groups were functionalized to various extents as bromomethyl groups. Although an ordered phase separation behavior was not

examined in this study, the block copolymer membrane produced much higher conductivity than the random sample. The block copolymer membrane with an IEC of 1.27 meq/g reached highest hydroxide conductivity of 84 mS/cm at 80 °C and 95% relative humidity.

1.3.4 Anionic Polymerization for Block Copolymers

Living anionic polymerization of vinyl monomers is very useful for the formation of block copolymers and functionalized polymers. Through the use of living anionic polymerization, polymers can be synthesized with controlled molecular weight, composition, and functional groups.[109, 110] The use of living polymerizations provides for the design of polymers for specific properties and applications.

Considerable interest in anionic polymerization of vinyl monomers has continued since the 1950's when Michael Szwarc first demonstrated the benefits of a living polymerization. In a living anionic polymerization, the reactive site persists throughout the reaction so that no termination or chain transfer occurs on the timescale of the reaction. Because there is no termination, monomers can be polymerized sequentially to yield well-defined block copolymers. In addition, the reactive sites can be readily terminated with an electrophile to form functionalized polymers. Additional living or controlled polymerization techniques have since been developed, but the control afforded by the anionic polymerization of vinyl monomers offers significant advantages over the other polymerization methods. One advantage is that only anionic polymerization can control the microstructure of diene (e.g. isoprene, butadiene) polymerizations. High 1,4-structured polydiene can be obtained by applying anionic polymerization toward diene monomers in non-polar solvents, and it is well known that only the

1,4-structured polydienes leads to an elastomeric property. The 1,4-structured polydiene can be further hydrogenated to produce semi-crystalline polyethylene material.

Although the exquisite control over block copolymer synthesis offered by living anionic polymerization is well understood, the block copolymer as fuel cell membrane prepared by living anionic polymerization has not been investigated to the best of our knowledge. Therefore, living anionic polymerization is designed in this thesis to provide a unique technique for the preparation of anion exchange membranes with controlled chemical structures and phase separated morphologies.

1.4 Conclusion

Fuel cells are provide a potentially sustainable and energy efficient technology for future clean energy solution. Alkaline fuel cells have gained renewed interest since its alkaline operating environment and resulting kinetics offer various advantages over proton exchange membrane fuel cell, including the ability of running alkaline fuel cells with non-precious metal catalyst and low operation temperature. Although the drawbacks in traditional liquid electrolyte alkaline fuel cells can be overcome by replacing the liquid electrolyte with anion exchange membrane, the polymer electrolyte must meet several distinct requirements for fuel cell application.

A variety of chemistries have been investigated toward improving membranes toward high ionic conductivity and low water uptake or swelling while maintaining good mechanical and alkaline stability. Some of the polymers produced exhibit promising membrane performances that could benefit further anion exchange membrane research. It is found that

phase separation plays an important role in optimizing the anion exchange membrane performance. The microphase structure control displays a tremendous influence on membrane properties, resulting in a good balance between conductivity and mechanical stability. Anionic polymerization offers exquisite control over block copolymer synthesis and diene microstructures, which could benefit the membrane properties. As a result, future research directed toward making anion exchange membrane with controlled phase separated morphology should be done. The understanding of anion exchange membrane properties and performance related to polymer structure is still demanded and more research toward membrane and cation improvements is needed.

1.5 Thesis Statement

The goal of this thesis is to develop different polymer systems (blend, block, graft, and crosslinked polymers) in order to understand alkaline fuel cell membranes in many aspects and to design optimized anion exchange membranes with better alkaline stability, mechanical integrity and ion conductivity.

Although basic knowledge on the factors that affect the anion exchange membrane (AEM) performance have been determined, the further understanding of AEM design is highly demanded and can be significantly improved through answering the following scientific questions in this thesis.

Question 1: Can the formation of miscible blends improve mechanical properties while maintaining high ionic conductivity through formation of phase separated ionic domains?

Vinylbenzyl chloride is a commercially available styrene based monomer and can be readily block copolymerized[111] and functionalized. Poly(vinylbenzyl chloride)-b-polystyrene (PVBC-b-PS) copolymers have shown the ability to prepare anion exchange membranes in previous studies, however its anticipated brittleness limits its potential application. In order to achieve desired mechanical properties, poly(phenylene oxide) (PPO) is used to blend with styrene based block copolymers as AEMs in Chapter 2. Although it is well known that PPO is compatible with PS in a wide range of compositions[112-118], the miscibility of PVBC-b-PS copolymer and PVBC-b-PS/PPO blend were investigated in this study. The PPO blended AEMs were prepared with different blend compositions and the mechanical properties of blend membranes were investigated. The water uptake and conductivity were studied and correlated to the ion exchange capacity. Annealing methods were applied on blend membranes to develop greater phase separation, and the membrane morphology and properties (water uptake and conductivity) after annealing were compared with sample before annealing.

In order to further expand the understanding developed in PPO blend membranes, brominated PPO (BrPPO) is also designed to blend with the PVBC-b-PS in Chapter 3 to study the additional functional group effect on blend AEMs. The compatibility study of BrPPO and PVBC-b-PS was also performed. The quaternized membrane properties were studied through the water uptake and ionic conductivity, which were compared with PPO blended AEMs to further study the effect of quaternized PPO group in BrPPO blend membranes.

Question 2: Can a polyethylene based block copolymer form well defined structures to enhance the ionic conducting property while providing good mechanical properties and alkaline stability?

In order to have controlled phase separation in anion exchange membranes, anionic polymerization is used to offer exquisite control over the synthesis of a block copolymer. In Chapter 4, polybutadiene-b-poly(4-methylstyrene) (PB-b-P4MS) is synthesized by anionic polymerization as precursors for AEMs. PB block is selected for the copolymer because it can be readily hydrogenated to form a polyethylene (PE) block to form a membrane matrix. PE derived from the hydrogenation of high 1,4-PB is a semi crystalline polymer providing dimensional and alkaline stable membrane. The P4MS block can be post modified to form quaternary ammonium cations by bromination and quaternization reactions. The final quaternary ammonium functionalized membranes with four block compositions are prepared in order to study the morphology effects by varying the block composition. The morphology of PE-b-P[VBTMA][Br] is examined by small angle x-ray scattering (SAXS) spectroscopy. The scanning transmission electron microscopy (STEM) was combined with SAXS to study the morphology of this PE block copolymer AEM. The water uptake of PE based AEMs was studied with their ion exchange capacity and correlated to ionic conductivity and activation energy. Tensile testing was performed on PE based AEMs to study their mechanical properties.

Question 3: Can the incorporation of hydrophilic polymer increase the hydration number of AEM to improve ionic conductivity while reducing the dependence of conductivity on relative humidity?

Most anion exchange membranes developed currently exhibit great loss of conductivity at low humidity conditions, limiting their application. Membrane performance at low humidity needs to be improved and an understanding of water and ionic conductivity is needed. By comparing proton exchange membranes and anion exchange membranes in hydration number,

anion exchange membranes usually possess a lower hydration number and also show relatively higher dependence of conductivity on humidity. In order to study the hydration number effect on ion conductivity of AEMs, a graft AEM system is designed in Chapter 5 to increase hydration numbers independently of ion exchange capacity. Mono methoxy polyethylene glycol (mPEG) is a hydrophilic polymer absorbing enough water to increase hydration number in AEM. The mPEG has a single hydroxyl group on one polymer chain end and can be readily grafted to the benzyl chloride groups in PVBC-b-PS.[119] The remaining benzyl chloride groups can be converted to quaternary ammonium groups. Hydroxide and chloride conductivity are found to increase with an increase in mPEG grafting extent. The chloride conductivities of mPEG grafted membranes were tested at different humidity levels to study the dependence of conductivity on humidity, and the hydroxide conductivity was also studied.

Question 4: Can the formation of quaternary ammonium crosslinks be quantitatively achieved while maintaining high ionic conductivity and mechanical properties?

Quaternary ammonium crosslinks in anion exchange membrane has been proved to have an efficient effect on reducing swelling. In Chapter 6, quaternary ammonium crosslinked membrane was prepared by dimethylamine crosslinking reaction through PVBC-b-PS block copolymer for potential AEM application. The membranes were crosslinked to different extents and aminated to produce pendent benzyltrimethyl ammonium cationic groups. The amount of quaternary ammonium crosslinking groups and pendent benzyltrimethyl ammonium cations were quantified through infrared spectroscopy and ion exchange capacity measurements. Hydroxide and chloride conductivities of the copolymer membranes were measured by electrochemical

impedance spectroscopy, and the thermal stability of crosslinked AEM was also studied. Conductivity and thermal stability of crosslinked AEMs were compared to the non-crosslinked analogue. It is important to mention that the crosslinking structure also can act as ion conducting group during the fuel cell operation.

CHAPTER 2 POLY(2,6-DIMETHYL-1,4-PHENYLENE OXIDE) BLENDED WITH POLY(VINYLBENZYL CHLORIDE)-B-POLYSTYRENE FOR THE FORMATION OF ANION EXCHANGE MEMBRANE

2.1 Introduction

Alkaline fuel cells (AFCs) using anion exchange membranes (AEMs) as electrolyte have recently received considerable attention.[9, 10] AFCs offer some advantages over proton exchange membrane (PEM) fuel cells, including the potential of non-noble metal (e.g. nickel, silver)[120] catalyst on the cathode, which can dramatically lower the fuel cell cost. The main drawback of traditional AFCs is the use of liquid electrolyte (e.g. aqueous KOH), which can result in the formation of carbonate precipitates by reaction with carbon dioxide. AEMs with bound cationic functional groups eliminate the precipitates formed in traditional AFCs.

The goal of useful AEMs for AFC applications is to obtain a robust membrane with high ionic conductivity and good mechanical properties that can be operated in a high pH environment. Therefore, it is important to investigate a variety of cationic functional groups and polymer backbones. The most widely studied AEMs contain quaternary ammonium functional groups,[29] which are relatively simple to effect functionalization and have demonstrated moderate alkaline stability.[27] The polymer backbone chain structure is an additional important component of AEMs. Efforts have been directed to develop various polymer backbones for AEMs containing quaternary ammonium cations, including poly(arylene ether)s,[23, 53, 54, 56] poly(phenylene),[83] polyethylene[68, 88] and polystyrene derivatives.[34, 35, 37] There is a particular interest in styrenic block copolymer structures because they can be readily synthesized

and functionalized, as well as the possibility to develop well-defined morphologies upon film formation.

Styrenic block copolymers are attractive materials for conversion into AEMs, however their anticipated brittleness and other poor mechanical properties limits their potential. One method that may lead to improved mechanical properties of styrenic block copolymers is to blend with poly(2,6-dimethyl-1,4-phenylene oxide) (PPO). PPO is an engineering plastic with high strength, chemical resistance[121] and high glass transition temperature (Tg ≈ 220°C).[122] PPO has also been widely used as a backbone polymer to prepare anion exchange membranes for fuel cell application by utilizing the pendent methyl groups for functionalization.[74, 76, 82, 108, 123] Furthermore, PPO is well known to form miscible blends with polystyrene and some polystyrene copolymers.[112-118] Recently, PPO has been blended in polystyrene-based ionic polymers to prepare PEMs where the blended membrane shows improved thermal stability and limited water uptake.[124, 125] Research has not been done on blending styrenic block copolymers with PPO as a means of improving properties of the materials for AEMs.

In the current study, we demonstrate a methodology to prepare PPO blended polystyrene based AEMs. The formation of the membrane involves the synthesis of polyvinylbenzyl chloride-b-polystyrene (PVBC-b-PS) by nitroxide mediated polymerization, followed by solvent casting of PVBC-b-PS/PPO blends from chloroform, and subsequently reacting the PVBC-b-PS/PPO blend films with trimethylamine to convert the benzyl chloride pendent groups into quaternary ammonium cations. A series of PPO blended membranes are prepared and the cationic functionality or ionic exchange capacity is tuned by varying the PPO content of the membrane. The research investigates in detail the preparation of quaternized PPO blend membranes, and the effect of PPO on the membrane properties including water uptake, ionic

conductivity, and mechanical properties. Additionally, the blend membranes are annealed by thermal and solvent vapor methods to study the effect on water uptake, ionic conductivity and morphology.

2.2 Experimental Section

2.2.1 Materials

Styrene (99%) and 4-vinylbenzyl chloride (VBC) (90%) were obtained from Aldrich, dried over calcium hydride and distilled under reduced pressure right before use. 2,2,6,6-tetramethyl-piperidine-1-oxyl (TEMPO) (Aldrich, 98%) was sublimed twice before use. Anhydrous trimethylamine gas (99%) was used as received. Benzoyl peroxide (BPO) was purified by recrystallization from chloroform/methanol. PPO homopolymer was purchased from Aldrich (M_n= 20,000 g/mol) and used as received.

2.2.2 Synthesis of PVBC-b-PS by Nitroxide Mediated Polymerization (NMP)

All glassware was dried at ~150 °C overnight before the polymerization. The purified VBC (10.0 mL), BPO (56 mg, 0.4 mmol), and TEMPO (62 mg 0.4 mmol) were added into a 50 mL round bottom flask containing a magnetic stir bar and capped with a rubber septum. After dissolution, the round bottom flask was purged with Ar for 30 min. The mixture was heated to 125°C for 3 hours to allow for polymerization. The TEMPO terminated PVBC (PVBC-TEMPO) was purified by several precipitations in methanol, and further dried in a vacuum oven before use. PVBC-TEMPO was then used as a macro-initiator to copolymerize styrene in a bulk

polymerization. PVBC-TEMPO (250 mg) was weighed into a 50 mL round bottom flask, and an excess of styrene (10 mL) was injected into the flask. After PVBC-TEMPO was dissolved in styrene, the round bottom flask was purged with Ar for 30 min. The bulk polymerization was carried out at 125 °C for 1 hr. The copolymer was isolated by precipitation in methanol, and was purified by re-precipitating after re-dissolving in chloroform. The copolymer was then dried under vacuum at room temperature.

2.2.3 PPO Blended AEM Preparation

PPO and PVBC-b-PS materials were dried in a vacuum oven before blending and then dissolved together in chloroform under sonication with a range of different mass ratios (PVBC-b-PS : PPO = 40:60, 50:50, 60:40, 70:30, 80:20). All blend concentrations were prepared at 5g/100mL. Polymer blend solutions were drop cast on glass slides by pipet and the solvent was allowed to evaporate slowly at room temperature. The glass slide was immersed in deionized water to remove the polymer film. All films (PVBC-b-PS/PPO) obtained were transparent. PVBC-b-PS/PPO films were then rinsed with methanol and soaked in round bottom flasks filled with methanol. A 500% excess of anhydrous trimethylamine gas was introduced to the round bottom flask and allowed to react over 48 hours at room temperature to convert PVBC-b-PS/PPO films into poly(vinylbenzyltrimethylammonium chloride)-b-polystyrene/PPO (P[VBTMA][Cl]-b-PS/PPO). The PPO blend membranes containing quaternary ammonium cations were soaked repeatedly with methanol and then deionized water. All quaternized membranes were dried in a vacuum oven at 60°C overnight.

2.2.4 Membrane Annealing

Annealing was attempted by the following methods: (1) membranes were suspended in boiling deionized water for 12 hours; (2) membranes were annealed at 125°C -140°C under dry conditions for 12 hours; (3) membranes were annealed at 125°C -140°C with deionized water for 12 hours in a sealed pressure vessel; and (4) membranes were annealed in a sealed pressure vessel at 70 °C over a 50/50 THF/water solution for 12 hours. Quaternized blend membranes were dried in a vacuum oven after annealing.

2.2.5 Ion Exchange to Hydroxide

The P[VBTMA][Cl]-b-PS/PPO membranes were soaked in 1M KOH solution for 48hr to exchange chloride to hydroxide and were subsequently rinsed repeatedly with degassed deionized water to remove residual salts.

2.2.6 Characterization

Molecular weights of PVBC-TEMPO and PVBC-b-PS were determined by gel permeation chromatography (GPC) using a Waters HPLC pump equipped with a Wyatt Technology Optilab RI detector and a Wyatt Technology miniDAWN multiangle laser light scattering (MALLS) detector. Elutions were carried out with two polymer laboratories Mixed-D columns at room temperature with THF at a flow rate of 1.0 mL/min, and the molecular weights were measured by calibration of a series of polystyrene standards and also using software (Astra) supplied by Wyatt Technology. ^{1}H NMR spectra of PVBC-b-PS were obtained using a JEOL

500 MHz spectrometer. All polymer samples were dissolved in $CDCl_3$ with respect to tetramethylsilane (TMS). IR measurements were performed on a Thermo FT-IR spectrometer in a spectral range of 500 – 4000 cm^{-1}. Glass transition temperatures (T_g) of blend membranes were performed by differential scanning calorimetry (DSC) on TA DSC-20 running TA software with three repeated heating loops and a heating rate of 10 °C/min under a nitrogen purge. Thermal stability was determined by thermogravimetric analysis (TGA) on a Seiko TGA/DTA320 at a heating rate of 10 °C/ min under a nitrogen atmosphere.

Theoretical ionic exchange capacities (IECs) were calculated based on 100% conversion of benzyl chloride to quaternary ammonium. IECs of blend membranes were also measured in hydroxide form by using an established literature titration method[31]. Before the measurements, about 0.02 g of vacuum dried blend membranes in hydroxide form were immersed in 10.00 mL of 0.00987 M standardized HCl solution for 48 hr, the actual IEC was calculated by titration of unreacted HCl with 0.01053 M standardized NaOH solution. The titrations were repeated 3 times for each blend membrane. The IEC (mmol/g) was obtained by

$$IEC\ (mmol/g) = \frac{M_{ohr,HCl} - M_{48hr,Hcl}}{m_{dry\ membrane}} \qquad (1)$$

where $M_{0h,\ HCl}$ is millimoles (mmol) of HCl determined before blend membranes neutralization, $M_{48h,\ HCl}$ is mmol determined after neutralization of membranes (after 48 hr), and $m_{dry\ membrane}$ is the dry mass (g) of membrane in hydroxide form.

In order to determine water uptake[126] of AEMs, membranes were pre-soaked in deionized water. After 24 hours of soaking, the fully hydrated membranes were removed from the water and any residual bulk water on the membrane surface was blotted dry with Kimwipes™ , and the sample was weighed immediately. The membranes were immersed again

into deionized water for another 15min to let them re-hydrate. This method was repeated 5 times to obtain the average mass of hydrated membranes ($m_{hydrated}$). The membranes were subsequently vacuum dried at 60 °C for 24 hr to obtain a dry mass (m_{dry}). The water uptake (WU) was determined by

$$WU\ (\%) = \frac{m_{hydrated} - m_{dry}}{m_{dry}} \times 100\% \qquad (2)$$

Synchrotron small angle x-ray scattering (SAXS) experiments were performed at the Advanced Photon Source at Argonne National Laboratory. A beam energy of 12keV with x-ray wavelength at 1 Å was employed to measure samples in transmission mode. The transmission intensity was normalized to exposure time and flux of the direct beam through the sample. The films were held in place using Kapton tape to the sample holder and placed in a custom built four-sample oven that controlled the humidity and temperature of the samples during scattering experiments.[127, 128] The humidity of the sample environment was controlled using a combination of wet and dry nitrogen with a humidity probe positioned in the sample oven to provide real time humidity readout. Based on the humidity measurement, gas flows were adjusted to achieve the desired temperature and humidity condition. The 2D scattering patterns were radially integrated to obtain intensity versus scattering vector (q) plots.

The in-plane ionic conductivities of blend membranes were measured by four probe electrochemical impedance spectroscopy (EIS) using a BioLogic VMP3 potentiostat over a frequency of 0.1 – 10^6 Hz. The conductivity can be calculated from the membrane resistance

$$\sigma = \frac{l}{R \cdot A} \qquad (3)$$

where R is the membrane resistance, l is the distance between the electrodes, A is the cross-

sectional area of the sample. The hydroxide and chloride conductivities were measured in water at room temperature and 60 °C.

High Angle Annular Dark Field Scanning Transmission Electron Microscopy (HAADF STEM) was performed at US Army Research Laboratory. The HAADF STEM samples with a thickness of approximately 90 nm were prepared by microtome. The detailed sample preparation was described as follows: membrane samples were microtomed on a Leica Ultra cut UCT with a EMFCS cryostage using a microstar diamond knife with a 6° cutting angle at -10 °C. The microtomed samples were transferred from the cryostage to a dessicator in capsules to minimize interaction with water vapor. The samples were tested using a JEOL 2100F operated at 200kV and HAADF 5 camera length.

Tensile properties of blended membranes were measured at dry and hydrated conditions on an Instru-Met frame tensile tester (by MTS Model: A30-33) using a 1000-pound load cell (with a resolution less than 0.1 pound) and a crosshead speed of 5 mm/min at room temperature. The dry samples were prepared by drying membranes in a vacuum oven at 60 °C for 24 hours, and the hydrated samples were prepared by soaking membranes in deionized water at room temperature for 24 hours. Blend membranes were cut into strips of approximately 60 mm x 8 mm and membrane thicknesses were measured in a range of 50 to 80 microns. Stress was calculated from the cross sectional area of the film and the strain is obtained by the percentage increase of film gauge length. The Young's modulus was determined by the initial slope of the stress vs. strain curve at very low strains (0.2 – 0.3%). Five replicates were performed on each sample to obtain the average values of stress, strain and Young's modulus.

2.3 Results and Discussion

Recently, block copolymers that form well-defined morphology have attracted considerable attention in polymer electrolyte design, and styrenic block copolymers have aroused interest for study in AEMs.[104, 105] PS is believed to be stable under alkaline fuel cell conditions,[129] the poor flexibility of PS somewhat limits its use as a membrane material for fuel cell applications. PPO is a commercially available polymer and the miscibility of PPO/PS blends has been well recognized for decades.[130] PPO is an engineering polymer with high mechanical strength and a significant amount of research on PPO blends has been done to improve the mechanical properties of styrenic copolymers for different applications. Here, a PPO blended AEM preparation method is designed where a PVBC-b-PS block copolymer is first synthesized and subsequently blended with PPO and solvent cast to prepare blend films. The quaternization of benzyl chloride groups is accomplished through the reaction with trimethylamine and all the preparation steps are depicted in Scheme 2.1.

Scheme 2.1 Strategy of PPO blended AEM preparation

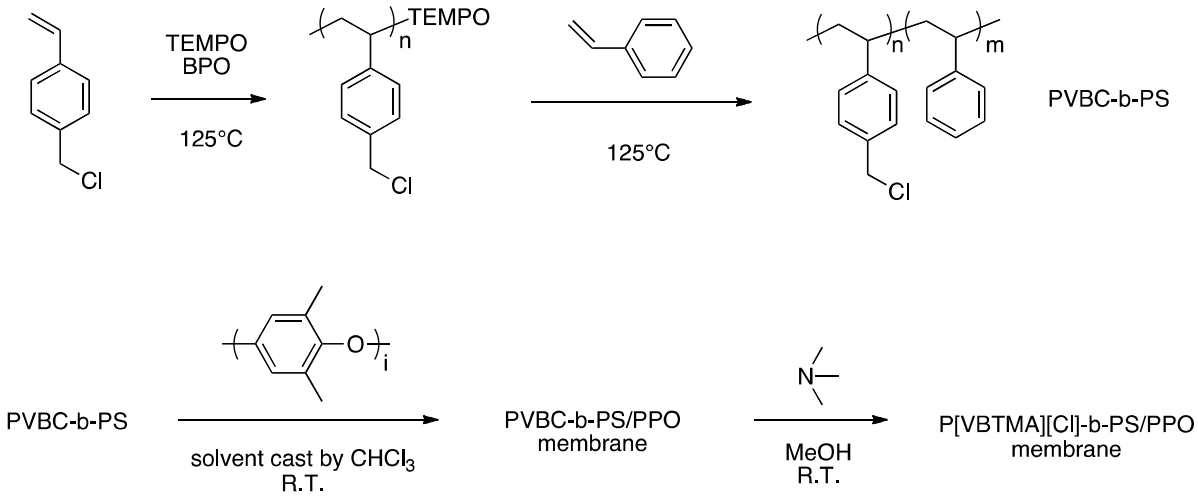

Numerous methods can be used to synthesize polystyrene-based block copolymers with controlled molecular weight, composition and functional groups, including living radical polymerization techniques (RAFT, ATRP and NMP). Block copolymers can be sequentially synthesized, to provide phase-separated materials with controlled morphologies. NMP was selected to synthesize the diblock, since this technique allows the polymerization of VBC, furthermore, it offers the control over molecular weight of PVBC-b-PS and composition of each block.[111] The polymerization of VBC was carried out using BPO as radical initiator in the presence of TEMPO[131, 132] and then the resulting PVBC-TEMPO was used as macrointiator to polymerize a styrene block. The PVBC with a TEMPO functional chain end (PVBC-TEMPO) was analyzed by GPC to determine a M_n = 30,500 g/mol and M_w/M_n = 1.90. Several precipitations were conducted on PVBC-TEMPO in order to remove any remaining VBC monomer. The nitroxide mediated copolymerization of styrene was initiated by the purified PVBC-TEMPO macroinitiator at 125 °C in bulk. The conversion of styrene reached ~10% after 30 minutes of reaction. The results of GPC analysis of PVBC-TEMPO and PVBC-b-PS diblock copolymer are depicted in Figure 2.1.

The molecular weight of PVBC-b-PS was determined by GPC to find M_n = 85,700 g/mol and M_w/M_n = 1.86. The GPC chromatogram of PVBC-TEMPO shows a small amount of tailing to low molecular weights, resulting in the broad peak feature. The broad molecular weight distribution may be attributed to the high reactivity of VBC monomer and uncontrolled initiation by using TEMPO as an additive rather than preforming a nitroxide initaitor.[133, 134] After the block copolymerization from the PVBC macroinitiator, the GPC chromatogram of PVBC-b-PS shows a significant shift to lower elution volume from the initial PVBC-TEMPO peak, as well as an increase in molecular weight as determined by light scattering detection compared to the

initial PVBC-TEMPO block. The peak shift indicates an efficient initiation from the PVBC-TEMPO macroinitiator to form the diblock copolymer.

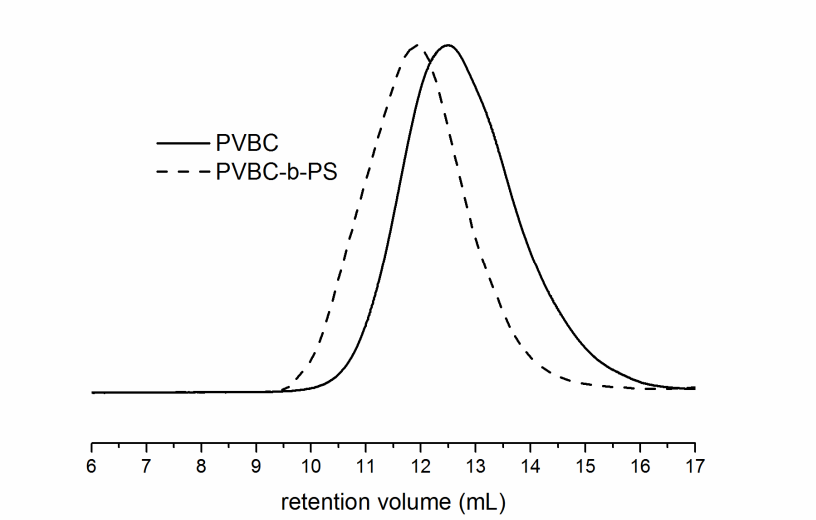

Figure 2.1 The GPC curves of TEMPO functionalized PB and PB-b-PS diblock copolymer.

Figure 2.2 depicts the ^{1}H NMR spectrum of the PVBC-b-PS with 0.5 hr polymerization of styrene. The PVBC-b-PS copolymer was re-precipitated in methanol several times to remove residual styrene monomer before ^{1}H NMR spectroscopy analysis. The spectrum exhibits both PVBC and PS characteristic peaks and the composition can be determined by the peak ratios. The amount of PVBC in the diblock can be calculated from integration of the benzyl peaks at 4.2 – 4.8 ppm. The determination of the amount of PS in diblock is complicated, as the aromatic peaks of both the PVBC and PS overlap. However, by subtracting the molar amount of PVBC aromatic peaks determined from the benzyl peaks, the amount of PS can be determined. The composition of PVBC and PS can be calculated by comparing the molar amount of PVBC and PS. The mass ratio of PVBC:PS is calculated to be 32:68 , in good agreement with the mass ratio determined by GPC.

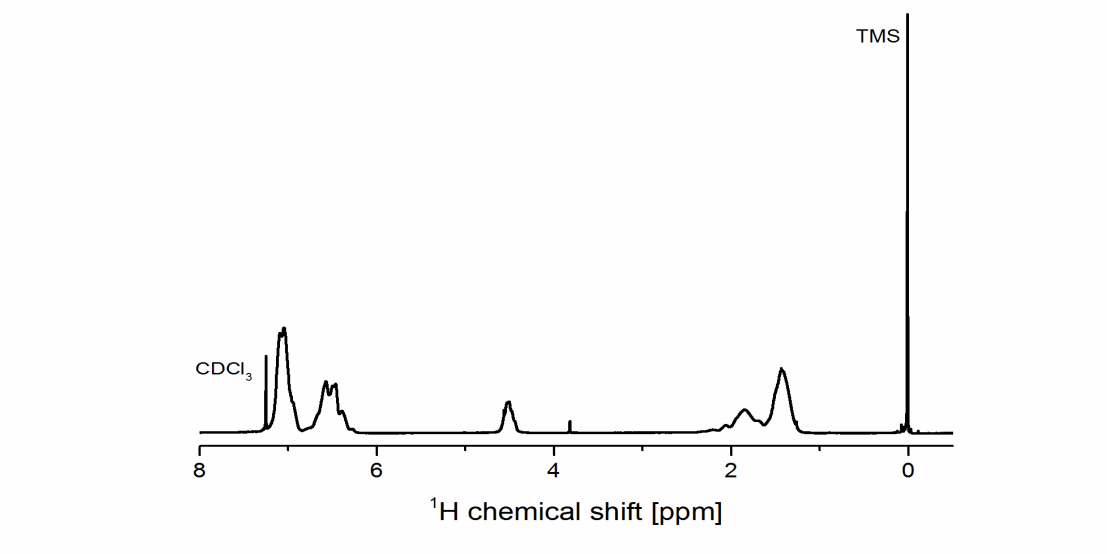

Figure 2.2 The ^{1}H NMR spectrum of PVBC-b-PS by bulk copolymerization.

PPO and PS are well known to be miscible at all compositions and the miscibility of a large number of polystyrene derivatives and polystyrene copolymers with PPO have been studied to find compatibility over a composition range.[135-139] The miscibility of PVBC with PPO and PVBC-b-PS with PPO, however, has not been reported. Because our objective is to form blends of copolymer with PPO, it was important to study the miscibility of these three different components in a blend.

The first thing to investigate was the miscibility of the PVBC-b-PS copolymer. The glass transition temperatures of PVBC and PS homopolymers with similar molecular weights as in the copolymer were measured by DSC to be 121 °C and 97 °C, respectively. The glass transition temperatures of PVBC and PS homopolymers are displayed in Figure 2.3 and clearly depict the two distinct transitions. The DSC curve for PVBC-b-PS copolymer displays only one glass transition at 107 °C, indicating the compatibility of PVBC and PS. A PVBC/PS blend of the two

homopolymers was prepared at the same composition as the PVBC-b-PS copolymer in order to further investigate the miscibility of PVBC and PS at this particular composition. The homopolymer blend also shows only a single glass transition in the DSC trace with similar temperature value suggesting PVBC and PS at this composition are miscible.

The miscibility of PPO and the PVBC-b-PS was also investigated. The glass transition temperature of PPO was measured to be 223 °C. The PPO homopolymer was then blended with the PVBC-b-PS copolymer in a range of compositions for the miscibility study. DSC was used to examine each PVBC-b-PS/PPO blend and only one glass transition temperature is observed in each of the blends. The glass transition temperature increases with the increase in PPO composition of blend films as expected. Figure 3 shows one example of PPO blend films with 50 wt% of PPO and the glass transition temperature of this particular blend membrane is at 153 °C.

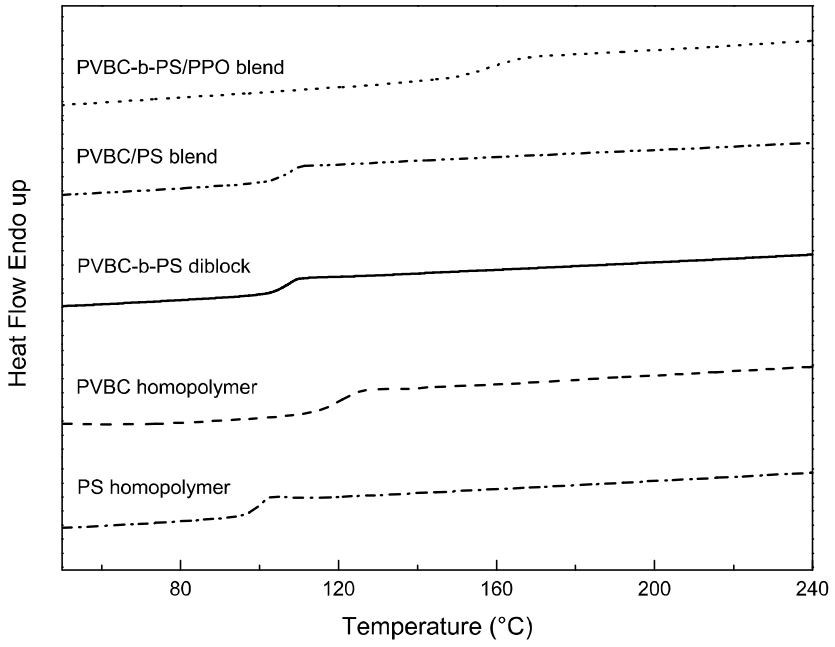

Figure 2.3 DSC traces of PVBC homopolymer, PS homopolymer, PVBC-b-PS diblock, PVBC/PS (30/70) blend and PVBC-b-PS/PPO (50/50) blend membranes.

The glass transition temperatures of PVBC-b-PS/PPO blends are plotted as a function of PPO loading contents (wt%) and the trend can be observed in Figure 2.4. Since one can predict the T_g of miscible blend by the Fox equation,

$$\frac{1}{T_g} = \sum_{i=1}^{n} \frac{w_i}{T_{g,i}} \qquad (4)$$

where w_i is the weight fraction of one blend component and $T_{g,i}$ is the glass transition temperature of that component in the blend. The theoretical T_g of PPO blend predicted by the Fox equation show a close match with the measured values also indicating the PPO is compatible with PVBC-b-PS in the concentration range investigated.

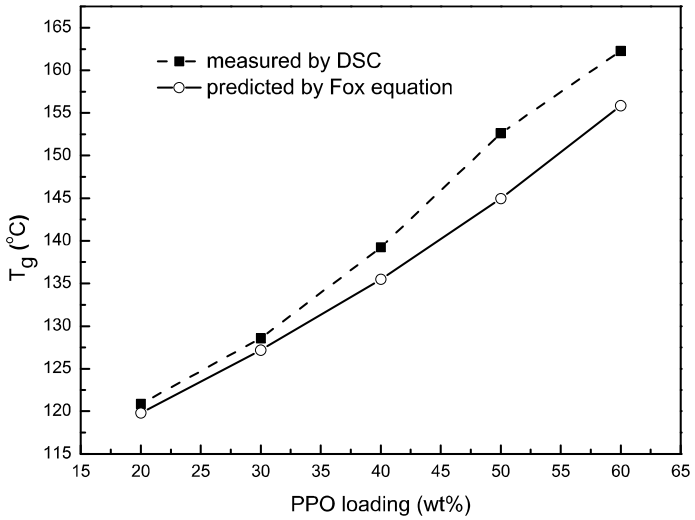

Figure 2.4 Measured T_g values (dashed) of PPO/PS-b-PVBC and theoretical values (solid) versus PPO loading (using T_g of 107 °C for block copolymer).

PPO was blended with PVBC-b-PS copolymer to prepare blend films (PVBC-b-PS/PPO) by solvent casting. The PVBC-b-PS copolymer and PPO homopolymer (M_n = 20,000 g/mol) were dried in a vacuum oven overnight, and then weighed into 20 mL vials with the range of blend compositions in Table 2.1. Polymer blends were prepared with concentration of 5g/100mL

in chloroform and sonication was applied to dissolve the polymers. The solutions were drop cast onto glass slides, the solvent evaporated, and the transparent films were separated from the glass slides by soaking in water.

Table 2.1 PVBC-b-PS/PPO blends composition, theoretical IEC and titrated IEC

AEM	PVBC-b-PS (wt%)	PPO (wt%)	Theoretical IEC[a] (mmol/g)	Titrated IEC[b] (mmol/g)
A	40	60	0.82	0.75
B	50	50	1.01	0.87
C	60	40	1.20	1.02
D	70	30	1.39	1.17
E	80	20	1.57	1.34

a) estimated by ^{1}H NMR spectrum and blend ratio;
b) determined by back titration of blended membranes after OH^- counter-ion exchange

The drop cast PVBC-b-PS/PPO films were converted to quaternary ammonium functionalized membranes. The films were immersed in methanol and the benzyl chloride groups converted to quaternary ammonium groups through reaction with trimethylamine. A large excess of trimethylamine gas was introduced to the reaction vessel in order to reach a high reaction conversion. The blend membranes were allowed to react for 48 hours and became less transparent over time, indicating reaction between the membrane and trimethyamine. The resulting membrane was washed with water and vacuum dried at 40 °C overnight.

The membranes were characterized by FT-IR spectroscopy and the spectra confirmed the formation of quaternary ammonium cation in the membrane. Figure 2.5b depicts the IR spectrum of PVBC-b-PS/PPO, showing clear chloromethyl (-CH_2-Cl) functional group absorption peaks at 571 cm^{-1} and 1224 cm^{-1}. After the quaternization reaction, the absorption peak at 571 cm^{-1} and 1224 cm^{-1} have almost completely disappeared, indicating reaction of the chloromethyl (-CH_2-

Cl) functional group. The strong peak at 3365 cm^{-1} in Figure 2.5a represents the water peak associated with the formation of the hygroscopic quaternary ammonium groups.

The ion exchange capacities (IECs) of the blend membranes were measured by hydroxide back titration[31] and are presented in Table 2.1. The hydroxide ion exchange was done in 1 M degassed KOH solution for 48 hr, the excess hydroxide was removed by washing with DI water. The completion of quaternization reaction can be estimated by comparing the actual IEC with the theoretical IEC, which can be easily calculated by assuming the complete conversion of benzyl chloride groups into quaternary ammonium functional groups. The conversion to quaternary ammonium reached 84% to 91% for the different membranes.

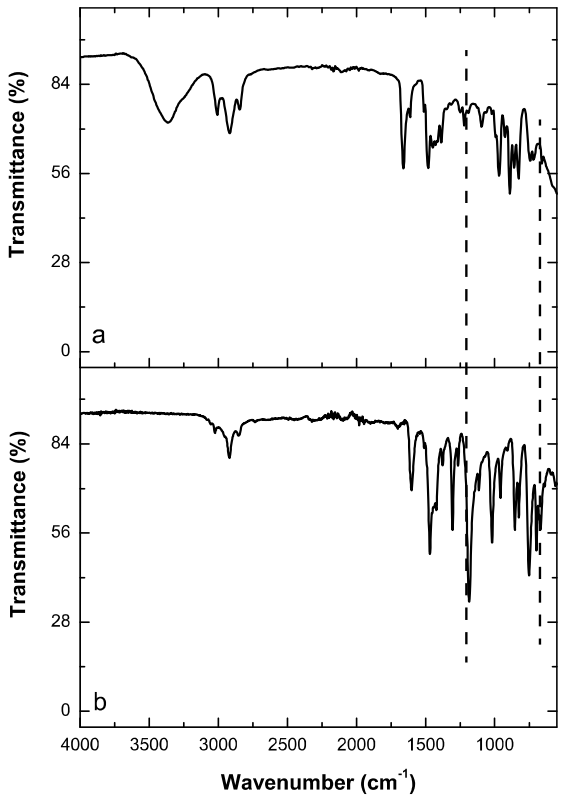

Figure 2.5 The FT-IR spectrum of PVBC-b-PS/PPO before quaternization (a) and P[VBTMA][Cl]-b-PS/PPO after quaternization (b)

After quaternization, the three-component miscible blend is expected to become incompatible, as the benzyl chloride groups of the PVBC block are converted to benzyl trimethylammonium cationic groups to form a poly[vinylbenzyltrimethylammonium] [chloride] (P[VBTMA][Cl]) block. The new functionalized material should now comprise a miscible blend between the PPO and the PS block with the now hydrophilic cationic P[VBTMA][Cl] immiscible with the blend. However, the phase separation between the hydrophilic and hydrophobic components is restricted because the high glass transition temperature of the PS/PPO blend does not allow reorganization of the structure at low temperatures. It is expected that an organized, phase separated morphology could have a positive effect on anion exchange membrane conductivity,[25, 56] therefore experiments were designed to anneal the PPO blend membranes under different conditions and then to examine their conductivity and water uptake, and attempt to relate the properties to a resulting phase morphology.

In order to maximize the phase separation of hydrophilic and hydrophobic components in the blend membranes, thermal and solvent vapor annealing methods were selected under both dry and humidified conditions. PS/PPO is a well-studied blend system and the blend glass transition temperature can be predicted by the Fox equation (Table 2.2). The thermal annealing temperatures for P[VBTMA][Cl]-b-PS/PPO membranes are required to be lower than the degradation temperature, while approaching the glass transition temperature of PS/PPO if possible. Annealing in the presence of water was expected to increase the volume of the hydrophilic component. Since the thermal stability of P[VBTMA][Cl]-b-PS/PPO is important to determine the annealing temperature, the thermal stability of P[VBTMA][Cl]-b-PS/PPO was first examined by TGA. The derivative curve of the thermogravimetric trace (DTG) (Figure 2.6) shows three main degradation regions. The beginning of the first decomposition region starts at

143 °C, presumably corresponding to the degradation of the benzyltrimethylammonium chloride group and indicates the upper limit for thermal annealing temperatures of the P[VBTMA][Cl]-b-PS/PPO membranes. Because the P[VBTMA][Cl]-b-PS/PPO membrane starts to degrade at 143 °C, thermal annealing temperatures were chosen to be lower than the degradation temperature. Solvent and water vapor annealing conditions were also examined as a way to avoid the higher temperatures where thermal degradation occurs.

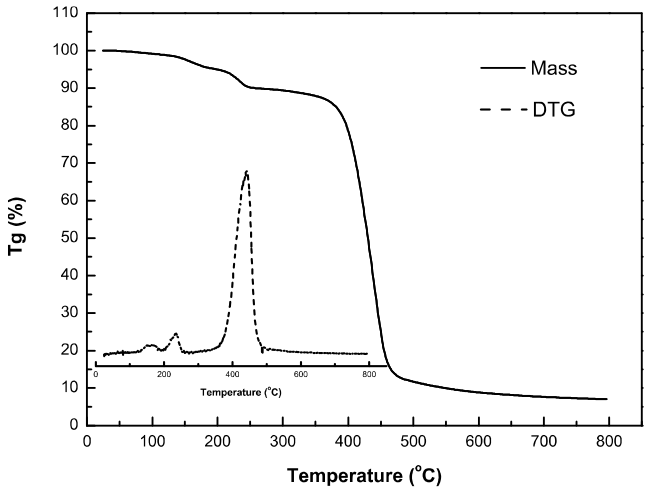

Figure 2.6 TGA and DTG (inset) curves of P[VBTMA][Cl]-b-PS/PPO.

Four separate annealing methods were investigated of the membrane films (Table 2.2): 1) annealing in boiling water; 2) at 125- 140 °C without water; 3) under pressure in the presence of water at 125 – 140 °C; 4) solvent vapor annealing over a 50/50 mixture of THF/water. The simplest method was to boil blend membranes in water, but the temperature (94 °C at altitude) of boiling water does not approach the glass transition temperature of the hydrophobic component (PS/PPO). Membranes were annealed at higher temperatures (125 – 140 °C) under pressure in the presence of water. For the samples with lower PPO composition (C, D, and E) the annealing temperature was above the T_g. For comparison, membranes were annealed at high temperatures

(125 – 140 °C) without water. Solvent vapor annealing was investigated over a THF/water mixture to plasticize the PS/PPO component while also providing a hydrated environment for the hydrophilic component.

Table 2.2 T_g of PVBC-b-PS/PPO & PPO/PS after quaternization reaction and annealing conditions[a] of P[VBTMA][Cl]-b-PS/PPO membrane

AEM	T_g[b] of PS/PPO (°C)	Boil in water[c] (°C)	Anneal with water[d] (°C)	Anneal without water[d] (°C)	Anneal with solvent vapor[e] (°C)
A	157	94	140	140	70
B	145	94	140	140	70
C	135	94	140	140	70
D	125	94	135	135	70
E	116	94	125	125	70

a) all annealing methods were conducted for 12 hours; b) T_g of PS/PPO after quaternization and calculated by Fox equation for PPO/PS system; c) calculated based on the elevation; d) determined by both predicted T_g for PPO/PS and degradation temperature from TGA; e) temperature was directly obtained from oil bath.

After thermal annealing, the IECs were re-measured for each membrane to investigate the stability of the cationic group. The titrated IECs of membrane after annealing were determined by hydroxide back titration and are compared with the values before annealing. No measurable change is observed in the IECs after any of the annealing techniques, implying a low occurrence of thermal degradation or leaching of hydrophilic component from the membrane.

All blend membranes before and after annealing were investigated by SAXS at 60 °C by sweeping the relative humidity (RH) from 25% to 95%RH. All as-cast blend membranes prior to annealing exhibited no features in the SAXS profiles as expected from casting the compatible blend and subsequent quaternization.. The membranes after different thermal treatments also exhibited no noticeable features in the SAXS. Only the solvent vapor annealed sample with the highest ion exchange capacity (Sample E) displayed a significant scattering peak after annealing.

The other solvent annealed membranes (A, B, C, and D) showed mostly featureless profiles, with only sample D showing some change after annealing and a small scattering peak. The SAXS profiles of membranes D and E are presented in Figure 2.7 as representatives to illustrate the effect of solvent annealing. Figure 2.7 indicates an amorphous morphology in membrane D and E before annealing, corresponding to the initially miscible PVBC-b-PS/PPO blend. In contrast, the solvent annealed membrane E displayed an ordered phase separation with a distinct peak at q = 0.013 A^{-1} and broad second and third order peaks at approximately q = 0.024 A^{-1} and 0.050 A^{-1}. Additionally, all SAXS profiles showed little response to changes in humidity revealing that the PPO blend AEMs possess desired dimensional stability under changing humidity conditions.

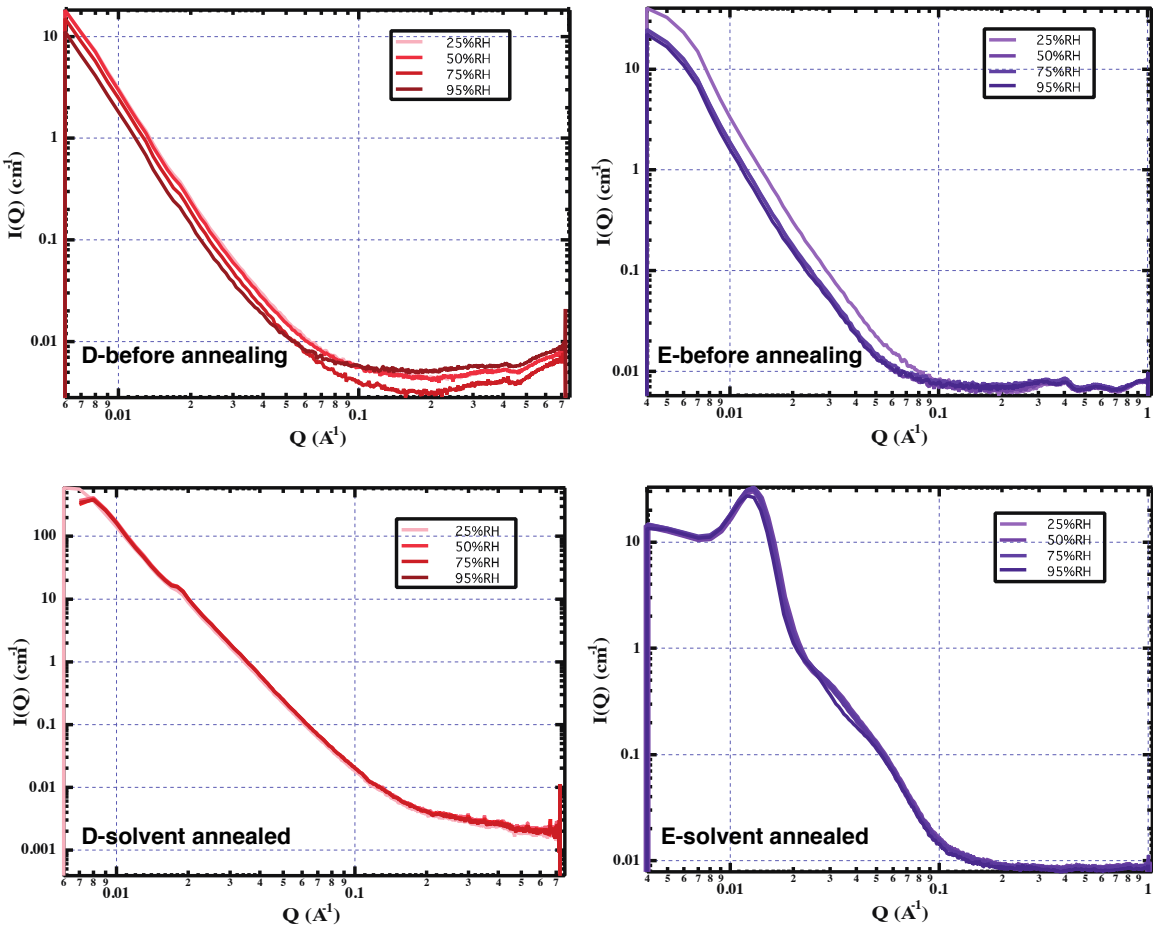

Figure 2.7 SAXS profiles (60 °C) of membranes (D & E) before and after solvent annealing.

High angle annular dark field scanning transmission electron microscopy (HAADF STEM) was performed on membrane E after solvent annealing, since the membrane E after annealing displayed relatively broad SAXS peaks to identify the actual morphology in membrane, although features were observed in SAXS profiles. The corresponding HAADF STEM image of membrane E in Figure 2.8 revealed the distinct hydrophilic and hydrophobic phase separation, with a domain size of approximately 25 nm. Lighter regions in images obtained through HAADF STEM corresponded to regions of high electron density. This is consistent with the presence of bromine and suggests that the hydrophilic regions aggregate into distinct clusters however, the hydrophilic components were randomly distributed in the matrix of PPO/PS blend.

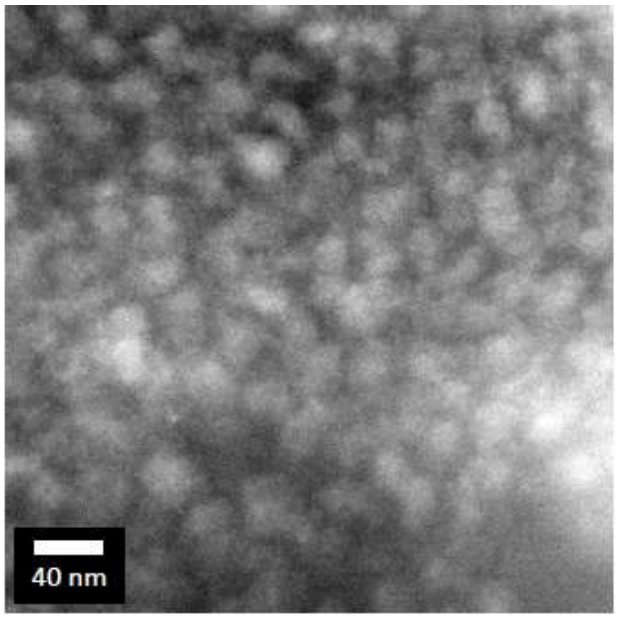

Figure 2.8 HAADF STEM image of membrane E after solvent annealing

The water uptake of all blend membranes before and after the different annealing conditions were measured at room temperature in the chloride form and compared (Figure 2.9a). The total number of ionic groups (as measured by IEC) varies with the amount of PPO in the

blend. The water uptake is found to increase with an increase in IEC, as expected, and the membranes before annealing show the water uptake increases from 9% to 28% as the amount of PPO in the blend decreases. A comparison between annealing methods reveals that almost no change occurs for samples boiled in water or for samples annealed at high temperature in the absence of water. Only the samples that were annealed at high temperature in the presence of water or over THF/water solutions showed any dramatic change in the water uptake. The change is related to these two annealing techniques allowing the rearrangement of the PPO/PS blend while also hydrating the hydrophilic component.

Table 2.3 Conductivity[a] (hydroxide and chloride[b]) comparison between membranes before and after annealing

AEM	IEC (mmol/g)	σ_0 (mS/cm)	σ_1 (mS/cm)	σ_2 (mS/cm)	σ_3 (mS/cm)	σ_4 (mS/cm)
A	0.75	6.0 (1.9)	5.8 (1.7)	6.9 (2.0)	9.0 (3.0)	10 (3.6)
B	0.87	8.0 (2.1)	7.0 (2.5)	9.0 (3.5)	17 (4.9)	17 (4.7)
C	1.02	11 (3.9)	11 (3.4)	12 (4.3)	25 (6.3)	23 (7.0)
D	1.17	15 (5.5)	14 (6.2)	17 (7.2)	32 (13)	30 (11)
E	1.34	18 (8.0)	18 (8.6)	22 (10)	43 (18)	35 (13)

a) The subscripts of IEC stand for the annealing methods: 0 represents the membranes before annealing; 1 represents the membranes after boiling in water; 2 represents the membranes after annealing at high temperature without water; 3 represents the membranes after annealing at high temperature with water; and 4 represents the membranes after annealing with solvent vapor;
b) chloride conductivity is in the parenthesis

Conductivity of all membranes were measured in either the hydroxide or chloride forms at 60 °C in water by electrochemical impedance spectroscopy. Similar to water uptake, the ionic conductivity is found to increase with increasing IEC for both hydroxide and chloride form (Figure 2.9b), and the detailed conductivity data is listed in Table 2.3. The hydroxide

conductivities are 2-4 times higher than chloride conductivities for all membranes as observed in other work.[69, 140] Also similar to the water uptake results, annealing at high temperature in the presence of water or over THF/water solutions exhibited a significant effect on the membrane ionic conductivity, while membranes boiled in water or annealed at high temperature in the absence of water show little change in conductivity. Hydroxide conductivity of membrane E (IEC = 1.34 mmol/g) increases from 16 mS/cm to 43 mS/cm on going from non-annealed membrane to after high temperature water annealing, which is consistent with the trend observed in water uptake. The effect of ionic conductivity with increased water uptake indicates that the conductivity is highly dependent on the water uptake.

In order to get better understanding of conductivity variation of the membranes with different annealing conditions, hydroxide conductivity of the membranes before and after annealing (solvent vapor and water at high temperature) as a function of water uptake is plotted in Figure 2.10. The enhancement in hydroxide conductivity is generally accompanied with an increase in water uptake. A close comparison reveals that membranes with similar water uptake display comparable conductivity. For instance, membrane E before annealing (water uptake = 28.1%) displays similar water uptake as membrane B after solvent vapor annealing (water uptake = 28.5%) and they show close conductivity values, however, the IEC differences between membranes E (IEC = 1.34 mmol/g) and B (IEC = 0.87 mmol/g) are quite significant. In addition, the membrane after high temperature water annealing displayed the highest water uptake and conductivity, but the membrane annealed by solvent vapor exhibited a different conductivity versus water uptake relationahip, whereby a relatively higher conductivity is for a given water uptake is observed. This implies that the solvent vapor annealed membrane can use water more

efficiently, which could be a result of the more developed phase separation morphology in the solvent annealed membrane.

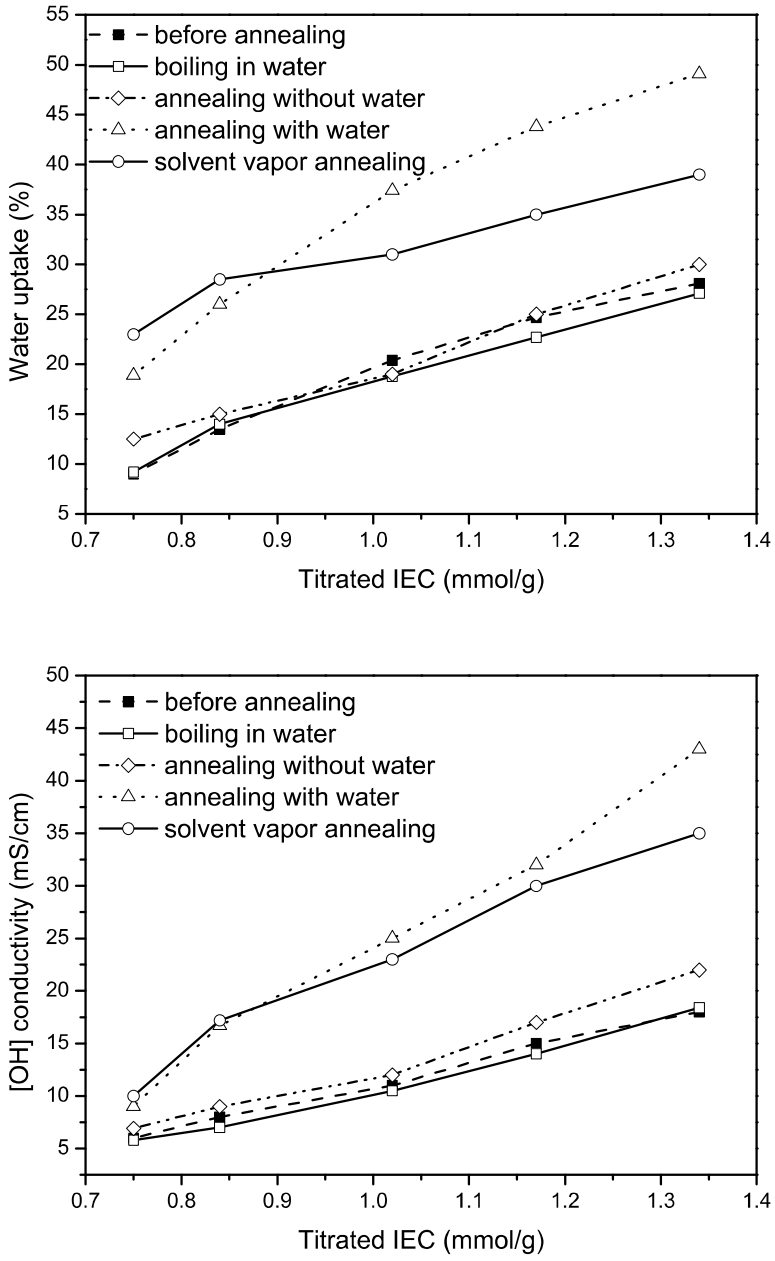

Figure 2.9 Water uptake (a) and hydroxide conductivity (b) comparison of membranes before and after annealing methods versus IEC

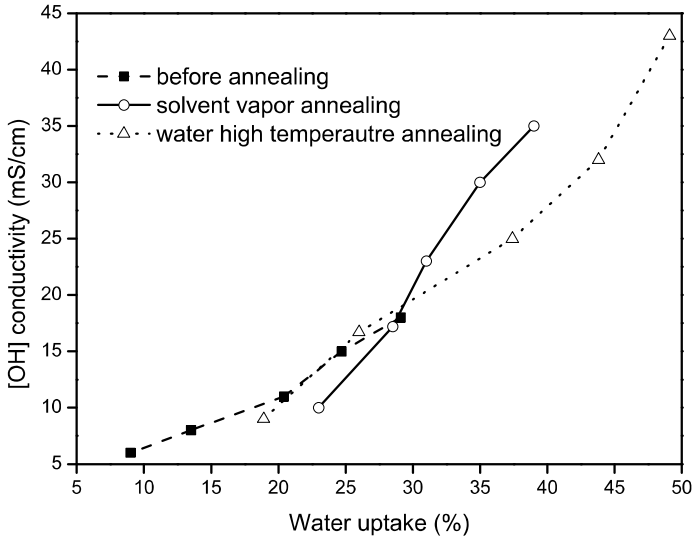

Figure 2.10 Hydroxide conductivities of membranes before and after annealing as a function of water uptake

The tensile properties (Young's modulus, stress at break and strain at break) of the various compositions of PPO blend AEMs were measured at room temperature under both dry and hydrated conditions to examine the effects of PPO content and water absorption (Figure 2.11). In addition to the PPO blend AEM, a quaternized film of P[VBTMA] [Cl]-b-PS copolymer with no added PPO was also prepared for comparison by soaking PVBC-b-PS copolymer membrane directly in a trimethylamine aqueous solution for 48 hours. Five replicate measurements were performed for each sample to obtain average values. For membranes tested at dry condition, the Young's modulus decreased from roughly 2 GPa to 1 GPa going from 0 wt% to 60 wt% PPO in the blend, and the stress (25.9 MPa to 35.4 MPa) as well as elongation (0.9% to 4.5%) generally increased when the PPO content increased consistent with known properties of PS/PPO blends.[121, 141, 142] The hydrated blend membranes show noticeable improvement in tensile properties from those under a dry condition. The hydrated membranes display significantly lower Young's modulus and stress (ranging from15 MPa to 26 MPa) as well

as higher elongation (ranging from 4.9% to 9.4%) than their dry analogues. Water in the quaternized membrane can act as plasticizer to decrease the modulus and increase the membrane elongation.[143] The Young's moduli for hydrated membranes are found to decrease from 945 MPa to 488 MPa as the PPO loading increases. However, no clear trend is observed for stress and elongation data from the hydrated membrane, and membrane C (40 wt% PPO loading) shows the highest elongation of 9.4%.

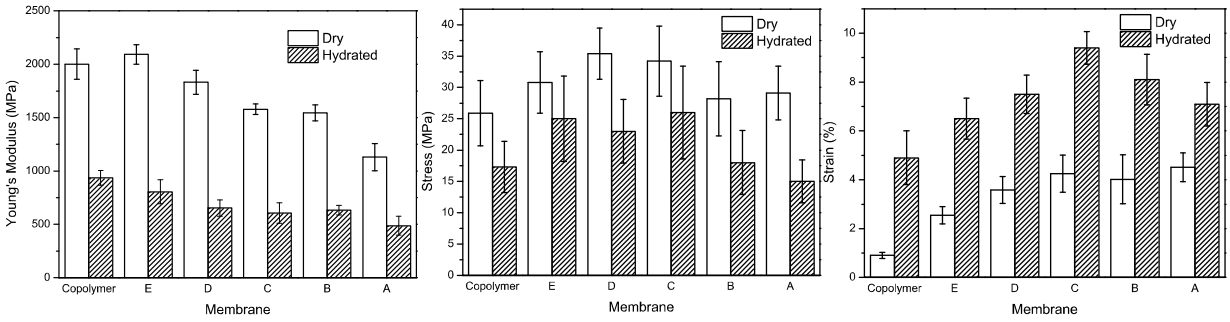

Figure 2.11 Young's modulus, stress at break and stain at break of PPO blend membranes at room temperature under dry and hydrated condition

2.4 Conclusion

We have demonstrated the preparation of AEMs by blending PPO with PVBC-b-PS to form miscible blends and subsequent trimethylamine quaternization. The addition of PPO improves the mechanical properties over that of the styrenic block copolymer. Annealing of the blend membranes is necessary to obtain good conductivity values because of the way the films are cast as miscible blends and then converted into quaternary ammonium functionalized materials. Only the annealing procedures that provide both a hydrated environment for the cationic component and conditions where the high T_g matrix can reorganize are effective for increasing both the water uptake and the conductivity. While an ordered morphology is

observed for some membranes, no strong correlation of conductivity with morphology is determined for these membranes.

2.5 Acknowledgement

This work was funded by the Army Research Office through a MURI (grant # W911NF-10-1-0520). NMR spectroscopy was made possible through a grant from the NSF MRI program (grant # CHW-0923537). The authors also want to thank Blake Whitley and Prof. Kip Findley for the assistance of membrane tensile test.

CHAPTER 3 BROMINATED POLY(2,6-DIMETHYL-1,4-PHENYLENE OXIDE) BLENDED WITH POLY(VINYLBENZYL CHLORIDE)-B-POLYSTYRENE FOR ANION EXCHANGE MEMBRANES

3.1 Introduction

In recent years, fuel cell research has been extensively focused on the proton exchange membrane fuel cell (PEMFC). Although perfluorosulfonic acid ionomers, such as Nafion®,[144, 145] have been commercialized as the polymer electrolyte, the high production cost of polymer electrolyte and the needs of precious metal catalyst as components of electrodes limit the commercialization of PEMFC.[146]

The alkaline fuel cell (AFC) offers an alternative way to solve the drawbacks in PEMFC. The AFC operates in a high pH environment, which enables the faster redox reaction and capability to use non-precious metal catalyst including nickel and silver.[12-15] However, AFC traditionally uses aqueous potassium hydroxide as electrolyte,[16, 147] which could cause many engineering issues, such as corrosion and leakage of electrolyte. In addition, carbonate precipitates can form in the electrolyte due to the presence of carbon dioxide in the air or fuel, impeding transport to the electrode.[17, 18] More recently, anion exchange membrane (AEM) has been investigated in AFCs as a potential solution for problems in traditional AFCs.[8, 10, 11]

The AEMs are typically tethered by cationic functional groups for hydroxide conduction. Benzyltrimethylammonium has been widely used as ion conducting group for AEM study, since it has moderate alkaline stability[27, 28] and can be readily functionalized through polystyrene or its derivative (e.g. polyvinylbenzyl chloride).[31, 32, 34-38, 40-42] Therefore, polystyrene block copolymers, such as polyvinylbenzyl chloride-b-polystyrene (PVBC-b-PS), become a very interesting material for AEM study due to the commercial availability of monomers and the

ability of morphological control offered by its block copolymer.[104-107] Although the polystyrene based films generally exhibit low flexibility, poly(1,4-dimethylphenylene oxide) (PPO) has been well studied to form a miscible blend with polystyrene in order to improve its mechanical property.[121, 141, 142]

Our previous work in Chapter 2 has demonstrated that the mechanical properties of PPO blended polystyrene block copolymer AEM is apparently enhanced compared to the AEM directly prepared by polystyrene block copolymer. Despite the improvements in mechanical properties that are observed, the PPO blend membrane still produces insufficient ionic conductivity, which is partially due to the low cationic functionality in membrane. Brominated poly(phenylene oxide) (BrPPO) has been incorporated in the synthesis of poly(vinylbenzyl chloride-divinylbenzene) network to increase the AEM functionality.[81] However, the leakage of BrPPO has been observed during quaternization, which could correspond to the incompatibility between BrPPO and the polymer network.[81] By blending BrPPO with polystyrene block copolymer to prepare AEM, it is expected that the unfunctionalized PPO can form a miscible blend with the PS to enhance the mechanical properties while the additional cationic functional group in PPO could improve the ionic conductivity of blended membrane. In addition, the functionality of BrPPO needs be controlled to maintain membrane integrity in water after quaternization.

In the current study, a BrPPO blended polystyrene block copolymer AEM system with functional groups in both BrPPO and block copolymer is investigated. The preparation of BrPPO blended membrane involves the bromination of PPO on the benzyl methyl groups, followed by blending BrPPO with PVBC-b-PS through solvent casting. The quaternary ammonium conducting groups are finally formed by reacting bromomethyl groups and chloromethyl groups

with trimethylamine. The ion exchange capacity is varied through changing the blend composition of BrPPO and PVBC-b-PS. The following research investigates in detail the preparation of BrPPO blended AEMs as well as the membrane properties including thermal stability, water uptake, and ionic conductivity. In addition, high temperature annealed membranes are also prepared to study the annealing effect on membrane properties.

3.2 Experimental

3.2.1 Materials

PVBC-b-PS copolymer was prepared by following literature procedures,[111] and the copolymer was several times dissolved in chloroform and precipitated into methanol to remove impurities before use. Poly(2,6-dimethyl-1,4-phenylene oxide) (PPO) (Aldrich, M_n ~32000 g/mol), bromine (Br_2) (AlfaAeser, 98%), 1,1,2,2-tetrachloroethane (TCE) (Aldrich, 98%), and aqueous trimethylamine solution (Aldrich 25 wt%) were used as received. Other reagents were used without further purification.

3.2.2 Synthesis of BrPPO

PPO (2.00g, 16.7 mmol repeat unit) was weighed into a 3 neck 500mL round bottom flask equipped with a magnetic stirbar, condenser, addition funnel and argon bubbler. 200 mL TCE was added and the mixture was stirred until the polymer had completely dissolved. The solution was heated to reflux. The addition funnel was charged with bromine (0.85mL, 16.59mmol) and TCE (85mL) and was added dropwise over 8 hours. The solution was stirred at reflux for an additional hour. Excess TCE was removed by distillation. The polymer was precipitated from methanol, filtered and dried in a vacuum oven at 80 °C overnight. All BrPPO

samples used in this study were supplied by Dr. Nate Rebeck.[148]

3.2.3 BrPPO Blended AEM Preparation

Both BrPPO and PVBC-b-PS samples were dried in a vacuum oven overnight before blending and then dissolved in chloroform with a range of different mass ratios (PVBC-b-PS : BrPPO = 40:60, 50:50, 60:40, 70:30, 80:20) by sonication at room temperature. All blend concentrations were around 5g/100mL. Polymer blend solutions were drop cast on glass slides and the solvent was allowed to evaporate slowly at room temperature. The glass slide was immersed in deionized water to remove the polymer film. All PVBC-b-PS/BrPPO blend membranes obtained were transparent and were dried in a vacuum oven at 60 °C overnight.

3.2.4 Amination of PVBC-b-PS/BrPPO Blend Membranes

About 0.2 g PVBC-b-PS/BrPPO membrane was soaked in a beaker containing 150 mL 25% aqueous trimethylamine solution to convert both chloromethyl and bromomethyl groups to quaternary ammonium caition functional groups. After 48 hours soaking at room temperature, BrPPO blend membranes containing quaternary ammonium cation were soaked repeatedly in fresh deionized water and dried in a vacuum oven at 60 °C overnight.

3.2.5 Ion Exchange of Aminated Membranes

The directly quaternized membranes were soaked in 1 M KCl solution for 48 hours to exchange any ammonium bromide to chloride for easier property comparison and the excess chloride solution was removed by rinsing the membrane repeatedly in deionized water. Hydroxide membrane was also produced by soaking quaternized membrane in 1M KOH solution

for 48hr in order to exchange chloride to hydroxide and subsequently soaking the membranes repeatedly in degassed deionized water to remove extra hydroxide ions

3.2.6 Membrane Annealing

All quaternized membranes were annealed in an acid digestion bomb at 125 °C under both dry and hydrated conditions for 12 hours. Quaternized membranes were dried in a vacuum oven after annealing.

3.2.7 Characterization

^{1}H NMR spectra of BrPPO and PS-b-PVBC were performed on a JEOL ECA-500 MHz spectrometer. All polymer samples were dissolved in dilute $CDCl_3$ solution at concentration of 50 mg/mL. Gel permeation chromatography was performed on a system consisting of a Water 600 Pump and two PL-gel 5 μm Mixed C columns. A Wyatt MiniDAWN light scattering instrument and Wyatt Optilab DSP refractometer were used as detectors. Differential scanning calorimetry (DSC-20) was used to obtain the glass transition temperatures (T_g) of blend membranes with 3 heating loops and heating rate at 10 °C/min under a nitrogen purge, and the data was analyzed by TA software. Thermal degradation temperatures were measured on Seiko TGA/DTA320 thermogravimetric analysis (TGA) at a heating rate of 10 °C/ min under a nitrogen atmosphere. Fourier transform infrared (FTIR) spectroscopy was performed on films with a Thermo-Electron Nicolet 4700 spectrometer utilizing Nicolet's OMNIC software.

Theoretical ionic exchange capacities (IECs) were calculated based on the complete conversion of chloromethyl and bromomethyl groups to benzylammonium groups. IECs of blend membranes were also measured by hydroxide back titration.[34, 55] Typically, about 0.02 g of

vacuum dried blend membranes in hydroxide form were immersed in 10.00 mL of 0.01007 M standardized HCl solution. After 48 hours, unreacted HCl was titrated by 0.01103 M standardized NaOH solution. The titrations were repeated 3 times for each blend membrane. The IEC (mmol/g) was obtained by

$$\text{IEC (mmol/g)} = \frac{M_{0hr,\,HCl} - M_{48hr,\,Hcl}}{m_{dry\ membrane}} \qquad (1)$$

where $M_{0h,\,HCl}$ is milimoles (mmol) of HCl determined before blend membranes neutralization, $M_{48h,\,HCl}$ is mmol determined after neutralization of membranes (after 48 hr), and $m_{dry\ membrane}$ is the dry mass (g) of membrane in hydroxide form.

Water uptake of BrPPO blended AEM was determined by comparing the hydrated and dry mass of membranes. The membranes were pre-soaked in deionized water for 24 hours. The excess water on surface of fully hydrated membranes was blotted dry with kimwipes, and weighed immediately. The membrane was re-hydrated again in deionized water to obtain an average mass of wet membrane. The film was finally vacuum dried at 60 °C until a constant mass was reached. The water uptake (WU) was determined by

$$\text{WU (\%)} = \frac{m_{hydrated} - m_{dry}}{m_{dry}} \times 100\% \qquad (2)$$

where $m_{hydrated}$ is hydrated mass of membrane after removing all surface water, and m_{dry} is dry mass of membrane after drying in vacuum oven.

The in plane ionic conductivities of blend membranes were measured by four platinum probe testing cell in electrochemical impedance spectroscopy (EIS) using a BioLogic VMP3 potentiostat under controlled temperature and relative humidity in a TestEquity H1000 oven, and

data was collected using EC Laboratories software. The conductivity can be calculated from the membrane resistance

$$\sigma = \frac{l}{R \cdot A} \qquad (3)$$

where R is the membrane resistance, l is the distance between the electrodes, A is the cross-section area of the sample. In this work, the chloride conductivities were measured at 95%RH by sweeping the temperature and hydroxide conductivities were measured in water at 60 °C by the testing cell.

Small angle x-ray scattering (SAXS) experiments were performed on beamline 12 ID-B at the Advanced Photon Source at Argonne National Laboratory. A beam energy of 12keV with x-ray wavelength at 1 Å was employed to measure samples in transmission mode. The scattering data was collected by a Pliatus 2M SAXS detector. The two-dimensional SAXS patterns were radially integrated to obtain the transmission intensity with respect to the scattering vector q. The typical experiment was performed using a customized environmental chamber with controlled temperature and humidity. The humidity of the chamber was controlled by mixing wet and dry nitrogen gas. Temperature was maintained at 60 °C while the humidity was varied from 25%RH to 95%RH.

3.3 Results and Discussion

The PPO homopolymer blended AEM study in Chapter 2 demonstrated the concept of the formation of miscible PPO/PS blends to enhance the mechanical properties of polystyrene block copolymer AEMs. Although the ionic conductivity (up to 43 mS/cm) was significantly

enhanced through high temperature and solvent annealing in the presence of water, desired high hydroxide conductivity is still not achieved.

The main goal of incorporating BrPPO in blend is to enhance the mechanical properties of polystyrene block copolymer while introducing more cationic functional groups in blend membranes for ion conduction. Furthermore, the additional functionality provided by BrPPO could exist in the membrane formation components between the ionic domains ultimately formed by the PVBC block. In order to maintain the similar mechanical strength as PPO blend AEM but improve the ionic conductivity, a BrPPO blended AEM is designed by taking advantage of the preparation method developed for PPO blended AEMs. As shown in Scheme 3.1, a BrPPO blended AEM is first prepared through the formation of PVBC-b-PS/BrPPO blend films by solution casting and then the solvent cast BrPPO blend film was isolated and subsequently functionalized by trimethylamine quaternization. The obtained membrane was soaked in KCl solution to exchange all counterions to chloride.

Scheme 3.1 Preparation of BrPPO blended AEM

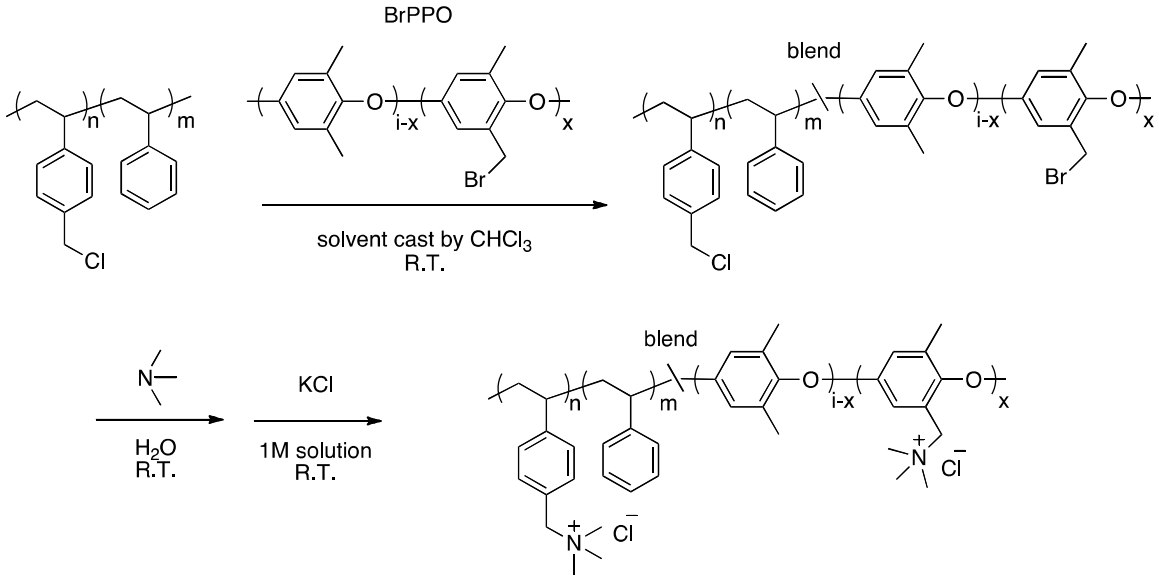

The PVBC-b-PS block copolymer was synthesized by nitroxide-mediated polymerization to control both molecular weight and the relative block composition.[111] The polymerization of vinylbenzyl chloride (VBC) (10 mL) was first carried out using benzoyl peroxide (56 mg, 0.4 mmol) as radical initiator in the presence of TEMPO[131, 132, 149] (62 mg 0.4 mmol) at 125 °C for 3 hours. The resulting TEMPO end-capped PVBC (PVBC-TEMPO) was isolated by precipitation in methanol and separated from any remaining monomer by several re-precipitations. The PVBC-TEMPO was analyzed by gel permeation chromatography to determine a number average molecular weight of 30,500 g/mol. PVBC-TEMPO (2.3 g) was dissolved in 20 mL styrene and used as macrointiator to copolymerize the styrene block in bulk at 125 °C for 30 minutes. The diblock copolymer was isolated and purified by precipitation in methanol. The diblock copolymer was characterized by gel permeation chromatography and had a total molecular weight of 85,700 g/mol and molecular weight distribution of 1.85. The diblock copolymer was prepared with the composition of 32 wt% PVBC block and 68 wt% PS block calculated from the ^{1}H NMR spectrum of the copolymer.

Scheme 3.2 Bromination of PPO

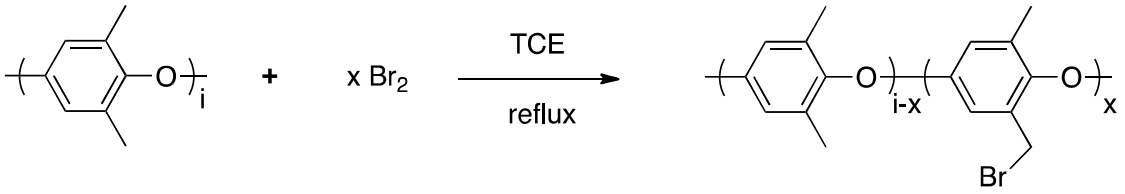

The bromination of commercially available PPO is depicted in Scheme 3.2, and the reaction was carried out using bromine as bromination agent directly according to a literature procedure.[150]. The tetrachloroethane diluted bromine was used in order to limit the local

bromine concentration and selectively brominate the 4-methyl groups. The degree of bromination (Figure 3.1) can be determined using ^{1}H NMR spectroscopy by comparing the integration values of the peaks associated with the bromomethyl group (noted as d peak) and the remaining unreacted methyl groups (noted as e peak). The peaks designated as a, b, and c correspond to the aromatic protons on the backbone. In Figure 3.1, the brominated repeat units in BrPPO were calculated to be 90 wt%. A series of bromination reactions was performed on PPO by varying the ratio of bromine to PPO repeat unit, and excess amount of bromine was used in order to achieve the desired degree of bromination. Gel permeation chromatography was performed on all samples after bromination in order to examine the stability of polymers under the reaction condition. It was found that all samples in chromatograms showed a shift to high molecular weight region without tailing to low molecular weight indicating no degradation occurred during the harsh bromination reaction condition.[148]

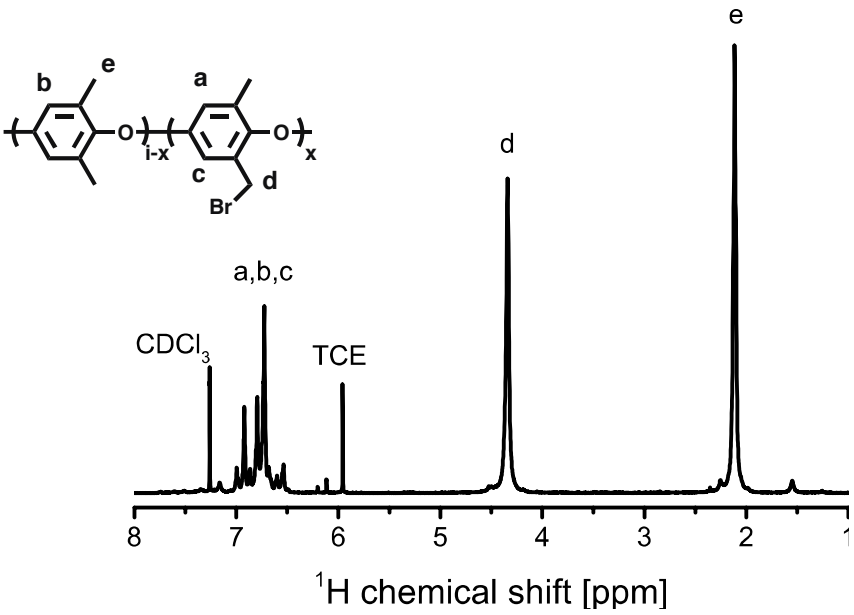

Figure 3.1 ^{1}H NMR spectrum of BrPPO

The BrPPO films with a series of bromination levels were drop cast from chloroform and quaternized in trimethylamine solution to convert benzylbromide groups to benzyltrimethylammonium bromide. Quaternized PPO films containing functional groups on approximately more than 0.18 per repeat units (25 wt% bromine functionalized PPO in BrPPO) became water-soluble. Since only the quaternized PPO with good mechanical integrity in water can be used for blend membrane preparation, the BrPPO with 25 wt% brominated repeat units was used in this research.

The previous study of PPO homopolymer blended AEMs investigated the miscibility of PVBC with PS and PVBC-b-PS with PPO. Compatibility was found in PVBC-b-PS copolymer and PVBC-b-PS/PPO blends for the compositions that were prepared. The miscibility of PVBC-b-PS with BrPPO is necessary to be investigated in this study due to the additional bromomethyl groups in BrPPO. The miscibility study of BrPPO and PVBC-b-PS was performed on the blend membrane samples. The glass transition temperature of BrPPO and PVBC-b-PS copolymer was firstly measured at 230 °C and 107 °C respectively. The BrPPO was blended with PVBC-b-PS copolymer in a range of compositions for the miscibility study. DSC was applied to examine all BrPPO blend materials and only one glass transition peak was shown in all BrPPO blend membranes. The glass transition temperature increases with the increase in BrPPO composition of blend membranes as expected. Figure 3.2 shows one example of BrPPO blend membrane with 40 wt% of BrPPO loading and the glass transition temperature of this particular blend membrane is at 135 °C indicating that the BrPPO is compatible with PVBC-b-PS in the blend composition investigated in this study.

BrPPO was blended with PVBC-b-PS in chloroform at the concentration of 5g/100mL and the PVBC-b-PS/BrPPO blend film was obtained by solution casting on a glass slide and

slow solvent evaporation. BrPPO blend membranes with a series of blend compositions were prepared and are listed in Table 3.1. The chloromethyl groups in the blend membranes decreased with the increase of BrPPO content in blend, whereas the number of bromomethyl groups followed the opposite order. So, it is expected that the ion exchange capacity only varies in a small range.

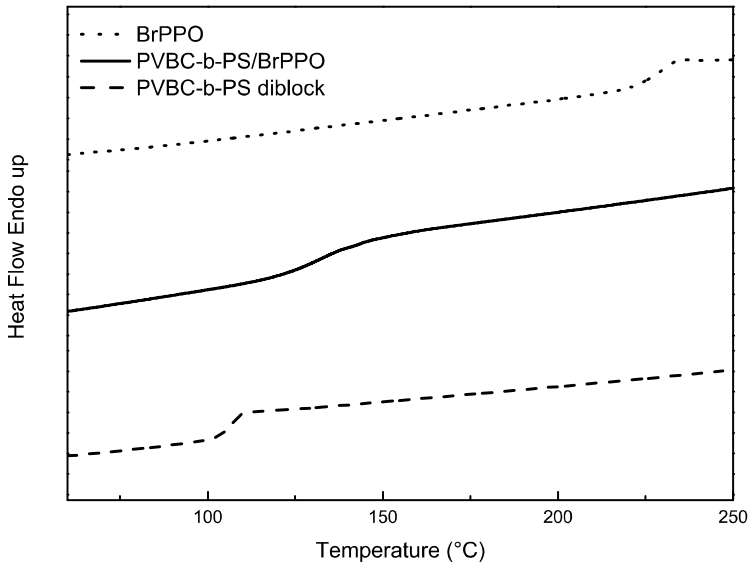

Figure 3.2 DSC traces of PVBC-b-PS diblock, PVBC-b-PS/BrPPO (60/40) blend membrane, and BrPPO (25wt% bromine repeat units)

Table 3.1 PVBC-b-PS/PPO blends composition, theoretical IEC and titrated IEC

AEM	PVBC-b-PS (wt%)	BrPPO (wt%)	Theoretical IEC[a] (mmol/g)	Titrated IEC[b] (mmol/g)
A	40	60	1.54	1.26
B	50	50	1.61	1.33
C	60	40	1.67	1.37
D	70	30	1.74	1.46
E	80	20	1.80	1.59

a) estimated by ^{1}H NMR spectrum and blend ratio; b) determined by back titration of blended membranes after OH^- counter-ion exchange

The PVBC-b-PS/BrPPO membranes were transparent and immersed in aqueous trimethylamine solution to convert both chloromethyl and bromomethyl groups to quaternary ammonium groups for ion conduction. A large excess of trimethylamine solution was used in order to reach a high reaction conversion. The blend membranes were left to react for 48 hours and the obtained AEM was vacuum dried at 60 °C overnight. Infrared spectroscopy qualitatively confirmed the formation of quaternary ammonium in blend membrane in Figure 3.3. The disappearance of C-Cl and C-Br stretching at about 580 to 680 cm^{-1} indicates the conversion of chloromethyl and bromomethyl groups and the formation of a peak at 3400 cm^{-1} represents the water peak associated with the formation of hygroscopic quaternary ammonium groups.

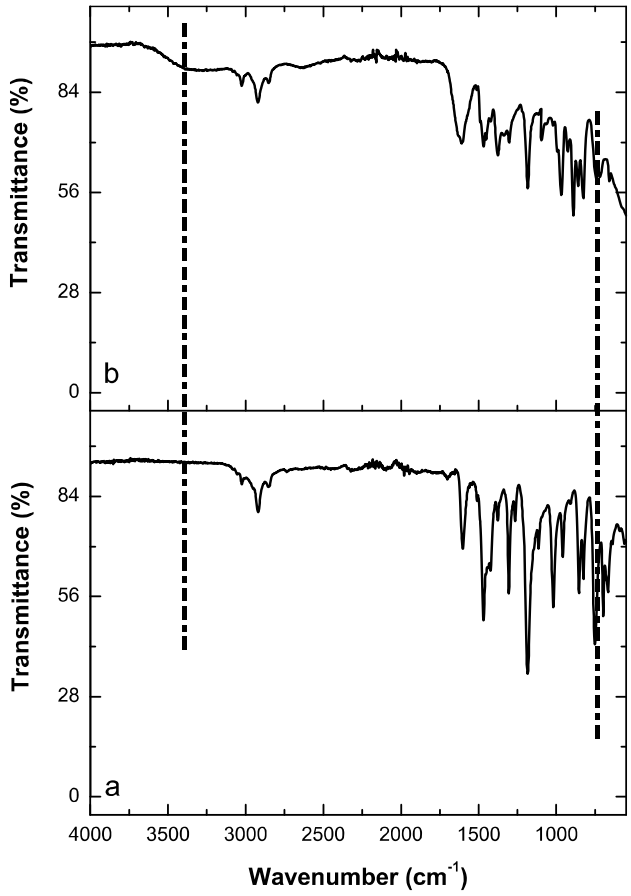

Figure 3.3 The FT-IR spectrum of (a) BrPPO blend membrane before quaternization and (b) BrPPO blend membrane after quaternization

In order to quantitatively examine the conversion following the amination reaction, hydroxide back titration was used to determine the titrated IEC of BrPPO blend membrane. The blend membranes were soaked in 1 M degassed KOH solution for 48 hr to exchange halide to hydroxide. The membranes were immersed in fresh deionized water every 4 hours to remove excess hydroxide ions. The conversion of quaternization reaction was calculated in a range of 82% to 88% by comparing the value between theoretical IEC and titrated IEC.

The blend membrane was expected to become an immiscible system after the quaternization reaction, but the phase separation between hydrophobic and hydrophilic components in membrane might be limited due to the formation of quaternized membrane from a pre-cast miscible blend. Since a significant enhancement in ionic conductivity was observed in previous PPO blend membranes as well as other fuel cell materials after annealing,[151] experiments were designed to anneal the BrPPO blend membranes under different conditions and then to examine their membrane properties, including water uptake and ionic conductivity.

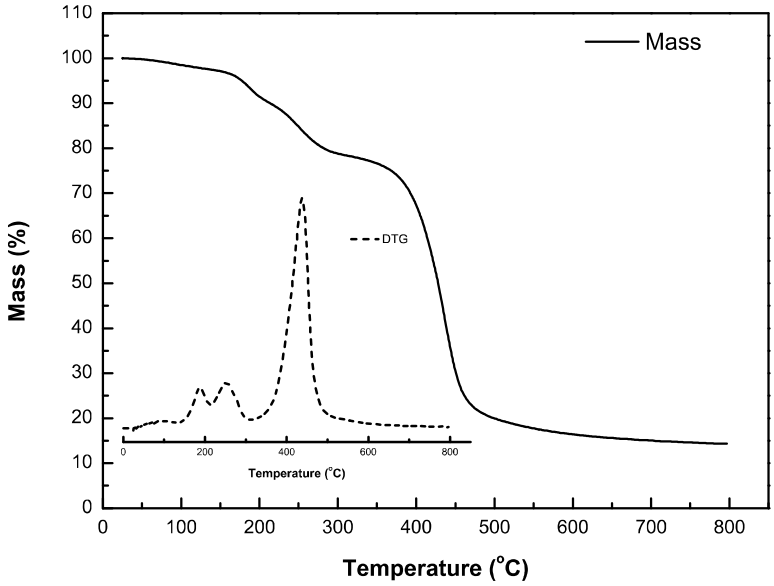

Figure 3.4 TGA and DTG (inset) curves of BrPPO blended AEM

In order to perform the annealing on BrPPO blend membranes, the thermal degradation of quaternized BrPPO blend membranes was investigated. The thermal stability of BrPPO blend AEM was studied by thermogravimetric analysis. The derivative of the thermogravimetric trace is plotted as a function of temperature in Figure 3.4, and it displays the degradation temperature of BrPPO blend AEM starts approximately at 131 °C, which is slightly lower than that observed for the pure PPO blend. All BrPPO blended AEMs were annealed at 125 °C at dry and hydrated conditions in order to stay below the observed degradation temperature.

Table 3.2 Titrated IECs[a] comparison of membranes before and after annealing

AEM	IEC_0 (mmol/g)	IEC_1 (mmol/g)	IEC_2 (mmol/g)
A	1.26	1.09	0.80
B	1.33	1.17	0.88
C	1.37	1.23	1.05
D	1.46	1.32	1.09
E	1.59	1.43	1.21

a) The subscripts of IEC stand for the annealing methods: 0 represents the membranes before annealing; 1 represents the membranes after annealing at high temperature without water; 2 represents the membranes after annealing at high temperature with water

Since the membrane obtained directly after quaternization reaction had a mixture of chloride and bromide as counterions, the membrane was soaked in 1 M KCl solution to exchange all counterions to chloride for easier property comparison. The water uptake of all membranes in chloride form before and after annealing were investigated at room temperature, and the water uptake as a function of IEC is shown in Figure 3.5. The water uptake is found to correlate with IEC as expected, and the membranes before annealing show the water uptake value increases from 23% to 42% going from the lowest quaternary ammonium functionalized sample to the most highly functionalized sample. However, the water uptake generally displays a decrease after annealing at 125 °C in dry and hydrated conditions, which correspond to the functionality

loss during the harsh annealing conditions. The most significant decrease in water sorption is observed in membrane annealed at high temperature with water and the values range from 12% to 21%, which agrees well with the trend observed in IEC measurements after annealing.

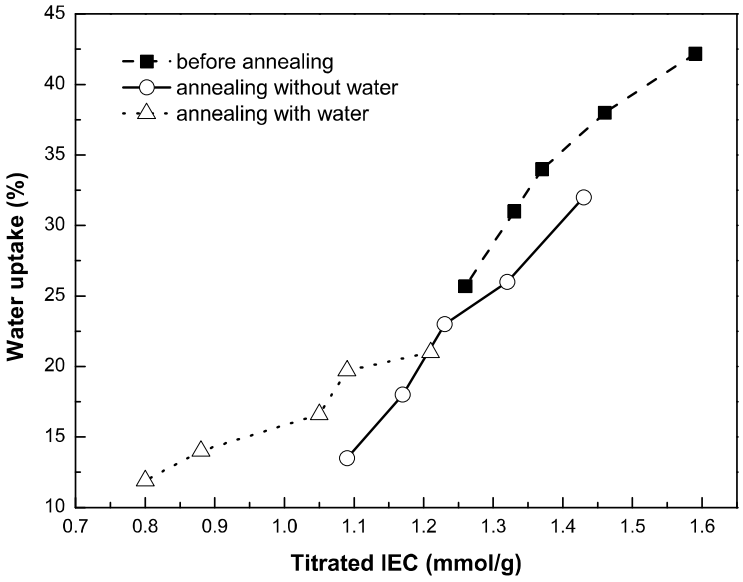

Figure 3.5 Water uptake comparison between membrane before and after annealing

Table 3.3 Conductivity[a] (chloride and hydroxide[b]) comparison between membranes before and after annealing

AEM	IEC (mmol/g)	σ_0 (mS/cm)	σ_1 (mS/cm)	σ_2 (mS/cm)
A	1.26	7.3 (22)	5.1	3.0
B	1.33	9.5 (30)	6.6	3.5
C	1.37	10 (34)	7.9	5.6
D	1.46	13 (41)	9.5	6.0
E	1.59	15 (46)	12	7.3

a) The subscripts of IEC stand for the annealing methods: 0 represents the membranes before annealing; 1 represents the membranes after annealing at high temperature without water; 2 represents the membranes after annealing at high temperature with water; b) hydroxide conductivity in parenthesis

Conductivities of all membranes were measured in the chloride form using electrochemical impedance spectroscopy at 95%RH by sweeping the temperature from 50-90 °C and the values at 60 °C are reported in Table 3.3. The chloride conductivity is dependent on the

ion exchange capacity as expected and the value increases with the increased functionality (Figure 3.6). The highest chloride conductivity is observed in the membranes before annealing, which is consistent with the observation in IEC and water uptake changes. The hydroxide conductivity was measured in water at 60 °C and only for the membranes before annealing due to the occurrence of degradation in membranes after annealing. The hydroxide conductivities are approximately 3 times higher than chloride conductivities for all membranes.

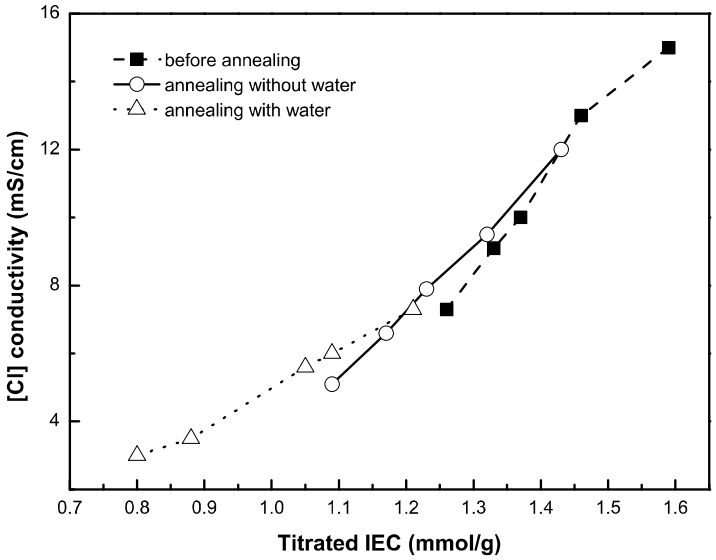

Figure 3.6 Chloride conductivity comparison of membranes before and after annealing methods versus IEC

In order to get a better comparison of ion conduction property on PPO and BrPPO blend membranes, hydroxide conductivities of PPO blended and BrPPO blended membrane before annealing as a function of water uptake is exhibited in Figure 3.7. Although the conductivities of both membranes show the same trend relative to water uptake, the BrPPO blended membranes display significantly higher hydroxide conductivity than PPO blended membranes, which could correspond to the higher functionality in BrPPO blends. Furthermore, it is also found that the BrPPO blended AEMs with similar IEC display higher water uptake and hydroxide conductivity

than the PPO blended samples, which indicates the high dependence of ionic conductivity on water uptake. For membranes with similar IEC values, BrPPO blend (IEC = 1.33 mmol/g) consisted of both quaternized PPO and quaternized PVBC, while PPO blend (IEC = 1.34 mmol/g) only consisted of quaternized PVBC but at higher concentration than the quaternized PVBC in BrPPO blend. This implies that the introduction of quaternized PPO has greater enhancement on water uptake and ionic conductivity in the blend membrane than quaternary ammonium functional groups provided by PVBC in block copolymer.

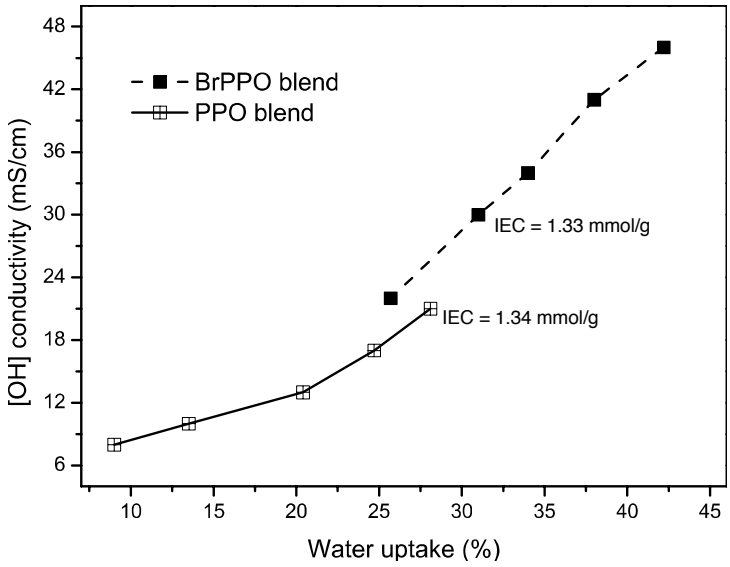

Figure 3.7 Hydroxide conductivities of PPO and BrPPO blended membranes before annealing as a function of water uptake

Small angle x-ray scattering (SAXS) experiments were performed on all BrPPO blended AEMs before annealing at 60 °C by sweeping the humidity from 25% RH to 95% RH. All as-cast BrPPO blend membranes prior to annealing exhibited no distinct peaks in the SAXS profiles as expected from casting the miscible blend and subsequent quaternization at temperature well below the T_g of all components in the membrane, which is consistent with the SAXS patterns observed in PPO blended AEM before annealing. The SAXS profile of BrPPO membranes E is

presented in Figure 3.8 as a representative to demonstrate the amorphous morphology in BrPPO membranes before annealing. Since the thermal annealing causes degradation in the BrPPO blended AEM, the membranes after annealing were not analyzed in this study. In addition, all SAXS profiles showed little response toward humidity change revealing that the desirable membrane dimensional stability under humidified condition was achieved by BrPPO blended AEMs.

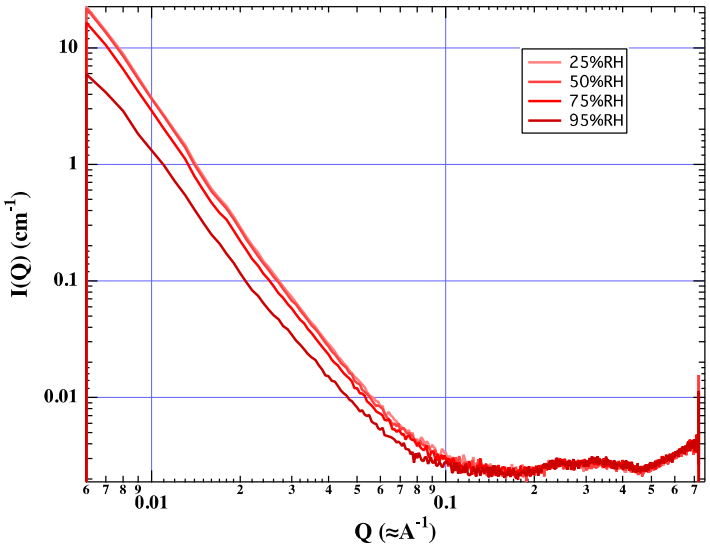

Figure 3.8 SAXS profile of BrPPO blend membranes E before annealing

3.4 Conclusion

BrPPO blend membranes were successfully prepared by blending BrPPO with PVBC-b-PS copolymer, solvent casting miscible blend membranes, and subsequent heterogeneous trimethyalmine quaternization. The membranes before annealing possessed the highest water uptake and hydroxide conductivity, as thermal degradation was found in membranes annealed at high temperature under both dry and hydrated conditions. The ionic conductivity was found to be highly dependent on water uptake and the incorporation of quaternary ammonium functionality

in PPO seems to have a greater effect on water uptake and ionic conductivity of blend membranes than increasing the functionality in the block copolymer.

3.5 Acknowledgement

The funding was provided by the US Army Research Office through a MURI on Ion Transport in Complex Heterogeneous Organic Materials (grant # W911NF-10-1-0520). NMR spectroscopy was made possible through a grant from the NSF MRI program (grant # CHW-0923537).

CHAPTER 4 POLYETHYLENE BASED BLOCK COPOLYMERS FOR ANION EXCHANGE MEMBRANE

4.1 Introduction

Alkaline fuel cells (AFCs) are being actively studied due to a number of advantages over proton exchange membrane fuel cells (PEMFCs), including their facile electrochemical kinetics and the capability to utilize non-precious metal catalysts (i.e., nickel[13] or silver).[8, 10, 11] However, the use of liquid electrolyte such as aqueous potassium hydroxide in traditional AFCs results in carbonate or bicarbonate precipitates from the exposure of potassium hydroxide to carbon dioxide in the air, resulting in reduced performance.[9] Recently, AFC research has focused on the development of anion exchange membranes (AEMs) with various tethered cationic functional groups, including quaternary ammonium[27, 29, 82, 84, 152] and phosphonium[85, 88], as solid polymer electrolytes for AFCs to eliminate the formation of precipitates. However, a major challenge in the development of AEMs is the preparation of a chemically stable polymer membrane with sufficient mechanical properties and ionic conductivity under the AFC operating conditions.

Polyethylene has been investigated as a component of blend membrane materials for PEMFC to provide mechanical properties and to control membrane swelling, and methanol permeability.[64, 65] AFC membranes containing polyethylene as membrane material have also been recently reported. Research has been performed to synthesize cationic functionalized cyclooctene, randomly copolymerize with cyclooctene by ring opening metathesis polymerization, and subsequently hydrogenate the polymer to form solvent processable

polyethylene AEMs with good mechanical and ion conductive properties.[68, 88] Another strategy to incorporate polyethylene in AEMs investigates the radiation graft reaction of vinylbenzyl chloride monomer onto commercially available polyethylene and subsequent conversion of benzyl chloride to quaternary ammonium cation.[153, 154] AEMs based on polyethylene have also been reported by blending anion exchange particles with linear polyethylene and a water soluble additive to prepare heterogeneous membranes.[155]

Although cationic functionalized polyethylene has been designed as a component of AEMs, the studies are based on the polymers with random cationic functional groups. Other research on AEMs has been directed toward preparing well-defined block copolymers that have a hydrophobic block that forms the matrix for mechanical strength and a hydrophilic (cationic) block for conductivity.[25, 104-108] The block copolymers for AEMs can provide phase-separated materials with controlled morphology for ion conduction by controlling the block composition. A notable strategy in the synthesis of well-defined block copolymers is to use living anionic polymerization. Anionic polymerization offers various benefits to prepare block copolymers as the reactive site in a living anionic polymerization persists throughout the reaction so that no termination or chain transfer occurs on the timescale of the reaction. Because there is no termination, monomers can be sequentially polymerized to yield well-defined block copolymers. Through the use of anionic living polymerization, polymers can be synthesized with controlled molecular weight, composition, and functional groups. Anionic polymerization can be used to control the microstructure of diene (e.g. isoprene, butadiene) polymerizations, and high 1,4-structured polybutadiene can be obtained by performing anionic polymerization of butadiene in non-polar solvents. Subsequent hydrogenation of high 1,4-content polybutadiene leads to a polyethylene structure. Through this sequence, polyethylene-based block copolymers

as AEMs can be prepared by living anionic polymerization and post functionalization.

In this study, polybutadiene-b-poly(4-methylstyrene) (PB-b-P4MS) block copolymer was synthesized by living anionic polymerization. The high 1,4-structured polybutadiene block was hydrogenated to polyethylene-like block and the poly(4-methylstyrene) block was ultimately converted to an ion conductive block. The following research investigates in detail the block copolymerization, hydrogenation, and cationic group functionalization reactions. The polyethylene block copolymer membranes are prepared to study their properties, including water uptake, hydration number, ionic conductivity, and morphology.

4.2 Experimental Section

4.2.1 Materials

4-Methylstyrene (Sigma-Aldrich, 96%) was dried over calcium hydride and distilled under reduced pressure two times before use. 1,3-Butadiene (Sigma-Aldrich, ≥99%) was transferred from the gas cylinder to an argon purged pressure vessel containing calcium hydride and a stir bar while cooling the vessel to -78 °C with an acetone/dry ice bath. The butadiene stirred over the calcium hydride for approximately 20 minutes right before use. *sec*-Butyllithium (*sec*-BuLi) (1.4 M in cyclohexane) solution and di-*n*-butylmagnesium (1.0 M in heptane) solution were obtained from Sigma-Aldrich and used as received. 2,2'-Azobisisobutyronitrile (AIBN) (Sigma-Aldrich, 98%) was purified by recrystallization in methanol, and N-bromosuccinimide (NBS) was recrystallized from deionized water. HPLC grade cyclohexane from Fisher was purified by passing through columns on a Pure Solv solvent purification system (Innovative Technology). 2,6-Di-*tert*-butyl-*p*-cresol (BHT, Eastman), xylenes (Mall, ACS

reagent grade), *p*-toluenesulfonyl hydrazide (TSH) (Sigma-Aldrich, 97%), carbon tetrachloride (Sigma-Aldrich, 99.9%) and trimethylamine (Sigma-Aldrich, 25 wt% aqueous solution) were used without further purification. All polymerization glassware, glass syringes, needles, and stir bars were dried in the oven at 180 °C overnight and the glassware was further flame dried under an argon purge after equipped with stir bar and sealed with a rubber septum.

4.2.2 Anionic Polymerization of Polybutadiene-b-Poly(4-Methylstyrene) (PB-b-P4MS)

Polymerizations were conducted at room temperature. A series of block copolymers (A, B, C, and D) were synthesized following the same polymerization procedure while varying the relative composition of butadiene and 4-methylstyrene blocks. A typical procedure (copolymer A) is as follows.

Dry cyclohexane (50 mL) from solvent purifier was added to a septum sealed, flame dried and argon purged 100 mL round bottom flask equipped with a stir bar. *sec*-BuLi (100 μL, 0.14 mmol) was then injected with a 250 μL syringe. The solution turned to a pale yellow and was allowed to stir for 15 min. An argon purged pressure vessel containing butadiene (7.22 g, 0.133 mol) over calcium hydride was connected to the round bottom flask with a cannula. The pressure vessel was gently warmed and the butadiene was transferred from the pressure vessel to reaction flask over 15 to 20 min. The cannula was then removed and the reaction was left to stir for 24 hrs. An aliquot (1 mL) of reaction solution was removed by syringe after 24 hours and added to argon degassed methanol to terminate a sample of polybutadiene. 4-methylstyrene (5.10 mL, 39.5 mmol) was introduced into the reaction flask using a 5 mL syringe. A bright orange color was immediately observed and the reaction solution was left to stir for 12 hrs. After this time, a small amount of argon-purged methanol was introduced by syringe to terminate the

living polymer chain ends as observed by the disappearance of the orange color. The polymer solution was precipitated into excess methanol containing 2,6-di-*tert*-butyl-*p*-cresol (0.2 g, about 0.02 wt% of polymer) as radical inhibitor, and the polymer was isolated by filtration, washed with more methanol, and dried in the vacuum oven at 40 °C overnight. The conversion of styrene was determined to be approximately 50%. ^{1}H NMR (500 MHz, $CDCl_3$, δ): 2.25-2.35 (s 3H –CH_3); 4.85-5.00 (m 2H -CH_2-CH(CH=CH_2)-); 5.28-5.51 (m 2H -CH_2-CH=CH-CH_2-); 5.65-5.80 (m 1H -CH_2-CH(CH=CH_2)-); 6.33-7.19 (m 4H ArH).

4.2.3 Hydrogenation of PB-b-P4MS Block Copolymer

Hydrogenation of the polybutadiene block in the copolymer was performed by using *p*-toluenesulfonyl hydrazide to form polyethylene-b-poly(4-methylstyrene) (PE-b-P4MS). In a general procedure for copolymer A, PB-b-P4MS (1.012 g, 0.015mol butadiene repeat units) was weighed into a 250 mL three neck round bottom flask equipped with a magnetic stirbar, a condenser, and an argon bubbler. Xylenes (80 mL) was added into the reaction flask and after dissolution the reaction flask was immersed in an oil bath and heated to 120 °C. *p*-Toluenesulfonyl hydrazide (22.3 g, 0.12 mmol) was added, and the solution was allowed to stir for 12 hrs. The hot solution was precipitated in an excess of methanol, filtered, and the white powder was washed with hot deionized water to remove byproducts. The final polymer was recovered by filtration and dried in the vacuum oven at 80 °C overnight.

4.2.4 Bromination of P4MS Homopolymer

The bromination of the poly(4-methylstyrene) block in PE-b-P4MS was performed by using NBS and BPO following a modified literature procedure.[32, 156] P4MS (0.3556 g, 3.00

mmol 4-methylstyrene repeat units) was weighed into a two neck 50 mL round bottom flask equipped with a magnetic stirbar, a condenser, and an argon bubbler. Carbon tetrachloride (15 mL) was added and the polymer was suspended in solution. The reaction flask was immersed in an oil bath and heated to 72 °C. The mixture was stirred until the copolymer dissolved. AIBN (0.0075 g, 0.045 mmol) was added followed by NBS (0.481 g, 2.70 mmol, 90 mol% to the amount of 4-methylstyrene) under argon flow. The solution was refluxed and allowed to stir for 24 hrs during which the solution turned yellow. The hot solution was precipitated into excess methanol, filtered, and the yellow powder was washed with deionized water to remove byproducts. The product was filtered and dried in the vacuum oven at 80 °C overnight.

4.2.5 Bromination of PE-b-P4MS Block Copolymer

The bromination of poly(4-methylstyrene) block in PE-b-P4MS was performed by using the same condition as bromination of P4MS homopolymer. In a typical reaction condition (copolymer A), PE-b-P4MS (1.3837 g, 2.70 mmol 4-methylstyrene repeat units) was dissolved in 50 mL of carbon tetrachloride in a two neck 150 mL round bottom flask. The solution was heated in oil bath to 72 °C with stirring under the argon atmosphere. AIBN (0.0065 g, 0.040 mmol) was first added into reaction and NBS (0.432 g, 2.43 mmol, 90% to the amount of 4-methylstyrene) were added right after AIBN into reaction flask with argon protection. The solution was refluxed and allowed to stir for 24 hrs. The color turned to yellow after the bromination. The hot solution was precipitated in excess of methanol, filtered, and the yellow powder was precipitated repeatedly by methanol to remove byproducts. The polyethylene-b-polyvinylbenzyl bromide (PE-b-PVBBr) was finally filtered and dried in the vacuum oven at 80 °C overnight.

4.2.6 PE-b-PVBBr Block Copolymer Membrane Preparation

PE-b-PVBBr block copolymer powder was dissolved at 90 °C in xylenes with a concentration of 3g/100mL. The solution was drop cast on a 80 °C pre-heated glass slide and the xylenes was allowed to evaporate. The resulting membrane was dried in vacuum oven at 80 °C overnight to remove remaining xylenes.

4.2.7 Amination of PE-b-PVBBr Block Copolymer Membrane

The PE-b-PVBBr membrane was soaked in a 25 wt% aqueous trimethylamine solution for 48 hours to convert benzyl bromide to benzyltrimethylammonium bromide ([VBTMA][Br]). The PE-b-P[VBTMA][Br] membrane was then repeatedly immersed in fresh deionized water multiple times, rinsed thoroughly with water, and then dried in a vacuum oven at 60 °C overnight.

4.2.8 Ion Exchange of Hydroxide Membrane

The quaternary ammonium functionalized block copolymer membranes were soaked in 1M KOH solution for 48 hrs to exchange bromide to hydroxide. The membranes were subsequently immersed in deionized water for a few hours with the deionized water exchanged several times during the soaking process.

4.2.9 Characterization

The molecular weights and molecular weight distributions for polybutadiene and PB-b-P4MS were determined by gel permeation chromatography (GPC) using a Waters 600 HPLC pump equipped with a Wyatt Technology Optilab RI detector and a Wyatt Technology

miniDAWN multiangle laser light scattering (MALLS) detector. Elutions were carried out with two Polymer Laboratories PLgel 5μm Mixed-D columns at room temperature with THF at a flow rate of 1.0 mL/min. Samples were dissolved in THF at 5 mg/mL and molecular weights were measured using Astra software supplied by Wyatt Technology. ^{1}H NMR spectra of copolymers were obtained using a JEOL 500 MHz spectrometer. All polymer samples were dissolved in $CDCl_3$ using tetramethylsilane (TMS) as standard. IR measurements were performed by attenuated total reflectance (ATR)-Fourier transform infrared (FTIR) spectroscopy using a Thermo-Electron Nicolet 4700 spectrometer with a Smart Orbit attachment in a spectral range of 500 – 4000 cm^{-1}. Glass transition temperatures (T_g) and crystallinity of membranes were determined by differential scanning calorimetry (DSC) on TA DSC-20 running TA software with a heating rate of 10 °C/min under a nitrogen purge. The degree of crystallinity was calculated by comparing the enthalpy of the DSC tested sample with the enthalpy value for 100% crystallized polyethylene.[157, 158]

Theoretical ionic exchange capacities (IECs) were calculated based on the complete conversion of benzyl bromide to quaternary ammonium. Titrated IEC was determined for samples in the bromide form by the Mohr's titration method.[54, 159] The membranes were dried in a vacuum oven at 60 °C for 24 hours, and their dry weights were quickly measured. About 0.10 g membrane was accurately weighed and soaked in 50 mL 0.2 M $NaNO_3$ solution for 8 hours. After 8 hours, the film was transferred into fresh 0.2 M $NaNO_3$ solution for another 8 hours. This process was repeated a total of 3 times in 24 hours to exchange the bromide ion to nitrate. The $NaNO_3$ solution was titrated to determine the amount of free bromide ions with 0.0992 M $AgNO_3$ solution by using K_2CrO_4 as color indicator. The bromide titration was repeated three times and the titrated IEC was calculated with the equation,

$$\text{IEC}\ (\text{mmol/g}) = \frac{c_{AgNO_3} V_{AgNO_3}}{m_{\text{dry membrane}}}$$

where c is the concentration of $AgNO_3$ solution, V is the volume of the $AgNO_3$ solution consumed during titration, and $m_{\text{dry membrane}}$ is the dry mass of the membrane.

In order to determine water uptake of AEMs, membranes were pre-soaked in deionized water. After 24 hrs soaking, the fully hydrated membranes were removed from the water and the extra water on the membrane surface was blotted dry with kimwipes, and the membrane was weighed immediately. The quaternized membranes were immersed again into deionized water for another 15min to let them re-hydrate. This method was repeated 5 times to obtain the average mass of hydrated membranes. The membranes were finally vacuum dried at 60 °C for 24 hr. The water uptake (WU) was determined by

$$\text{WU}\ (\%) = \frac{m_{\text{hydrated}} - m_{\text{dry}}}{m_{\text{dry}}} \times 100\%$$

where m_{hydrated} is hydrated mass of membrane after removing all surface water, and m_{dry} is dry mass of membrane after drying in the vacuum oven.

Synchrotron small angle x-ray scattering (SAXS) experiments were performed at the Advanced Photon Source at Argonne National Lab. Measurements were taken in a transmission geometry using a Pliatus 2M SAXS detector with an acquisition time of 1 s at a beam energy of 12 keV and incoming x-ray wavelength of 1 Å. The 2D scatter was radially integrated to obtain data of intensity versus scattering vector q. The transmission intensity was normalized to exposure time and flux of the direct beam through the sample. An environmental chamber was used to control the temperature and humidity.[127, 128] The humidity was stepped from 25% to 50%, 75%, and 95%RH every 20 minutes in order to hydrate the membrane.

High Angle Annular Dark Field Scanning Transmission Electron Microscopy (HAADF

STEM) was performed using a JEOL 2100F operated at 200kV and HAADF 5 camera length. Samples for HAADF STEM were microtomed on a Leica Ultra cut UCT with a EMFCS cryostage using a microstar diamond knife with a 6° cutting angle. Samples were microtomed at -10 °C to a thickness of 90nm. Samples were transferred from the cryostage to a dessicator in capsules to minimize interaction with water vapor.

The ionic conductivity of quaternized membranes was measured by electrochemical impedance spectroscopy (EIS) using a Bio-Logic VMP3 potentiostat under controlled temperature, and data was collected using EC Laboratories software. Membranes were held in four electrode cells with platinum electrodes. In this work, EIS was performed by changing temperature from 50 °C to 90 °C in water. Activation energy (E_a) of ionic conductivity can be determined by using an Arrhenius relationship between the conductivity and temperature, which can be expressed as

$$\sigma_T = \sigma_0 e^{\frac{-E_a}{RT}}$$

where σ is the ionic conductivity, σ_0 is Arrhenius constant, R is gas constant, and E_a is the activation energy of ionic conductivity under certain relative humidity.

Tensile properties of block copolymer membranes were measured at dry and hydrated conditions on an Instru-Met frame tensile tester (by MTS Model: A30-33) using a 1000-pound load cell (with a resolution less than 0.1 pound) and a crosshead speed of 5 mm/min at room temperature. The dry samples were prepared by drying membranes in a vacuum oven at 60 °C for 24 hours, and the hydrated samples were prepared by soaking membranes in deionized water at room temperature for 24 hours. Samples were cut into strips with dimension of approximately 60 mm x 8 mm and membrane thicknesses were measured in a range of 50 to 80 microns. Stress was calculated from the cross-sectional area of the film and the strain was obtained by measuring

the increase of the film gauge length. The Young's modulus was determined by the initial slope of the stress vs. strain curve at very low strains (0.3%).

4.3 Results and Discussion

Studies have demonstrated random polyethylene copolymers for anion exchange membranes, with the polyethylene providing good mechanical properties, decreased dimensional swelling, and good chemical stability.[63-65] However, well-defined diblock copolymers containing polyethylene as the hydrophobic block for fuel cell membranes have not been investigated. In this work, a polyethylene block copolymer with quaternary ammonium functionality is prepared through a series of reactions. The reaction sequence is designed through a living anionic polymerization to form polybutadiene (PB) with high 1,4 content as a precursor to polyethylene and the controlled polymerization of poly(4-methylstyrene) as a precursor to a benzyl bromide functionality, and ultimately, a benzyltrimethyl ammonium functionality.

PB-b-P4MS block copolymer was synthesized through the sequential anionic polymerization of butadiene and 4-methylstyrene initiated by *sec*-BuLi in cyclohexane (Scheme 4.1). Living anionic polymerization was selected since this technique offers significant advantages over other polymerization methods to synthesize a well-defined PB block with high 1,4 enchainment of monomer. While the anionic polymerization of butadiene has been widely studied, very few references to the anionic polymerization of 4-methylstyrene exist.[160, 161] A block copolymer of butadiene and 4-methylstyrene can be produced through either reacting butadiene or 4-methylstyrene as the first block. However, the chain transfer to toluene in butyllithium initiated anionic polymerization of styrene is well studied,[162] and chain transfer

to the *para*-methyl group is possible during the polymerization. 4-methylstyrene homopolymer has previously been prepared by anionic polymerization and the research indentified the importance of low temperature polymerization and limiting the conversion to less than than 60% in order to avoid chain transfer.[163] In order to synthesize well-defined linear block copolymer and minimize any chain transfer to pendent benzylic methyl groups, the block copolymerization was designed to polymerize butadiene first, followed by polymerization of the 4-methylstyrene. In addition, the 4-methylstyrene polymerization was terminated prior to high monomer conversion.

Scheme 4.1 Sequential anionic polymerization of PB-b-P4MS block copolymer

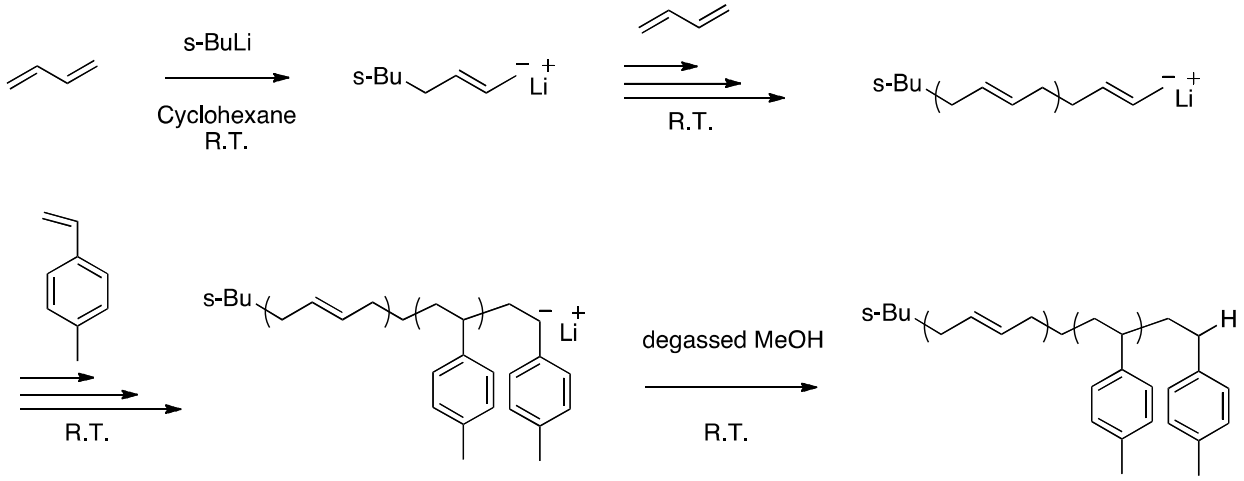

In the first step, the anionic polymerization of butadiene was carried out using *sec*-BuLi in cyclohexane at room temperature following a procedure previously reported.[164] *sec*-BuLi initiated anionic polymerization of butadiene in non-polar cyclohexane solvent has been demonstrated to result in predominately 1,4-structured PB.[165] Linear polybutadienyllithium chains were formed by adding butadiene monomer to the solution of *sec*-BuLi in cylcohexane, resulting in a light yellow color during butadiene polymerization. Once the butadiene

polymerization was completed, a small amount of polymer solution (1 mL) was removed and terminated with degassed methanol for analysis. A series of four PB polymers were produced with molecular weights controlled by the molar ratios of [butadiene]/[sec-BuLi]. The molecular weights were targeted to range between 33,000 and 50,000 g/mol. GPC was used to analyze the molecular weights attained for each PB polymerization and found excellent agreement between the actual and targeted molecular weights, (Table 4.1) indicating complete conversion of butadiene monomer to polymer. The molecular weight distributions of the PB samples are relatively narrow and in the range of 1.05-1.09.

Table 4.1 Characterization of PB and PB-b-P4MS copolymers

Samples	PB block				PB-b-P4MS copolymer			
	[Bd] /[*sec*-BuLi]	M_n[a] (g/mol)	M_w/M_n[a]	1,4-PB[b] (%)	[4MS]/[*sec*-BuLi]	M_n[a] (g/mol)	M_w/M_n[a]	PB : P4MS[b] (wt%)
A	950	50,100	1.08	92	282	64,800	1.16	77 : 23
B	750	39,800	1.06	92	370	61,000	1.08	68 : 32
C	898	47,300	1.09	95	526	75,400	1.13	60 : 40
D	590	32,700	1.05	95	646	68,900	1.14	51 : 49

a) determined by light scattering (GPC); b) measured by ^{1}H NMR spectroscopy

The diblock copolymer was prepared by adding 4-methylstyrene to the living polybutadienyllithium chains. As the 4-methylstyrene was introduced, the solution color changed from light yellow (polybutadienyllithium) to bright orange immediately indicating the successful initiation of 4-methylstyrene. The block copolymerization was terminated by the introduction of degassed methanol and the bright color immediately turned to colorless indicating the termination of all living polymer chains. The polymer solution was precipitated into an excess of

methanol to isolate the block copolymer. A series of PB-b-P4MS diblock copolymers (Table 4.1) was prepared by varying the molar ratio of [4-methylstyrene]/[*sec*-BuLi]. The molecular weight of the P4MS blocks in the different copolymer samples was determined by the difference in the molecular weight of the PB block and the final copolymer measured by GPC. The conversion of 4-methylstyrene was calculated to be approximately 43% to 49% based on the value of [4-methylstyrene]/[*sec*-BuLi].

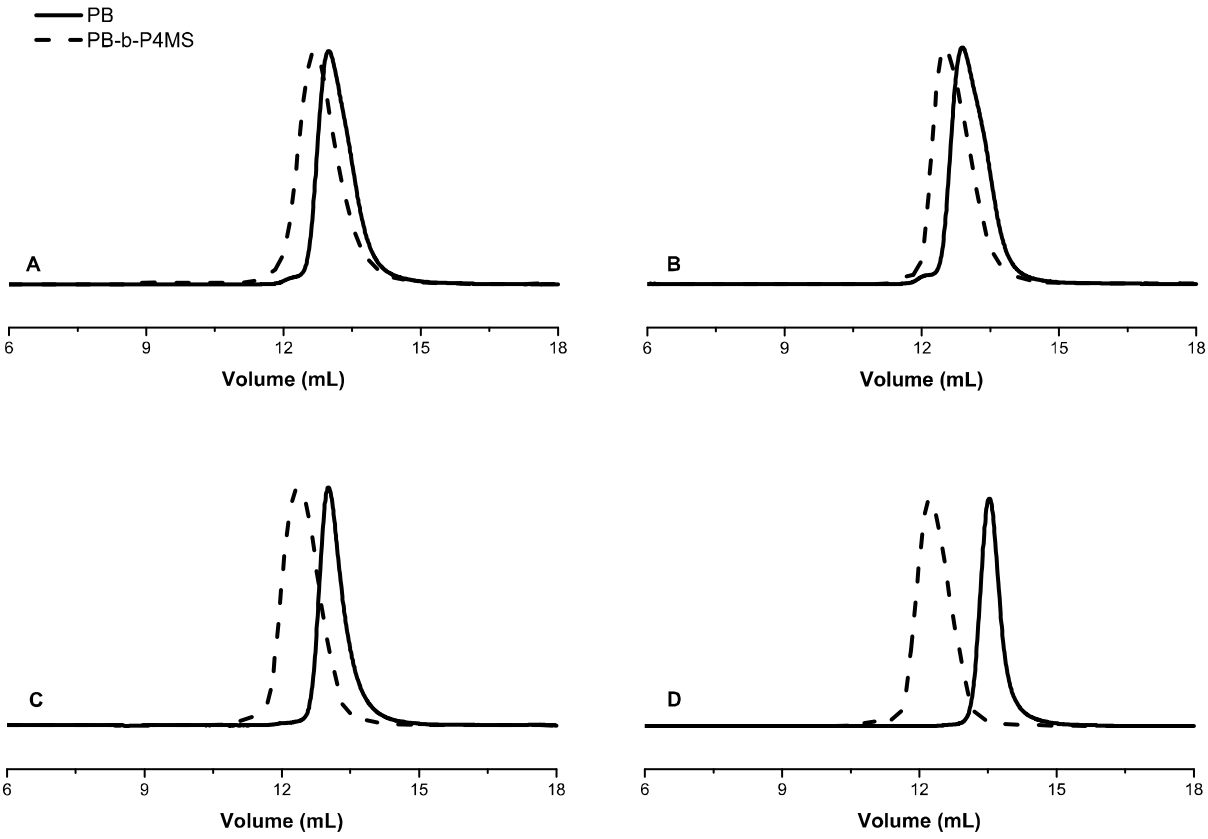

Figure 4.1 a) GPC chromatograms of PB-b-P4MS copolymers a) copolymer A; b) copolymer B; c) copolymer C and d) copolymer D

The progression of the copolymerizations is clearly demonstrated by the GPC chromatograms in Figures 4.1a-d for the four different copolymerizations (copolymers A, B, C

and D). Solid lines represent the first block (PB homopolymer) and the dashed lines show the complete separation from the PB homopolymer in the formation of the PB-b-P4MS copolymer. The dashed peaks shift significantly in all chromatograms indicating complete crossover from polybutadienyllithium to polybutadiene-b-poly(4-methylstyrenyl)lithium. Molecular weight distributions of the block copolymers (M_w/M_n = 1.08-1.16) become only slightly higher after adding the second block. The slight increase in polydispersity could be due to a slow crossover from polybutadienyllithium to polybutadiene-b-poly(4-methylstyrenyl)lithium or to a small amount of chain transfer to the *para*-methyl group. Small shoulders in the high molecular weight region are observed in some chromatograms, presumably a result from polymer chain coupling by oxygen during termination reactions.

The microstructure of the PB block and block composition of copolymers were determined by ^{1}H NMR spectroscopy. Figure 4.2a shows the spectrum of one PB-b-P4MS copolymer (sample C) consisting of characteristic signals of polybutadiene and poly(4-methylstyrene). The peaks at 4.85-5.00 ppm and 5.65-5.80 ppm are signals from the 1,2-structured PB. The peaks at 5.28-5.51 correspond to the two olefinic protons from the 1,4-structured PB.[164] The microstructure in the PB block can be calculated based on the integration of 1,2-structured PB and 1,4-structured PB. The amount of 1,4 configuration is predominant in the microstructure of PB as expected and the composition varies from 92% to 95% for the 4 different samples (Table 4.1). The chemical shift at 2.25 ppm is attributed to the benzylic methyl group from 4-methylstyrene, and the peaks at 6.33-7.19 ppm represent aromatic protons of 4-methylstyrene. The molar composition of PB and P4MS can be readily estimated by comparing integration of characteristic peaks for PB and P4MS. For this sample (copolymer C), the mass composition of PB and P4MS is determined to be 60% and 40%, respectively.

The diblock copolymer was subsequently reacted to hydrogenate the PB block and then quaternary ammonium functionality was introduced to the P4MS block (Scheme 4.2). The hydrogenation and bromination of para-methyl groups were each done in a homogenous reaction, while the final conversion of bromomethyl groups to benzyltrimethylammonium groups was done as a heterogeneous reaction on a solution cast film.

Scheme 4.2 Hydrogenation, bromination and quaternization

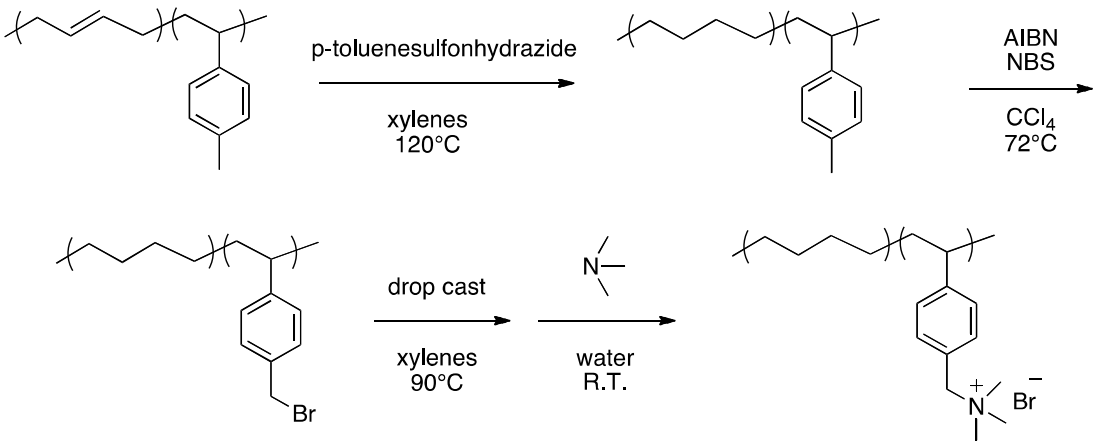

Because the majority of the PB is 1,4-structured, hydrogenation of the PB block results in a predominantly polyethylene-like block with 5-8% ethyl branches. The thermal decomposition of *p*-toluenesulfonhydrazide in xylenes is a common method for converting polydienes to hydrogenated polymers.[166-168] A large excess (molar ratio of [TSH]/[butadiene repeat units] = 8/1) of *p*-toluenesulfonhydrazide was added in this reaction to ensure complete hydrogenation. The resulting hydrogenated polymer remained soluble in xylenes at high temperature, so the polymer was precipitated into methanol while the solution was still hot. The resulting polymers were washed by boiling water for 30 min in order to remove *p*-toluenesulfonic acids formed during the reaction. The hydrogenated polymers were no longer soluble or only partially soluble

in common solvents at room temperature, including THF, toluene, chloroform, tetrachloroethane, and xylenes. The polymer was soluble enough in chloroform at low concentration to perform ^{1}H NMR spectroscopy in order to quantify the extent of the hydrogenation reaction. Figure 4.2b shows the ^{1}H NMR spectrum of PE-b-P4MS copolymer. Comparison with the PB-b-P4MS in Figure 4.2a shows that olefinic proton signals of PB at 4.85-5.80 ppm (including 1,2-structuured and 1,4-structured) completely disappear and new peaks form at 1.51 ppm corresponding to the methylene protons from polyethylene demonstrating the complete hydrogenation.

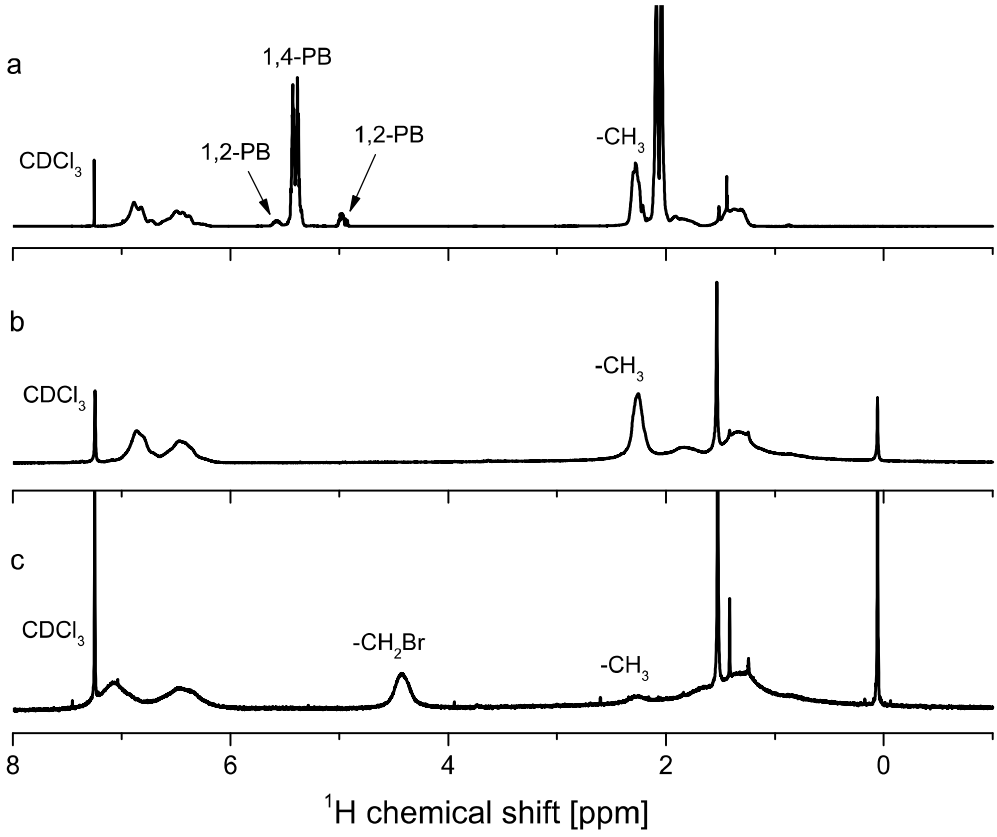

Figure 4.2 ^{1}H NMR spectra comparison of (a) PB-b-P4MS, (b) PE-b-P4MS and (c) PE-b-PVBBr copolymers in $CDCl_3$

A model reaction to brominate the P4MS homopolymer was examined in order to study the bromination of 4-MS repeat units in block copolymer. The reaction was carried out in the presence of AIBN with less than the stoichiometric conversion ([NBS]/[4-methyl group] = 0.9/1

molar ratio) in order to selectively brominate the 4-methyl group with out reacting the tertiary benzylic protons on backbone. ^{1}H NMR spectroscopy was used to evaluate the reaction (Figure 4.3). The intensity of the peak corresponding to the 4-methyl groups at 2.25 ppm reduces after bromination while a new peak at 4.51 ppm represents to the formation of benzyl bromide groups. The degree of bromination reaction can be calculated based on the integration ratio between benzyl bromide groups and aromatic groups. Furthermore, the integration ratio between methylene protons (1.34 – 1.64 ppm) and tertiary benzylic proton (1.64 – 2.05 ppm) on backbone remained the same after the bromination reaction. From the results, it is expected that the reaction could be used to quantitatively synthesize the PE-b-PVBBr block copolymers with only 4-methyl groups bominated.

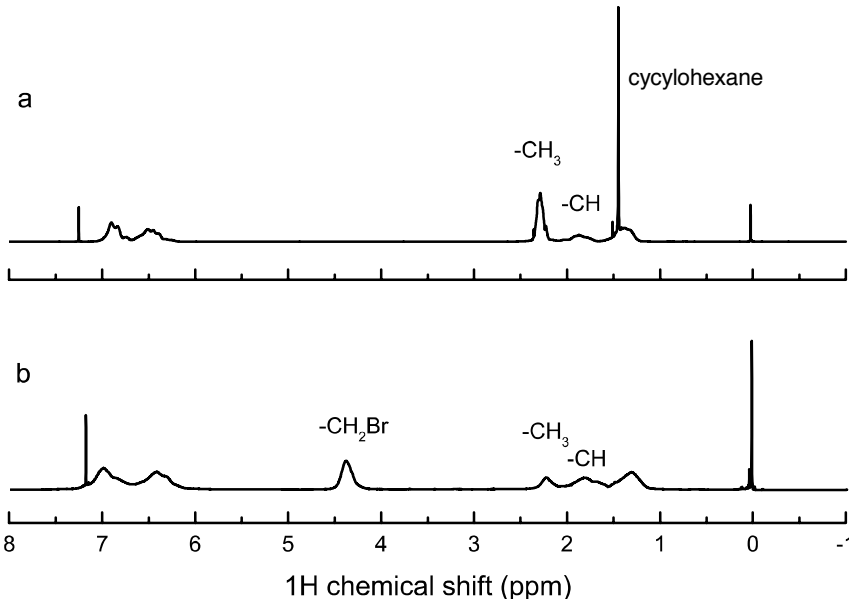

Figure 4.3 ^{1}H NMR spectra of (a) P4MS homopolymer and (b) P4MS after bromination reaction

Bromination of PE-b-P4MS copolymer was conducted after hydrogenation reaction, since the selective bromination of the 4-methyl groups is desired. The bromination reaction was

carried out at 72 °C in carbon tetrachloride and the polymer remained in solution during the reaction. The solution color changed to light yellow when NBS was added, and the stoichiometric ratio of NBS and 4-methyl groups was the same as the model bormination reaction in order to exclusively introduce bromine functional group on 4-methyl groups. After 12 hours of reaction, the light yellow polymer (PE-b-PVBBr) was obtained by precipitation in methanol and isolation by filtration. Figure 4.2c shows the ^{1}H NMR spectrum of PE-b-PVBBr after vacuum drying and it is compared with ^{1}H NMR spectrum of PE-b-P4MS (Figure 4.2b). The chemical shift at 2.25 ppm corresponding to 4-methyl groups reduces significantly after bromination, at the same time, a new peak at 4.51 ppm corresponding to benzyl bromide is observed in Figure 4.2c. It is reasonable to observe some remaining 4-methyl groups after bromination since NBS with less than 1 equiv of 4-MS was used in this reaction. The degree of bromination on 4-MS can be determined by the integration ratio between benzyl bromide groups and aromatic groups. The degree of bromination is calculated in a range of 81.8% to 84.6% (Table 4.2) depending on copolymer samples. Therefore, quantitative control over bromination of 4-MS block was successfully achieved.

The PE-b-PVBBr was cast into membrane prior to the amination reaction, since the amphiphilic material after quaternization is difficult to process into a membrane. PE-b-PVBBr powder was dissolved in 90 °C xylenes and cast on a hot plate held at 80 °C, keeping the copolymer in solution while the solvent slowly evaporated. The PE-b-PVBBr membrane remained clear and homogeneous after holding at 80 °C for 1 hr. The membrane was then dried in a vacuum oven at 80 °C to remove remainin xylenes. The PE-b-PVBBr copolymer membranes were examined by DSC to determine the degree of crystallinity of the PE component in the film.

All membranes were found to have a similar amount of crystalline structure in the range of 24.1% to 25.7% (Table 4.2).

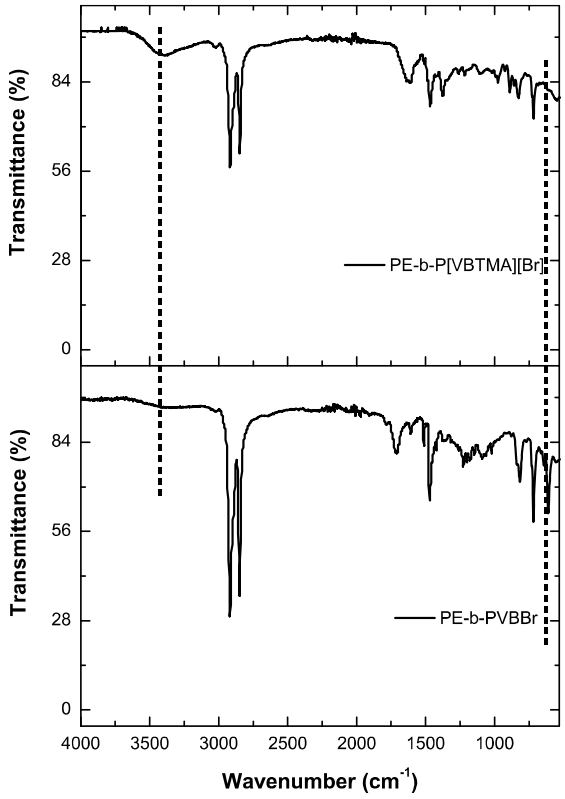

Figure 4.4 Infrared spectra of PE-b-PVBBr and PE-b-P[VBTMA][Br]

The amination reaction was done by soaking PE-b-PVBBr membrane in trimethylamine aqueous solution at room temperature for 48 hr. The resulting PE-b-P[VBTMA][Br] membrane was immersed in deionized water, then rinsed with large amount of water and dried in vacuum oven to remove extra trimethylamine. Examination of the quaternization reaction was done by IR spectroscopy (Figure 4.4). The characteristic peak at 618 cm^{-1} corresponding to a C-Br stretch mostly disappears after amination, indicating high conversion in the quaternization reaction. Additionally, a new peak forms at 3364 cm^{-1} corresponding to water from the hygroscopic quaternary ammonium cation in membrane.

The theoretical IECs of the quaternized membranes were compared with their titrated IECs in Table 4.2. The theoretical IEC was calculated based on the composition of 4-MS in the copolymer and the degree of bromination in each of the different copolymers. The titrated IEC was determined by the well-established Mohr's titration method. The comparison shows that the quaternization reaction reached high conversion of 83-93%, in agreement with the IR spectroscopy results.

Table 4.2 IEC, water uptake, and conductivity of PE based anion exchange membranes

Copoly -mer AEMs	Degree of Bromination[a] (%)	Degree of crystallinity[b] (%)	Theoretical IEC[c] (mmol/g)	Titrated IEC[d] (mmol/g)	Water uptake[e] (%)	σ[f] (mS/cm)
A	82.5	24.1	1.38	1.17	15	24 (7.1)
B	84.6	25.7	1.78	1.66	26	47 (11)
C	83.1	25.1	2.07	1.87	35	70 (18)
D	81.8	24.3	2.30	1.92	37	73 (19)

a) determined by ^{1}H NMR spectroscopy; b) estimated by DSC; c) ^{1}H NMR spectroscopy and complete $N(CH_3)_3$ quaternization; d) determined by Mohr's titration; e) measured in bromide form at room temperature; f) hydroxide and bromide conductivity measured by EIS at 60 °C in water (bromide conductivity in parentheses)

Small angle x-ray scattering (SAXS) characterization was done to examine phase separation of the hydrophobic and hydrophilic components. The quaternized block copolymer membranes were prepared in the bromide counterion form, and SAXS experiments were performed in an environmental chamber at 60 °C by varying the relative humidity from 25% RH to 95% RH. Ordered morphologies were observed in all membranes tested and they all displayed a distinct first order peak and a weak second order peak as shown in Figure 4.5. The d-spacing of

the membranes increased from 48.3 nm to 69.8 nm on going from the lowest cationic functionalized sample to the most highly functionalized sample. The increase in d spacing could be due to the increase in the molecular weight of the hydrophobic domain in membranes. All SAXS profiles displayed little response during the humidity change, indicating all membranes are dimensionally stable under changing humidity conditions. This could be due to the semi-crystalline structure in membrane matrix causing restricted structural swelling.

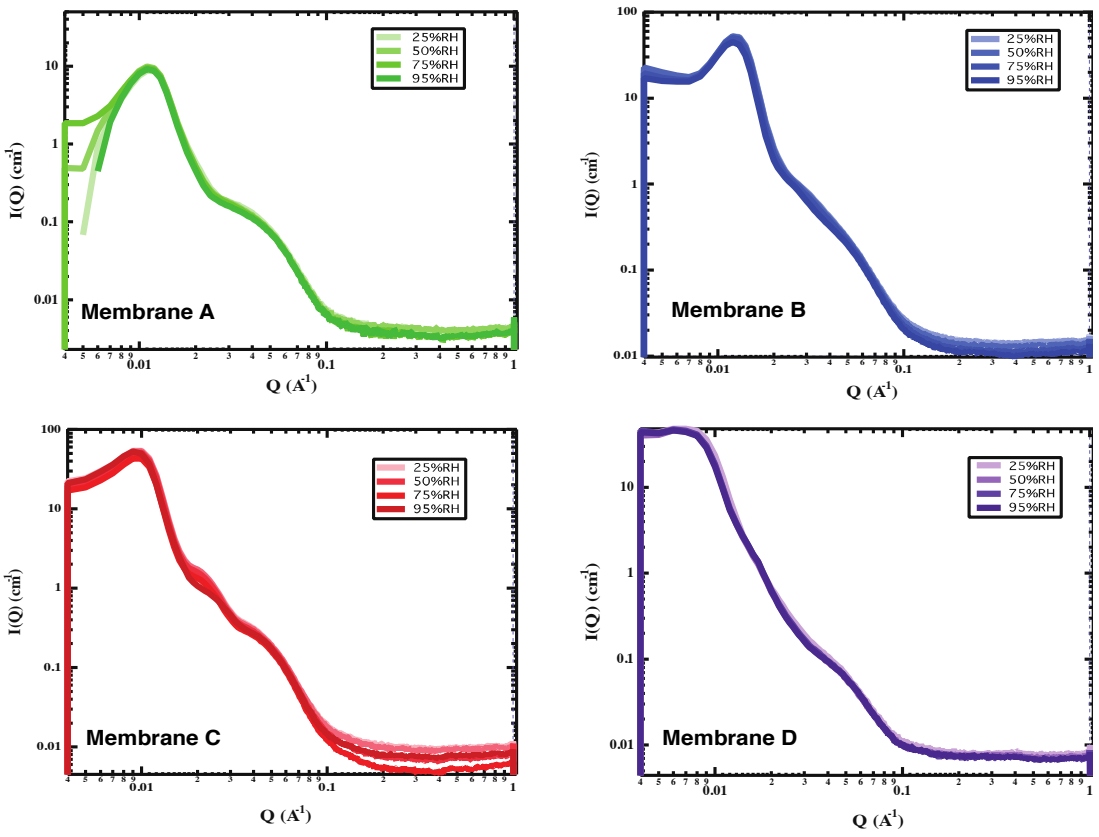

Figure 4.5 SAXS profiles of quaternized polyethylene block copolymer AEMs

Although the structural features were observed in all SAXS profiles, the peaks were relatively broad in all cases leading to the difficulty in the interpretation of the membrane morphologies. Therefore, high angle annular dark field scanning transmission electron microscopy (HAADF STEM) was performed on all membranes to further study the phase-

separated morphology in the PE block copolymer membranes. The corresponding HAADF STEM images revealed distinct hydrophilic (represented by bright areas) and hydrophobic (represented by dark areas) phase separation. The STEM image of membrane C in Figure 4.6 clearly exhibits a bi-continuous morphology with a domain size of approximately 35 nm.

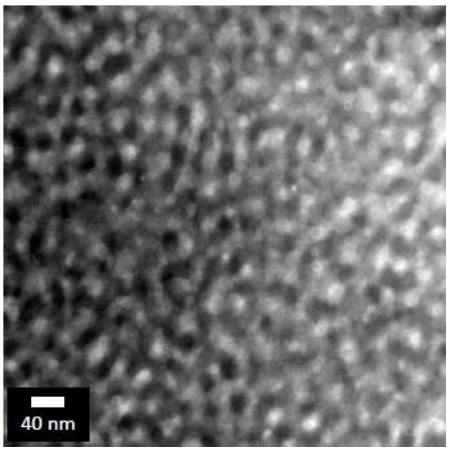

Figure 4.6 HAADF STEM of images of PE block copolymer membrane C

The four different polymer membranes were prepared with a range of ion exchange capacities that is dependent on the block composition of the copolymer precursor and the extent of bromine functionalization. The water uptake of the block copolymer membranes increases with increasing ion exchange capacity from 15% to 37% going from the low functionalized membrane to the most highly functionalized membrane. The water uptake values of block copolymer membranes are relatively lower than other AEMs with similar ion exchange capacity and the same cationic functional groups,[23, 56, 68, 169] which could be attributed to the crystalline structure in the hydrophobic matrix.

The bromide and hydroxide conductivity of all block copolymer AEMs were measured by electrochemical impedance spectroscopy and are reported for measurements at 60 °C in Table 4.2. The ionic conductivity is found to increase with increasing IEC and the concomitant water

uptake as expected, due to the increase in the number of charge carriers. The membranes C and D show close values in ionic conductivity, in agreement with the observation in their ion exchange capacities. The hydroxide conductivities are approximately 4 times higher than the bromide conductivity.

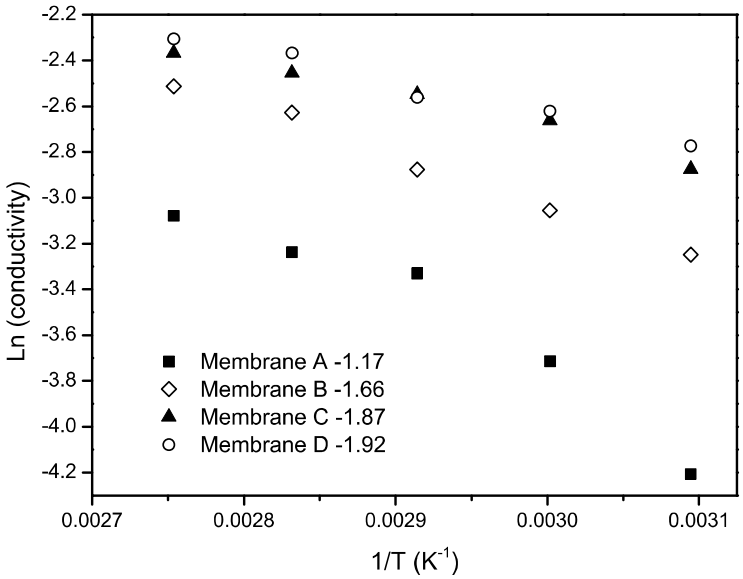

Figure 4.7 Conductivity temperature dependence of PE based block copolymer anion exchange membranes

The hydroxide conductivities of block copolymer membranes were further examined in Figure 4.7 by sweeping temperature from 50 °C to 90 °C and the conductivity increases with the increasing temperature in all membranes. Furthermore, this method allows the calculation of activation energy for ion conduction in block copolymer membranes by an Arrhenius relationship. The activation energy was found to be dependent on the ion exchange capacity. The higher functionalized membrane shows lower activation energy and the activation energy calculated for hydroxide membranes ranged from 27 kJ/mol to12 kJ/mol going from the least functionalized to the most highly functionalized membranes. The activation energies of

hydroxide membrane are only slightly higher compared to the activation energies reported for Nafion (5-20 kJ/mol).[34, 170, 171] However, the activation energies determined for block copolymer membranes are very comparable with the values for other AEMs,[24, 34, 54, 172] which could correspond to the formation of some extent of ordered morphological structure for ion conduction.

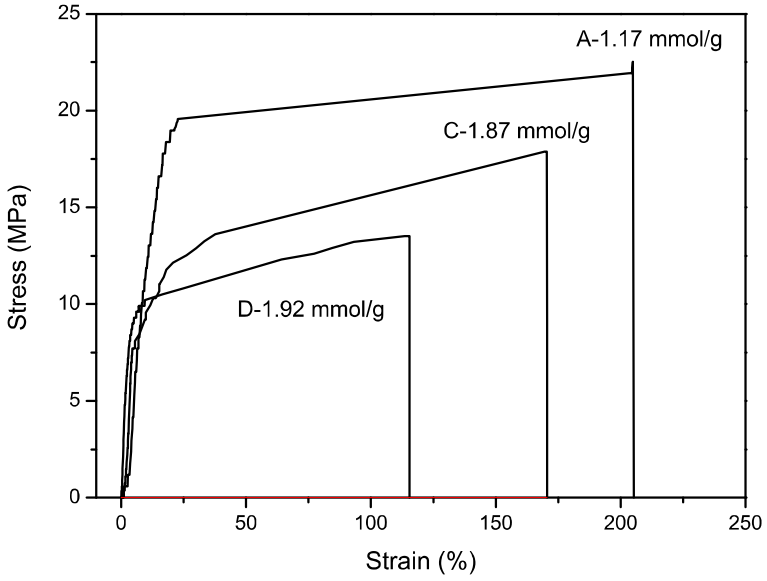

Figure 4.8 Stress vs. strain curves of membrane A, C, and D at room temperature and dry condition

4.4 Conclusion

Polyethylene block copolymer AEMs were formed through the preparation of anionic polymerization of PB-b-P4MS and subsequent post functionalization reactions. The PB with high 1,4-configuration was hydrogenated to a polyethylene hydrophobic block with semicrystalline structure. The polyethylene block copolymer AEM exhibited excellent tensile properties with a high strain at break (over 100%). The block compositions were varied to alter the IEC and control the morphology. The ordered morphologies were observed in all membranes

and bi-continuous morphology was found in the membrane with high IEC. The activation energy was strongly dependent on IEC and the sample with higher IEC displayed values comparable to Nafion. The results suggest promise for utilizing semi-crystalline block copolymer for AEM application.

4.5 Acknowledgement

This work was funded by the Army Research Office through a MURI (grant # W911NF-10-1-0520). NMR spectroscopy was made possible through a grant from the NSF MRI program (grant # CHW-0923537). The authors also want to thank Blake Whitley and Prof. Kip Findley for their assistance with membranes tensile testing.

CHAPTER 5 MONO METHOXY POLY(ETHYLENE GLYCOL) GRAFTED BLOCK COPOLYMERS FOR ALKALINE EXCHANGE MEMBRANE

5.1 Introduction

Alkaline fuel cells using anion exchange membranes as electrolyte have recently aroused considerable interest because it can overcome the carbonate precipitation issue in traditional alkaline fuel cells (aqueous KOH as electrolyte) while still maintaining the advantages of a traditional alkaline fuel cell.[8, 11] The main advantages of anion exchange membrane fuel cell (AEMFC) include facile electrokinetics at the cathode and the ability to use non-precious metal catalysts under the high pH operation conditions.[9, 10, 22]

However, AEMFCs suffer from a few drawbacks compared to proton exchange membrane fuel cell (PEMFC). First, the conducting ion in AEMFC, hydroxide, has a lower diffusion coefficient than protons due to its larger size compared to proton.[23, 173] Therefore, the anion exchange membranes (AEMs) commonly exhibit lower ion conductivity than proton exchange membranes (PEMs), which could result in a difficulty to reach a similar fuel cell performance as PEM. Secondly, it is found that the conductivity of AEMs exhibit strong dependence on the humidity. Research has been performed to study the humidity effect on conductivity of benzyltrimethylammonium functionalized AEM compared to the PEM, Nafion.[24] Although the humidity dependence problem is also observed in PEM,[174] the benzyltrimethylammonium functionalized AEM displays a more significant decrease in conductivity relative to Nafion when the humidity drops. Consequently, both drawbacks could limit the broad application of AEMFC.

Various strategies have been applied to overcome the drawbacks in current AEMs. Research efforts have recently sought to increase hydroxide conductivity of membranes by incorporation of new cationic functional groups and the control of the microphase separation.[69, 82, 85, 88-90, 94] AEM studies have also focused on water movement of AEMFC in order to reduce the dependence of conductivity on humidity by improving the water management.[175] Additionally, a hybrid fuel cell has been developed to take the advantages of high conducting electrolyte (such as Nafion) in PEMFC and better electrokinetics in AEMFC.[176, 177] This hybrid fuel cell comprises an acidic electrode from PEMFC as anode and a basic electrode from AEMFC as cathode. The formation of water at the junction of PEM and AEM makes this hybrid electrolyte possess a self-humidifying feature, which could potentially reduce the humidity effect on conductivity.

Although research efforts have attempted to solve the drawbacks of AEMs through various methods, the importance of AEM water affinity on conducting properties and its humidity dependence are not fully understood. It is found that the sulfonic acid functionalized PEM has a higher hydration number (average water molecules per functional group) than the quaternary ammonium functionalized AEM with similar number of functional groups.[178] Furthermore, in order to attain the same level of conductivity, AEM commonly requires the presence of more water or a higher hydration number than PEM.[56, 108, 169, 179, 180] This can be explained by the lower dissociation constant of quaternary ammonium hydroxide in AEM compared to sulfonic acid in PEM, so more water molecules are required for quaternary ammonium hydroxide to dissociate to reach the high conductivity.[181, 182] However, the increase in hydration number is generally achieved by increasing ion exchange capacity in most studies,[34, 83, 95] which could complicate the study of hydration effect on membrane

properties.

In order to investigate the hydration number effect on membrane properties independently without increasing the functionality, we have developed a simple method to graft hydrophilic polymer onto AEM with no increase in ion exchange capacity. Mono methoxy polyethylene glycol (mPEG) is a water soluble polymer that can be used to graft onto polyvinylbenzyl chloride-b-polystyrene (PVBC-b-PS) copolymer. The mPEG grafted PVBC-b-PS can be further converted to cationic functionalized polymer for ion conduction. The overall result is to graft mPEG onto what ultimately becomes the ion conducting component of the block copolymer. The research investigates in detail the grafting reactions of PVBC-b-PS and the subsequent amination reaction. The effect of mPEG grafts on the membrane properties, including water uptake, hydration number, ionic conductivity and its dependence on humidity, is also investigated.

5.2 Experimental

5.2.1 Materials

Styrene (99%) and 4-vinylbenzyl chloride (VBC) (90%) were obtained from Aldrich, dried over calcium hydride, and distilled under reduced pressure right before use. 2,2,6,6-tetramethyl-1-piperidinyloxy (TEMPO) (Aldrich, 98%) was sublimed twice before use. Mono methoxy poly(ethylene glycol) (mPEG) (Aldrich, M_n = 2,000 g/mol), sodium hydride (Aldrich, powder) and trimethylamine (Aldrich, 25 wt% aqueous solution) were used as received. Benzoyl peroxide (BPO) was purified by recrystallization from 40:60 chloroform:methanol.[183] HPLC grade THF and toluene from Mall were purified by passing through columns on a

commercial system (Innovative Technology). Other reagents were used without further purification.

5.2.2 Synthesis of PVBC-b-PS by Nitroxide Mediated Polymerization

10 mL distilled VBC was introduced into a 50 mL round bottom flask containing BPO (56 mg, 0.4 mmol), and TEMPO (62 mg 0.4 mmol), and the reaction flask was sealed with a rubber septum. The mixture was stirred to dissolve reagents while purging with argon for 30 minutes. The reaction flask was heated to 125 °C for 3 hours, and the nitroxide end-functionalized PVBC was purified by repeated precipitation in methanol. Nitroxide end-functionalized PVBC was vacuum dried at 60 °C for 20 hours and used as a macro-initiator to copolymerize styrene in a bulk reaction. 10 mL styrene was added into a round bottom flask with 250 mg macro-initiator. The copolymerization was carried out at 125 °C for 1 hour and the reaction solution was precipitated into methanol to isolate the block copolymer. The copolymer was purified by re-precipitation in methanol and dried in a vacuum oven at 60 °C. ^{1}H NMR (500 MHz, $CDCl_3$, δ): 6.21-7.26 (9H, ArH), 4.37-4.65 (2H, CH_2Cl), 1.65-2.18 (2H, CH), 1.19-1.65 (4H, CH_2).

5.2.3 Synthesis of mPEG Grafted PVBC-b-PS

PVBC-b-PS copolymers were grafted by reacting the pendent benzyl chloride groups on PVBC block with the hydroxyl end group on mPEG. mPEG and PVBC-b-PS copolymer were dried by azeotropic distillation in toluene at 170 °C before the reaction.[184] An example procedure follows (membrane D-1): All reactions were conducted under an argon atmosphere and carried out at room temperature. 0.52 g azeotropic dried mPEG polymer (0.26 mmol of

hydroxyl end groups) was weighed and dissolved in 5 mL dry THF. The mPEG polymer solution was subsequently added dropwise into a stirred flask with an excess amount of sodium hydride (12 mg, 0.50 mmol) dissolved in dry THF. The deprotonation reaction was carried out for 2 hours and the obtained alkoxide solution was again added slowly into another flask containing 3.5 g azeotropic dried PVBC-b-PS (7.8 mmol of benzyl chloride groups) and 15 mL dry THF, and the resulting reaction was left to stir for 48 hours. The mPEG grafted copolymer was isolated by precipitation in the deionized water. The final polymer was purified by repeated precipitation in hot (80 °C) deionized water. Other samples were grafted using the same procedure with different amounts of mPEG calculated to produce the desired number of grafts in the copolymer and the amount of sodium hydride calculated as approximately twice the amount of hydroxyl groups in mPEG.

5.2.4 Membrane Preparation And Water Solubility Test

mPEG grafted polymer was dried overnight in a vacuum oven at 60 °C. A solution of approximately 5 wt% copolymer in THF was prepared and sonicated for 30 minutes. The copolymer solution was drop-cast onto a glass slide and the membrane isolated by evaporating the THF in the fume hood. The obtained membrane was dried in a vacuum oven at 60 °C overnight and immersed in water to determine its solubility in water.

5.2.5 Amination of mPEG Grafted Membranes

The water insoluble films were soaked in 100 mL of 25 wt% aqueous trimethylamine solution for 48 hours, then immersed in deionized water, and rinsed repeatedly with more deionized water. The quaternized membranes were dried in a vacuum oven at 60 °C overnight.

5.2.6 Characterization

Average molecular weights and molecular weight distributions were determined by gel permeation chromatography at a flow rate of 1 mL/min THF using a Waters 600 Pump equipped with a Wyatt Optilab DSP refractive index detector, Wyatt MiniDAWN light scattering detector, and 2 PL-gel 5μ Mixed-D columns. ^{1}H NMR measurements were performed on a JEOL ECA-500 spectrometer using $CDCl_3$ as solvent.

Theoretical ionic exchange capacities (IECs) were calculated based on the mPEG graft extent and complete conversion of remaining benzyl chloride to benzyltrimethylammonium chloride. Actual IECs of membranes were measured by hydroxide back titration.[31, 55] Quaternized membranes in the chloride form were immersed in 1 M KOH solution to exchange chloride to hydroxide. The resulting membrane was rinsed with deionized water until the rinse water was neutral. About 0.02 g vacuum dried membranes in hydroxide form were immersed in 10.00 mL of 0.00987 M standardized HCl solution for 48 hr, and the actual IEC was calculated by titration of unreacted HCl using 0.01053 M standardized NaOH solution. The back titration was repeated 3 times for each membrane. The IEC (mmol/g) was obtained by

$$\text{IEC (mmol/g)} = \frac{M_{0hr,\,HCl} - M_{48hr,\,Hcl}}{m_{dry\ membrane}} \qquad (1)$$

where $M_{0hr,\,HCl}$ is the original moles of HCl calculated before hydroxide membrane titration, $M_{48hr,\,HCl}$ is determined by moles of NaOH used in back titration after 48 hours soaking in HCl, and $m_{dry\ membrane}$ is the dry mass (g) of membrane after ion exchange.

Water uptake was measured comparing wet and dry weights of the membranes. The film was soaked in deionized water for two days before the measurement. The surface water was removed and the mass of the hydrated film was determined. The film was immersed in deionized

water again for 15 minutes, and the measurements were repeated 5 times for each sample. The films was then dried in a vacuum oven at 60 °C for 24 hours until constant weight was achieved. The water uptake was calculated using the equation,

$$WU\ (\%) = \frac{m_{hydrated} - m_{dry}}{m_{dry}} \times 100\% \qquad (2)$$

where $m_{hydrated}$ is hydrated mass of membrane after removing all surface water, and m_{dry} is dry mass of membrane after drying in vacuum oven. The hydration number (λ), which is described as average number of water per quaternary ammonium can be calculated based on the given water uptake and titrated IEC,

$$\lambda = \frac{WU}{mw_{H_2O} \times IEC} \qquad (3)$$

Water sorption of the membrane was also tested using a SMS dynamic vapor sorption (DVS) instrument. The sample after drying in the vacuum oven overnight was loaded in the glass sample pan hanging from an ultra sensitive microbalance. The relative humidity is achieved by a proportionally mixing a dry gas (nitrogen) and a water vapor stream controlled by mass flow controllers. Conditions for the experiment were set at 60 °C with different humidity cycles. Samples were first kept at 0% relative humidity for 8h, then the humidity was increased in the sequence of 20%, 40%, 60%, 80%, 95% and then decreased to 0% with the same 20% humidity steps. the sample equilibrated at each humidity for 2h and the cycle was run twice. The equilibrium mass at the end of each step was used to calculate water uptake and hydration number from the isotherm of mass variation versus relative humidity.

Conductivity was measured by electrochemical impedance spectroscopy using a four electrode cell with platinum electrodes equipped with a Bio-Logic VMP3 potentiostat. The

impedance spectra were collected over a frequency range of 0.1 HZ to 10^5 Hz using EC Laboratories software. The hydroxide conductivity was measured under fully hydrated condition at room temperature and 60 °C with the cell immersed in water. Chloride conductivity was measured in an environmental chamber (TestEquity Model 1007H, Moorpark, CA) to control the temperature at 60 °C and varying the humidity from 50%RH to 95%RH. Both conductivity values were calculated with the equation (4),

$$\sigma = \frac{l}{R \times t \times w} \qquad (4)$$

where l, R, t, and w represent the distance between the electrodes, resistance of membrane measured, the thickness, and width of the membrane, respectively.

5.3 Results and Discussion

Despite recent improvement in hydroxide conductivity of AEMs, most AEMs still demonstrate a lower conductivity than Nafion with the same level of charge carriers (measured as ion exchange capacity). In addition, a strong dependence of conductivity on high relative humidity limits the potential for application of AEMs in alkaline fuel cells. Although water management and humidified gas supply might be able to maintain membrane performance, this complicates the engineering that goes into the fuel cell. Moreover, research has shown that ionic conductivity increases with an increase in hydration level,[54] so the effect of hydration number on membrane properties is an important area of investigation.

In order to investigate the hydration effect independently of the cationic functional groups, a sytem is designed to alter hydrophilicity of a membrane with the introduction of a hydrophilic mPEG polymer graft. PVBC-b-PS block copolymer was selected for a grafting

reaction, since the mPEG can be grafted through substitution on the pendent benzyl chloride groups in the PVBC block. The remaining benzyl chloride groups in the polymer are subsequently quaternized by trimethylamine to form the final mPEG grafted anion exchange membrane. The overall sequence of reaction is outlined in Scheme 5.1.

Scheme 5.1 The preparation of mPEG grafted AEM

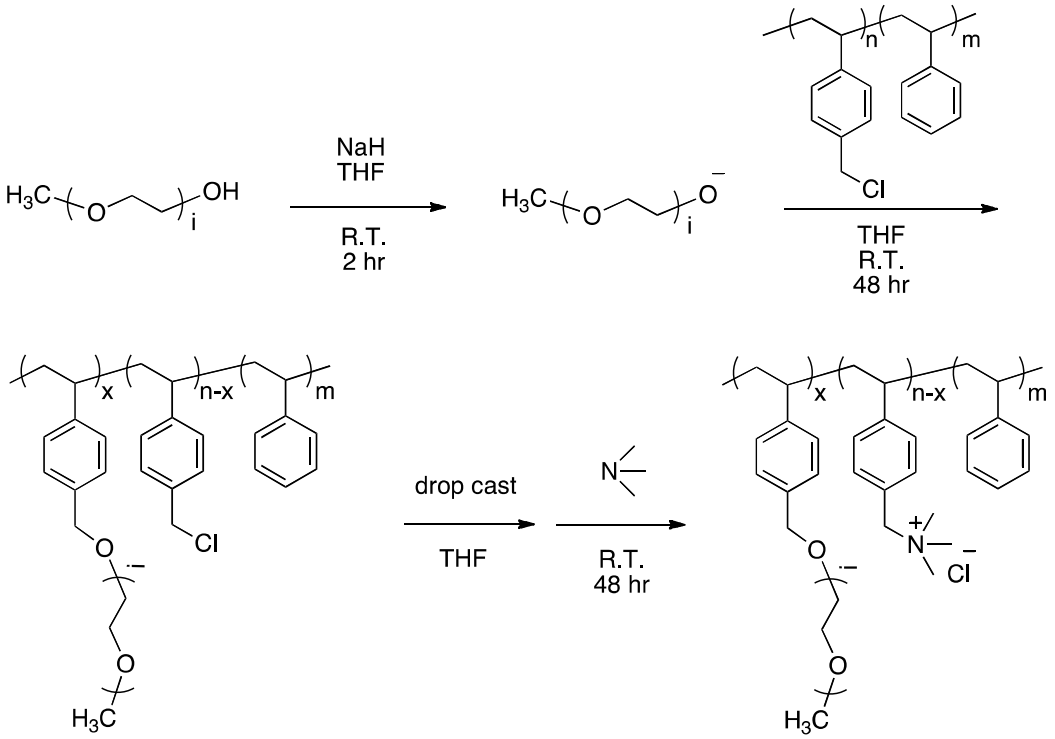

The PVBC-b-PS block copolymer was synthesized by nitroxide mediated polymerization to provide controlled molecular weight and block composition material. The polymerization of VBC was first carried out using BPO as radical initiator in the presence of TEMPO[131, 132, 149] and then the resulting TEMPO end capped PVBC was used as macrointiator to polymerize a styrene block. The procedure and results are more completely described in the Chapter 2. The diblock copolymer was characterized by gel permeation chromatography and had a total

molecular weight of 79,600 g/mol. The diblock copolymer was prepared with the composition of 34 wt% PVBC block and 66 wt% PS block as determined from the ^{1}H NMR spectrum of the copolymer.

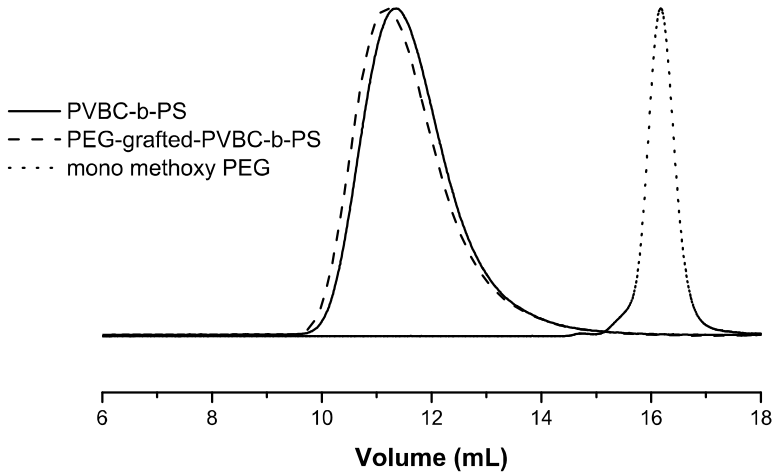

Figure 5.1 GPC chromatograms of mPEG, PVBC-b-PS copolymer, and grafted polymer

The mPEG grafting reaction occurs in two steps, where sodium hydride deprotonates the hydroxyl end functional group in mPEG and then the resulting alkoxide anion can further react with a pendent benzyl chloride to produce the graft structure. First, a simple deprotonation reaction was achieved by reacting mPEG with calculated amount of sodium hydride for 2 hours, as reported in a similar reaction.[119, 185] The resulting alkoxide anion solution was transferred to react with PVBC-b-PS copolymer in THF and the reaction solution became viscous during the reaction. The grafting reaction was left to stir for 48 hours to reach high conversion. Several precipitations were conducted to remove unreacted mPEG homopolymer residue. The graft polymer, PVBC-b-PS and mPEG homopolymer were vacuum dried and subsequently analyzed by GPC (Figure 5.1.) The GPC chromatogram of grafted polymer shows (dash line) a slight but clean separation on both low molecular weight and high molecular weight regions from the

initial PVBC-b-PS copolymer peak. The slight peak shift corresponds to the low graft extent of low molecular weight mPEG after grafting. Signal corresponding to mPEG homopolymer is not observed in the grafted polymer sample, indicating the complete grafting reaction and successful removal of unreacted mPEG homopolymer.

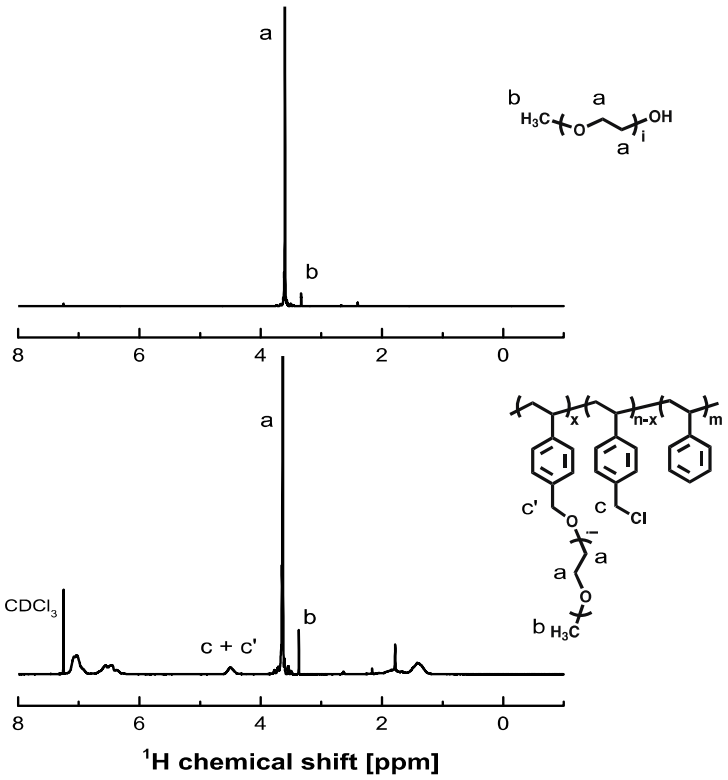

Figure 5.2 ^{1}H NMR spectra of mPEG (top) and mPEG grafted PVBC-b-PS polymer (bottom)

Knowing that no residual mPEG remains after reaction and purification, the ^{1}H NMR spectrum of mPEG grafted PVBC-b-PS is compared with mPEG homopolymer in Figure 5.2 in order to determine the amount of mPEG grafts in the copolymer. The characteristic peak at 4.45 ppm corresponds to the benzylic protons from benzyl chloride and mPEG grafted structure while the protons on the methoxy end group in mPEG have a chemical shift of 3.36 ppm. The amount of mPEG grafted through substitution of the benzyl chloride groups can be calculated based on

the integration of the corresponding peaks. As a result, the mol% of mPEG incorporated through benzyl chloride substitution can be calculated and a wide range of materials with 0.5 mol% to 46 mol% of mPEG grafts are obtained. The amount of mPEG graft in copolymer also can be evaluated as the wt% of mPEG incorporated into copolymer by the equation,

$$\frac{m_{mPEG}}{m_{PVBC\text{-}b\text{-}PS}} = \frac{w_{PVBC} \times G \times MW_{mPEG}}{MW_{VBC}} = 4.46 \cdot G \qquad (5)$$

where m_{mPEG} is the mass of mPEG, $m_{PVBC\text{-}b\text{-}PS}$ is the mass of PVBC-b-PS copolymer, w_{PVBC} is wt% of PVBC block in copolymer, G is the mol% of benzyl chloride grafted, MW_{mPEG} is the molar mass of mPEG, and MW_{vbc} is the molar mass of VBC repeat unit.

PVBC-b-PS copolymers with nine different graft compositions were prepared through the reaction with mPEG. The amount of mPEG graft is reported as both wt% of mPEG added onto PVBC-b-PS copolymer and mole% of benzyl chloride groups reacted by mPEG (Table 5.1). From equation (5), it should be noted that with only a small amount of benzyl chloride groups grafted by mPEG, the mass of mPEG added into the copolymer could be significant. Highly grafted polymers show a good agreement between the theoretically calculated amount of graft and the measured value, indicating high efficiency of the mPEG grafting reaction. However, samples with low graft contents (membranes A and B) displayed a large difference between theoretical and measured graft values, which could be a result from impurities or less control with small amounts of mPEG.

Membrane films were prepared using the THF soluble mPEG grafted PVBC-b-PS materials by drop casting at 5% wt/vol concentration on glass slides. It was expected that polymers with higher mPEG graft content would result in a large increase in the hydrophilicity of the membrane, thus leading to loss of mechanical stability in water or complete dissolution.

Membranes were isolated from glass slides and soaked in deionized water to determine solubility. The results are shown in Table 5.1 and membranes with high graft contents (H-1 and I-1) became soluble in water after the grafting reaction.

Table 5.1 Characterization of mPEG grafting reaction and water solubility

mPEG grafted membrane	Theoretical mPEG grafted[b] (wt%)	Actual mPEG grafted[c] (wt%)	Actual VBC grafted[d] (mole%)	Solubility in water after mPEG graft	Solubility in water after quaternization
A-1	5	2.2	0.5	-	-
B-1	8	4.9	1.1	-	-
C-1	10	7.6	1.7	-	-
D-1	15	13	2.8	-	-
E-1	20	21	4.8	-	+
F-1	40	36	8.0	-	+
G-1	50	40	9.0	-	+
H-1	70	67	15	+	+
I-1	200	205	46	+	+

a) estimated by the feed ratio of sodium hydride, mPEG and PVBC-b-PS; b) wt% of mPEG polymer grafted onto PVBC-b-PS copolymer; c) wt% of benzyl chloride groups grafted and calculated by the equation ^{1}H NMR spectroscopy and (5); d) mol% of VBC reacted by mPEG and measured by ^{1}H NMR spectroscopy.

The grafted membranes that remained insoluble in water were soaked in aqueous trimethylamine solution for 48 hours to convert remaining benzyl chloride groups to quaternary ammonium groups. As the cationic functional groups were formed through substitution of benzyl chloride for trimethylamine, the polymers became even more hydrophilic and the membranes (E-1, F-1, and G-1) with relatively high mPEG graft content became water. The membranes that remained water insoluble were removed from the trimethylamine aqueous solution and subjected to repeated soaking in fresh deionized water every 4 hours. The membranes were finally rinsed with deionized water and dried in a vacuum oven to remove any residual trimethylamine.

The membranes obtained after quaternization with trimethylamine were titrated to determine the conversion of benzyl chloride groups to quaternary ammonium groups. The quaternized membranes in the chloride form were subsequently exchanged to hydroxide in 1 M KOH for 24 hours. The actual IEC was determined by hydroxide back titration method and the results are shown in Table 5.2. The conversion of quaternization reaction can be determined by comparing titrated IEC with theoretical IEC, which can be calculated by assuming complete conversion of remaining benzyl chloride groups in mPEG grafted membrane to benzyltrimethylammonium groups.

Table 5.2 Characterization of mPEG grafted and non-grafted membranes

mPEG grafted membrane[a]	Theoretical IEC[b] (mmol/g)	Titrated IEC[c] (mmol/g)	Water uptake[d] (%)	λ	σ^{e}_{OH} (mS/cm) R.T.	σ^{e}_{OH} (mS/cm) 60 °C
A-2	1.99	1.68	58	19	10	33
B-2	1.94	1.60	80	28	17	44
C-2	1.88	1.57	91	32	22	50
D-2	1.79	1.49	108	40	27	61
J	2.04	1.73	28	9	7.8	25

a) Membrane A-2, B-2, C-2, D-2 were prepared by reacting A-1, B-1, C-1, D-1 with $N(CH_3)_3$, and membrane J was prepared by directly soaking PVBC-b-PS in $N(CH_3)_3$ without grafting reaction; b) estimated by ^1H NMR spectroscopy and complete $N(CH_3)_3$ quaternization; c) determined by hydroxide back titration; d) measured in chloride form at room temperature; e) hydroxide conductivity measured by EIS in water

A non-grafted and quaternized block copolymer membrane was also prepared for comparison by soaking PVBC-b-PS membrane directly in a trimethylamine aqueous solution for 48 hours without any mPEG graft reaction step (membrane J in Table 5.2). The theoretical and titrated IEC of the resulting membrane was also measured by hydroxide back titration, and the conversions for all membranes were determined to be greater than 82%.

The water uptake and hydration number (λ) of all membrane samples were determined at room temperature and compared (Figure 5.3) to study the effect of mPEG grafts on polymer. Because the grafting reaction requires substitution of some benzyl chloride groups, the total number of ionic groups (as measured by IEC) is decreased relative to the non-grafted membrane (J). However, since only a small amount of benzyl chloride groups are reacted, only small IEC differences between grafted membranes are observed. The water uptake and hydration number are found to increase with the number of mPEG grafts on the membrane, and the trends can be observed in Figure 5.3. The hydration numbers increase from 9 to 40 going from the non-grafted membrane to the most highly mPEG grafted membrane. Hydration number follows the reverse order of IEC, therefore it is clear that the mPEG grafts increase the hydration number independently of the number of cationic groups. The water uptake value is also plotted and shows the same trend as hydration number. The highest water uptake reaches 108% with only 2.8 mol% benzyl chloride groups reacted with mPEG.

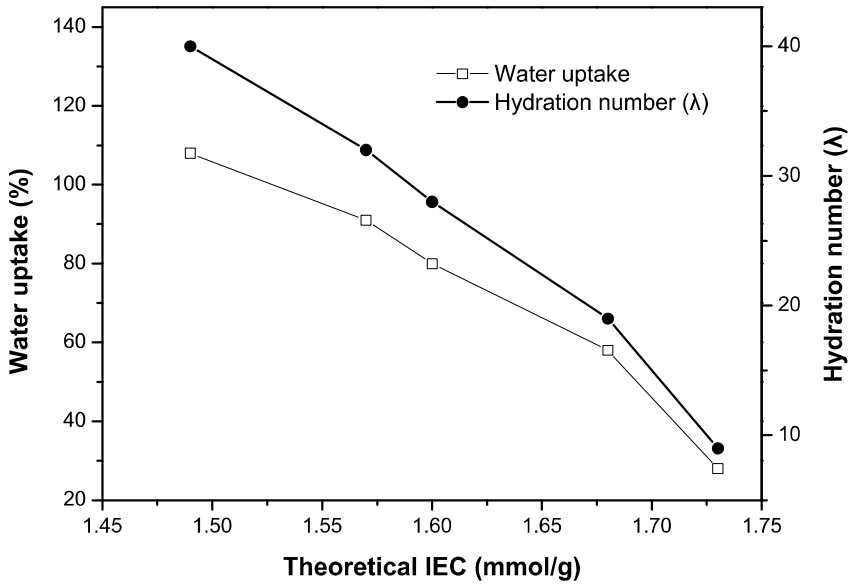

Figure 5.3 Water uptake and hydration number versus titrated IEC of PEG grafted AEMs

Conductivity of each membrane in their hydroxide form was measured at room temperature and 60 °C in a fully hydrated condition by electrochemical impedance spectroscopy. The ionic conductivity is found to increase with increasing hydration number and the amount of mPEG grafts, and the results can be observed in Table 5.2. Although the IEC only varies over a small range of 1.73 mmol/g to 1.49 mmol/g, the most highly grafted samples, which have the lowest IEC, display a significant increase in hydroxide conductivity (61 mS/cm) relative to the non-grafted sample (25 mS/cm). Therefore, the increase in water content, due to the high hydrophilicity of mPEG in these membranes shows a greater effect on the ion transport than the small difference in IEC. The trends of hydroxide conductivity at room temperature and 60 °C are also plotted as a function of water uptake in Figure 5.4 to further study the mPEG graft effect in anion exchange membrane. The conductivities at both temperatures show high dependence on water uptake. The conductivity increases with the increase in water uptake as expected, which correspond to the increase in mPEG graft contents.

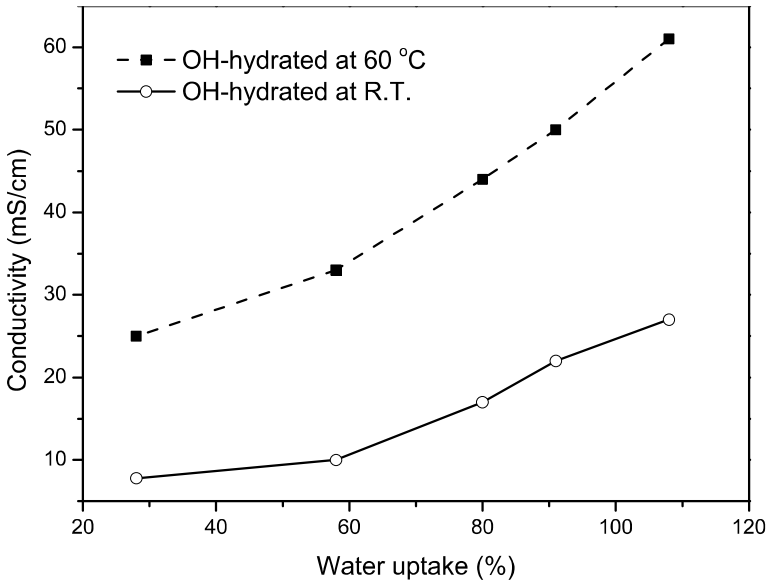

Figure 5.4 Conductivity of mPEG grafted and non-grafted membranes as a function of water uptake at room temperature and 60 °C

The role of mPEG on water sorption and its effect on the anion exchange membrane was further examined by dynamic vapor sorption (DVS). The water uptake of the most highly mPEG grafted membrane (D-2) was measured by varying the relative humidity from 0%RH to 95%RH and compared with the non-grafted membrane in Figure 5.5. Water uptake and hydration number increase with the increased humidity for both membranes, but the mPEG grafted membrane displayed greater water sorption than non-grafted membrane, as expected. Figure 5.5 shows that both grafted and ungrafted membranes absorb similar water at a low humidity range of 0%RH to 20%RH. However, the mPEG grafted membrane absorbs significantly greater amounts of water than the non-grafted membrane as humidity increases above 20% RH. This further confirms the mPEG content is responsible for the high water affinity in the grafted membranes.

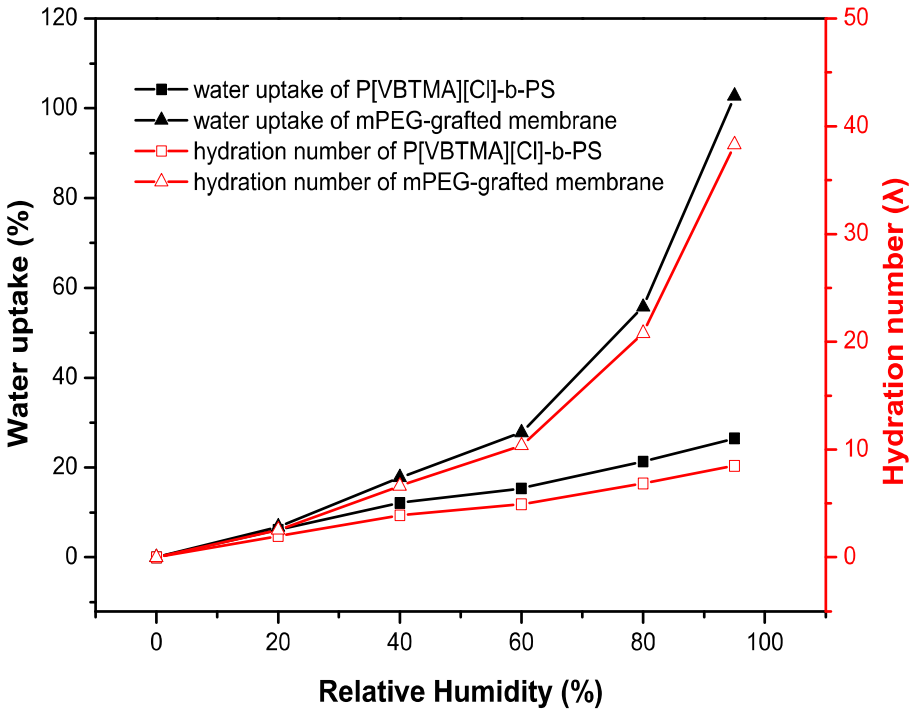

Figure 5.5 DVS study of mPEG grafted membrane D-2 (▲,△) and non-grafted membrane J (■,□) at 60 °C (solid symbols represent the water uptake and hollow symbols represent the hydration number)

In order to investigate the dependence of conductivity on humidity, the conductivity of all membranes were measured at 60 °C by sweeping relative humidity from 50-95 %RH in an environmental chamber. Since the reactivity of hydroxide ion with carbon dioxide could cause complication upon exposure to air in the environmental chamber during measurements, the membranes were examined in their chloride form for the conductivity tests. The conductivities of mPEG grafted membranes at different relative humidities (50%, 80%, and 95%) are plotted as a function of titrated IEC in Figure 5.6. The chloride conductivities at all humidity conditions increase with the increase in the amount of mPEG grafting and related increased hydration level, which agrees well with the trend observed in hydroxide conductivity.

The conductivity is found to generally decrease with reduced relative humidity, which is consistent with the observation in other anion exchange membrane studies.[24, 105, 175] For instance, the conductivity of the non-grafted membrane decreases by more than 50% on going from 95%RH to 80%RH and reduces to 13% of its 95%RH value on going to 50%RH. This strong humidity dependence in conductivity corresponds to the low availability of water molecules at low humidity condition. However, the conductivity of the highly mPEG grafted sample, membrane D-2, displayed much less of a humidity dependence. The conductivity of membrane D-2 shows only a small decrease from 28 mS/cm to 22 mS/cm (21% decrease) on going from 95%RH to 80%RH, indicating the ability of the mPEG grafts in the membrane to hold water at 80 %RH compared to the non-grafted membrane. The mPEG grafted membranes still experience a significant conductivity loss on going to 50%RH, nonetheless, this methodology demonstrates the potential to reduce the conductivity dependence on humidity at least at humidity changes from 95 %RH to 80 %RH.

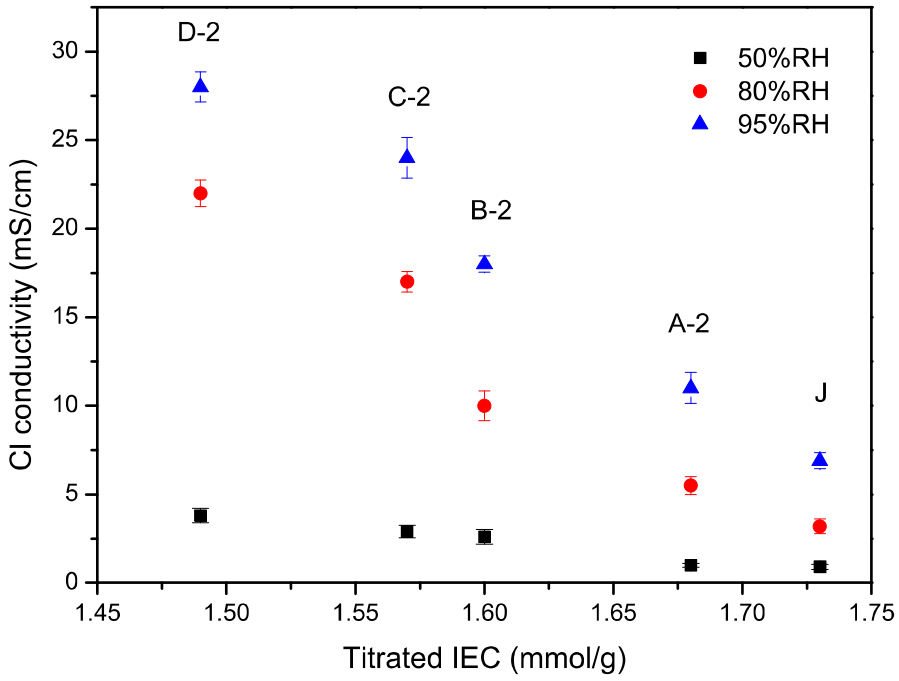

Figure 5.6 Cl conductivity comparison (50%, 80% and 95%RH) of PEG grafted AEM at 60 °C

5.4 Conclusion

mPEG homopolymer is utilized as a hydrophilic polymer to modify the anion exchange membrane properties through grafting reaction. The mPEG grafted AEMs enhanced the water uptake and hydration number due to an increased membrane water affinity by mPEG even with decreased IEC. The hydroxide and chloride conductivity increased with an increase in mPEG graft content due to the greater water sorption in the membrane for ion transport. The investigation of dependence of conductivity on humidity indicated that the mPEG grafts seem to have little effect on reducing the humidity dependence of conductivity at 50 %RH, but this humidity dependence is apparently reduced for mPEG grafted membrane at 80%RH and higher humidity. The results suggest promise for utilizing hydrophilic polymer to improve the ion conduction and its performance at low humidity condition

5.5 Acknowledgement

This work was funded by the Army Research Office through a MURI (grant # W911NF-10-1-0520). NMR spectroscopy was made possible through a grant from the NSF MRI program (grant # CHW-0923537).

CHAPTER 6 QUATERNARY AMMONIUM CROSSLINKED BLOCK COPOLYMERS FOR ALKALINE EXCHANGE MEMBRANES

6.1 Introduction

The alkaline fuel cell (AFC) is a competitive fuel cell technology to the proton exchange membrane (PEM) fuel cell.[9] However, the traditional liquid electrolyte, KOH, can negatively affect the performance of the AFC, as the carbon dioxide in air reacts with KOH to form carbonate precipitates in the electrolyte, which block pores in the electrodes.[35] The development of solid-state electrolytes (i.e., anion exchange membranes) can eliminate the carbonate precipitate problem.

To be effective, the anion exchange membrane must possess certain properties and research efforts have been directed to address these characteristics. Foremost, the cationic conducting group must be stable in an alkaline environment. Among the different cationic functional groups that have been examined, quaternary ammonium has demonstrated good thermal and chemical stability and the benzyltrimethylammonium cation has been widely studied because of its relative ease of synthesis.[26-28, 54] Secondly, the polymer backbone must be chemically stable under the alkaline conditions. Styrenic polymers are alkaline stable materials and can be readily functionalized, resulting in several studies[34, 35, 37, 40] that have incorporated polyvinylbenzylammonium groups into polymer structures for anion exchange membrane preparation. Moreover, an important requirement for robust anion exchange membrane is high ionic conductivity. The primary method for ionic conductivity enhancement involves introducing more ion conducting functional groups. However, as the degree of functionality increases, the anion exchange membrane may lose its mechanical integrity in water

or fuel. In order to solve this problem, the introduction of crosslinking may effectively enhance the membrane insolubility[8]. In addition, crosslinking may also improve the thermal and chemical stability in the membrane, but the crosslinking also has the potential to render the membranes more brittle.

Various strategies have been used to prepare crosslinked polymers for anion exchange membranes. Research has been performed to brominate arylmethyl groups on a poly(aryl ether sulfone) and then to use the resulting benzyl bromide groups in a self-crosslinking reaction at high temperature by Friedel-Crafts reaction between the benzyl bromide groups and aromatic rings on the polymer backbone.[186, 187] Another crosslinking strategy investigated the design of a tetraalkylammonium functionalized cyclooctene as both crosslinker and monomer for ring opening metathesis polymerization.[69] Recently, the diamine, 1,4-diazabicyclo[2,2,2]octane (DABCO) was used to react with polyvinylbenzyl chloride grafts to crosslink anion exchange membranes.[188, 189] Diethylamine has also been investigated as a crosslinker to form crosslinks in poly(arylene ether sulfone)[190] or poly(vinylbenzyl chloride) composite membranes[191] and effectively reduce the membrane dimensional swelling in water, however, the reaction left with moderate contents of tertiary amine in the membrane.

We have investigated a simple method to react dimethylamine with a portion of pendent benzyl chloride groups in order to crosslink block copolymer chains. The remaining pendent benzyl chloride groups are then reacted with trimethylamine to form additional cationic functionality. The block copolymer is chosen since it offers the potential for controlled morphology, which can be tuned by varying the block composition. The overall result is to crosslink what ultimately becomes the hydrophilic part of the membrane, while potentially retaining the mechanical properties of the hydrophobic matrix. Additionally, the quaternary

ammonium crosslinking unit can act as an ionic conducting group to maintain ionic conductivity. The research investigates in detail the crosslinking and amination reactions of poly(vinylbenzyl chloride)-b-polystyrene (PVBC-b-PS) in the formation of membranes. The effect of crosslinking on the membrane properties, including water uptake, ionic conductivity, thermal stability, and mechanical property is also investigated.

6.2 Experimental Section

6.2.1 Materials

Styrene (99%) and 4-vinylbenzyl chloride (VBC) (90%) were obtained from Aldrich, dried over calcium hydride, and distilled under reduced pressure right before use. 2,2,6,6-tetramethyl-1-piperidinyloxy (TEMPO) (Aldrich, 98%) was sublimed twice before use. Benzyl chloride (Mallinkrodt, analytical reagent), potassium carbonate (Fisher Scientific, anhydrous), dimethylamine (Aldrich, 40 wt% aqueous solution) and trimethylamine (Aldrich, 25 wt% aqueous solution) were used as received. Benzoyl peroxide (BPO) was purified by recrystallization from 40:60 chloroform:methanol. Other reagents were used without further purification.

6.2.2 Synthesis of Dibenzyldimethylammonium Chloride

Benzyl chloride (1.0 mL, 8.7 mmol) and potassium carbonate (1.2 g, 8.7 mmol) were added to a 50 mL round bottom flask followed by 10 mL methanol. Dimethylamine (40 wt% aqueous solution) (0.5 mL, 4.35 mmol) was introduced into the flask by microliter syringe. The reaction flask was capped with a rubber septum and heated to 60 °C for 24 hours. The potassium carbonate was separated by filtration and the methanol fraction was concentrated by rotary

evaporation. The final product was isolated by precipitation in hexane and dried under vacuum overnight. Pure yield: 89%. ^{1}H NMR (500 MHz, D_2O, δ): 7.33-7.60 (10H, ArH), 4.42 (4H, CH_2Cl), 2.81 (6H, CH_3).

6.2.3 Synthesis of PVBC-b-PS by Nitroxide Mediated Polymerization (NMP)

All glassware was dried overnight at ~150 °C before the polymerization. The purified VBC (10.0 mL), BPO (56 mg, 0.4 mmol), and TEMPO (62 mg 0.4 mmol) were introduced into a 50 mL round bottom flask containing a magnetic stir bar and capped with a rubber septum, and contents were purged with argon for 30 min. The mixture was then heated to 125°C for 3 hours. The resulting TEMPO-terminated PVBC (PVBC-TEMPO) was purified by repeated precipitations in methanol, and further dried in a vacuum oven at room temperature overnight before use.

PVBC-TEMPO was used as a macro-initiator to copolymerize with styrene in a bulk polymerization. PVBC-TEMPO (250 mg) was weighed into a 50 mL round bottom flask and the flask capped with a rubber septum. An excess of styrene (10 mL) was then added to the flask by syringe. After the PVBC-TEMPO dissolved in the styrene, the round bottom flask was purged with argon for 30 min. The bulk polymerization was carried out at 125 °C for 1 hr. The copolymer was isolated by precipitation in methanol, and was purified by re-precipitating after re-dissolving in chloroform. The copolymer was then dried under vacuum at room temperature. ^{1}H NMR (500 MHz, $CDCl_3$, δ): 6.21-7.26 (9H, ArH), 4.37-4.65 (2H, CH_2Cl), 1.65-2.18 (2H, CH), 1.19-1.65 (4H, CH_2).

6.2.4 Formation of Crosslinked Membranes

Films were crosslinked by reaction between the pendent benzyl chloride groups and dimethylamine. An example procedure follows (membrane A-1): PVBC-b-PS copolymer was dried overnight in a vacuum oven at room temperature. A solution of approximately 5 wt% copolymer in chloroform was prepared and sonicated for 15 minutes. The copolymer solution was drop-cast onto a glass slide and the chloroform was allowed to evaporate in the fume hood. The copolymer film that was obtained was immersed in water to separate from the glass slide, and then held for 20 hours in a vacuum oven at 40 °C. 0.55 g of dry copolymer film (1.15 mmol of benzyl chloride groups) was weighed into a single neck 100 mL round bottom flask equipped with a magnetic stir bar. Based on the amount of desired reaction, potassium carbonate (63 mg, 0.46 mmol) and 30 mL methanol were added to round bottom flask. 26.0 μL of a 40 wt% aqueous dimethylamine solution (0.23 mmol) was introduced to the round bottom flask using a micro-liter syringe. The reaction flask was capped with a rubber septum and heated to 60 °C for 24 hours. The crosslinked membrane was removed from the flask and rinsed with water. Other samples were crosslinked using the same procedure with the amount of dimethylamine calculated to produce the desired number of crosslinks and the amount of potassium carbonate calculated as twice the amount of dimethylamine.

6.2.5 Quaternization of Crosslinked Membrane by Trimethylamine

The crosslinked membranes were soaked in 100 mL 25 wt% aqueous trimethylamine solution for 48 hours, then immersed in deionized water, and rinsed thoroughly with more deionized water. The quaternized membranes were dried in vacuum oven at room temperature overnight.

6.2.6 Characterization

^{1}H NMR spectroscopy was performed on samples in $CDCl_3$ using a JEOL ECA-500 spectrometer. Gel permeation chromatography was performed using a system consisting of a Waters 600 Pump, Wyatt Optilab DSP refractive index detector, Wyatt MiniDAWN light scattering detector, and 2 PL-gel 5μ Mixed D columns. Fourier transform infrared (FTIR) spectroscopy was performed using a Thermo-Electron Nicolet 4700 spectrometer with a Smart Orbit attachment utilizing Nicolet's OMNIC software. Thermal stability was determined by thermogravimetric analysis (TGA) on a Seiko TGA/DTA320 at a heating rate of 10 °C/ min under a nitrogen atmosphere.

Chloride conductivity was measured by electrochemical impedance spectroscopy using a Bio-Logic VMP3 potentiostat under controlled temperature and relative humidity in a TestEquity H1000 oven, whereas hydroxide conductivity was measured by electrochemical impedance spectroscopy in water by sweeping the temperature from 60 to 90 °C. All membranes were held in four electrode cells with platinum electrodes, and data was collected using EC Laboratories software.

Theoretical ion exchange capacity (IEC) was calculated for membranes both after crosslinking and after final quaternization reactions. The theoretical IEC after the crosslinking reaction was determined by dimethylamine feed ratio, and the theoretical IEC of the final membrane was calculated based on the assumption of complete trimethylamine quaternization reaction. Titrated IEC was determined by the Mohr's chloride titration method[159]. The desired membranes were dried in a vacuum oven at 60 °C for 24 hours, and their dry weights were quickly measured. About 0.10 g membrane was accurately weighed and soaked in 50 mL 0.2 M $NaNO_3$ solution for 24 hours to exchange the chloride ion to nitrate. The $NaNO_3$ solution was

titrated to determine the amount of free chloride ions with 0.0992 M $AgNO_3$ solution by using K_2CrO_4 as color indicator. The end point of the titration was identified as the appearance of light red brown color, indicating all the chloride ions were consumed and Ag_2CrO_4 was formed. The chloride titration was repeated three times and the titrated IEC was calculated with the equation,

$$\text{IEC}\,(\text{mmol/g}) = \frac{c_{AgNO_3} V_{AgNO_3}}{m_{\text{dry membrane}}}$$

where c is the concentration of $AgNO_3$ solution, V is the volume of the $AgNO_3$ solution consumed during titration, and $m_{\text{dry membrane}}$ is the dry mass of the membrane.

Water uptake was measured comparing wet and dry weights of the membranes. The film was soaked in water for two days. Excess water was removed with a Kimwipe and the mass of the hydrated film was determined. The film was then dried in a vacuum oven at 60 °C for 24 hr until constant weight was achieved. The water uptake was calculated using the equation,

$$\text{WU}\,(\%) = \frac{m_{\text{hydrated}} - m_{\text{dry}}}{m_{\text{dry}}} \times 100\%$$

where m_{hydrated} is hydrated mass of membrane after removing all surface water, and m_{dry} is dry mass of membrane after drying in vacuum oven.

Mechanical properties of crosslinked and non-crosslinked membranes were performed using an Instru-Met frame tensile tester (by MTS Model: A30-33) with a 1000-pound load cell (a resolution less than 0.1 pound). The samples were dried in a vacuum oven at 60 °C for 24 hours before testing and were cut into approximately 60 mm x 8 mm strips with a thickness of about 100 microns. The test was performed at crosshead speed of 5 mm/min at room temperature in dry condition.

6.3 Results and Discussion

In order to attain the desired conducting performance of anion exchange membranes, high cation functionality is typically introduced into the polymer structure. Although incorporation of more cationic functional groups (as measured by an increased ion exchange capacity) can enhance the membrane ionic conductivity, this method will increase the membrane hydrophilicity and may result in the loss of its mechanical integrity under hydrated conditions. The goal of current study is to develop a method to increase the membrane integrity is water without damaging its mechanical property. Research has been directed toward making block copolymers that have a hydrophobic block that forms the matrix for mechanical strength and a hydrophilic (cationic) block for conductivity.[25, 105, 108] Here, the amount of cationic groups is still limited because at a certain content, the hydrophilic portion can become the majority phase or otherwise promote solubility or high levels of swelling in water. We introduce a variation in the use of block copolymers where the hydrophilic cationic phase is crosslinked to limit the hydration and swelling while allowing for a large number of ionic groups.

Scheme 6.1 Synthesis route for crosslinked AEM

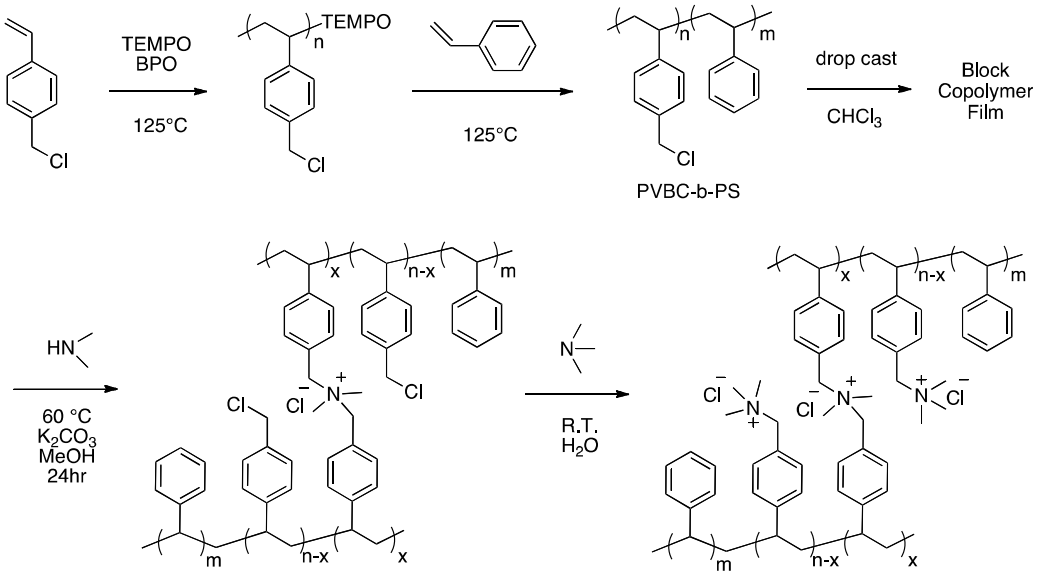

A method (Scheme 6.1) was developed with poly(vinylbenzyl chloride)-b-polystyrene (PVBC-b-PS) block copolymer to form quaternary ammonium crosslinking structures in what ultimately becomes the hydrophilic portion of the membrane by using dimethylamine as crosslinker. The remaining benzyl chloride groups in the polymer are subsequently quaternized by trimethylamine to form the final crosslinked membrane.

Block copolymers can be synthesized to provide phase-separated materials with controlled morphologies, and living radical polymerization techniques are suited for a variety of monomers and functional groups. Nitroxide mediated polymerization is selected in this work to synthesize a PVBC-b-PS diblock copolymer.[111, 134] This technique allows the sequential polymerization of both styrene and VBC with control over molecular weight of PVBC-b-PS and composition of each block. A simple procedure using free TEMPO stable radical is used here. The polymerization of VBC was carried out using BPO as radical initiator in the presence of TEMPO[131, 132] ([BPO]/[TMEPO] = 200) in bulk at 125 °C for 3.5 hours. The resulting PVBC with a TEMPO functional chain end (PVBC-TEMPO) was analyzed by GPC to determine a M_n = 30,500 g/mol and M_w/M_n = 1.90. Several precipitations were conducted on PVBC-TEMPO in order to remove any remaining VBC monomer. The nitroxide mediated copolymerization of styrene was initiated by the purified PVBC-TEMPO macroinitiator at 125 °C in bulk. The conversion of styrene reached ~10% after 30 minutes of reaction. The results of GPC analysis of PVBC-TEMPO and PVBC-b-PS diblock copolymer are depicted in Figure 6.1.

The molecular weight of PVBC-b-PS was determined by GPC to find M_n = 85,700 g/mol and M_w/M_n = 1.86. The styrene conversion was calculated by using the molecular weight of the PS block in PVBC-b-PS diblock copolymer divided by the molecular weight of complete (100%)

styrene conversion determined by initial molar ratio of styrene to PVBC-TEMPO macro-initiator. The GPC chromatogram of PVBC-TEMPO shows a small amount of tailing to low molecular weights, resulting in the broad peak feature. The broad molecular weight distribution may be attributed to the high reactivity of VBC monomer and uncontrolled initiation.[133, 192] After the block copolymerization from the PVBC macroinitiator, the GPC chromatogram of PVBC-b-PS shows a significant separation from the initial PVBC-TEMPO peak, as well as an increase in molecular weight as determined by light scattering detection compared to the initial PVBC-TEMPO block. The significant peak shift indicates an efficient initiation from the PVBC-TEMPO macroinitiator to form the diblock copolymer.

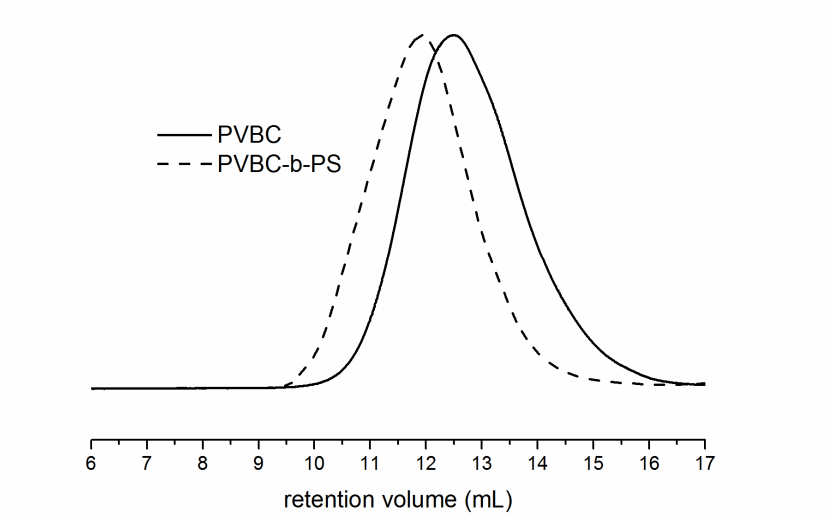

Figure 6.1 The GPC chromatograms of TEMPO functionalized PVBC (——) and PVBCB-b-PS (----) diblock copolymer.

^{1}H NMR spectroscopy was applied to determine the amount of benzyl chloride groups in the copolymer. Figure 6.2 shows the spectrum of PVBC-b-PS copolymer with the benzylic protons at 4.37-4.65 ppm and aromatic protons at 6.21 to 7.26 ppm. The mass composition of PVBC and PS blocks can be calculated based on these two major characteristic peaks, in this

case, the PVBC block is calculated to be 32 wt% of the copolymer. At this composition, the membrane will not be soluble in water after the quaternization reaction, so different analytical methods can be applied to explore the effect of crosslinking on membrane properties (e.g. water uptake and conductivity). Since materials are impossible to cast into membranes after the crosslinking reaction, films were prepared using the soluble PVBC-b-PS copolymers by drop casting from chloroform at 5% wt/vol concentration on glass slides. Isolated films could then be crosslinked by reaction with dimethylamine.

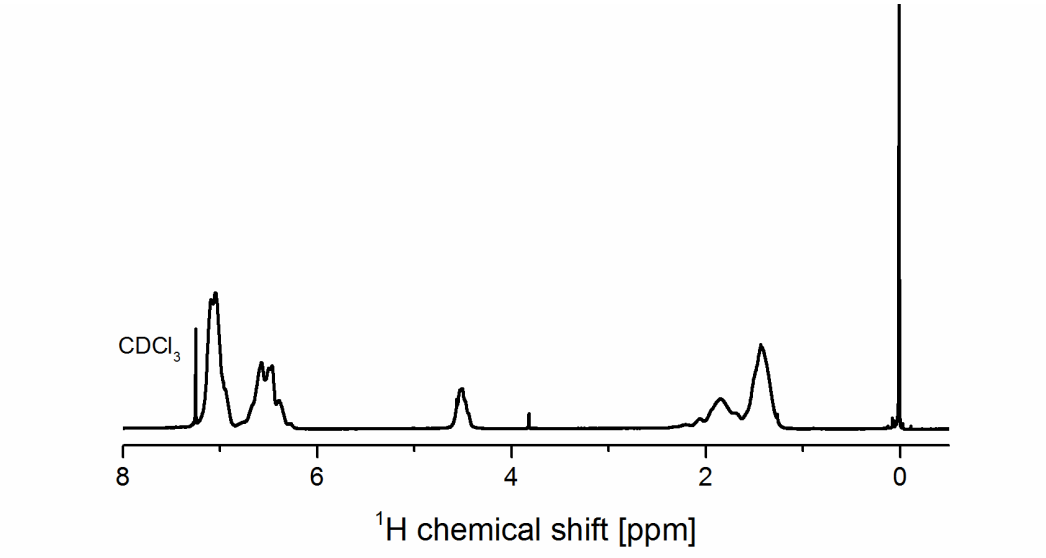

Figure 6.2 The ^{1}H NMR spectrum of PVBC-b-PS by bulk copolymerization in $CDCl_3$

In order to study the crosslinking reaction in the membrane, a model reaction to synthesize dibenzyldimethylammonium chloride was examined (Scheme 6.2). The reaction was carried out with excess amount of potassium carbonate and the pure product can be easily isolated in nearly quantitative yield (89%). From this result, it was expected that the reaction could be used to quantitatively synthesize crosslinked structures in the PVBC-b-PS block copolymer membranes.

Scheme 6.2 Synthesis of dibenzyldimethylammonium chloride as model for the crosslinking reaction

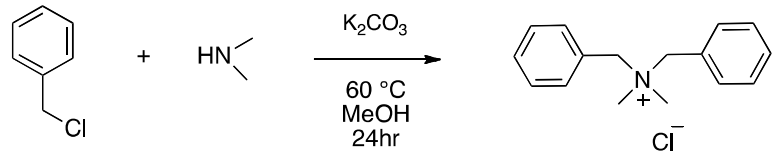

Scheme 6.3 Crosslinking reaction by dimethylamine

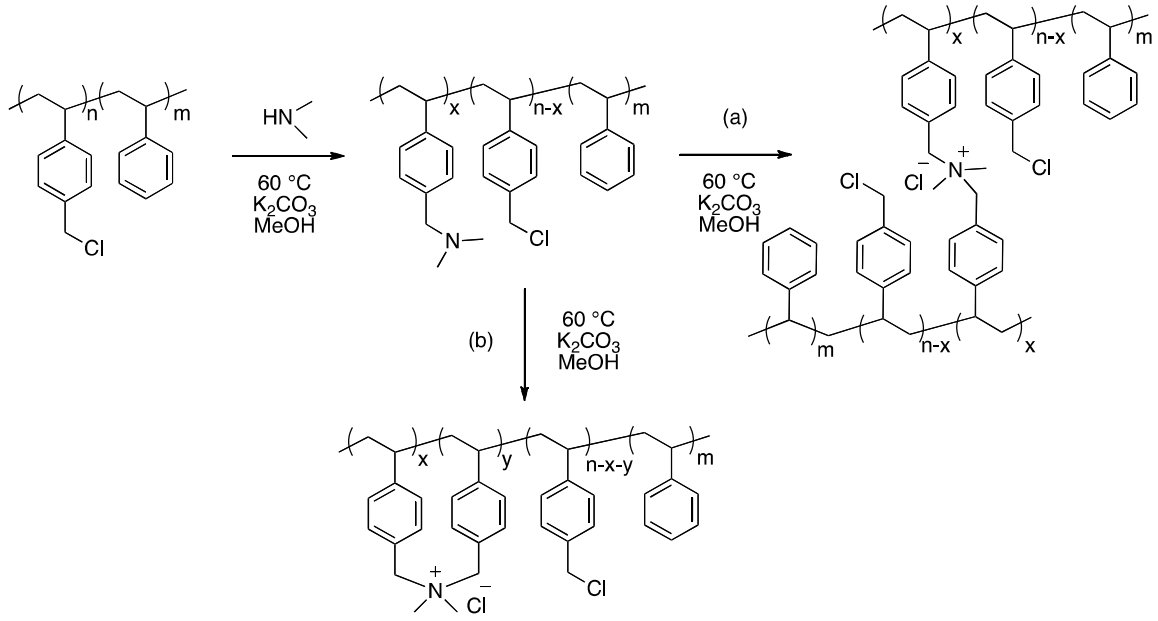

The crosslinking reaction occurs in two steps (Scheme 6.3), where dimethylamine reacts with a pendent benzyl chloride and the resulting tertiary amine can then further react with another benzyl chloride group to produce a crosslink that is itself a quaternary ammonium cation. While crosslinking is the major reaction expected, the formation of some non-crosslinked structures through intramolecular reactions like that shown in Scheme 6.3(b) can also occur. Because of these possible side reactions, the exact crosslink density cannot be readily determined, however the overall extent of reaction can be found through titration. Further, the formation of

crosslinks can be qualitatively determined by testing the solubility of films after reaction. It is expected that an increase in crosslinks will result from an increase in the amount of dimethylamine added.

The crosslinking reaction with dimethylamine was carried out for 24 hours on films suspended in methanol at 60 °C. After about 5 hours the membrane turned from transparent to an opaque white. After 24 hours, the reaction was stopped and the membrane was removed and soaked in different solvents (chloroform, toluene, THF, DMF, and DMSO) to test the solubility of the crosslinked membrane. The membranes did not dissolve after soaking in any solvent indicating the formation of crosslinked structures. The reaction with dimethylamine is further confirmed by FT-IR spectroscopy. Figures 6.3a and 6.3b show the FT-IR spectra of PVBC-b-PS copolymer membrane and the membrane after reaction with dimethylamine. The characteristic peak at 669 cm^{-1} corresponds to the C-Cl stretch and this peak decreases after the reaction, but does not disappear completely, indicating benzyl chloride groups are still available after the dimethylamine crosslinking reaction, as expected from the stoichiometry.

Membranes with four different crosslink compositions were prepared through the reaction with dimethylamine (Table 6.1). The amount of reacted groups is presented as a percentage of the total number of benzyl chloride groups available. The number of quaternary ammonium cations, which is also the ion exchange capacity (IEC), resulting from the reaction with dimethylamine can be determined by titration. The estimated IEC was calculated based on the feed ratio of PVBC-b-PS and dimethylamine. The actual IEC value was determined by Mohr's chloride titration method. The membranes were first dried to measure the dry weight and were then exchanged from chloride to nitrate for titration. Since this is a direct titration method, a large amount of membrane (about 0.1 g) was utilized in order to produce a large amount of

chloride ions in solution. The crosslinked compositions of each membrane are shown in Table 6.1. All membranes show good agreement between titrated and estimated values, indicating the high conversion of crosslinking reaction between dimethylamine and two benzyl chloride groups. This implies the low existence of any tertiary amine, which would be the result of reaction between dimethylamine and only one benzyl chloride group and would not titrate.

Table 6.1 Characterization of crosslinked membranes

Crosslinked membranes[a]	Theoretical PVBC reacted (%)[b] by feed ratio	Estimated IEC[c] (mmol/g) after reacting with $N(CH_3)_2$	Titrated IEC[d] (mmol/g) after reacting with $N(CH_3)_2$	Actual PVBC reacted (%)[b]
A-1	40	0.41	0.33	32
B-1	30	0.31	0.26	25
C-1	20	0.21	0.17	16
D-1	10	0.10	0.09	9

a) Membrane A-1, B-1, C-1, and D-1 were crosslinked by different amounts of $N(CH_3)_2$ using the same PVBC-b-PS copolymer; b) mole% of benzyl chloride groups reacted; c) estimated by feed ratio of $N(CH_3)_2$; d) determined by Mohr's chloride titration.

The remaining pendent benzyl chloride groups were then converted into quaternary ammonium groups by reaction with trimethylamine. The crosslinked membranes were suspended in aqueous trimethylamine solution at room temperature for 48 hours. The membranes were removed and were subjected to repeated soaking in fresh deionized water every 4 hours. The membranes were finally rinsed with deionized water and dried in a vacuum oven to remove any residual trimethylamine. The trimethylamine quaternization reaction was examined by FT-IR spectroscopy. The C-Cl characteristic peak disappears in the FT-IR spectrum (Figure 6.3c) indicating the reaction of the benzyl chloride groups. The strong peak at 3300 cm^{-1} is presumably due to the presence of water in the membrane from the increased hygroscopic nature of the quaternary ammonium group.

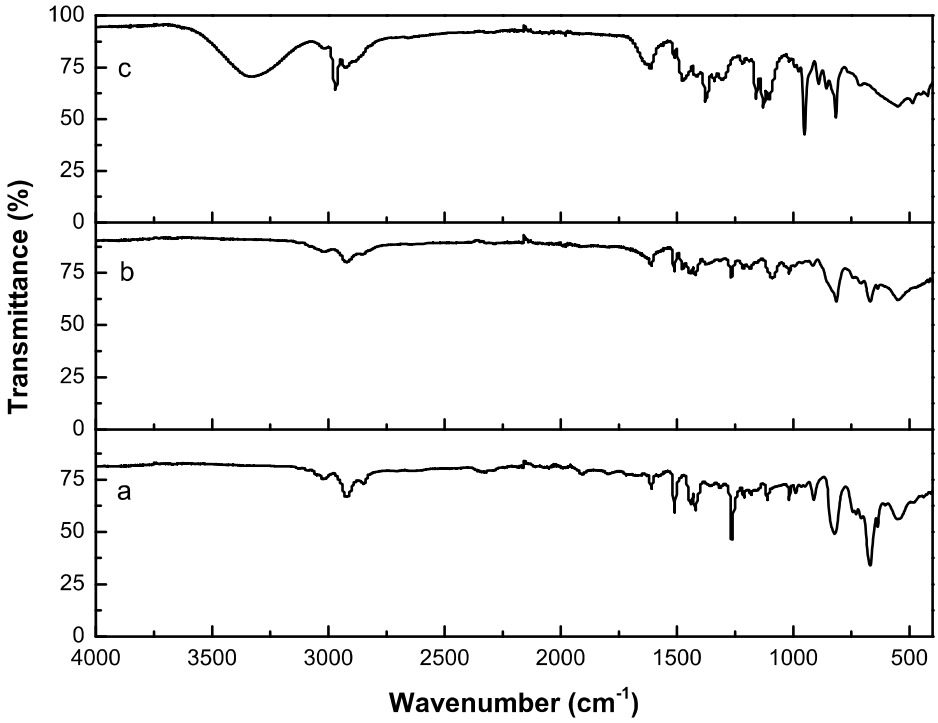

Figure 6.3 FT-IR spectra of a) PVBC-b-PS membrane before reaction, b) membrane after crosslinking reaction by $N(CH_3)_2$ and c) crosslinked membrane after final quaternization reaction by $N(CH_3)_3$

The membranes obtained after quaternization with trimethylamine were titrated to determine the overall conversion of benzyl chloride groups. The titrated IECs are compared with the theoretical IEC's in Table 6.2. The theoretical IECs were calculated by assuming 100% conversion of remaining benzyl chloride groups in crosslinked membrane to benzyltrimethylammonium chloride groups. The titrated IEC was again determined by Mohr's direct titration method. The titrated values compared well to the theoretical values, indicating a high conversion of 88-95% of the benzyl chloride groups in agreement with the qualitative FTIR results.

A non-crosslinked, quaternized membrane was also prepared for comparison by soaking PVBC-b-PS membrane directly in a trimethylamine aqueous solution for 48 hours without any

dimethylamine reaction step (sample E in Table 6.2). The theoretical and titrated IEC of the resulting membrane was also measured by Mohr's chloride titration, and the conversion was determined to be greater than 95%.

Table 6.2 IEC, water uptake and conductivity of crosslinked and non-crosslinked membranes

Cross-linked AEMs[a]	Theoretical IEC[b] (mmol/g)	Titrated IEC[c] (mmol/g)	Water uptake[d] (%)	Conductivity[e] 60 °C	70 °C	80 °C	90 °C
A-2	1.60	1.40	12	12 (4.3)	16 (5.5)	18 (6.6)	10 (9.1)
B-2	1.66	1.49	16	18 (5.3)	21 (6.2)	22 (7.4)	25 (11)
C-2	1.74	1.62	20	23 (6.4)	25 (7.7)	27 (9.1)	30 (13)
D-2	1.79	1.69	23	24 (6.8)	26 (8.4)	31 (9.7)	34 (14)
E	1.87	1.78	29	26 (7.4)	28 (8.9)	33 (10)	35 (15)

a) Membrane A-2, B-2, C-2, D-2 were prepared by reacting A-1, B-1, C-1, D-1 with $N(CH_3)_3$, and membrane E was prepared by directly soaking PVBC-b-PS in $N(CH_3)_3$ without crosslinking ; b) estimated by ^1H NMR spectroscopy and complete $N(CH_3)_3$ quaternization; c) determined by Mohr's chloride titration; d) measured in chloride form; e) hydroxide measured by EIS in water and chloride conductivity measured by EIS at 95 %RH (chloride conductivity in parentheses)

The water uptake and ionic conductivity of all membrane samples were measured and compared (Table 6.2) to study the effect of crosslinking and IEC. Because the crosslinking reaction requires two benzyl chlorides to produce one ionic group, the total number of ionic groups (as measured by IEC) is decreased relative to the non-crosslinked membrane (E). The water uptake is found to increase with the number of cationic groups or IEC as expected, and the water uptake values decrease from 29% to 12% going from the non-crosslinked membrane to the most highly crosslinked membrane. It is not clear whether the crosslinking decreases the water uptake independently of the effect on IEC. Conductivity of all membranes were measured in both the hydroxide and chloride forms by sweeping temperature from 60-90 °C in

electrochemical impedance spectroscopy. The ionic conductivity is found to increase with increasing IEC and the concomitant water uptake, as expected and the trends can be observed in Figure 6.4. The hydroxide conductivities are 2-4 times higher than chloride conductivities for all membranes. While the most highly crosslinked samples display a significant decrease in conductivity relative to the non-crosslinked sample, which could correspond to a restriction in motion because of the tight crosslinking and a restriction in the hydration of the cationic groups, samples with light amounts of crosslinking do not show a significant decrease in conductivity. The level of hydroxide conductivity for D-2 is only slightly decreased from that observed for membrane E. Therefore, small levels of crosslinking may not only maintain the membrane integrity in water, but also maintain desired ionic conductivity. This methodology can be used to allow anion exchange membranes with high cation functional group density to overcome the hydrophilicity problem, with little side effect on ion conductivity.

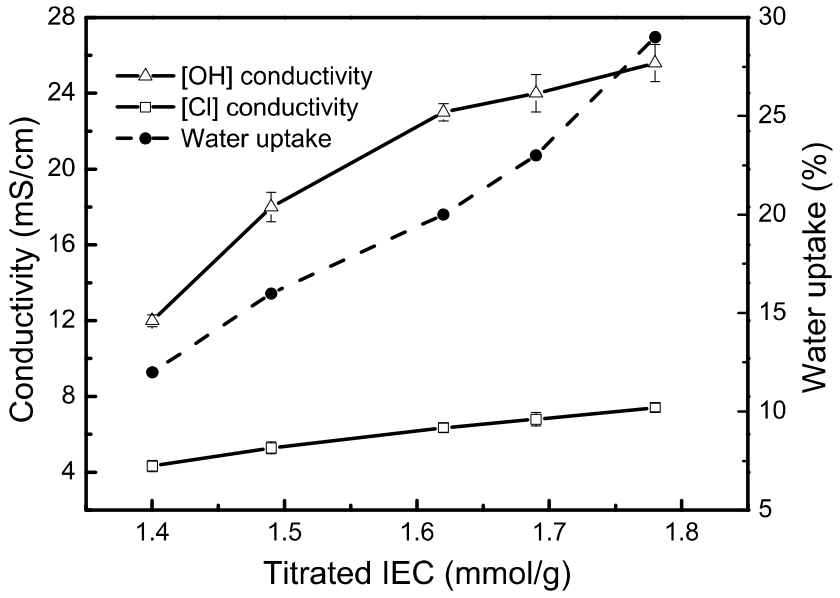

Figure 6.4 Ionic conductivity (60°C) and water uptake of membrane A-2, B-2, C-2, D-2, E versus their titrated IECs

The thermal stability of AEMs is also an important factor for ultimate application in a fuel cell. The thermal stabilities of crosslinked AEM (membrane D-2) and non-crosslinked membrane E were examined by thermogravimetric analysis in a nitrogen atmosphere. The derivative curves (DTG) of both membranes are plotted in Figure 6.5 and indicate that the crosslinked AEM has slightly better thermal stability than the non-crosslinked membrane, which is in agreement with research results on the thermal stability of other crosslinked versus non-crosslinked materials[189, 193, 194]. The crosslinked AEM exhibited an initial decomposition temperature starting at 154 °C, which is 13 °C higher than the non-crosslinked sample.

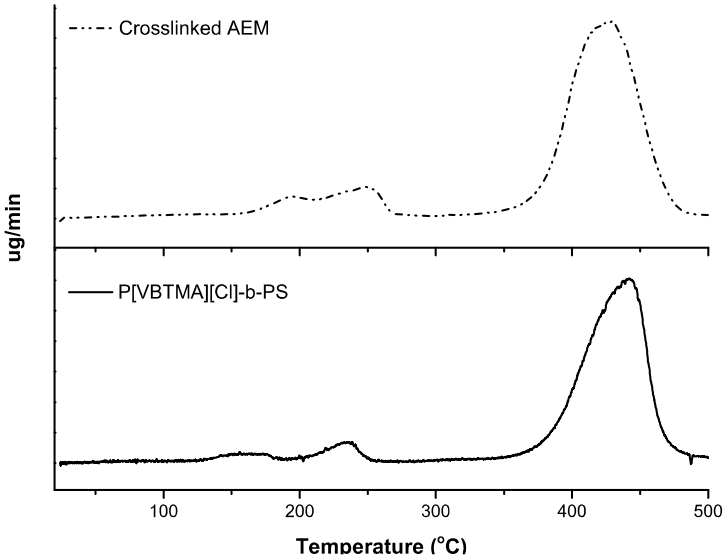

Figure 6.5 DTG curve comparison between crosslinked (dashed line) and non-crosslinked (solid line) membranes

In order to investigate the crosslinking effect on membrane mechanical properties, the tensile test was performed on dried crosslinked membrane and compared with non-crosslinked membrane at room temperature in Figure 6.6. The membrane D-2 (9 mol% benyl chloride crosslinked) displayed a maximum stress and stain at break of 34 MPa and 2.1% with a Young's

modulus of 1.79 GPa, which are the similar tensile properties compared to non-crosslinked AEM (30 MPa maximum stress, 2.2% stain at break, and 1.66 GPa Young's modulus). The comparable mechanical properties between crosslinked and non-crosslinked AEMs confirms that the crosslinking structure formed exclusively in hydrophilic components could in fact maintain the membrane mechanical properties.

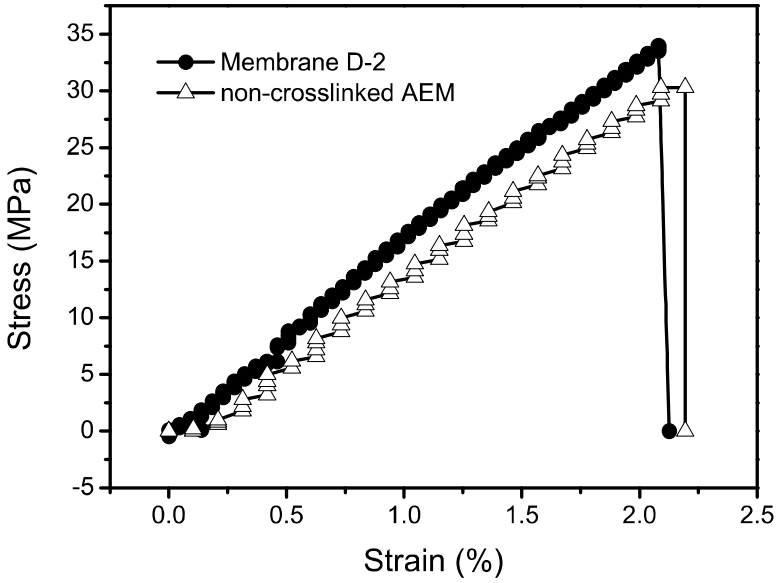

Figure 6.6 Stress versus stain curve of crosslinked AEM (D-2) and non-crosslinked AEM.

6.4 Conclusion

Block copolymers of PVBC-b-PS were synthesized through nitroxide-mediated polymerization. A solid film of the copolymer reacts to high conversions with dimethylamine in an aqueous solution by a two-step amination reaction to form quaternary ammonium crosslinks in what ultimately become the hydrophilic domains. The remaining benzyl chloride groups are converted to benzyltrimethyl ammonium cations. The FT-IR spectra and IEC values confirm the nearly quantitative control over crosslinking and final quaternization reactions. The crosslinked

membranes show a decreased water uptake due to a decreased IEC and presumably also because of the crosslinking. The crosslinked membranes display an expected decrease in conductivity from their lower water uptake and lower IEC, however, for samples with low extents of crosslinking, only a small decrease in conductivity is observed. Thermogravimetric and mechanical analysis determined a slightly higher thermal stability and comparable mechanical property of the quaternary ammonium crosslinked membranes compared to non-crosslinked analogy. The results suggest promise for utilizing quaternary ammonium crosslinks to improve the integrity of membranes with high ionic functionality under aqueous conditions without a deleterious effect on ionic conductivity.

6.5 Acknowledgement

This work was funded by the Army Research Office through a MURI (grant # W911NF-10-1-0520). NMR spectroscopy was made possible through a grant from the NSF MRI program (grant # CHW-0923537).

CHAPTER 7 CONCLUSION AND FUTURE WORK

7.1 Conclusion

Anion exchange membrane has demonstrated its promise to use as polymer electrolyte in AFC for renewable energy solutions, however, current anion exchange membranes still suffer from high material cost, low alkaline stability, poor mechanical and conductive performance. Although new chemistries have been designed to overcome the drawbacks, the understanding of AEM design and its performance are still limited. Therefore, it is important to direct the research in developing AEMs with desired alkaline stability, mechanical properties and ionic conductivity.

Phase separated block copolymers can lead to a positive effect on ion conduction by tuning their morphologies. Block copolymer with controlled molecular weight, composition and functional groups can be synthesized through various methods including living radical polymerization (e.g. nitroxide mediated polymerization) and anionic polymerization.

Polyvinylbenzyl chloride-b-polystyrene (PVBC-b-PS) block copolymers provided a versatile platform for cation functionalization and morphology control to study AEMs. Furthermore, its relatively poor mechanical properties could be improved by blending poly(1,4-dimethyl-phenylene oxide) (PPO) with PVBC-b-PS to form a miscible blend. The PPO blended PS block copolymer membrane exhibited noticeable improvement in mechanical properties. The membranes with higher water affinity possessed better ionic conducting properties with hydroxide conductivity up to 43 mS/cm in water at 60 °C, which was achieved by thermal annealing in the presence of water and through solvent annealing. The PPO miscible blend improves the mechanical properties of PS block copolymer membrane while maintaining high ionic conductivity through the formation of phase separated ionic domains.

In order to expand the knowledge of PPO blend AEM, brominated poly(1,4-dimethyl-phenylene oxide) (BrPPO) was also designed to blend with PVBC-b-PS to produce AEMs with additional functionality in the PPO component. Although ordered phase separation in BrPPO blend membrane was not achieved, the BrPPO blends showed higher ionic conductivity than PPO blends before annealing even though the ion exchange capacities between both blend AEMs were similar.

In addition to blend AEM system, amphiphilic block copolymer membranes containing polyethylene block as membrane formation material were prepared by anionic polymerization and post functionalizations. The polyethylene block prepared through anionic polymerization was a semicrystalline (approximately 30% crystallinity) material and could provide good alkaline stability and necessary hydrophobic support for the membrane. Bi-continuous morphology was observed in membranes with higher ion exchange capacity. The PE block copolymer membranes exhibited excellent properties, including extraordinary mechanical properties (up to 205% strain), high hydroxide conductivity (up to 73 mS/cm in water at 60 °C), and low activation energy of conduction (down to 12 kJ/mol). The well defined morphology along with the great membrane properties indicated the ionic conducting property can be enhanced through the formation of well defined morphology of amphiphilic block copolymer while increasing the alkaline stability and mechanical properties by the semicrystalline membrane matrix.

AEM properties were also investigated through varying the hydration number in the membrane due to the low water affinity and high dependence of conductivity on humidity compared to proton exchange membrane. Mono methoxy poly(ethylene glycol) (mPEG), a hydrophilic polymer, could be grafted onto benzyl chloride groups in PVBC-b-PS to only

investigate hydration number independently without increasing the functionality. The mPEG grafted AEM displayed significant increase in water uptake and hydration number with only small amount of benzyl chloride groups grafted by mPEG. The membranes with higher mPEG graft contents also showed higher ionic conductivity with much less dependence on humidity. The results revealed the significance of hydration number on ion conduction and its performance at low relative humidity.

The ionic conductivity is commonly increased by increasing the ion exchange capacity, but the membrane could eventually become water soluble due to the increased hydrophilicity of the membrane. Therefore, a quaternary ammonium crosslinked membrane was prepared by dimethylamine crosslinking reaction through PVBC-b-PS block copolymer to solve this problem. The overall result was that the crosslink structure only forms in what ultimately became the hydrophilic part of the membrane, while retaining the mechanical properties of the hydrophobic matrix. Additionally, quaternary ammonium crosslinking could act as an ionic conducting group, so no deleterious effect was observed in conductivity between slightly crosslinked membranes and non-crosslinked membranes.

7.2 Future work

We have reviewed four different polymer systems (blend, block, grafted, and crosslinked polymer) in this thesis and built the further understanding of anion exchange membranes for alkaline fuel cells. However, there are still many aspects to be studied in order to improve our knowledge in the design of fuel cell membranes.

The concept of blending PPO and its derivative (BrPPO) to enhance the mechanical properties of PS block copolymer is demonstrated, however, two main areas can be exploited to

further understand this material. One approach is to blend PPO with PS block copolymer (PVBC-b-PS) in much narrower molecular weight distribution. Although a low polydispersity block copolymer is not required for phase separation morphology,[195, 196] the block copolymer with low dispersity could possibly result in a more defined morphology. Therefore, the ionic conductivity and water affinity can be combined to study the polydispersity effect on blend membrane properties, which can be further correlate with the phase separated morphologies in both blends.

In Chapter 3 the quaternized BrPPO exhibits great effect on ionic conductivity before annealing, however, degradation was observed in the membrane after thermal annealing. Since the solvent vapor annealing only requires moderate temperature, this method may be able to anneal the BrPPO blend AEM without degradation. Small angle x-ray scattering and transmission electron microscopy can be combined to study the solvent annealed membrane morphology, which can be related to the water uptake and ionic conductivity. This can provide a more complete understanding of blend membrane design that leads to higher membrane performance.

Previous semi-crystalline block copolymer AEMs show the outstanding performance in mechanical properties, ion conducting and water swelling control. Low activation energy for hydroxide conduction is also observed, which could correspond to the formation of a bicontinuous morphology in the block copolymer AEM. As a result, the understanding of bicontinuous morphology formation in this particular block copolymer becomes more significant. Since the AEM is formed by the quaternization of polyethylene-b-polyvinylbenzyl bromide (PE-b-PVBBr) at room temperature, the phase reorganization after quaternization is limited and the Flory-Huggins parameter (χ) between PE and PVBBr block becomes an important factor in the

phase-separated morphology. It is possible to measure χ by small angle x-ray scattering of PE-b-PVBBr at a variety of block compositions.[197-199] The second virial coefficient, which is related to χ, can be obtained by constructing a Zimm plot. In this case, the complete morphological diagram of this system (at least for the morphologies in which we are interested) can be further studied experimentally by preparing a series of PE block copolymers along with the characterization by electron microscopy and x-ray scattering.

We examine the effect of hydration number independently on block copolymer membrane properties in Chapter 5 and conclude that the ionic conductivity and its dependence on humidity can be improved by grafting hydrophilic polymer (mPEG), but the mPEG grafted AEM needs to be understood in more aspects. The major area can be explored is to study the effect of mPEG grafts on random copolymers, since it is not dertermined how the water absorbed by mPEG is involved in the ion transport. This problem can be indirectly solved by preparing a mPEG grafted random copolymer (PVBC-r-PS) with similar molecular weight, functionality and graft content compared to its block copolymer analogue. The ionic conductivity and water uptake along with morphological structure can be compared between both grafted AEMs in order to study the random and block copolymer effect on membrane properties. It is believed that the mPEG grafts prepared using block copolymer can have higher probability to provide water for the ionic domains.

The benefit of studying mPEG grafted AEM is to understand hydration number effect on membrane ion conducting property. mPEG increases the water uptake and hydration number while also increasing the probability of losing membrane integrity in water. For example, copolymer with 20 wt% mPEG grafted became water soluble after quaternization reaction. One simple route to study high mPEG grafted membrane is to take advantage of crosslinking

technique developed in Chapter 6. The high mPEG grafted PVBC-b-PS backbone, and this resulting polymer can be cast into membranes from THF. The pre-cast mPEG grafted PVBC-b-PS membrane can react with dimethylamine to form a crosslinked membrane and the trimethylamine quaternization can be performed during the last step. Since grafting reaction needs to consume functional groups, the balance between hydrophilic grafts and cationic functional groups can be further studied by comparing highly grafted membrane with the slightly grafted membrane, which could advance the understanding of hydrophilic effect on membrane.

Due to the excellent membrane properties, PE block copolymer AEM can be used as backbone to study new cationic functional groups for hydroxide conduction. Although benzyl-trimethylammonium [BTMA] cation can be readily tethered onto the polymer backbone, the alkaline stability of [BTMA] is less stable in an alkaline environment compared to other cations.[84, 88] For example, tris(2,4,6-trimethoxyphenyl) quaternary phosphonium (TPQP) has been reported to have a high hydroxide conductivity and alkaline stability and it can be introduced through the benzyl chloride group.[85, 86] As a result, polybutadiene-b-polyvinylbenzyl chloride (PB-b-PVBC) developed in Appendix B can be quaternized by TPQP and solution cast to form TPQP functionalized film. The heterogeneous hydrogenation of PB block can be further accomplished by using Crabtree's catalyst and hydrogen gas.[68, 200] Once the preparation of PB-b-PVBC is optimized and finalized, a series of hydrogenated TPQP films can be produced and characterized to study their membrane properties through water affinity, ionic conductivity and morphology. Additionally, since the cationic functionalization is carried out on PB-b-PVBC copolymer and the PB block has a T_g well below the room temperature, the phase reorganization between PB and ionic block in as-cast membranes is expected to be significant. Therefore, this strategy provides a great opportunity to manipulate the morphology

by using variety of cationic functional groups and block compositions while still taking advantage of the benefits provided by polyethylene.

APPENDIX A BULK ANIONIC POLYMERIZATION OF α-METHYLSTYRENE AND ISOPRENE BLOCK COPOLYMERS

A.1 Introduction

Poly(α-methylstyrene) (PAMS) is a polymer with high glass transition temperature (~173ºC)[201, 202] that has not achieved high use in part because of the difficulty in its formation. There is a well-established ceiling temperature[203] for the polymerization of α-methylstyrene (AMS) that inhibits high conversion to polymer.[204, 205] The ceiling temperature precludes the polymerization at moderate temperature to high temperature, and the only successful polymerizations of AMS are anionic[206-215] and cationic[216] polymerization at low temperature.

PAMS has been incorporated as hard phase in block copolymers to prepare thermoplastic elastomers for high temperature application, and most PAMS block copolymer syntheses are accomplished by living anionic polymerization. Due to the low ceiling temperature of AMS, a common strategy of AMS diblock copolymer preparation is to react AMS in the first step at very low temperature (-78 °C) in polar solvent or with a polar additive in order to yield a defined PAMS block with high conversion of AMS monomer to polymer.[217-220] However, this strategy usually results in a low level of control when diene monomer is copolymerized with AMS, since the polar solvents or additives will cause more 1,2- or 3,4-addition instead of 1,4-addtion during diene polymerization,[218, 219] and it is well known that only the 1,4-structured polydiene leads to an elastomeric property.

Researchers have also synthesized triblock copolymers through di-functional initiators (e.g. dilithio compound) with comonomer block in the middle and PAMS blocks in both ends.[221-225] In this case, PAMS block copolymer is polymerized right after the completion of comonomer. This method allows the polymerization of diene monomer in non-polar solvent, but the crossover reaction from polydiene to AMS polymerization is usually quite slow in non-polar solvent. It is found that the crossover reaction to AMS can be significantly enhanced through introducing small amounts of styrene monomer or polar additives (e.g. dimethyl ether, THF, and trimethylamine) before AMS addition.[221, 222, 226]

Our objective is to take the advantage of the low ceiling temperature and weak reactivity of AMS to develop a sequential synthetic pathway for the block copolymer formation by bulk anionic polymerization. In the current study, we investigate the anionic polymerization of AMS in bulk and the reactivity of AMS-isoprene system. We have developed a simple method using *sec*-butyllithium as an initiator and block copolymers are synthesized sequentially with good control over molecular weight and molecular weight distribution. The synthesis of diblock copolymer (PAMS-b-PI) involves the formation of a PAMS block first, and then isoprene is introduced into the reaction in order to switch the polymerization from AMS to isoprene. N,N,N′,N′-tetramethylethylenediamine (TMEDA) was introduced as a polar additive to produce the triblock copolymer (PAMS-b-PI-b-PAMS). Here we report the detailed synthesis of AMS and isoprene block copolymers and their results.

A.2 Experimental Section

A.2.1 Materials

AMS (Aldrich, 99%) and isoprene (Aldrich, 99%) were first dried over calcium hydride and then distilled over di-n-butylmagnesium under reduced pressure right before use. N,N,N′,N′-tetramethylethylenediamine (TMEDA) (Aldrich, 99%) was purified by calcium hydride and sodium metal by the procedures described in the literature.[227, 228] *sec*-Butyllithium (*sec*-BuLi) (1.4 M in cyclohexane) solution and di-*n*-butylmagnesium (1.0 M in heptane) solution were purchased from Aldrich and used as received. Cyclohexane was purified by passing through columns on a commercial solvent purifier system (Innovative Technology). 2,6-Di-*tert*-butyl-*p*-cresol (BHT, Eastman) and other reagents were used without further purification. All polymerization glassware, glass syringes, needles and stir bars were oven-dried at 180°C overnight and the glassware was further flame dried under an argon purge after equipped with stir bar and septum.

A.2.2 Bulk Anionic Polymerization of α-Methylstyrene Homopolymer

Freshly distilled AMS (18 mL) was transferred into a flame-dried and Ar-purged 50 mL round bottom flask equipped with septum and stir bar. *sec*-BuLi was added dropwise to titrate any protic impurities until a pale orange color was observed. The calculated amount of *sec*-BuLi (50 μL, 0.07 mmol) was then injected by a 250 μL syringe and the color of reaction turned to red orange. The bulk homopolymerization was carried out at room temperature. Homopolymer samples were taken at different times (0.5 hr, 1 hr, 2 hr, 3 hr, 3.5 hr, 4.5 hr, and 5 hr) during the polymerization.

A.2.3 Reactivity Ratio Determination

The procedure for monomer reactivity study is as follows. AMS (18 mL) and isoprene (2 mL) were re-distilled from di-*n*-butylmagnesium right before the reaction and transferred into the septum sealed, flame-dried and argon-purged 50 mL round bottom flask before initiation. A calculated amount of *sec*-BuLi (50 μL, 0.07 mmol) was injected after the titration, and the polymerization was left to react at room temperature. An aliquot of reaction solution (1 mL) was removed during the bulk polymerization at different reaction times (1 hr, 1.5 hr, 2 hr, 2.5 hr, 3 hr, 3.5 hr, 4 hr and 24 hr). The monomer reactivity ratio can be calculated from the experimental results depending on the feed ratio (f) and copolymer composition (F).

$$f = \frac{m_1}{m_2} \qquad \text{and} \qquad F = \frac{M_1}{M_2}$$

where m_1 and m_2 are the mole fractions of isoprene and AMS estimated from the molecular weight data respectively, moreover, the M_1 and M_2 are the mole fractions of isoprene and AMS in copolymer determined by ^{1}H NMR spectroscopy respectively. The reactivity ratio can be obtained by the calculations of the feed ratio and copolymer composition according to the Fineman–Ross (FR) method,[229]

$$\frac{f(F-1)}{F} = r_1 \frac{f^2}{F} - r_2$$

A plot of $f(F-1)/F$ versus f^2/F give the linear regression, where the intercept is r_2 and slope is r_1.

A.2.4 Anionic Polymerization of AMS and Isoprene Block Copolymers

AMS and isoprene block copolymers were synthesized by sequential bulk anionic polymerization. An example procedure follows (Experiment 1) : AMS (18 mL) was re-distilled and transferred to a flame-dried 50 mL round bottom flask equipped with stir bar and septum

under the pressurized argon atmosphere. sec-BuLi was added dropwise to titrate the impurities until a pale orange color was observed. The calculated amount of sec-BuLi (50 μL, 0.07 mmol) was then injected. After 30 min, an aliquot (1 mL solution) was removed from reaction and terminated with argon-purged methanol. After the sample was taken, 2 mL fresh purified isoprene was then added into the reaction solution by gas-tight syringe. The reaction was left to stir for 4 hours under room temperature. An aliquot (1 mL solution) was removed for analysis and previously distilled TMEDA (0.25 mL) was subsequently injected into the reaction solution. 1 hr after the addition of TMEDA, argon-purged methanol was introduced to terminate the polymerization. The polymer solution was isolated and purified by precipitation in 10 times excess of methanol with 0.2 wt% of 2,6-*tert*-dibutyl-*p*-cresol (BHT) to prevent oxidation of the polyisoprene block.

A.2.5 Characterization

Gel permeation chromatography (GPC) was used to determine the molecular weight and molecular weight distribution for homopolymer and block copolymer samples, and all GPC samples were prepared at a concentration of approximately 5 mg/mL in the volumetric flask. GPC was performed in THF at room temperature using a Waters model 600 high pressure liquid chromatograph with the flow rate at 1 mL/min using two Polymer Laboratories PL-gel 5 μm Mixed-D columns. The columns were connected to a calibrated Wyatt R401 differential refractometer and a Wyatt Technology miniDAWN multi-angle laser light scattering (MALLS) detector. Astra software (supplied by Wyatt Technology) was used to calculate molecular weight and molecular weight distribution.

^{1}H NMR spectra of all block copolymers were obtained from a JEOL 500 MHz spectrometer to determine the block composition and microstructure of polyisoprene. All polymer samples were dissolved in $CDCl_3$ and chemical shifts are reported with respect to tetramethylsilane (TMS) (δ 0.00).

A.3 Results and Discussion

PAMS has been successfully synthesized by anionic polymerization. Solution polymerization is the most reported method,[206, 207, 209-211] while a few studies investigate the bulk polymerization of AMS.[230] In order to understand the anionic polymerization of AMS in bulk, the homopolymerization of AMS was designed and samples were taken during the reaction. The reaction can be carried out at room temperature since bulk AMS polymerization has a ceiling temperature at ~ 57 ºC,[203, 208] however, the low ceiling temperature also indicates that the polymerization of AMS will reach equilibrium at room temperature.[205, 231-233] This bulk anionic polymerization used *sec*-BuLi as initiator ([AMS]/[*sec*-BuLi] = 1980.0) due to its high reactivity. According to our observation, the reaction solution color changed to red in only a few seconds after *sec*-BuLi was introduced, which was much faster than the initiation time reported for *n*-BuLi initiated AMS bulk polymerization.[230] Seven samples were taken during the bulk polymerization and terminated by degassed methanol for analysis. The color of the solution stayed red orange during the whole reaction, suggesting low occurrence of termination during the sampling process. GPC was used to analyze molecular weight and molecular weight distributions (M_w/M_n) of all homopolymer samples and the M_w/M_n values are in the range of 1.06-1.17, which are much narrower than the results (M_w/M_n = 1.55-2.20) reported by *n*-BuLi initiated AMS bulk study.[230] The AMS conversion can be determined by

using molecular weight of PAMS over the molecular weight of complete (100%) AMS conversion calculated by initial molar ratio of AMS to *sec*-BuLi.

Table A.1 Molecular weight and composition data of AMS and isoprene reactivity study

Rxn Time (hr)	M_n[a] (g/mol)	M_w/M_n[a]	PI (mol%)[b]	PAMS (mol%)[b]
1	9,900	1.04	98.3	1.7
1.5	12,900	1.04	98.6	1.4
2	14,300	1.05	98.5	1.5
2.5	16,700	1.03	98.3	1.7
3	17,900	1.10	98.0	2.0
3.5	18,100	1.10	97.7	2.3
4	18,900	1.07	97.6	2.4
24	46,900	1.79	46.9	53.1

a) determined by light scattering (GPC); b) determined by ^{1}H NMR spectroscopy

The reactivity of AMS and isoprene was also investigated before the block copolymerization, since it was observed in previous studies that the crossover reaction from polybutadienyl anion to AMS is quite slow[221-223] and the reactivity of AMS-isoprene system in bulk anionic polymerization has not been investigated to the best of our knowledge. The reaction solution with 18 mL AMS and 2 mL isoprene was prepared at high concentration of AMS monomer (AMS/isoprene = 90/10 v/v). The polymerization was carried out using *sec*-BuLi as initiator ([AMS]/[*sec*-BuLi] = 1980.0 and [isoprene]/[*sec*-BuLi] = 258.6) at room temperature, and both monomers were initiated at the same time. However, after the calculated amount of *sec*-BuLi was added into the reaction, the color of the reaction turned to light yellow instead of red orange indicating that isoprene was the major monomer to be polymerized, since the color of polyisoprenyl anion is light yellow. The reaction color stayed light yellow for over 8 hours, but the color changed to red in the end of reaction (after 24 hour) and the reaction solution became

more viscous than first 8 hour reaction. Small amount of polymer solutions were taken at different times in first 4 hours of reaction, and the polymer samples were terminated by degassed methanol and precipitated in methanol for several times to remove extra AMS monomer. All polymer samples were analyzed by GPC to determine the molecular weight and the ^{1}H NMR spectroscopy was used to determine the monomer composition in polymer samples, the results are shown in Table A.1.

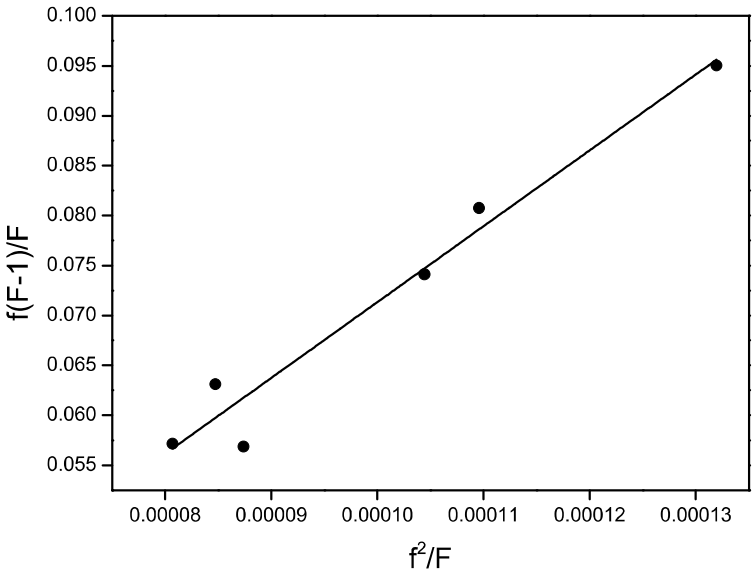

Figure A.1 Fineman–Ross plot for reactivity ratio study

In the first 4 hours of reaction, the molecular weight of polymer samples increased with the reaction time and the narrow molecular weight distributions (M_w/M_n = 1.03 – 1.10) were observed in all samples indicating the successful initiation and polymerization. The composition of PI and PAMS in polymer samples was calculated from the PI and PAMS characteristic peaks in the ^{1}H NMR spectra. During the first 4 hour reaction, all samples showed high PI composition (97.6 to 98.6 mol%) showing only small amounts of AMS monomer was incorporated in the

polymer samples, which agrees well with the light yellow color observed during the polymerization. In order to have a better understanding of AMS and isoprene copolymerization, the Fineman–Ross linear curve is plotted in Figure A.1 to determine the isoprene-AMS reactivity ratio. The experimental value of reactivity ratio reveals that isoprene monomer (r_1 = 752.6) is much more favorable to react with itself in this condition compared to the addition of AMS monomer, while the AMS (r_2 = 0.0019) polymerization is almost negligible even at a high concentration.

The reactivity ratio further confirmed that only isoprene polymerization took place at room temperature in first 4 hours. The conversion of isoprene can be calculated by comparing the molecular weight of polymer sample with the initial molar ratio of [isoprene]/[*sec*-BuLi]. After 4 hr reaction, polymer has a M_n of 18,900 g/mol indicating a high conversion of isoprene, since the theoretical M_n of 19,300 g/mol can be calculated for complete conversion of isoprene. Interestingly, the reaction solution became red after 24 hours and the polymer sample was also analyzed in GPC and ^{1}H NMR spectroscopy. Table A.1 exhibited that sample after 24 hours had much higher molecular weight than the earlier ones and the polymer sample had significant amount of AMS incorporated indicating that the AMS could still be polymerized without the polar additives as long as the isoprene monomer is completed. However, the final molecular weight distribution (M_w/M_n = 1.79) is relatively broad, which could correspond to the slow crossover reaction from polyisoprenyl anion to AMS leading to a low efficient initiation reaction. Therefore, the addition of polar additives might be still important when fast initiation process from polyisoprenyl anion to AMS is desired.

As discussed above, research has been conducted to prepare PAMS triblock copolymer using di-functional initiator,[221-224] however, the benefits of AMS's low ceiling temperature

and its weak reactivity have not been fully realized. Since the isoprene can be predominantly polymerized in AMS, a bulk anionic polymerization method (Scheme A.1) can be developed to synthesize AMS-isoprene diblock and triblock copolymers sequentially. The synthesis first involves the polymerization of AMS and subsequently the isoprene is introduced for diblock copolymer preparation. The triblock copolymer synthesis is finally achieved by adding polar additive (TMEDA) for AMS polymerization again after the completion of isoprene monomer.

Scheme A.1 Anionic polymerization of PAMS-PI diblock and triblock copolymer

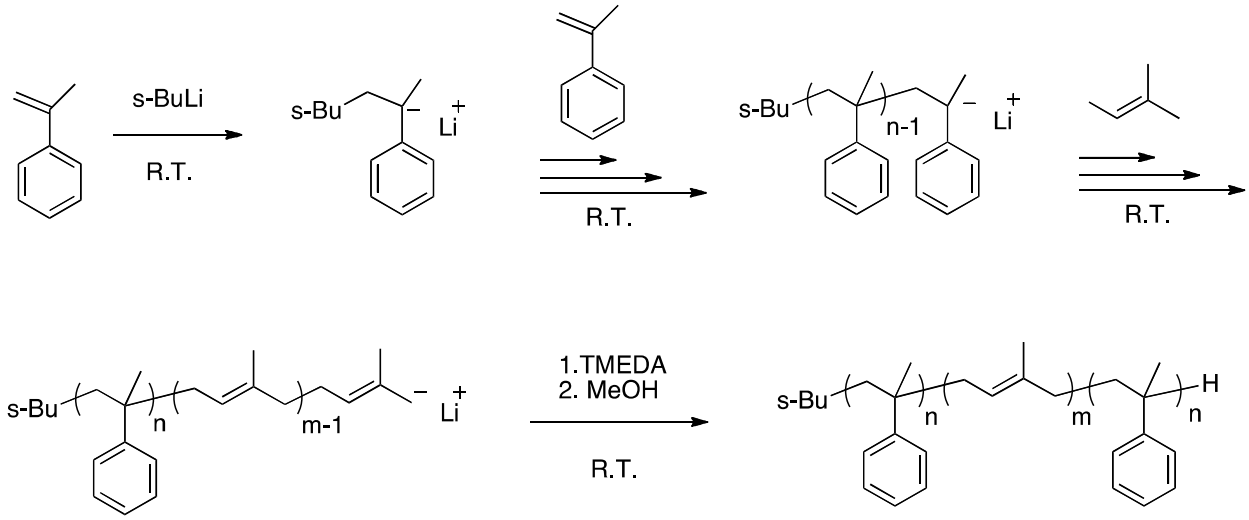

In the first step, anionic polymerization of AMS (18 mL) was carried out using *sec*-BuLi at room temperature in bulk. The *sec*-BuLi was shown to be a good initiator for bulk polymerization of AMS in homopolymerization experiments. The color of reaction stayed red during the AMS polymerization indicating the formation of PAMS anion. After 30 min reaction, a small amount of polymer solution (1 mL) was taken and terminated with degassed methanol for analysis. A series of experiments were performed and GPC was used to analyze all initial PAMS block samples. The molecular weights of PAMS blocks in all experiments were found in

a small range of 16,100 to 17,600 g/mol (Table A.2), which show a good consistence of initial PAMS block polymerizations. The molecular weight distributions of PAMS samples are also relatively narrow with a range of 1.05-1.13. Since the AMS polymerization will eventually reach the equilibrium, the concentration of AMS plays an important role in triblock copolymerization and can be determined by comparing the conversion of AMS monomer with initial AMS concentration (7.69 mol/L). The concentrations of AMS after 30 min bulk reaction in all experiments were estimated in a range of 7.11 to 7.15 mol/L (based on the molecular weight of PAMS), which are still much higher than the equilibrium concentration (~ 2.23 mol/L) of AMS polymerization at room temperature.[205]

Table A.2 Characterization of PAMS and PAMS-b-PI copolymers

Exp.	M_n[a](g/mol) of PAMS	M_w/M_n[a] of PAMS	isoprene (mL)	M_n[a](g/mol) of diblock	M_w/M_n[a] of diblock	PAMS : PI[b] (wt%)	1,4-PI[b]
1	16,300	1.05	2	37,100	1.15	43.8 : 56.2	94.2
2	17,200	1.09	2	38,800	1.16	41.8 : 58.2	93.6
3	17,600	1.02	4	39,400	1.04	46.0 : 54.0	93.6
4	16,900	1.13	4	47,700	1.14	29.8 : 70.2	93.4
5	16,100	1.03	4	60,400	1.05	25.4 : 74.6	93.9

a) determined by light scattering (GPC); b) determined by ^{1}H NMR spectroscopy

The diblock copolymerization was accomplished by introducing isoprene to the living PAMS chains. It is concluded from our reactivity ratio study that this reaction should switch to isoprene polymerization when isoprene was introduced, although there was a significant amount of AMS left. As the isoprene was introduced, the color of the reaction solution changed from red orange to light yellow immediately, indicating the fast crossover reaction from AMS polymerization to isoprene, and the color stayed light yellow during the reaction. A small amount

of polymer solution (1 mL) was also taken for analysis. A series of diblock polymer samples (Table A.2) were synthesized by varying the amount of isoprene monomers with corresponding reaction time (more monomers require longer reaction time). It should be noted that the unsaturated polymer might not be stable due to oxidative degradation even under ambient condition, therefore, radical inhibitor, BHT, was used in methanol with a concentration of 0.2 wt% during the polymer precipitation.

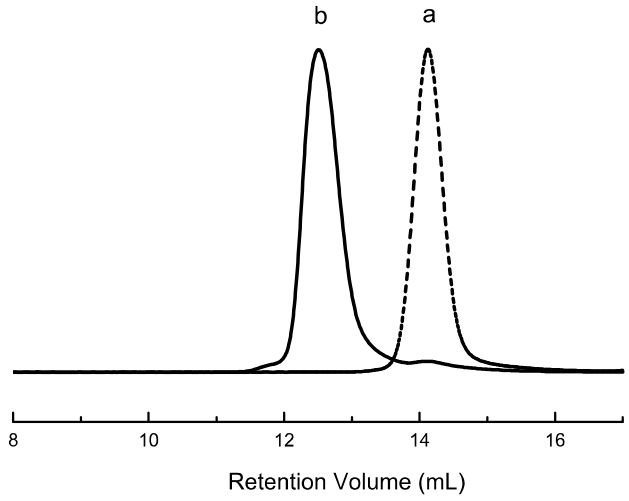

Figure A.2 GPC chromtograms of Exp.5. a) PAMS and b) PAMS-b-PI

The progression of copolymerization is demonstrated clearly by GPC chromatograms in Figure A.2 for diblock copolymerization experiment (Exp. 5). Dashed line represents the first block of PAMS homopolymer, and the solid line shows the complete separation from PAMS homopolymer to PAMS-b-PI copolymer. The diblock peak completely shifts to higher molecular weight in the chromatogram demonstrating the efficient crossover reaction from poly(α-methylstyrenyl)lithium to poly(α-methylstyrenyl)-b-polyisoprenyllithium. The molecular weight distributions (M_w/M_n = 1.05-1.16) of all diblock samples become only slightly higher after adding the second block indicating the successful isoprene initiation and polymerization. A tiny

peak in the low molecular weight region is observed in diblock copolymer and also it is overlapped with first PAMS block. This extra small peak could result from the introduction of impurities during the PAMS homopolymer sampling or the isoprene addition. The molecular weight of PI block can be estimated by comparing the molecular weights of block copolymers with the initial PAMS block in order to determine the isoprene conversion. Based on the initial molar ratio of [isoprene]/[*sec*-BuLi], it is calculated that isoprene in Exp. 1, 2 and 5 reached almost complete conversion, whereas Exp. 3 and 4 had isoprene conversion at approximately 56% and 79% respectively.

The block composition of copolymers and microstructure of the PI block were determined by ^{1}H NMR spectroscopy. Figure A.3 shows the spectrum of PAMS-b-PI copolymer (Exp. 5) consisting of characteristic chemical shifts of PI and PAMS. The chemical shifts at 6.5 – 7.2 ppm region are attributed to the aromatic protons from AMS, and the peaks at 4.9-5.8 ppm represent olefin protons of isoprene. The molar composition of PB and P4MS can be readily estimated by comparing integration of characteristic peaks for PAMS and PI. Furthermore, the weight fraction of PAMS and PI blocks in copolymer is determined at 25.4% : 74.6% for Exp. 5 (Table A.2). The block composition can also be estimated by the molecular weight of initial PAMS block and PAMS-b-PI, and the spectroscopy data matches very well with the composition calculated from molecular weight method. As a result, we can further conclude from spectroscopy results that almost no AMS was polymerized during the isoprene reaction. The peaks at 4.6-4.9 ppm represent the two olefinic protons from 3,4-structured PI and the chemical shift at 5.0-5.3 corresponds to the single olefinic protons from1,4-structured PI. Therefore, the microstructure compositions in PI block can be calculated based on the resonance integration of 3,4-structured PI and 1,4-structured PI. The amount of 1,4 conformation is predominant in the

microstructure of PI and only varies in a small range (93.4% to 94.2%) in Table A.2. The microstructure results of PI is in a good agreement with the value expected for anionic polymerization of diene monomers in nonpolar solvents, which further indicates that AMS worked well as a nonpolar solvent for isoprene polymerization. Additionally, the chemical shifts at 1.6 ppm and 1.7 ppm correspond to the *trans* and *cis* isomers of 1,4-PI. It is very clear to identify that *cis*-1,4-PI (approximately 70%) is the predominating structure in 1,4-PI.

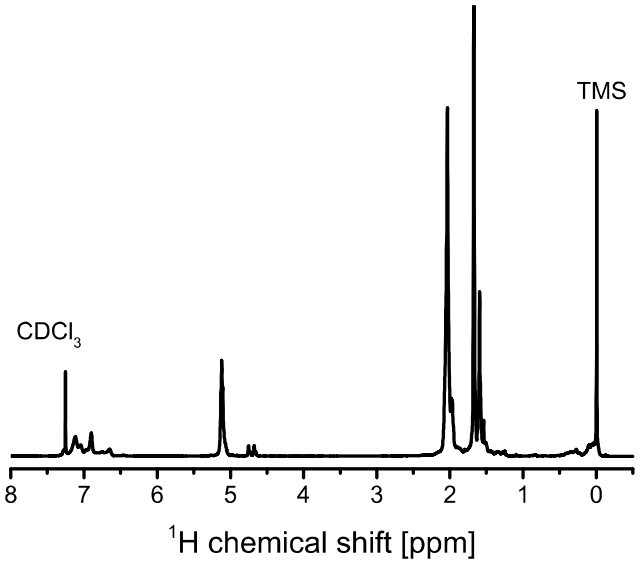

Figure A.3 ^{1}H NMR spectrum of PAMS-b-PI (exp.5) in $CDCl_3$ with respect to TMS

After isoprene polymerization, a large amount of AMS was still left in the polymerization system, however the amount of isoprene added into the reaction solution can dilute the AMS monomer concentration. Since almost no AMS polymerization occurred during isoprene reaction, the AMS concentration after diblock copolymer formation can be estimated in a range of 5.82 - 6.44 mol/L depending on the amount of isoprene added. The value is still much higher than the room temperature equilibrium concentration of AMS indicating that AMS can be polymerized again to form triblock copolymers. Previous study indicated that although the polyisoprenyllithium could switch to AMS polymerization after isoprene is finished, the

crossover reaction was quite slow resulting in the broad molecular weight distribution. In order to synthesize the well defined triblock copolymer, the efficiency of AMS re-initiation reaction needs to be enhanced. Different additives have been used for increasing the crossover reaction, such as styrene, THF and hexamethylene phosphoric triamide (HMPT),[221, 222] however, TMEDA has not been investigated as polar additive for this crossover reaction.

Table A.3 Characterizations of TMEDA addition reaction

Exp.	TMEDA (mL)	M_n[a](g/mol) of triblock	M_w/M_n[a] of triblock	PAMS : PI[b] (wt%)	1,4-PI[b]
1	0.25	52,100	1.25	61.2 : 38.8	94.0
2	0.25	56,800	1.20	60.7 : 39.3	93.4
3	0.25	65,800	1.26	25.0 : 75.0	62.2
4	0.25	70,000	1.14	28.2 : 71.8	78.9
5	0.25	76,500	1.16	36.2 : 63.8	93.9

a) determined by light scattering (GPC); b) determined by ^{1}H NMR spectroscopy

The final PAMS-b-PI-b-PAMS polymerization was carried out by adding TMEDA as polar additive into reaction solution at room temperature to increase the crossover reaction from poly(isoprenyl)lithium to AMS. When calculated amount of TMEDA (0.25 mL, [TMEDA]/[*sec*-BuLi] = 23.9) was introduced, the reaction color changed from light yellow to red orange immediately suggesting the successful re-initiation of AMS. The color stayed red orange during the reaction and the solution became noticeably viscous demonstrating that high molecular weight polymer was formed. The final polymer samples were also analyzed by GPC to determine the molecular weight, which is in a range of 52,100 to 76,500 g/mol. The molecular weight distributions are still relatively reasonable (M_w/M_n = 1.14 – 1.25), which are shown in Table A.3. The GPC chromatogram of the final polymer sample in Figure A.4 clearly demonstrates a clear separation from diblock peak, as well as an increase in molecular weight

from PAMS-b-PI indicating the successful initiation from the poly(α-methylstyrene)-b-polyisoprenyllithium to AMS. The molecular weight of third block can be easily calculated by comparing the molecular weight data of triblock in Table A.3 with diblock molecular weight. The GPC chromatogram of triblock copolymer (Exp. 5) also shows a little peak at low molecular weight region, which is overlapping with both the small bump in diblock sample and initial PAMS block. This implies that the TMEDA were successfully purified and functioned in the polymerization of AMS.

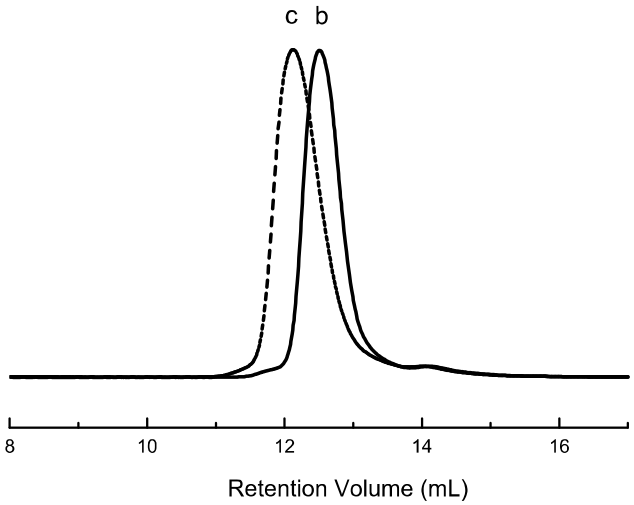

Figure A.4 GPC chromatograms of Exp. 5 b) PAMS-b-PI and c) PAMS-b-PI-b-PAMS

The ^{1}H NMR spectroscopy was also applied to determine the composition after the final synthetic step. The composition data for reaction after TMEDA addition is also shown in Table A.3, and can be compared with composition data in Table A.2. Due to the incomplete conversion of isoprene before TMEDA addition in Exp. 3 and 4, the final polymerization step was expected to involve both AMS and isoprene monomers. Therefore, the composition of PAMS in final polymer (Exp. 3, and 4) decreased while the final polymer samples in Exp. 1, 2, and 5 displayed a significant increase in PAMS contents after the TMEDA addition. Furthermore, it is observed

in ^{1}H NMR results that the microstructure of PI in Exp. 1, 2 and 5 still remain the same after the TMEDA addition, but the Exp. 3 and 4 lose the control over microstructures of PI with a dramatically decrease in the amount of 1,4-structured PI after the final-step polymerization. Both composition and microstructure data confirm that the polymer samples after TMEDA addition in Exp. 3 and 4 resulting in a tapered block copolymer with AMS and monomer in the third block. Nonetheless, Exp. 1, 2 and 5 only synthesize the AMS in the final step, so the clean PAMS-b-PI-b-PAMS triblock copolymers are prepared in the final step.

A.4 Conclusion

We have demonstrated that *sec*-BuLi initiated anionic polymerization of AMS can be carried out in bulk with a good control on molecular weight and its distribution in this work. The reactivity study of AMS and isoprene in bulk indicated that isoprene could be predominantly polymerized until completion in the presence of high AMS concentration (90% v/v). Well-defined diblock copolymers were prepared through sequential addition strategy in the large amount AMS monomer. The polar additive, TEMDA, can be used to effectively enhance the rate of crossover reaction from poly(α-methylstyrene)-b-polyisoprenyllithium to AMS polymerization. The tapered and clean triblock copolymers were prepared depending on the isoprene conversion before TMEDA addition.

A.5 Acknowledgement

NMR spectroscopy was made possible through a grant from the NSF MRI program (grant # CHW-0923537).

APPENDIX B AMPHILIPHILIC BLOCK COPOLYMERS CONTAINING QUATERNARY AMMONIUM CATION SYNTHESIZED BY LIVING POLYMERIZATION

B.1 Introduction

Alkaline anion exchange membranes (AAEMs) have received considerable attention recently as electrolytes in alkaline fuel cells (AFCs).[9, 10, 29] The disadvantage of traditional AFCs is the liquid electrolyte (e.g. KOH), which results in the formation of precipitated carbonate by reaction with CO_2. AAEMs can overcome the problem of carbonate precipitates in AFC electrolytes. Right now, amphiphilic block copolymers containing quaternary ammonium cation are an interesting class of AAEMs and have potential application in AFCs.[27]

Numerous methods can be used to synthesize amphiphilic block copolymers. Living polymerization is one powerful method to form these unique structures. This method not only results in controlled molecular weight and molecular weight distribution,[111, 234] but also good phase separation, which is particularly useful for morphology control. In the current study, we demonstrate combining two living polymerization techniques (anionic polymerization and nitroxide mediated polymerization) to synthesize amphiphilic block copolymers containing quaternary ammonium cation for potential AAEM applications.

B.2 Experimental

B.2.1 Materials

Butadiene (≥99%) was purified by the procedure described in the literature.[235] sec-Butyllithium (1.4M) in cyclohexane solution, Br_2 (%), 2,2,6,6-tetramethyl-1-(2-bromo-1-phenylethoxy) piperidine (TEMPO) (98%) and anhydrous trimethylamine gas (99%) were used

as received. Styrene (99%) and vinylbenzyl chloride (VBC) (90%) were purified by distillation under reduced pressure right before use. Polymerization solvents (cylcohexane, THF) were purified by passing through columns on a commercial system (Innovative Technology). Other reagents were used without further purification.

B.2.2 Synthesis of Nitroxide Functionalized Polybutadiene (PB-TEMPO)

Glassware and a stir bar were dried at ~150 °C overnight before the polymerization. s-BuLi (80 μL) was injected into a flame-dried 50 mL round bottom flask with dry cylcohexane (25 mL) from the solvent purifier. Purified butadiene (12.5 mL) was transferred into the round bottom flask by cannula at room temperature, and the polymerization was left to stir for 20 hr. 2,2,6,6-tetramethyl-1-(2-bromo-1-phenylethoxy) piperidine (Br-TEMPO) was synthesized by the procedure described in the literature,[235-238] and Br-TEMPO (200 mg) was dissolved in dry THF and transferred into reaction flask to terminate the polymerization.

B.2.3 Synthesis of Polybutadiene-b-Polystyrene (PB-b-PS) by Nitroxide Mediated Polymerization

PB-TEMPO was used as a macroinitiator to polymerize styrene. PB-TEMPO (100 mg) was added to a 50 mL round bottom flask, and styrene (10 mL) was injected into round bottom flask. After PB-TEMPO was dissolved in styrene, the round bottom flask was purged by Ar for 30 min. This bulk polymerization was carried out at 125 °C for 5 hrs.

B.2.4 Synthesis of Polybutadiene-b-Poly(vinylbenzyl chloride) (PB-b-PVBC) by Nitroxide Mediated Polymerization

PB-TEMPO was used as a macroinitiator to polymerize VBC. PB-TEMPO (200 mg) was weighed into a 50 mL round bottom flask, and VBC (10 mL) was then injected into the flask. After PB-TEMPO was dissolved in styrene, and the round bottom flask was purged with Ar for 30 min. The bulk polymerization was carried out at 125 °C for 4 hrs.

B.2.5 Synthesis of Polybutadiene-b-Poly(vinylbenzyltrimethylammonium chloride) (PB-b-P[VBTMA][Cl])

PB-b-PVBC (300 mg) was dissolved in 15 mL chloroform in a 25 mL round bottom flask sealed with a septum. Anhydrous trimethylamine gas was added into the polymer solution to form PB-b-P[VBTMA][Cl]. The precipitates formed immediately as the trimethylamine was added. Preparation of PB-b-P[VBTMA][Cl] membrane. The PB-b-P[VBTMA][Cl] was solvent cast in a chloroform/methanol co-solvent at room temperature.

B.2.6 Characterization

Gel permeation chromatography (GPC) was performed in THF at 30 ^{o}C using a Waters model 600 high pressure liquid chromatograph with the flow rate at 1 mL/min, and connected to a calibrated Wyatt R401 differential refractometer and a Wyatt Technology miniDAWN multi-angle laser light scattering (MALLS) detector.

^{1}H NMR spectra of polymers were obtained from a JEOL 500 MHz spectrometer. All polymer samples were dissolved in $CDCl_3$ using tetramethylsilane (TMS) as standard. IR measurements were performed on a Thermo FT-IR spectrometer.

B.3 Results and Discussion

PB-TEMPO and PB-b-PS. The anionic polymerization of butadiene was carried out using s-BuLi as initiator ([Bd]/[s-BuLi] = 735.3) in cyclohexane at room temperature, and the PB was functionalized by Br-TEMPO to form TEMPO end capped PB[6]. This termination reaction was carried out using a 2.0-fold molar excess of terminator in cyclohexane/THF for 24 hr[6] at 10 °C. The functionalized PB was analyzed and it had a M_n = 50,000 and M_w/M_n = 1.10. In order to prove the formation of PB-TEMPO, bulk copolymerization of PB-b-PS was conducted on PB-TEMPO macroinitiator and styrene at 125 °C.

The living radical copolymerization of styrene (10 ml) was initiated by TEMPO functionalized PB. The conversion of styrene reached 56% after 6 hr. The results of GPC analysis of PB-TEMPO and the PB-b-PS diblock copolymer are shown in Figure B.1.

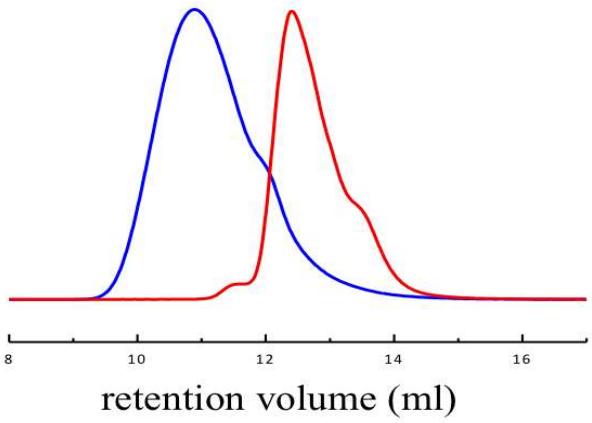

Figure B.1 The GPC curves of TEMPO functionalized PB and PB-b-PS diblock copolymer

The molecular weight of PB-b-PS was measured by GPC and it had M_n = 250,000 and a broadened molecular weight distribution with M_w/M_n = 1.90. The styrene conversion was determined by using molecular weight of PS block in PB-b-PS over the molecular weight of 100% styrene conversion calculated by initial molar ratio of styrene to the PB-TEMPO. The

GPC curve of PB-b-PS shows a small amount of tailing in the low molecular weight region, and it shows a significant separation from the initial PB-TEMPO block. Some portion of PB-TEMPO initiator may not convert to diblock, but most of the macroinitiator was reacted to form diblock.

PB-b-PVBC. Different block compositions of PB-b-PVBCs were also synthesized by using PB-TEMPO as macroinitiator to bulk polymerize VBC (10 ml) in different polymerization times at 125 °C (Scheme B.1). The PB-b-PVBC copolymers were analyzed by GPC and ^{1}H NMR spectroscopy, and the results are shown in Table B.1. GPC curves of PB-b-PVBC copolymers depict the increase in molecular weight from initial PB-TEMPO block

Scheme B.1 Synthesis of PB-b-PS by TEMPO functionalized PB

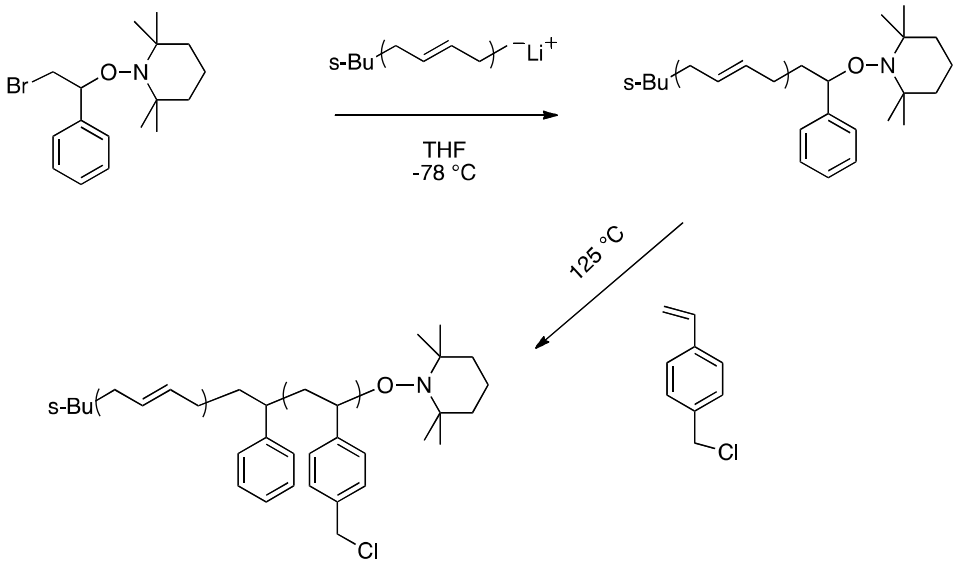

Table B.1 Molecular weight and composition data of PB-b-PVBC copolymers

Rxn time of VBC	M_n[a]	PDI[a]	PVBC (wt%)[b]	1,4-PB (%)[b]
2.5 hr	61,210	1.46	28.3	95.4
3.5 hr	73,150	1.7	39.3	95.0
5 hr	100,010	1.82	53.1	94.9

a) determined by light scattering (GPC); b) determined by ^{1}H NMR spectroscopy

Figure B.2 shows the PB-b-PVBC with 3.5 hr polymerization of VBC. The spectrum exhibits both PB and PVBC characteristic resonances. The composition of PB and PVBC can be determined by comparing the resonances at 4.9-5.8 ppm with those at 4.58 ppm. It is well known that the microstructure of PB can be quantified by comparing the integrations of resonance between 4.9-5.1 ppm and 5.1-5.8 ppm, which represent for the 1,2- and 1,4-PB. From Figure 2, the 1,4-PB was estimated to be about 94.5%, which is in agreement with the value expected for anionic polymerization of diene monomers in nonpolar solvents.

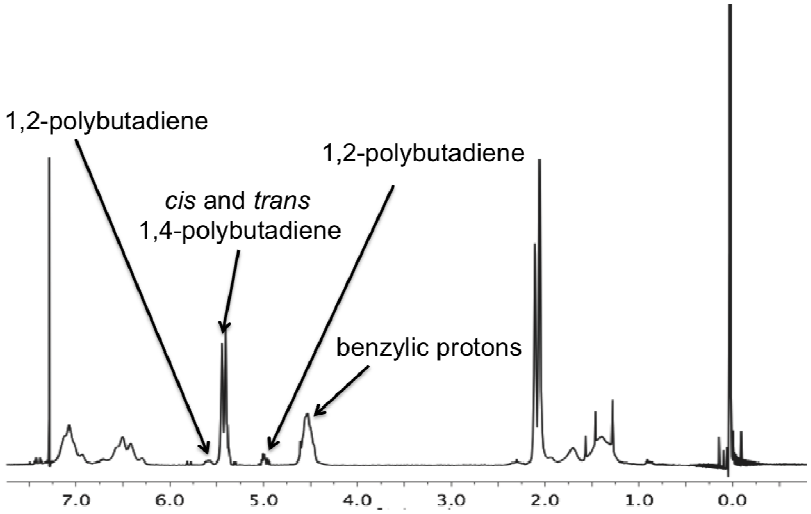

Figure B.2 ^{1}H NMR spectrum of PB-b-PVBC with 3.5 hr VBC bulk polymerization

PB-b-P[VBTMA][Cl]. The resulting PB-b-PVBC copolymers were dissolved in chloroform and reacted with a large excess of anhydrous trimethylamine at room temperature. The FT-IR spectroscopy confirms the formation of quaternary ammonium cation. Figure B.3(a) depicts the IR spectrum of PB-b-PVBC, which shows a very clear chloromethyl ($-CH_2-Cl$) functional group with absorption peaks at 571.1 cm^{-1} and 1263.8 cm^{-1}. By comparing Figure B.3(a) with Figure 3(b), the 571.1 cm^{-1} and 1263.8 cm^{-1} absorption peaks in Figure 3(b) have almost disappeared, which indicates the reaction on the chloromethyl ($-CH_2$ -Cl) functional group. The absorption peak at 3364.5 cm^{-1} in Figure 3(b) represents the water peak associated

with the formation of quaternary ammonium groups. Final PB-b-P[VBTMA][Cl] was solvent cast by chloroform/methanol co-solvent at room temperature on teflon substrate. Other properties will be investigated in the future.

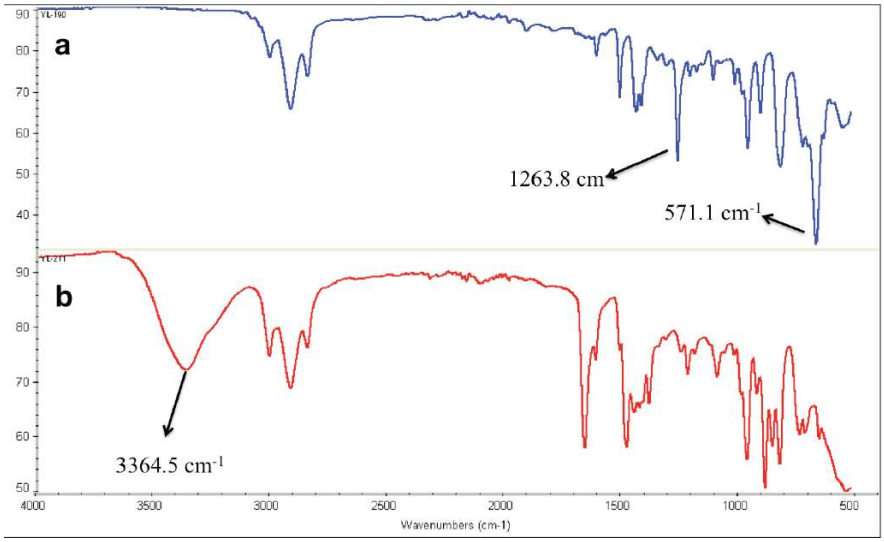

Figure B.3 The FT-IR spectrum of (a) PB-b-PVBC and (b) PB-b- P[VBTMA][Cl]

B.4 Conclusion

In this study, we demonstrate a synthetic pathway to combine two living polymerization techniques (anionic polymerization and nitroxide mediated polymerization) to produce the amphiphilic block copolymer PB-b-P[VBTMA][Cl]. The formation of TEMPO functionalized PB was proved by further polymerization of PB-b-PS by NMP, and GPC curve of PB-b-PS showed complete separation from that of the PB-TEMPO. Subsequently, bulk copolymerization was carried out on PB-TEMPO macroinitiator and VBC at 125°C, and GPC curves and ^{1}H NMR characterization proved the formation of PB-b-PVBC. The PB-b-PVBC diblock copolymers with different block compositions were investigated. FT-IR was used to characterize the formation of

quaternary ammonium cation by trimethylamine. The membranes made from PB-b-P[VBTMA][Cl] were solvent cast, and could potentially extend the application in AAEMs.

B.5 Acknowledgement

Funding was provided by the Army Research Office through a MURI (grant # W911NF-10-1-0520). NMR spectroscopy was made possible through a grant from the NSF MRI program (grant # CHW-0923537)

APPENDIX C COPYRIGHT PERMISSIONS

American Chemical Society's Policy on Theses and Dissertations

If your university requires you to obtain permission, you must use the RightsLink permission system.
See RightsLink instructions at http://pubs.acs.org/page/copyright/permissions.html.

This is regarding request for permission to include **your** paper(s) or portions of text from **your** paper(s) in your thesis. Permission is now automatically granted; please pay special attention to the **implications** paragraph below. The Copyright Subcommittee of the Joint Board/Council Committees on Publications approved the following:

Copyright permission for published and submitted material from theses and dissertations

ACS extends blanket permission to students to include in their theses and dissertations their own articles, or portions thereof, that have been published in ACS journals or submitted to ACS journals for publication, provided that the ACS copyright credit line is noted on the appropriate page(s).

Publishing **implications** of electronic publication of theses and dissertation material

Students and their mentors should be aware that posting of theses and dissertation material on the Web prior to submission of material from that thesis or dissertation to an ACS journal may affect publication in that journal. Whether Web posting is considered prior publication may be evaluated on a case-by-case basis by the journal's editor. If an ACS journal editor considers Web posting to be "prior publication", the paper will not be accepted for publication in that journal. If you intend to submit your unpublished paper to ACS for publication, check with the appropriate editor prior to posting your manuscript electronically.

Reuse/Republication of the Entire Work in Theses or Collections: Authors may reuse all or part of the Submitted, Accepted or Published Work in a thesis or dissertation that the author writes and is required to submit to satisfy the criteria of degree-granting institutions. Such reuse is permitted subject to the ACS' "Ethical Guidelines to Publication of Chemical Research" (http://pubs.acs.org/page/policy/ethics/index.html); the author should secure written confirmation (via letter or email) from the respective ACS journal editor(s) to avoid potential conflicts with journal prior publication*/embargo policies. Appropriate citation of the Published Work must be made. If the thesis or dissertation to be published is in electronic format, a direct link to the Published Work must also be included using the ACS Articles on Request author-directed link – see http://pubs.acs.org/page/policy/articlesonrequest/index.html

* Prior publication policies of ACS journals are posted on the ACS website at http://pubs.acs.org/page/policy/prior/index.html

If your paper has **not** yet been published by ACS, please print the following credit line on the first page of your article: "Reproduced (or 'Reproduced in part') with permission from [JOURNAL NAME], in press (or 'submitted for publication'). Unpublished work copyright [CURRENT YEAR] American Chemical Society." Include appropriate information.

If your paper has already been published by ACS and you want to include the text or portions of the text in your thesis/dissertation, please print the ACS copyright credit line on the first page of your article: "Reproduced (or 'Reproduced in part') with permission from [FULL REFERENCE CITATION.] Copyright [YEAR] American Chemical Society." Include appropriate information.

Submission to a Dissertation Distributor: If you plan to submit your thesis to UMI or to another dissertation distributor, you should not include the unpublished ACS paper in your thesis if the thesis will be disseminated electronically, until ACS has published your paper. After publication of the paper by ACS, you may release the entire thesis (**not the individual ACS article by itself**) for electronic dissemination through the distributor; ACS's copyright credit line should be printed on the first page of the ACS paper.

10/10/03, 01/15/04, 06/07/06, 04/07/10, 08/24/10, 02/28/11

Wiley and Sons Author Retained Rights

excerpt from Copyright FAQs on the Wiley website:

http://authorservices.wiley.com/bauthor/faqs_copyright.asp#1.7

7. What rights do I retain?

The Contributor or, if applicable, the Contributor's Employer, retains all proprietary rights other than copyright, such as patent rights, in any process, procedure or article of manufacture described in the contribution.

Contributors may re-use unmodified abstracts for any non-commercial purpose. For online use of the abstract, Wiley-Blackwell encourages but does not require linking back to the final published contribution.

Contributors may use the articles in teaching duties and in other works such as theses.

Contributors may re-use figures, tables, data sets, artwork, and selected text up to 250 words from their contributions, provided the following conditions are met:

Full and accurate credit must be given to the contribution.

Modifications to the figures, tables and data must be noted. Otherwise, no changes may be made.

The reuse may not be made for direct commercial purposes, or for financial consideration to the Contributor.

Re-use rights shall not be interpreted to permit dual publication in violation of journal ethical practices.

Additional re-use rights are set forth in the actual copyright Agreement.

Title: Anion Conductive Block Poly(arylene ether)s: Synthesis, Properties, and Application in Alkaline Fuel Cells

Author: Manabu Tanaka, Keita Fukasawa, Eriko Nishino, Susumu Yamaguchi, Koji Yamada, Hirohisa Tanaka, Byungchan Bae, Kenji Miyatake, and Masahiro Watanabe

Publication: Journal of the American Chemical Society

Publisher: American Chemical Society

Date: Jul 1, 2011

Quick Price Estimate

Permission for this particular request is granted for print and electronic formats, and translations, at no charge. Figures and tables may be modified. Appropriate credit should be given. Please print this page for your records and provide a copy to your publisher. Requests for up to 4 figures require only this record. Five or more figures will generate a printout of additional terms and conditions. Appropriate credit should read: "Reprinted with permission from {COMPLETE REFERENCE CITATION}. Copyright {YEAR} American Chemical Society." Insert appropriate information in place of the capitalized words.

If credit is given to another source for the material you requested, permission must be obtained from that source.

I would like to... reuse in a Thesis/Dissertation

Requestor Type Author (original

Portion

Number of Table/Figure/Micrographs 2

Format Print and

Select your currency USD - $

Quick Price Click Quick Price

QUICK PRICE | CONTINUE

This service provides permission for reuse only. If you do not have a copy of the article you are using, you may copy and paste the content and reuse according to the terms of your agreement. Please be advised that obtaining the content you license is a separate transaction not involving Rightslink.

Note: Individual Scheme and Structure reuse is free of charge and does not require a license. If the scheme or structure is identified as a Figure in the article, permission is required.

To request permission for a type of use not listed, please contact the publisher directly.

Title: Effect of Nanoscale Morphology on the Conductivity of Polymerized Ionic Liquid Block Copolymers

Author: Ryan L. Weber, Yuesheng Ye, Andrew L. Schmitt, Steven M. Banik, Yossef A. Elabd, and Mahesh K. Mahanthappa

Publication: Macromolecules

Publisher: American Chemical Society

Date: Jul 1, 2011

Quick Price Estimate

Permission for this particular request is granted for print and electronic formats, and translations, at no charge. Figures and tables may be modified. Appropriate credit should be given. Please print this page for your records and provide a copy to your publisher. Requests for up to 4 figures require only this record. Five or more figures will generate a printout of additional terms and conditions. Appropriate credit should read: "Reprinted with permission from {COMPLETE REFERENCE CITATION}. Copyright {YEAR} American Chemical Society." Insert appropriate information in place of the capitalized words.

If credit is given to another source for the material you requested, permission must be obtained from that source.

I would like to...	reuse in a Thesis/ Dissertation
Requestor Type	Author (original work)
Portion	Table/Figure/Micrograph
Number of Table/Figure/Micrographs	1
Format	Print and Electronic
Select your currency	USD - $
Quick Price	Click Quick Price

QUICK PRICE CONTINUE

This service provides permission for reuse only. If you do not have a copy of the article you are using, you may copy and paste the content and reuse according to the terms of your agreement. Please be advised that obtaining the content you license is a separate transaction not involving Rightslink.

Note: Individual Scheme and Structure reuse is free of charge and does not require a license. If the scheme or structure is identified as a Figure in the article, permission is required.

To request permission for a type of use not listed, please contact the publisher directly.

Copyright Clearance Center RightsLink®

Home | Create Account | Help

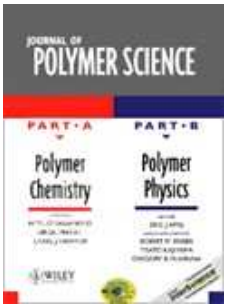

Title: Synthesis and structure–conductivity relationship of polystyrene-block-poly(vinyl benzyl trimethylammonium) for alkaline anion exchange membrane fuel cells

Author: Tsung-Han Tsai,Ashley M. Maes,Melissa A. Vandiver,Craig Versek,Sönke Seifert,Mark Tuominen,Matthew W. Liberatore,Andrew M. Herring,E. Bryan Coughlin

Publication: Journal of Polymer Science Part B: Polymer Physics

Publisher: John Wiley and Sons

Date: Sep 21, 2012

User ID

Password

Enable Auto Login

LOGIN

Forgot Password/User ID?

If you're a copyright.com user, you can login to RightsLink using your copyright.com credentials. Already **a RightsLink user** or want to learn more?

Quick Price Estimate

This permission does not apply to images that are credited to publications other than Wiley journals or books. For images credited to non-Wiley journal or book publications, you will need to obtain permission from the journal or book referenced in the figure or table legend or credit line before making any use of the image(s) or table(s).

John Wiley and Sons grants a license for all orders, including $0 orders. Please select the Continue button and place an order for this reuse.

This license allows only minor adaptations as required by the new publication format (with no additions, deletions or modifications to the text that materially alter the meaning of what the author has written). If you wish to make more significant changes to the work please select "I don't see my intended use" and provide full details of your proposed adaptation for review by John Wiley and Sons.

I would like to... reuse in a dissertation/ thesis

Requestor Type University/Academic

Format Print and electronic

Portion FigureAddle

Number of figures/tables 3

Will you be translating? No

Quick Price 0.00 USD

QUICK PRICE | CONTINUE

Content Delivery: This service provides permission for reuse only. If you do not have a copy of the content you are using, you may purchase it via Pay-Per-View.

REFERENCES CITED

1. Barnett, B.M. and Teagan, W.P., *The role of fuel cells in our energy future*. Journal of Power Sources, 1992. **37**(1–2): p. 15-31.

2. Du Melle, F., *The global and urban environment: the need for clean power systems*. Journal of Power Sources, 1998. **71**(1–2): p. 7-11.

3. Dufour, A.U., *Fuel cells – a new contributor to stationary power*. Journal of Power Sources, 1998. **71**(1–2): p. 19-25.

4. Bauen, A. and Hart, D., *Assessment of the environmental benefits of transport and stationary fuel cells*. Journal of Power Sources, 2000. **86**(1–2): p. 482-494.

5. Hart, D., *Sustainable energy conversion: fuel cells — the competitive option?* Journal of Power Sources, 2000. **86**(1–2): p. 23-27.

6. Carrette, L., Friedrich, K.A. and Stimming, U., *Fuel Cells – Fundamentals and Applications*. Fuel Cells, 2001. **1**(1): p. 5-39.

7. Kordesch, K.V. and Simader, G.R., *Environmental Impact of Fuel Cell Technology*. Chemical Reviews, 1995. **95**(1): p. 191-207.

8. Couture, G., Alaaeddine, A., Boschet, F. and Ameduri, B., *Polymeric materials as anion-exchange membranes for alkaline fuel cells*. Progress in Polymer Science, 2011. **36**(11): p. 1521-1557.

9. McLean, G.F., Niet, T., Prince-Richard, S. and Djilali, N., *An assessment of alkaline fuel cell technology*. International Journal of Hydrogen Energy, 2002. **27**(5): p. 507-526.

10. Varcoe, J.R. and Slade, R.C.T., *Prospects for Alkaline Anion-Exchange Membranes in Low Temperature Fuel Cells*. Fuel Cells, 2005. **5**(2): p. 187-200.

11. Merle, G., Wessling, M. and Nijmeijer, K., *Anion exchange membranes for alkaline fuel cells: A review*. Journal of Membrane Science, 2011. **377**(1-2): p. 1-35.

12. Gamburzev, S., Petrov, K. and Appleby, A.J., *Silver–carbon electrocatalyst for air cathodes in alkaline fuel cells*. Journal of Applied Electrochemistry, 2002. **32**(7): p. 805-809.

13. Abdel Rahim, M.A., Abdel Hameed, R.M. and Khalil, M.W., *Nickel as a catalyst for the electro-oxidation of methanol in alkaline medium*. Journal of Power Sources, 2004. **134**(2): p. 160-169.

14. Schulze, M. and Gülzow, E., *Degradation of nickel anodes in alkaline fuel cells*. Journal of Power Sources, 2004. **127**(1–2): p. 252-263.

15. Wagner, N., Schulze, M. and Gülzow, E., *Long term investigations of silver cathodes for alkaline fuel cells*. Journal of Power Sources, 2004. **127**(1–2): p. 264-272.

16. Gülzow, E., *Alkaline fuel cells: a critical view*. Journal of Power Sources, 1996. **61**(1–2): p. 99-104.

17. Cifrain, M. and Kordesch, K.V., *Advances, aging mechanism and lifetime in AFCs with circulating electrolytes*. Journal of Power Sources, 2004. **127**(1-2): p. 234-242.

18. Gülzow, E. and Schulze, M., *Long-term operation of AFC electrodes with CO2 containing gases*. Journal of Power Sources, 2004. **127**(1-2): p. 243-251.

19. Sata, T., *Studies on ion exchange membranes with permselectivity for specific ions in electrodialysis*. Journal of Membrane Science, 1994. **93**(2): p. 117-135.

20. Strathmann, H., *Chapter 6 Electrodialysis and related processes*, in *Membrane Science and Technology*, Richard, D.N. and Stern, S.A., Editors. 1995, Elsevier. p. 213-281.

21. Sata, T., Teshima, K. and Yamaguchi, T., *Permselectivity between two anions in anion exchange membranes crosslinked with various diamines in electrodialysis*. Journal of Polymer Science Part A: Polymer Chemistry, 1996. **34**(8): p. 1475-1482.

22. Hickner, M.A., *Ion-containing polymers: new energy & clean water*. Materials Today, 2010. **13**(5): p. 34-41.

23. Hibbs, M.R., Hickner, M.A., Alam, T.M., McIntyre, S.K., Fujimoto, C.H. and Cornelius, C.J., *Transport Properties of Hydroxide and Proton Conducting Membranes*. Chemistry of Materials, 2008. **20**(7): p. 2566-2573.

24. Varcoe, J.R., *Investigations of the ex situ ionic conductivities at 30 [degree]C of metal-cation-free quaternary ammonium alkaline anion-exchange membranes in static atmospheres of different relative humidities*. Physical Chemistry Chemical Physics, 2007. **9**(12): p. 1479-1486.

25. Elabd, Y.A. and Hickner, M.A., *Block Copolymers for Fuel Cells*. Macromolecules, 2010. **44**(1): p. 1-11.

26. Bauer, B., Strathmann, H. and Effenberger, F., *Anion-exchange membranes with improved alkaline stability*. Desalination, 1990. **79**(2,Äì3): p. 125-144.

27. Einsla, B.R., Chempath, S., Pratt, L., Boncella, J., Rau, J., Macomber, C. and Pivovar, B., *Stability of Cations for Anion Exchange Membrane Fuel Cells*. ECS Transactions, 2007. **11**(1): p. 1173-1180.

28. Chempath, S., Boncella, J.M., Pratt, L.R., Henson, N. and Pivovar, B.S., *Density Functional Theory Study of Degradation of Tetraalkylammonium Hydroxides*. The Journal of Physical Chemistry C, 2010. **114**(27): p. 11977-11983.

29. Jaeger, W., Bohrisch, J. and Laschewsky, A., *Synthetic polymers with quaternary nitrogen atoms--Synthesis and structure of the most used type of cationic polyelectrolytes*. Progress in Polymer Science, 2010. **35**(5): p. 511-577.

30. Sata, T., *Modification of properties of ion-exchange membranes. IV. Change of transport properties of cation-exchange membranes by various polyelectrolytes*. Journal of Polymer Science: Polymer Chemistry Edition, 1978. **16**(5): p. 1063-1080.

31. Danks, T.N., Slade, R.C.T. and Varcoe, J.R., *Alkaline anion-exchange radiation-grafted membranes for possible electrochemical application in fuel cells*. Journal of Materials Chemistry, 2003. **13**(4): p. 712-721.

32. Herman, H., Slade, R.C.T. and Varcoe, J.R., *The radiation-grafting of vinylbenzyl chloride onto poly(hexafluoropropylene-co-tetrafluoroethylene) films with subsequent conversion to alkaline anion-exchange membranes: optimisation of the experimental conditions and characterisation*. Journal of Membrane Science, 2003. **218**(1,Äì2): p. 147-163.

33. Dragan, E.S., Avram, E., Axente, D. and Marcu, C., *Ion-exchange resins. III. Functionalization–morphology correlations in the synthesis of some macroporous, strong basic anion exchangers and uranium-sorption properties evaluation*. Journal of Polymer Science Part A: Polymer Chemistry, 2004. **42**(10): p. 2451-2461.

34. Slade, R.C.T. and Varcoe, J.R., *Investigations of conductivity in FEP-based radiation-grafted alkaline anion-exchange membranes*. Solid State Ionics, 2005. **176**(5-6): p. 585-597.

35. Varcoe, J.R., Slade, R.C.T., Lam How Yee, E., Poynton, S.D., Driscoll, D.J. and Apperley, D.C., *Poly(ethylene-co-tetrafluoroethylene)-Derived Radiation-Grafted Anion-Exchange Membrane with Properties Specifically Tailored for Application in Metal-Cation-Free Alkaline Polymer Electrolyte Fuel Cells*. Chemistry of Materials, 2007. **19**(10): p. 2686-2693.

36. Luo, Y., Guo, J., Wang, C. and Chu, D., *Quaternized poly(methyl methacrylate-co-butyl acrylate-co-vinylbenzyl chloride) membrane for alkaline fuel cells*. Journal of Power Sources, 2010. **195**(12): p. 3765-3771.

37. Zeng, Q.H., Liu, Q.L., Broadwell, I., Zhu, A.M., Xiong, Y. and Tu, X.P., *Anion exchange membranes based on quaternized polystyrene-block-poly(ethylene-ran-butylene)-block-polystyrene for direct methanol alkaline fuel cells*. Journal of Membrane Science, 2010. **349**(1-2): p. 237-243.

38. Vinodh, R., Ilakkiya, A., Elamathi, S. and Sangeetha, D., *A novel anion exchange membrane from polystyrene (ethylene butylene) polystyrene: Synthesis and characterization*. Materials Science and Engineering: B, 2010. **167**(1): p. 43-50.

39. Cao, Y.-C., Wang, X., Mamlouk, M. and Scott, K., *Preparation of alkaline anion exchange polymer membrane from methylated melamine grafted poly(vinylbenzyl chloride) and its fuel cell performance*. Journal of Materials Chemistry, 2011. **21**(34): p. 12910-12916.

40. Faraj, M., Elia, E., Boccia, M., Filpi, A., Pucci, A. and Ciardelli, F., *New anion conducting membranes based on functionalized styrene–butadiene–styrene triblock copolymer for fuel cells applications*. Journal of Polymer Science Part A: Polymer Chemistry, 2011. **49**(15): p. 3437-3447.

41. Luo, Y., Guo, J., Wang, C. and Chu, D., *Fuel cell durability enhancement by crosslinking alkaline anion exchange membrane electrolyte*. Electrochemistry Communications, 2012. **16**(1): p. 65-68.

42. Sun, L., Guo, J., Zhou, J., Xu, Q., Chu, D. and Chen, R., *Novel nanostructured high-performance anion exchange ionomers for anion exchange membrane fuel cells*. Journal of Power Sources, 2012. **202**: p. 70-77.

43. Hao, J., Wang, W., Yang, P. and Zhao, Q., *The preparation of quaternized polysulfone membrane for low pressure reverse osmosis*. Desalination, 1991. **83**(1–3): p. 361-371.

44. Dal-Cin, M.M., Tam, C.M., Guiver, M.D. and Tweddle, T.A., *Polysulfone membranes. V. Poly(phenyl sulfone) (Radel R)–poly(vinyl pyrrolidone) membranes*. Journal of Applied Polymer Science, 1994. **54**(6): p. 783-792.

45. Rafe, A. and Razavi, S.M.A., *Water and hexane permeate flux through UF polysulfone amide membrane*. Desalination, 2009. **236**(1–3): p. 39-45.

46. Ahn, J., Chung, W.-J., Pinnau, I. and Guiver, M.D., *Polysulfone/silica nanoparticle mixed-matrix membranes for gas separation*. Journal of Membrane Science, 2008. **314**(1–2): p. 123-133.

47. Barbari, T.A. and Datwani, S.S., *Gas separation properties of polysulfone membranes treated with molecular bromine*. Journal of Membrane Science, 1995. **107**(3): p. 263-266.

48. Genova-Dimitrova, P., Baradie, B., Foscallo, D., Poinsignon, C. and Sanchez, J.Y., *Ionomeric membranes for proton exchange membrane fuel cell (PEMFC): sulfonated polysulfone associated with phosphatoantimonic acid*. Journal of Membrane Science, 2001. **185**(1): p. 59-71.

49. Kerres, J., Cui, W. and Reichle, S., *New sulfonated engineering polymers via the metalation route. I. Sulfonated poly(ethersulfone) PSU Udel® via metalation-sulfination-oxidation*. Journal of Polymer Science Part A: Polymer Chemistry, 1996. **34**(12): p. 2421-2438.

50. Li, L. and Wang, Y., *Quaternized polyethersulfone Cardo anion exchange membranes for direct methanol alkaline fuel cells*. Journal of Membrane Science, 2005. **262**(1-2): p. 1-4.

51. Wang, G., Weng, Y., Chu, D., Chen, R. and Xie, D., *Developing a polysulfone-based alkaline anion exchange membrane for improved ionic conductivity*. Journal of Membrane Science, 2009. **332**(1-2): p. 63-68.

52. Wang, J., Zhao, Z., Gong, F., Li, S. and Zhang, S., *Synthesis of Soluble Poly(arylene ether sulfone) Ionomers with Pendant Quaternary Ammonium Groups for Anion Exchange Membranes*. Macromolecules, 2009. **42**(22): p. 8711-8717.

53. Zhou, J., Unlu, M., Vega, J.A. and Kohl, P.A., *Anionic polysulfone ionomers and membranes containing fluorenyl groups for anionic fuel cells*. Journal of Power Sources, 2009. **190**(2): p. 285-292.

54. Yan, J. and Hickner, M.A., *Anion Exchange Membranes by Bromination of Benzylmethyl-Containing Poly(sulfone)s*. Macromolecules, 2010. **43**(5): p. 2349-2356.

55. Zhou, J., Ünlü, M., Anestis-Richard, I. and Kohl, P.A., *Crosslinked, epoxy-based anion conductive membranes for alkaline membrane fuel cells*. Journal of Membrane Science, 2010. **350**(1-2): p. 286-292.

56. Tanaka, M., Fukasawa, K., Nishino, E., Yamaguchi, S., Yamada, K., Tanaka, H., Bae, B., Miyatake, K. and Watanabe, M., *Anion Conductive Block Poly(arylene ether)s: Synthesis,*

Properties, and Application in Alkaline Fuel Cells. Journal of the American Chemical Society, 2011. **133**(27): p. 10646-10654.

57. Zhao, Z., Wang, J., Li, S. and Zhang, S., *Synthesis of multi-block poly(arylene ether sulfone) copolymer membrane with pendant quaternary ammonium groups for alkaline fuel cell*. Journal of Power Sources, 2011. **196**(10): p. 4445-4450.

58. Zhou, J., Ünlü, M., Anestis-Richard, I., Kim, H. and Kohl, P.A., *Solvent processible, high-performance partially fluorinated copoly(arylene ether) alkaline ionomers for alkaline electrodes*. Journal of Power Sources, 2011. **196**(19): p. 7924-7930.

59. Zschocke, P. and Quellmalz, D., *Novel ion exchange membranes based on an aromatic polyethersulfone*. Journal of Membrane Science, 1985. **22**(2–3): p. 325-332.

60. Wang, G., Weng, Y., Chu, D., Xie, D. and Chen, R., *Preparation of alkaline anion exchange membranes based on functional poly(ether-imide) polymers for potential fuel cell applications*. Journal of Membrane Science, 2009. **326**(1): p. 4-8.

61. Wang, G., Weng, Y., Zhao, J., Chen, R. and Xie, D., *Preparation of a functional poly(ether imide) membrane for potential alkaline fuel cell applications: Chloromethylation*. Journal of Applied Polymer Science, 2009. **112**(2): p. 721-727.

62. Wang, G., Weng, Y., Zhao, J., Chu, D., Xie, D. and Chen, R., *Developing a novel alkaline anion exchange membrane derived from poly(ether-imide) for improved ionic conductivity*. Polymers for Advanced Technologies, 2010. **21**(8): p. 554-560.

63. Han, X., Zhou, L., Liu, H. and Hu, Y., *Effect of in situ oxidization with potassium permanganate on the morphologies of SEBS membranes*. Polymer Degradation and Stability, 2007. **92**(1): p. 75-85.

64. Yildirim, M.H., Stamatialis, D. and Wessling, M., *Dimensionally stable Nafion–polyethylene composite membranes for direct methanol fuel cell applications*. Journal of Membrane Science, 2008. **321**(2): p. 364-372.

65. Mokrini, A., Huneault, M.A., Shi, Z., Xie, Z. and Holdcroft, S., *Non-fluorinated proton-exchange membranes based on melt extruded SEBS/HDPE blends*. Journal of Membrane Science, 2008. **325**(2): p. 749-757.

66. Nagarale, R.K., Gohil, G.S. and Shahi, V.K., *Recent developments on ion-exchange membranes and electro-membrane processes*. Advances in Colloid and Interface Science, 2006. **119**(2–3): p. 97-130.

67. Clark, T.J., Robertson, N.J., Kostalik Iv, H.A., Lobkovsky, E.B., Mutolo, P.F., Abruña, H.c.D. and Coates, G.W., *A Ring-Opening Metathesis Polymerization Route to Alkaline Anion Exchange Membranes: Development of Hydroxide-Conducting Thin Films from an Ammonium-Functionalized Monomer*. Journal of the American Chemical Society, 2009. **131**(36): p. 12888-12889.

68. Kostalik, H.A., Clark, T.J., Robertson, N.J., Mutolo, P.F., Longo, J.M., Abruña, H.c.D. and Coates, G.W., *Solvent Processable Tetraalkylammonium-Functionalized Polyethylene for Use as an Alkaline Anion Exchange Membrane*. Macromolecules, 2010. **43**(17): p. 7147-7150.

69. Robertson, N.J., Kostalik, H.A., Clark, T.J., Mutolo, P.F., Abruña, H.D. and Coates, G.W., *Tunable High Performance Cross-Linked Alkaline Anion Exchange Membranes for Fuel Cell Applications*. Journal of the American Chemical Society, 2010. **132**(10): p. 3400-3404.

70. Xu, T. and Yang, W., *Fundamental studies of a new series of anion exchange membranes: membrane preparation and characterization*. Journal of Membrane Science, 2001. **190**(2): p. 159-166.

71. Xu, T. and Zha, F.F., *Fundamental studies on a new series of anion exchange membranes: effect of simultaneous amination-crosslinking processes on membranes ion-exchange capacity and dimensional stability*. Journal of Membrane Science, 2002. **199**(1-2): p. 203-210.

72. Xu, T., Liu, Z. and Yang, W., *Fundamental studies of a new series of anion exchange membranes: membrane prepared from poly(2,6-dimethyl-1,4-phenylene oxide) (PPO) and triethylamine*. Journal of Membrane Science, 2005. **249**(1-2): p. 183-191.

73. Li, Y., Xu, T.W. and Gong, M., *Fundamental studies of a new series of anion exchange membranes: Membranes prepared from bromomethylated poly(2,6-dimethyl-1,4-phenylene oxide) (BPPO) and pyridine*. Journal of Membrane Science, 2006. **279**(1-2): p. 200-208.

74. Wu, L., Xu, T. and Yang, W., *Fundamental studies of a new series of anion exchange membranes: Membranes prepared through chloroacetylation of poly(2,6-dimethyl-1,4-phenylene oxide) (PPO) followed by quaternary amination*. Journal of Membrane Science, 2006. **286**(1-2): p. 185-192.

75. Zhang, S., Xu, T. and Wu, C., *Synthesis and characterizations of novel, positively charged hybrid membranes from poly(2,6-dimethyl-1,4-phenylene oxide)*. Journal of Membrane Science, 2006. **269**(1-2): p. 142-151.

76. Wu, L., Xu, T., Wu, D. and Zheng, X., *Preparation and characterization of CPPO/BPPO blend membranes for potential application in alkaline direct methanol fuel cell*. Journal of Membrane Science, 2008. **310**(1-2): p. 577-585.

77. Wu, L. and Xu, T.W., *Improving anion exchange membranes for DMAFCs by inter-crosslinking CPPO/BPPO blends*. Journal of Membrane Science, 2008. **322**(2): p. 286-292.

78. Li, Y. and Xu, T.W., *Fundamental Studies of a New Series of Anion Exchange Membranes: Membranes Prepared from Bromomethylated Poly(2,6-dimethyl-1,4-phenylene oxide) and 4-Vinylpyridine*. Journal of Applied Polymer Science, 2009. **114**(5): p. 3016-3025.

79. Wu, Y., Wu, C., Xu, T., Lin, X. and Fu, Y., *Novel silica/poly(2,6-dimethyl-1,4-phenylene oxide) hybrid anion-exchange membranes for alkaline fuel cells: Effect of heat treatment*. Journal of Membrane Science, 2009. **338**(1-2): p. 51-60.

80. Wu, Y., Wu, C., Varcoe, J.R., Poynton, S.D., Xu, T. and Fu, Y., *Novel silica/poly(2,6-dimethyl-1,4-phenylene oxide) hybrid anion-exchange membranes for alkaline fuel cells: Effect of silica content and the single cell performance*. Journal of Power Sources, 2010. **195**(10): p. 3069-3076.

81. Wu, L., Zhou, G., Liu, X., Zhang, Z., Li, C. and Xu, T., *Environmentally friendly synthesis of alkaline anion exchange membrane for fuel cells via a solvent-free strategy*. Journal of Membrane Science, 2011. **371**(1-2): p. 155-162.

82. Li, N., Leng, Y., Hickner, M.A. and Wang, C.-Y., *Highly Stable, Anion Conductive, Comb-Shaped Copolymers for Alkaline Fuel Cells*. Journal of the American Chemical Society, 2013. **135**(27): p. 10124-10133.

83. Hibbs, M.R., Fujimoto, C.H. and Cornelius, C.J., *Synthesis and Characterization of Poly(phenylene)-Based Anion Exchange Membranes for Alkaline Fuel Cells*. Macromolecules, 2009. **42**(21): p. 8316-8321.

84. Hibbs, M.R., *Alkaline stability of poly(phenylene)-based anion exchange membranes with various cations*. Journal of Polymer Science Part B: Polymer Physics, 2013. **51**(24): p. 1736-1742.

85. Gu, S., Cai, R., Luo, T., Chen, Z., Sun, M., Liu, Y., He, G. and Yan, Y., *A Soluble and Highly Conductive Ionomer for High-Performance Hydroxide Exchange Membrane Fuel Cells*. Angewandte Chemie International Edition, 2009. **48**(35): p. 6499-6502.

86. Gu, S., Cai, R., Luo, T., Jensen, K., Contreras, C. and Yan, Y., *Quaternary Phosphonium-Based Polymers as Hydroxide Exchange Membranes*. ChemSusChem, 2010. **3**(5): p. 555-558.

87. Gu, S., Cai, R. and Yan, Y., *Self-crosslinking for dimensionally stable and solvent-resistant quaternary phosphonium based hydroxide exchange membranes*. Chemical Communications, 2011. **47**(10): p. 2856-2858.

88. Noonan, K.J.T., Hugar, K.M., Kostalik, H.A., Lobkovsky, E.B., Abruña, H.D. and Coates, G.W., *Phosphonium-Functionalized Polyethylene: A New Class of Base-Stable Alkaline Anion Exchange Membranes*. Journal of the American Chemical Society, 2012. **134**(44): p. 18161-18164.

89. Wang, J., Li, S. and Zhang, S., *Novel Hydroxide-Conducting Polyelectrolyte Composed of an Poly(arylene ether sulfone) Containing Pendant Quaternary Guanidinium Groups for Alkaline Fuel Cell Applications*. Macromolecules, 2010. **43**(8): p. 3890-3896.

90. Lin, X., Wu, L., Liu, Y., Ong, A.L., Poynton, S.D., Varcoe, J.R. and Xu, T., *Alkali resistant and conductive guanidinium-based anion-exchange membranes for alkaline polymer electrolyte fuel cells*. Journal of Power Sources, 2012. **217**(0): p. 373-380.

91. Henkensmeier, D., Kim, H.-J., Lee, H.-J., Lee, D.H., Oh, I.-H., Hong, S.-A., Nam, S.-W. and Lim, T.-H., *Polybenzimidazolium-Based Solid Electrolytes*. Macromolecular Materials and Engineering, 2011. **296**(10): p. 899-908.

92. Thomas, O.D., Soo, K.J.W.Y., Peckham, T.J., Kulkarni, M.P. and Holdcroft, S., *Anion conducting poly(dialkyl benzimidazolium) salts*. Polymer Chemistry, 2011. **2**(8): p. 1641-1643.

93. Thomas, O.D., Soo, K.J.W.Y., Peckham, T.J., Kulkarni, M.P. and Holdcroft, S., *A Stable Hydroxide-Conducting Polymer*. Journal of the American Chemical Society, 2012. **134**(26): p. 10753-10756.

94. Rao, A.H.N., Thankamony, R.L., Kim, H.-J., Nam, S. and Kim, T.-H., *Imidazolium-functionalized poly(arylene ether sulfone) block copolymer as an anion exchange membrane for alkaline fuel cell*. Polymer, 2013. **54**(1): p. 111-119.

95. Weber, A.Z. and Newman, J., *Modeling Transport in Polymer-Electrolyte Fuel Cells*. Chemical Reviews, 2004. **104**(10): p. 4679-4726.

96. Kreuer, K.-D., Paddison, S.J., Spohr, E. and Schuster, M., *Transport in Proton Conductors for Fuel-Cell Applications: Simulations, Elementary Reactions, and Phenomenology*. Chemical Reviews, 2004. **104**(10): p. 4637-4678.

97. Peckham, T.J. and Holdcroft, S., *Structure-Morphology-Property Relationships of Non-Perfluorinated Proton-Conducting Membranes*. Advanced Materials, 2010. **22**(42): p. 4667-4690.

98. Kong, X., Wadhwa, K., Verkade, J.G. and Schmidt-Rohr, K., *Determination of the Structure of a Novel Anion Exchange Fuel Cell Membrane by Solid-State Nuclear Magnetic Resonance Spectroscopy*. Macromolecules, 2009. **42**(5): p. 1659-1664.

99. Jung, M.-s.J., Arges, C.G. and Ramani, V., *A perfluorinated anion exchange membrane with a 1,4-dimethylpiperazinium cation*. Journal of Materials Chemistry, 2011. **21**(17): p. 6158-6160.

100. Salerno, H.L.S., Beyer, F.L. and Elabd, Y.A., *Anion exchange membranes derived from nafion precursor for the alkaline fuel cell*. Journal of Polymer Science Part B: Polymer Physics, 2012. **50**(8): p. 552-562.

101. Förster, S. and Plantenberg, T., *From Self-Organizing Polymers to Nanohybrid and Biomaterials*. Angewandte Chemie International Edition, 2002. **41**(5): p. 688-714.

102. BATES, F.S., *Polymer-Polymer Phase Behavior*. Science, 1991. **251**(4996): p. 898-905.

103. (JASRI), J.S.R.R.I. *Developing Quasicrystals Comprised of Three-Component Block Copolymers*. Developing Quasicrystals Comprised of Three-Component Block Copolymers 2007; Available from: http://www.spring8.or.jp/en/news_publications/publications/scientific_results/soft_matter/topic10.

104. Weber, R.L., Ye, Y., Schmitt, A.L., Banik, S.M., Elabd, Y.A. and Mahanthappa, M.K., *Effect of Nanoscale Morphology on the Conductivity of Polymerized Ionic Liquid Block Copolymers*. Macromolecules, 2011. **44**(14): p. 5727-5735.

105. Tsai, T.-H., Maes, A.M., Vandiver, M.A., Versek, C., Seifert, S., Tuominen, M., Liberatore, M.W., Herring, A.M. and Coughlin, E.B., *Synthesis and structure–conductivity relationship of polystyrene-block-poly(vinyl benzyl trimethylammonium) for alkaline anion exchange membrane fuel cells*. Journal of Polymer Science Part B: Polymer Physics, 2013. **51**(24): p. 1751-1760.

106. Ye, Y., Sharick, S., Davis, E.M., Winey, K.I. and Elabd, Y.A., *High Hydroxide Conductivity in Polymerized Ionic Liquid Block Copolymers*. ACS Macro Letters, 2013. **2**(7): p. 575-580.

107. Ye, Y., Choi, J.-H., Winey, K.I. and Elabd, Y.A., *Polymerized Ionic Liquid Block and Random Copolymers: Effect of Weak Microphase Separation on Ion Transport*. Macromolecules, 2012. **45**(17): p. 7027-7035.

108. Rebeck, N.T., Li, Y. and Knauss, D.M., *Poly(phenylene oxide) copolymer anion exchange membranes*. Journal of Polymer Science Part B: Polymer Physics, 2013. **51**(24): p. 1770-1778.

109. Hsieh, H. and Quirk, R.P., *Anionic Polymerization: Principles and Practical Applications*. 1996: Taylor & Francis.

110. Baskaran, D. and Müller, A.H.E., *Anionic vinyl polymerization—50 years after Michael Szwarc*. Progress in Polymer Science, 2007. **32**(2): p. 173-219.

111. Ting, W.-H., Dai, S.A., Shih, Y.-F., Yang, I.K., Su, W.-C. and Jeng, R.-J., *Facile synthetic route toward poly(vinyl benzyl amine) and its versatile intermediates*. Polymer, 2008. **49**(6): p. 1497-1505.

112. Bair, H.E., *Quantitative thermal analysis of polyblends*. Polymer Engineering & Science, 1970. **10**(4): p. 247-250.

113. Oudhuis, A.A.C.M. and Ten Brinke, G., *Enthalpy relaxations and concentration fluctuations in blends of polystyrene and poly(oxy-2,6-dimethyl-1,4-phenylene)*. Macromolecules, 1992. **25**(2): p. 698-702.

114. Shultz, A.R. and Gendron, B.M., *Thermo-optical and differential scanning calorimetric observations of mobility transitions in polystyrene-poly(2,6-dimethyl-1,4-phenylene oxide) blends*. Journal of Applied Polymer Science, 1972. **16**(2): p. 461-471.

115. Lefebvre, D., Jasse, B. and Monnerie, L., *Fourier transform infra-red study of uniaxially oriented poly(2,6-dimethyl 1,4-phenylene oxide)-atactic polystyrene blends*. Polymer, 1981. **22**(12): p. 1616-1620.

116. Tucker, P.S., Barlow, J.W. and Paul, D.R., *Thermal, mechanical, and morphological analyses of poly(2,6-dimethyl-1,4-phenylene oxide)/styrene-butadiene-styrene copolymer blends*. Macromolecules, 1988. **21**(6): p. 1678-1685.

117. Yang, J., An, L. and Xu, T., *The glass transition temperatures of PS/PPO blends: Couchman volume-based equation and its verification*. Polymer, 2001. **42**(18): p. 7887-7892.

118. Mazard, C., Benyahia, L. and Tassin, J.-F., *Dynamic mechanical properties of polystyrene-based block copolymers blended with poly(2,6-dimethyl-1,4-phenylene oxide)*. Polymer International, 2003. **52**(4): p. 514-521.

119. Park, J.Y., Acar, M.H., Akthakul, A., Kuhlman, W. and Mayes, A.M., *Polysulfone-graft-poly(ethylene glycol) graft copolymers for surface modification of polysulfone membranes*. Biomaterials, 2006. **27**(6): p. 856-865.

120. Sanabria-Chinchilla, J., Asazawa, K., Sakamoto, T., Yamada, K., Tanaka, H. and Strasser, P., *Noble Metal-Free Hydrazine Fuel Cell Catalysts: EPOC Effect in Competing Chemical and Electrochemical Reaction Pathways*. Journal of the American Chemical Society, 2011. **133**(14): p. 5425-5431.

121. Hay, A.S., *Polymerization by oxidative coupling: Discovery and commercialization of PPO® and Noryl® resins*. Journal of Polymer Science Part A: Polymer Chemistry, 1998. **36**(4): p. 505-517.

122. Puskas, J.E., Kwon, Y., Altstädt, V. and Kontopoulou, M., *Blends of poly(2,6-dimethyl-1,4-phenylene oxide) (PPO) with polystyrene-based thermoplastic rubbers: A comparative study*. Polymer, 2007. **48**(2): p. 590-597.

123. Tongwen, X. and Weihua, Y., *Fundamental studies of a new series of anion exchange membranes: membrane preparation and characterization*. Journal of Membrane Science, 2001. **190**(2): p. 159-166.

124. Li, G.H., Lee, C.H., Lee, Y.M. and Cho, C.G., *Preparation of poly(vinyl phosphate-b-styrene) copolymers and its blend with PPO as proton exchange membrane for DMFC applications*. Solid State Ionics, 2006. **177**(11-12): p. 1083-1090.

125. Cho, C.G., Kim, S.H., Park, Y.C., Kim, H. and Park, J.-W., *Fuel cell membranes based on blends of PPO with poly(styrene-b-vinylbenzylphosphonic acid) copolymers*. Journal of Membrane Science, 2008. **308**(1-2): p. 96-106.

126. Fujimoto, C.H., Hickner, M.A., Cornelius, C.J. and Loy, D.A., *Ionomeric Poly(phenylene) Prepared by Diels-Alder Polymerization: Synthesis and Physical Properties of a Novel Polyelectrolyte*. Macromolecules, 2005. **38**(12): p. 5010-5016.

127. Liu, Y., Horan, J.L., Schlichting, G.J., Caire, B.R., Liberatore, M.W., Hamrock, S.J., Haugen, G.M., Yandrasits, M.A., Seifert, S. and Herring, A.M., *A Small-Angle X-ray Scattering Study of the Development of Morphology in Films Formed from the 3M Perfluorinated Sulfonic Acid Ionomer*. Macromolecules, 2012. **45**(18): p. 7495-7503.

128. Schlichting, G.J., Horan, J.L., Jessop, J.D., Nelson, S.E., Seifert, S., Yang, Y. and Herring, A.M., *A Hybrid Organic/Inorganic Ionomer from the Copolymerization of Vinylphosphonic Acid and Zirconium Vinylphosphonate*. Macromolecules, 2012. **45**(9): p. 3874-3882.

129. Hubner, G. and Roduner, E., *EPR investigation of HO/ radical initiated degradation reactions of sulfonated aromatics as model compounds for fuel cell proton conducting membranes*. Journal of Materials Chemistry, 1999. **9**(2): p. 409-418.

130. Horák, Z., Fortelný, I., Kolařík, J., Hlavatá, D. and Sikora, A., *Polymer Blends*, in *Encyclopedia of Polymer Science and Technology*. 2002, John Wiley & Sons, Inc.

131. Georges, M.K., Veregin, R.P.N., Kazmaier, P.M. and Hamer, G.K., *Narrow molecular weight resins by a free-radical polymerization process*. Macromolecules, 1993. **26**(11): p. 2987-2988.

132. Hawker, C.J., *Molecular Weight Control by a "Living" Free-Radical Polymerization Process*. Journal of the American Chemical Society, 1994. **116**(24): p. 11185-11186.

133. Kazmaier, P.M., Daimon, K., Georges, M.K., Hamer, G.K. and Veregin, R.P.N., *Nitroxide-Mediated "Living" Free Radical Polymerization: A Rapid Polymerization of (Chloromethyl)styrene for the Preparation of Random, Block, and Segmental Arborescent Polymers*. Macromolecules, 1997. **30**(8): p. 2228-2231.

134. Lacroix-Desmazes, P., Delair, T., Pichot, C. and Boutevin, B., *Synthesis of poly(chloromethylstyrene-b-styrene) block copolymers by controlled free-radical polymerization*. Journal of Polymer Science Part A: Polymer Chemistry, 2000. **38**(21): p. 3845-3854.

135. Shultz, A.R. and Beach, B.M., *Thermo-Optical, Differential Calorimetric, and Dynamic Viscoelastic Transitions in Poly(2,6-dimethyl-1,4-phenylene oxide) (PPO Resin) Blends with Poly-p-chlorostyrene and with Styrene-p-Chlorostyrene Statistical Copolymers*. Macromolecules, 1974. **7**(6): p. 902-909.

136. Brinke, G.T., Karasz, F.E. and MacKnight, W.J., *Phase behavior in copolymer blends: poly(2,6-dimethyl-1,4-phenylene oxide) and halogen-substituted styrene copolymers*. Macromolecules, 1983. **16**(12): p. 1827-1832.

137. Zacharius, S.L., Ten Brinke, G., MacKnight, W.J. and Karasz, F.E., *Evidence for critical double points in blends of polystyrene and poly(o-chlorostyrene)*. Macromolecules, 1983. **16**(3): p. 381-387.

138. Vukovic, R. and Bogdanic, G., *Phase Behavior and Miscibility in Binary Blends Containing Polymers and Copolymers of Styrene, of 2,6-Dimethyl-1,4-Phenylene Oxide, and of Their Derivatives*. Journal of Physical and Chemical Reference Data, 1999. **28**(3): p. 851-868.

139. Kambour, R.P., Gundlach, P.E., Wang, I.-C.W., White, D.M. and Yeagert, G.W., *Miscibility of poly(2,6-dimethyl-1,4-phenylene oxide) with several styrenic homopolymers: dependence of interaction parameters from critical molecular weights on cohesive energy densities*. Polymer Communications, 1988. **29**.

140. Sudre, G., Inceoglu, S., Cotanda, P. and Balsara, N.P., *Influence of Bound Ion on the Morphology and Conductivity of Anion-Conducting Block Copolymers*. Macromolecules, 2013. **46**(4): p. 1519-1527.

141. Fried, J.R., MacKnight, W.J. and Karasz, F.E., *Modeling of tensile properties of polymer blends: PPO/poly(styrene-co-p-chlorostyrene)*. Journal of Applied Physics, 1979. **50**(10): p. 6052-6060.

142. Kleiner, L.W., Karasz, F.E. and MacKnight, W.J., *Compatible glassy polyblends based upon poly(2,6-dimethyl-1,4-phenylene oxide): Tensile modulus studies*. Polymer Engineering & Science, 1979. **19**(7): p. 519-524.

143. Fujimoto, C., Kim, D.-S., Hibbs, M., Wrobleski, D. and Kim, Y.S., *Backbone stability of quaternized polyaromatics for alkaline membrane fuel cells*. Journal of Membrane Science, 2012. **423–424**: p. 438-449.

144. Curtin, D.E., Lousenberg, R.D., Henry, T.J., Tangeman, P.C. and Tisack, M.E., *Advanced materials for improved PEMFC performance and life*. Journal of Power Sources, 2004. **131**(1–2): p. 41-48.

145. Hamrock, S.J. and Yandrasits, M.A., *Proton Exchange Membranes for Fuel Cell Applications*. Journal of Macromolecular Science, Part C, 2006. **46**(3): p. 219-244.

146. Borup, R., Meyers, J., Pivovar, B., Kim, Y.S., Mukundan, R., Garland, N., Myers, D., Wilson, M., Garzon, F., Wood, D., Zelenay, P., More, K., Stroh, K., Zawodzinski, T., Boncella, J., McGrath, J.E., Inaba, M., Miyatake, K., Hori, M., Ota, K., Ogumi, Z., Miyata, S., Nishikata, A., Siroma, Z., Uchimoto, Y., Yasuda, K., Kimijima, K.I. and Iwashita, N., *Scientific Aspects of Polymer Electrolyte Fuel Cell Durability and Degradation*. Chemical Reviews, 2007. **107**(10): p. 3904-3951.

147. Gülzow, E., *Alkaline Fuel Cells*. Fuel Cells, 2004. **4**(4): p. 251-255.

148. Rebeck, N.T., *Polymer Synthesis Toward Fuel Cell Membrane Materials*, 2012, Colorado School of Mines: PhD Thesis.

149. Moad, G., Rizzardo, E. and Solomon, D.H., *Selectivity of the reaction of free radicals with styrene*. Macromolecules, 1982. **15**(3): p. 909-914.

150. Cabasso, I., Jagur-Grodzinski, J. and Vofsi, D., *Synthesis and characterization of polymers with pendent phosphonate groups*. Journal of Applied Polymer Science, 1974. **18**(7): p. 1969-1986.

151. Shin, D.W., Lee, S.Y., Lee, C.H., Lee, K.-S., Park, C.H., McGrath, J.E., Zhang, M., Moore, R.B., Lingwood, M.D., Madsen, L.A., Kim, Y.T., Hwang, I. and Lee, Y.M., *Sulfonated Poly(arylene sulfide sulfone nitrile) Multiblock Copolymers with Ordered Morphology for Proton Exchange Membranes*. Macromolecules, 2013. **46**(19): p. 7797-7804.

152. Pan, J., Lu, S., Li, Y., Huang, A., Zhuang, L. and Lu, J., *High-Performance Alkaline Polymer Electrolyte for Fuel Cell Applications*. Advanced Functional Materials, 2010. **20**(2): p. 312-319.

153. Faraj, M., Boccia, M., Miller, H., Martini, F., Borsacchi, S., Geppi, M. and Pucci, A., *New LDPE based anion-exchange membranes for alkaline solid polymeric electrolyte water electrolysis*. International Journal of Hydrogen Energy, 2012. **37**(20): p. 14992-15002.

154. Sherazi, T.A., Yong Sohn, J., Moo Lee, Y. and Guiver, M.D., *Polyethylene-based radiation grafted anion-exchange membranes for alkaline fuel cells*. Journal of Membrane Science, 2013. **441**: p. 148-157.

155. Schauer, J., Hnát, J., Brožová, L., Žitka, J. and Bouzek, K., *Heterogeneous anion-selective membranes: Influence of a water-soluble component in the membrane on the morphology and ionic conductivity*. Journal of Membrane Science, 2012. **401–402**(0): p. 83-88.

156. Kim, H.K., Zhang, M., Yuan, X., Lvov, S.N. and Chung, T.C.M., *Synthesis of Polyethylene-Based Proton Exchange Membranes Containing PE Backbone and Sulfonated Poly(arylene ether sulfone) Side Chains for Fuel Cell Applications*. Macromolecules, 2012. **45**(5): p. 2460-2470.

157. Brandrup, J. and Immergut, E.H., *Polymer handbook*. 1966: Interscience Publishers.

158. Wunderlich, B., *Thermal analysis*. 1990: Academic Press.

159. Skoog, D.A., West, D.M. and Holler, F.J., *Fundamentals of Analytical Chemistry 7th Edition*. 1996: Thomson Learning, Inc, USA.

160. Hou, H.C., Tsiang, R.C.C. and Hsieh, H.C.C., *Preparing a functionalized thermoplastic elastomer: Chlorination and synthesis of poly(p-methylstyrene)-block-polyisoprene-block-poly(p-methylstyrene)*. Journal of Polymer Science Part a-Polymer Chemistry, 1997. **35**(14): p. 2969-2980.

161. Quirk, R.P., *New Block Copolymers for Higher Temperature Applications*. Abstracts of Papers of the American Chemical Society, 1985. **190**(SEP): p. 74-POY.

162. Gatzke, A.L., *Chain transfer in anionic polymerization. Determination of chain-transfer constants by using carbon-14-labeled chain transfer agents*. Journal of Polymer Science Part A-1: Polymer Chemistry, 1969. **7**(8): p. 2281-2292.

163. Mays, J.W. and Hadjichristidis, N., *Synthesis of High Molecular-Weight Near-Monodisperse Poly(4-methylstyrene) by Anionic Polymerization*. Polymer Bulletin, 1989. **22**(5-6): p. 471-474.

164. Bender, J.T. and Knauss, D.M., *Synthesis of low polydispersity polybutadiene and polyethylene stars by convergent living anionic polymerization*. Journal of Polymer Science Part A: Polymer Chemistry, 2006. **44**(2): p. 828-836.

165. Hsieh, H.L. and Quirk, R.P., *Anionic Polymerization: Principles and practical applications*. 1996, New York: Marcel Dekker, Inc.

166. Dounis, P. and James Feast, W., *A route to low polydispersity linear and star polyethylenes via ring-opening metathesis polymerization*. Polymer, 1996. **37**(12): p. 2547-2554.

167. Grassi, A., Caprio, M., Zambelli, A. and Bowen, D.E., *Synthesis and Characterization of Syndiotactic Styrene−Ethylene Block Copolymers*. Macromolecules, 2000. **33**(22): p. 8130-8135.

168. Phinyocheep, P., Pasiri, S. and Tavichai, O., *Diimide hydrogenation of isoprene–styrene diblock copolymers*. Journal of Applied Polymer Science, 2003. **87**(1): p. 76-82.

169. Price, S.C., Ren, X., Jackson, A.C., Ye, Y., Elabd, Y.A. and Beyer, F.L., *Bicontinuous Alkaline Fuel Cell Membranes from Strongly Self-Segregating Block Copolymers*. Macromolecules, 2013. **46**(18): p. 7332-7340.

170. Halseid, R., Vie, P.J.S. and Tunold, R., *Influence of Ammonium on Conductivity and Water Content of Nafion 117 Membranes*. Journal of The Electrochemical Society, 2004. **151**(3): p. A381-A388.

171. Saito, M., Hayamizu, K. and Okada, T., *Temperature Dependence of Ion and Water Transport in Perfluorinated Ionomer Membranes for Fuel Cells*. The Journal of Physical Chemistry B, 2005. **109**(8): p. 3112-3119.

172. Xiong, Y., Fang, J., Zeng, Q.H. and Liu, Q.L., *Preparation and characterization of cross-linked quaternized poly(vinyl alcohol) membranes for anion exchange membrane fuel cells*. Journal of Membrane Science, 2008. **311**(1-2): p. 319-325.

173. Vanvsek, P., *CRC Handbook of Chemistry and Physics*. 83rd ed. 2002: CRC Press: Boca Raton, FL.

174. Roy, A., Yu, X., Dunn, S. and McGrath, J.E., *Influence of microstructure and chemical composition on proton exchange membrane properties of sulfonated–fluorinated, hydrophilic–hydrophobic multiblock copolymers*. Journal of Membrane Science, 2009. **327**(1–2): p. 118-124.

175. Zhang, H., Ohashi, H., Tamaki, T. and Yamaguchi, T., *Direction and Management of Water Movement in Solid-State Alkaline Fuel Cells*. The Journal of Physical Chemistry C, 2012. **116**(14): p. 7650-7657.

176. U□nlu□, M., Zhou, J. and Kohl, P.A., *Hybrid Anion and Proton Exchange Membrane Fuel Cells*. The Journal of Physical Chemistry C, 2009. **113**(26): p. 11416-11423.

177. Ünlü, M., Zhou, J. and Kohl, P.A., *Self Humidifying Hybrid Anion–Cation Membrane Fuel Cell Operated Under Dry Conditions*. Fuel Cells, 2010. **10**(1): p. 54-63.

178. Disabb-Miller, M.L., Johnson, Z.D. and Hickner, M.A., *Ion Motion in Anion and Proton-Conducting Triblock Copolymers*. Macromolecules, 2013. **46**(3): p. 949-956.

179. Roziere, J. and Jones, D.J., *Non-fluorinated polymer materials for proton exchange membrane fuel cells*. Annual Review of Materials Research, 2003. **33**: p. 503-555.

180. Okada, T., Xie, G., Gorseth, O., Kjelstrup, S., Nakamura, N. and Arimura, T., *Ion and water transport characteristics of Nafion membranes as electrolytes*. Electrochimica Acta, 1998. **43**(24): p. 3741-3747.

181. Grew, K.N., Chu, D. and Chiu, W.K.S., *Ionic Equilibrium and Transport in the Alkaline Anion Exchange Membrane*. Journal of The Electrochemical Society, 2010. **157**(7): p. B1024-B1032.

182. Grew, K.N. and Chiu, W.K.S., *A Dusty Fluid Model for Predicting Hydroxyl Anion Conductivity in Alkaline Anion Exchange Membranes*. Journal of The Electrochemical Society, 2010. **157**(3): p. B327-B337.

183. Armarego, W.L.F. and Chai, C., *Chapter 1 - Common Physical Techniques Used in Purification*, in *Purification of Laboratory Chemicals (Seventh Edition)*, Armarego, W.L.F. and Chai, C., Editors. 2013, Butterworth-Heinemann: Boston. p. 1-70.

184. Kinard, L., Kasper, K. and Mikos, A., *Drying poly(ethylene glycol)*. Protocol Exchange, 2012.

185. Siyad, M.A. and Kumar, G.S.V., *Poly(ethylene glycol) grafted polystyrene dendrimer resins: Novel class of supports for solid phase peptide synthesis*. Polymer, 2012. **53**(19): p. 4076-4090.

186. Sun, H., Zhang, G., Liu, Z., Zhang, N., Zhang, L., Ma, W., Zhao, C., Qi, D., Li, G. and Na, H., *Self-crosslinked alkaline electrolyte membranes based on quaternary ammonium poly (ether sulfone) for high-performance alkaline fuel cells*. International Journal of Hydrogen Energy, 2012. **37**(12): p. 9873-9881.

187. Zhao, C.H., Gong, Y., Liu, Q.L., Zhang, Q.G. and Zhu, A.M., *Self-crosslinked anion exchange membranes by bromination of benzylmethyl-containing poly(sulfone)s for direct methanol fuel cells*. International Journal of Hydrogen Energy, 2012. **37**(15): p. 11383-11393.

188. Pandey, A.K., Goswami, A., Sen, D., Mazumder, S. and Childs, R.F., *Formation and characterization of highly crosslinked anion-exchange membranes*. Journal of Membrane Science, 2003. **217**(1-2): p. 117-130.

189. Fang, J., Yang, Y., Lu, X., Ye, M., Li, W. and Zhang, Y., *Cross-linked, ETFE-derived and radiation grafted membranes for anion exchange membrane fuel cell applications*. International Journal of Hydrogen Energy, 2012. **37**(1): p. 594-602.

190. Pan, J., Li, Y., Zhuang, L. and Lu, J., *Self-crosslinked alkaline polymer electrolyte exceptionally stable at 90 [degree]C*. Chemical Communications, 2010. **46**(45): p. 8597-8599.

191. Zhao, Y., Yu, H., Yang, D., Li, J., Shao, Z. and Yi, B., *High-performance alkaline fuel cells using crosslinked composite anion exchange membrane*. Journal of Power Sources, 2013. **221**: p. 247-251.

192. Devonport, W., Michalak, L., Malmström, E., Mate, M., Kurdi, B., Hawker, C.J., Barclay, G.G. and Sinta, R., *"Living" Free-Radical Polymerizations in the Absence of Initiators: Controlled Autopolymerization*. Macromolecules, 1997. **30**(7): p. 1929-1934.

193. Levchik, G.F., Si, K., Levchik, S.V., Camino, G. and Wilkie, C.A., *The correlation between cross-linking and thermal stability: Cross-linked polystyrenes and polymethacrylates*. Polymer Degradation and Stability, 1999. **65**(3): p. 395-403.

194. Wu, L. and Xu, T., *Improving anion exchange membranes for DMAFCs by inter-crosslinking CPPO/BPPO blends*. Journal of Membrane Science, 2008. **322**(2): p. 286-292.

195. Widin, J.M., Schmitt, A.K., Schmitt, A.L., Im, K. and Mahanthappa, M.K., *Unexpected Consequences of Block Polydispersity on the Self-Assembly of ABA Triblock Copolymers*. Journal of the American Chemical Society, 2012. **134**(8): p. 3834-3844.

196. Widin, J.M., Kim, M., Schmitt, A.K., Han, E., Gopalan, P. and Mahanthappa, M.K., *Bulk and Thin Film Morphological Behavior of Broad Dispersity Poly(styrene-b-methyl methacrylate) Diblock Copolymers*. Macromolecules, 2013. **46**(11): p. 4472-4480.

197. Wendorff, J.H., *Concentration fluctuations in poly(vinylidene fluoride)-poly(methyl methacrylate) mixtures*. Journal of Polymer Science: Polymer Letters Edition, 1980. **18**(6): p. 439-445.

198. Wendorff, J.H., *The structure of amorphous polymers*. Polymer, 1982. **23**(4): p. 543-557.

199. Riedl, B. and Prud'homme, R.E., *The determination of the thermodynamic interaction parameter χ in polymer blends*. Polymer Engineering & Science, 1984. **24**(17): p. 1291-1299.

200. Gilliom, L.R., *Catalytic hydrogenation of polymers in the bulk*. Macromolecules, 1989. **22**(2): p. 662-665.

201. Cowie, J.M.G. and Toporowski, P.M., *The dependence of glass temperature on molecular weight for poly [alpha]-methyl styrene*. European Polymer Journal, 1968. **4**(5): p. 621-625.

202. Curran, S., Kim, J.K. and Han, C.D., *On segmental mobility in a compatible poly(α-methylstyrene)-block-polystyrene copolymer*. Macromolecules, 1992. **25**(16): p. 4200-4205.

203. McCormick, H.W., *Ceiling Temperature of α-Methylstyrene*. Journal of Polymer Science, 1957. **25**(111): p. 488-490.

204. Mita, I. and Okuyama, H., *Anionic Bulk Polymerization of α-Methylstyrene. Stopping of Polymerization due to Vitrification and Equilibrium in Bulk*. Journal of Polymer Science, Part A-1, 1971. **9**: p. 3437-3452.

205. Cunningham, R.E., *Equilibrium monomer concentration for the anionic polymerization of a-methylstyrene in cyclohexane*. Polymer, 1978. **19**: p. 729-731.

206. Jones, G.D., Friedrich, R.E., Werkema, T.E. and Zimmerman, R.L., *Poly-alpha-methylstyrene*. Industrial & Engineering Chemistry, 1956. **48**(12): p. 2123-2131.

207. Worsfold, D.J. and Bywater, S., *Anionic Polymerization of a-Methylstyrene*. Journal of Polymer Science Part A: General Papers, 1957. **26**: p. 299-304.

208. Worsfold, D.J. and Bywater, S., *ANIONIC POLYMERIZATION OF α-METHYLSTYRENE PART 2. KINETICS*. Canadian Journal Of Chemistry, 1958. **36**: p. 1141-1145.

209. Wenger, F., *Monodisperse poly-α-methylstyrene*. Die Makromolekulare Chemie, 1960. **37**(1): p. 143-148.

210. Burge, D.E. and Bruss, D.B., *Preparation and properties of some poly-α-methylstyrenes*. Journal of Polymer Science Part A: General Papers, 1963. **1**(6): p. 1927-1935.

211. Baer, M., *Anionic block polymerization. II. Preparation and properties of block copolymers*. Journal of Polymer Science Part A: General Papers, 1964. **2**(1): p. 417-436.

212. Fujimoto, T., Ozaki, N. and Nagasawa, M., *Study of the effects of additives in homogeneous anionic polymerization of α-methylstyrene by n-butyllithium (to prepare polymers having narrow molecular weight distribution)*. Journal of Polymer Science Part A: General Papers, 1965. **3**(6): p. 2259-2274.

213. Dainton, F.S., Hui, K.M. and Ivin, K.J., *KINETICS OF ANIONIC POLYMERIZATION OF α-METHYLSTYRENE IN TETRAHYDROPYRAN*. European Polymer Journal, 1969. **5**(3): p. 379-386.

214. Malhotra, S.L., *ANIONIC-POLYMERIZATION OF ALPHA-METHYLSTYRENE .9. NATURE OF THE PROPAGATING SPECIES*. Journal of Macromolecular Science-Chemistry, 1981. **A15**(4): p. 533-552.

215. Ades, D., Fontanille, M., Leonard, J. and Thomas, M., *The anionic bulk polymerization of [alpha]-methylstyrene-II. Kinetic study of the propagation*. European Polymer Journal, 1983. **19**(4): p. 305-311.

216. Higashimura, T., Kamigaito, M., Kato, M., Hasebe, T. and Sawamoto, M., *Living cationic polymerization of .alpha.-methylstyrene initiated with a vinyl ether-hydrogen chloride adduct in conjunction with tin tetrabromide*. Macromolecules, 1993. **26**(11): p. 2670-2673.

217. Morton, M., Kammereck, R.F. and Fetters, L.J., *Synthesis and Properties of Block Polymers. II. Poly(α-methylstyrene)-Poly(propylene sulfide)-Poly(α-methylstyrene)*. Macromolecules, 1971. **4**(1): p. 11-15.

218. Hsiue, G.-H. and Yang, C.-H., *Morphology and properties of α-methylstyrene and butadiene diblock copolymers*. Journal of Applied Polymer Science, 1980. **25**(8): p. 1715-1722.

219. Hsiue, G. and Lee, S., *Domain structure and some properties of solvent-cast films from α-methylstyrene-butadiene block copolymer*. Journal of the Chinese Institute of Chemical Engineers, 1981. **12**(2): p. 61-8.

220. Lee, J. and Hogen-Esch, T.E., *Synthesis and characterization of well-defined poly(alpha-methylstyrene)-b-poly(dimethylsiloxane) block copolymers*. Macromolecules, 2001. **34**(7): p. 2095-2100.

221. Fetters, L.J. and Morton, M., *Synthesis and Properties of Block Polymers. I. Poly-α-methylstyrene-Polyisoprene-Poly-α-methylstyrene*. Macromolecules, 1969. **2**(5): p. 453-458.

222. Cunningham, R.E., *Preparation and stress-strain properties of ABA block copolymers of α-methylstyrene and butadiene*. Journal of Applied Polymer Science, 1978. **22**(10): p. 2907-2913.

223. Hsiue, G.-H. and Yang, W.-R., *Thermal properties and morphology of α-methylstyrene-butadiene-α-methylstyrene triblock copolymer*. Journal of Polymer Science: Polymer Chemistry Edition, 1984. **22**(6): p. 1525-1530.

224. Li, D. and Faust, R., *Polyisobutylene-Based Thermoplastic Elastomers. 3. Synthesis, Characterization, and Properties of Poly(.alpha.-methylstyrene-b-isobutylene-b-.alpha.-methylstyrene) Triblock Copolymers*. Macromolecules, 1995. **28**(14): p. 4893-4898.

225. Li, D. and Faust, R., *Living Carbocationic Sequential Block Copolymerization of Isobutylene with .alpha.-Methylstyrene*. Macromolecules, 1995. **28**(5): p. 1383-1389.

226. Roest, B.C. and Schepers, H.A.J., *Process of preparing A-B-C elastomeric block copolymers*, 1976, US Patents.

227. Baskaran, D., Müller, A.H.E. and Sivaram, S., *The effect of TMEDA on the kinetics of the anionic polymerization of methyl methacrylate in tetrahydrofuran using lithium as counterion*. Macromolecular Chemistry and Physics, 2000. **201**(14): p. 1901-1911.

228. Natori, I., Natori, S., Usui, H. and Sato, H., *Anionic Polymerization of 4-Diphenylaminostyrene: Characteristics of the Alkyllithium/N,N,N',N'-Tetramethylethylenediamine System for Living Anionic Polymerization*. Macromolecules, 2008. **41**(11): p. 3852-3858.

229. Fineman, M. and Ross, S.D., *Linear method for determining monomer reactivity ratios in copolymerization*. Journal of Polymer Science, 1950. **5**(2): p. 259-262.

230. Wyman, D.P. and Song, I.H., *The Butyllithium Initiated Bulk Anionic Polymerization of a-Methylstyrene*. Die Makromolekulare Chemie, 1968. **115**: p. 64-72.

231. Léonard, J. and Malhotra, S.L., *Equilibrium Anionic Polymerization of a-Methylstyrene in p-Dioxane*. Journal of Polymer Science Part A-1: Polymer Chemistry, 1971. **9**(7): p. 1983-1991.

232. Iveq, K.J., *The Effect of Polymer Concentration on the Equilibrium Monomer Concentration for the Anionic Polymerization of α-Methylstyrene in Tetrahydrofuran*. European Polymer Journal, 1970. **6**: p. 331-341.

233. Ivin, K.J. and LÈonard, J., *The effect of polymer concentration on the equilibrium monomer concentration for the anionic polymerization of [alpha]-methylstyrene in tetrahydrofuran*. European Polymer Journal, 1970. **6**(2): p. 331-341.

234. Kobatake, S., Harwood, H.J., Quirk, R.P. and Priddy, D.B., *Block Copolymer Synthesis by Styrene Polymerization Initiated with Nitroxy-Functionalized Polybutadiene*. Macromolecules, 1998. **31**(11): p. 3735-3739.

235. Kobatake, S., Harwood, H.J., Quirk, R.P. and Priddy, D.B., *Synthesis of Nitroxy-Functionalized Polybutadiene by Anionic Polymerization Using a Nitroxy-Functionalized Terminator*. Macromolecules, 1997. **30**(14): p. 4238-4240.

236. Tsoukatos, T., Pispas, S. and Hadjichristidis, N., *Complex Macromolecular Architectures by Combining TEMPO Living Free Radical and Anionic Polymerization*. Macromolecules, 2000. **33**(26): p. 9504-9511.

237. Kobatake, S., Harwood, H.J., Quirk, R.P. and Priddy, D.B., *Synthesis of Nitroxide-Functionalized Polybutadiene Using Halogen-Containing Benzyloxyamine as Terminators for Anionic Polymerization*. Macromolecules, 1999. **32**(26): p. 9080-9080.

238. Kobatake, S., Harwood, H.J., Quirk, R.P. and Priddy, D.B., *Nitroxide-mediated styrene polymerization initiated by an oxoaminium chloride*. Journal of Polymer Science Part A: Polymer Chemistry, 1998. **36**(14): p. 2555-2561.